
# A GEOCHEMICAL INVESTIGATION OF THE DARLING AND YSTERFONTEIN SALINE PANS, WESTERN CAPE, SOUTH AFRICA



**MERIS SMITH**
B. Sc. (Hons) (Geology) (Wits)

Submitted in partial fulfilment of the requirements of the degree of
**MASTER OF SCIENCE**
in the
Department of Geological Sciences
Faculty of Science
University of Cape Town
December 2000

# ABSTRACT

Saline pans are an important component of the hydrologic cycle in arid areas, and are common in South Africa. Natural saline pans on the coastal lowlands of the Western Cape Province, South Africa, were studied to determine the origin and evolution of salts within the pans. Samples of surface, subsurface, stream and spring water as well as pan sediments were collected from two large coastal pans near Ysterfontein, and eight smaller pans 10 – 20 km from the sea, on the inland side of the granitic Darling hills.

Pan waters have between 2 and 379 g/L of total dissolved salts (TDS) and are neutral to alkaline, with a pH of 6.5 to 9.2 buffered by carbonate precipitation. Inland pans can be divided into brine-type (168 – 379 g/L TDS) or brackish to saline types (2 – 64 g/L TDS). $\delta^{18}O$ and $\delta D$ values indicate a meteoric origin of water, with moderate evaporation of pan water. Ionic dominance and ion ratios of major elements in the brackish-saline, coastal and stream/spring samples are similar to seawater. The order of cation dominance is Na>>Mg>>Ca ≈K, and anion dominance is $Cl>>SO_4>>HCO_3$. With the exception of Ca, F, Si, alkalinity and U, all elements behave conservatively in streams and springs, brackish-saline pans and coastal pans. Calcium, alkalinity and perhaps F are depleted in all samples due to precipitation of calcite. Removal of elements from the brine-type pans is due to precipitation of high-Mg calcite, gypsum and fluorite (Ca, Mg, Sr, $HCO_3$, $SO_4$, F), immobilisation by redox (U, Se, S) and ion exchange or clay mineral formation (Mg, Si, K, Li, Br, Rb, Ba). Modelling using PHRQPITZ and PHREEQC indicates that pan waters are slightly undersaturated with respect to halite, but have reached equilibrium with gypsum, celestite, barite, quartz and are supersaturated with respect to calcite, dolomite, epsomite and kaolinite.

Evaporite mineral zonation in the inland pans shows the following stratigraphic sequence with depth: low-Mg calcite – high-Mg calcite – gypsum - halite, consistent with concentration of water by capillary evaporation. The sequence in coastal pans is low Mg-calcite – gypsum – halite, precipitated by complete evaporation of seawater. Precipitation of calcite and gypsum in the sediments permanently removes ions from solution whereas halite is not preserved in the sediments and dissolves on an annual basis. Salts precipitated in the catchment soils by evaporation of coastal rainfall are flushed out by heavy rains, salinising the regional groundwater and contributing directly to pans. Seasonal influxes of this brackish ground- and runoff-water result in accumulation of salts in the pans. Major ions (Na, Mg, Ca, K, Cl, $SO_4$) in inflow waters are derived from coastal rainfall and marine aerosols. Chemical weathering of granite contributes additional Ca and S to the inflow water, and is the main source of $HCO_3$ and trace elements (F, Se, As, Rb, Ba, U). Inland pans are estimated to be no more than a few thousand years old while coastal pans are relict Pleistocene marine evaporates currently cut off from the sea and being fed by terrestrial water.

Most pan waters are unfit for any human related use because of the extreme concentrations of ions (e.g. Na up to 4642 mmol/kg). Concentrations of Se (0.1 – 47 µmol/kg) and B (45 – 7310 µmol/kg) are sufficiently high in pan waters to be a hazard to wildlife and the livestock farmed in the area, a problem exacerbated by the mining of halite from pans, and by removal of natural vegetation from the hillsides.

Salts originate from coastal rainfall modified by contributions from chemical weathering of granite. As the pans evolve, mineral precipitation, ion exchange and redox processes affect the chemical signature of the pan.

# Acknowledgements

The author would like to thank the following people for their contributions to this thesis:

Dr. John Compton for making a thesis from scratch in 5 months an achievable goal;

Prof. Martin Fey for his infectious enthusiasm and wealth of knowledge;

Richard White (almost a Dr.) for providing helpful comments on writing;

A plethora of technical and academic staff who prioritised my analyses and offered their invaluable expertise:

Prof. Chris Harris and Fayrooza Rawoot for assistance with stable isotope sample preparation and analysis, and for constructive comments on this thesis;

Dr. Andreas Spath and Ilse Jones for assistance with ICP-MS sample preparation and analysis;

Patrick Sieas for analysing most of my samples on the IC first time round and trusting me with the instrument second time round.;

Shireen Mjacu AAS analysis;

The following people were ever-ready with advice, always knew of a useful reference and pitched in wherever they could:

Bernadette Azzie, Sarah Miller for ideas, encouragement and invaluable assistance in the lab;

Ross Campbell and Peter Azah Abanda, my classmates, for critical discussion throughout the year, and most of all for being slave labour during sampling trips;

Lisa Cave and John Weaver (CSIR, Stellenbosch) for sampling advice;

Toby Mills for helping out with everything, in particular database design;

All the farmers in the area for allowing me to collect samples on their land, and to Marius at Ysterfontein Gypsum Mine for allowing access to the pan.

# TABLE OF CONTENTS

## Chapter 4: Results



## Chapter 5: Discussion

# List of Figures

# List of Tables

# Glossary of terms and abbreviations

*AAS* – Atomic absorption spectrometry.

*Aeolian deposits* – Sediments deposited after transport by wind (Whitten and Brooks, 1972).

*Athalassic* - Pans with no connection to the sea (Seaman *et al.*, 1991).

*Back reaction* – equilibration reaction between fractionated brine and minerals that were precipitated earlier on in the evolution of the brine (Warren, 1999).

*Berg wind* – A warm dry wind generated when by the compression and heating of air drawn off the elevated plateau of the South African interior by a southwards moving offshore low-pressure cell (Nieman, 1981).

*Bittern salts* - The most soluble salts, precipitating only in the last increment of evaporation (Warren, 1999). They are so called because they decrease the quality of table salt, and the brine (or mother liquor) needs to be removed from a pan precipitating table salt before the bitterns precipitate (Hugo, 1974).

*Brackish* – Too saline to be potable, but significantly less saline than seawater (TDS 1-20 g/kg) (Drever, 1997).

*Calcrete* - Powdery to nodular to highly indurated calcium carbonate that displaces and replaces soil, rock or weathered material in the vadose zone (Goudie, 1983).

*Colluvial deposits* – Loose material deposited after transport by gravity at the foot of a cliff or slope (Parker, 1989).

*Congruent dissolution* - A mineral is completely dissolved into its constituent ions (Faure, 1992).

*Connate salt* - Originates from saline water trapped in sedimentary rocks that formed in a marine environment (Hugo, 1974).

*CSIR* – Council for Scientific and Industrial Research, a South African research institution.

*Cyclic salts* - Salts that originate as sea spray or vapour (Hugo, 1974).

*D-spacing* – Separation between mineral layers (Whittig and Allardice, 1986).

*Deflation* - The removal of material from a pan by aeolian processes (Verhagen 1991).

*DOC* – Dissolved organic carbon.

*Duricrust* – A strongly cemented layer found a short distance below the surface of unconsolidated sediments. The cement can be calcareous, siliceous or ferruginous (Whitten and Brooks, 1972).

*DWAF* – Department of Water Affairs and Forestry.

*EC* – Electrical conductivity. A measure of the number of ions in solution, and used as an estimate of TDS (Drever, 1997).

*EDTA* – Ethylene-diamine-tetraacetic acid.
*Efflorescence* – A surface encrustation of whitish powder found in arid zones, and consisting of one or more minerals (Parker, 1989).

*Eluviation* – The process of leaching in a soil, mainly removing iron and calcium (Whitten and Brooks, 1972).

*Endorheic* – Having no surface outflow (Shaw and Thomas, 1989).

*Fluvial deposits* – Sediments deposited after transport by water in streams or rivers (Branford, 1987).

*Fractional crystallization* – Separation of early-formed crystals from the parent fluid by gravity settling (Whitten and Brooks, 1972).

*Fragipan* – A hard, dense subsurface layer of soil which restricts the movement of water due to its compactness or density rather than due to cementation or clay content (Parker, 1989).

*Heuweltjies* – Afrikaans term for hillock, but used on the South African West Coast to describe large termite mounds (reference).

*Hillocky* – Describing topography dominated by small low hills (Parker, 1989).

*Hygroscopic* – Ability of a mineral to accelerate condensation of water vapour from the atmosphere (Parker, 1989).

*IC* – Ion chromatograph, more correctly in this study High Performance Liquid Chromatograph, an instrument for measuring concentrations of ions in solution (Weiss, 1986).

*ICP-MS* – Inductively coupled plasma mass spectrometer.

*ISE* – Ion selective electrode.

*Illuviation* – The process of deposition of leached material (Whitten and Brooks, 1972).

*Incongruent dissolution* - A mineral reacts with water to form a new mineral and in the process ions are released into solution (Faure, 1992).

*Lithosol* – Shallow soils containing rock fragments, with occasional bedrock exposure (Lambrechts, 1981).

*Lunette dune* - Found downwind of a pan, formed by accretion of fine-grained sand and clay flakes produced on desiccation in the pan and entrained by the wind (Shaw and Thomas, 1989).

*Pans* – A shallow natural depression or closed basin found in arid zones which are subject to ephemeral surface water flooding of varying frequency and extent (Shaw and Thomas, 1989).

*Planosolic soils* - Eluviated surface horizons underlain by clay pans or fragipans (Lambrechts, 1981).

*Renosterbos* – Afrikaans term for a dark coloured bush found in the Darling area (literally, Rhinoceros bush) *Elytropapps rhinocerotis* (Meadows, 1998).

*SA* – South Africa.

*Saline* – Salinity similar to or greater than seawater (TDS 20-50 g/kg) (Drever, 1997).

*Salinity* – This term is used in a similar way to TDS to describe the total quantity of dissolved salts in water (Drever, 1997; Parker, 1989).

*Solonetzic soils* - Thin porous topsoil underlain by a columnar, usually sodic horizon (Lambrechts, 1981).

*SPE* – Saturated paste extract. An analytical method for obtaining a representation of salts in a soil solution (Rhoades, 1982).

*Stokes' surface* – Flat floor of a pan, which defines the top of the capillary zone (Warren, 1999).

*TDS* – Total dissolved solids.

*Thalassic* – Coastal pans, either in direct continuity with the sea, or blind or residual estuarine embayments (Seaman *et al.*, 1991).

*Throughflow* – Lateral subsurface flow of infiltrated water through the soil down a slope (Schloeman, 1994).

*TISAB* – Total ionic strength adjustment buffer.

*UCT* – University of Cape Town.

*Vadose zone* – Unsaturated zone between the ground surface and the water table (Whitten and Brooks, 1972).

*Veld* – Open country, grassland, grazing land, non-urban land (Branford, 1987).

*Vlei* – Lake, swamp (Branford, 1987).

*XRD* – X-ray diffraction.

# 1. Introduction and Literature Review

## 1.1. INTRODUCTION

### 1.1.1. MOTIVATION

Small closed basins, or pans (Goudie, 1991) are important sources of water and salt for humans and animals in semi-arid to arid areas (Shaw and Thomas, 1989). Of all inland surface water in the world, almost half is found in water bodies occupying closed basins. Salt lakes are found on every continent, including Antarctica, and are an important component of the hydrological cycle (Williams, 1996). In many areas, pans are mined for salt (Shaw and Thomas, 1989). Pans are an integral part of the South African landscape, with pan density reaching 1.14 pans per $km^2$ in some areas (Goudie and Thomas, 1985; Figure 1.1). They are found in the more arid north-central to western areas of the country where evaporation exceeds precipitation. Pans can be a potential source of surface water but they are generally saline (total dissolved salts (TDS) 20-50 g/kg) and often associated with brackish (TDS 1-20 g/kg) to saline groundwater (Goudie and Thomas, 1985).

The coastal lowlands of the Western Cape Province, South Africa (SA) are semi-arid, receiving between 150 and 500 mm of rain per annum. Salt pans are a common feature of the coastal lowland areas. Some of the pans have been exploited for salt since the time of Jan van Riebeeck ($17^{th}$ century), the country's first colonist, and probably by indigenous people long before that (Hugo, 1974). Expansion of the Cape Town metropolis along this dry coastline places increasing pressure on the scarce water resources of the area. The establishment of industrial nodes at Atlantis and Saldanha Bay, north and south of Darling, has been hampered by a lack of water. Developments in the Saldanha Bay area receive water from the Berg River, over 30 km away, and the town of Atlantis relies on groundwater supplemented by artificial recharge (Figure 1.2). Groundwater is currently the main source of water for farmers and many of the small towns on the coastal plain.

Pans are accumulators and concentrators of salts, and provide a record of inputs from the catchment, including any hazardous elements. Both worldwide and in SA there is a shortage of information on the potentially harmful constituents of saline water bodies (Williams, 1996). Man-made saline pans are a common way of disposing of industrial and agricultural brines.

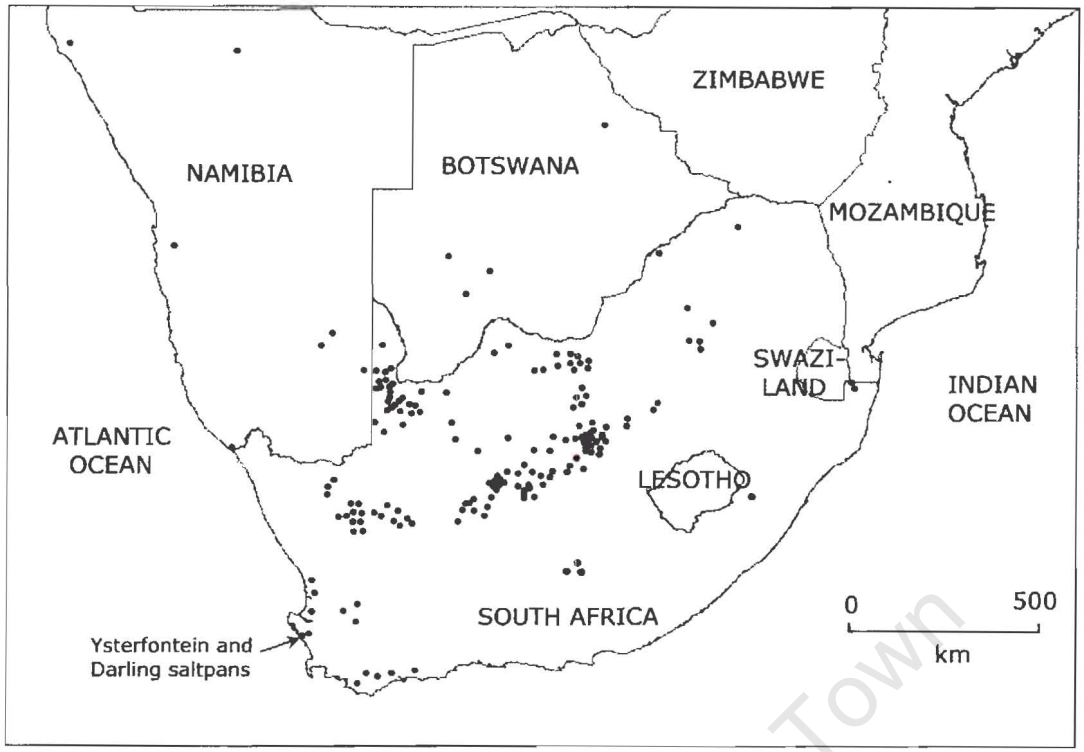


**Figure 1.1: Distribution of pans in Southern Africa. Each point may represent more than one pan. Study area indicated (adapted from Seaman *et al.*, 1991)**

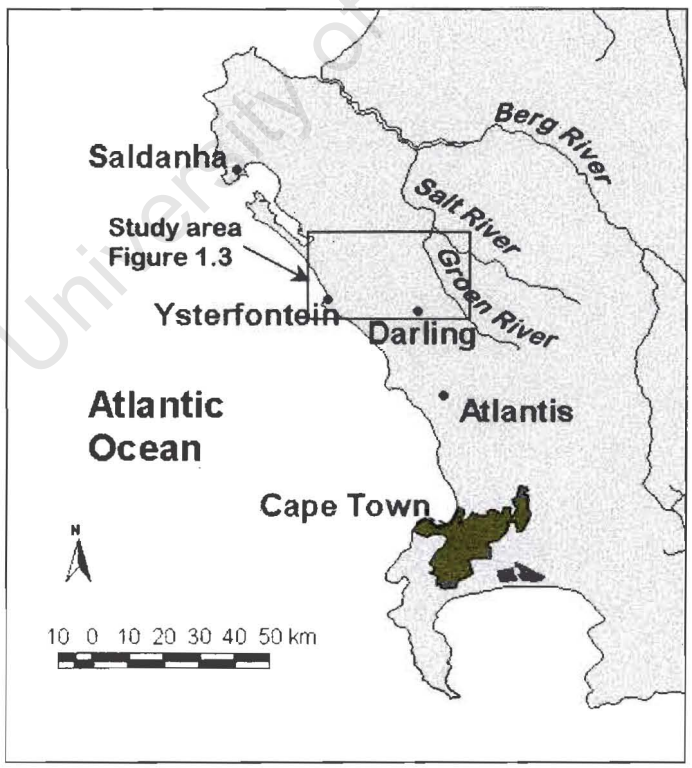


**Figure 1.2: Location of the study area, showing main towns and rivers of the coastal lowlands**

Only recently have the negative effects of these brines been seen, with the death of many birds in the USA at the Kesterson Reservoir in the San Joaquin valley (Tanner *et al.*, 1999). Agricultural drainage water enriched in selenium was used for the management of the Kesterson Reservoir wetlands. The deaths of the birds has been attributed to bioaccumulation of selenium in brine shrimp. Studying the accumulation and bioavailability of trace elements in natural systems will aid understanding of their behaviour in artificial systems. Trace element studies will also enable more accurate pinpointing of the origin of salts.

### 1.1.2. Objectives

Although the Darling and Ysterfontein salt pans have been studied as a salt resource, no comprehensive geochemical study has been undertaken. Most work on saline pans in South Africa mentions the Darling and Ysterfontein saltpans, but there is no study specifically of pans in the area. The most comprehensive information concerning the pans is Hugo (1974), but they are also mentioned in Visser and Schoch (1973), Seaman *et al.* (1991), Goudie and Thomas (1985), Day (1993) and Silberbauer and King (1991). The location of the pans and regional geology are shown in Figure 1.3. The aim of this study is to investigate the origin of salts in the pans by studying the geochemistry of subsurface water, pan water, sediments and soils in the area. The following questions will be addressed:

- What is the origin of salts in the brines?
- What are the relative contributions of groundwater, rain and surface water to the pans?
- Are there potentially harmful trace elements in the salt pans?
- Do the Darling saltpans fit the model of brine evolution proposed by Hardie and Eugster (1970), which states that the chemistry and mineralogy of saltpans is determined by the composition of dilute inflow waters?

### 1.1.3. Description of the study area

*Topography and drainage*

The northwest trending Darling Hills rise up to an altitude of about 300 m above the surrounding lowlying and undulating plain (Figure 1.4(a)). To the west of the hills is a short flat coastal plain, the Sandveld, and to the east an extensive plain interrupted occasionally by granite hills, the Swartland. The Swartland is known as hillocky veld (grassland) because of the occurrence of large termite mounds locally known as *heuweltjies* (small hills). The termite mounds are clearly visible on aerial photographs even though ploughed by farmers.

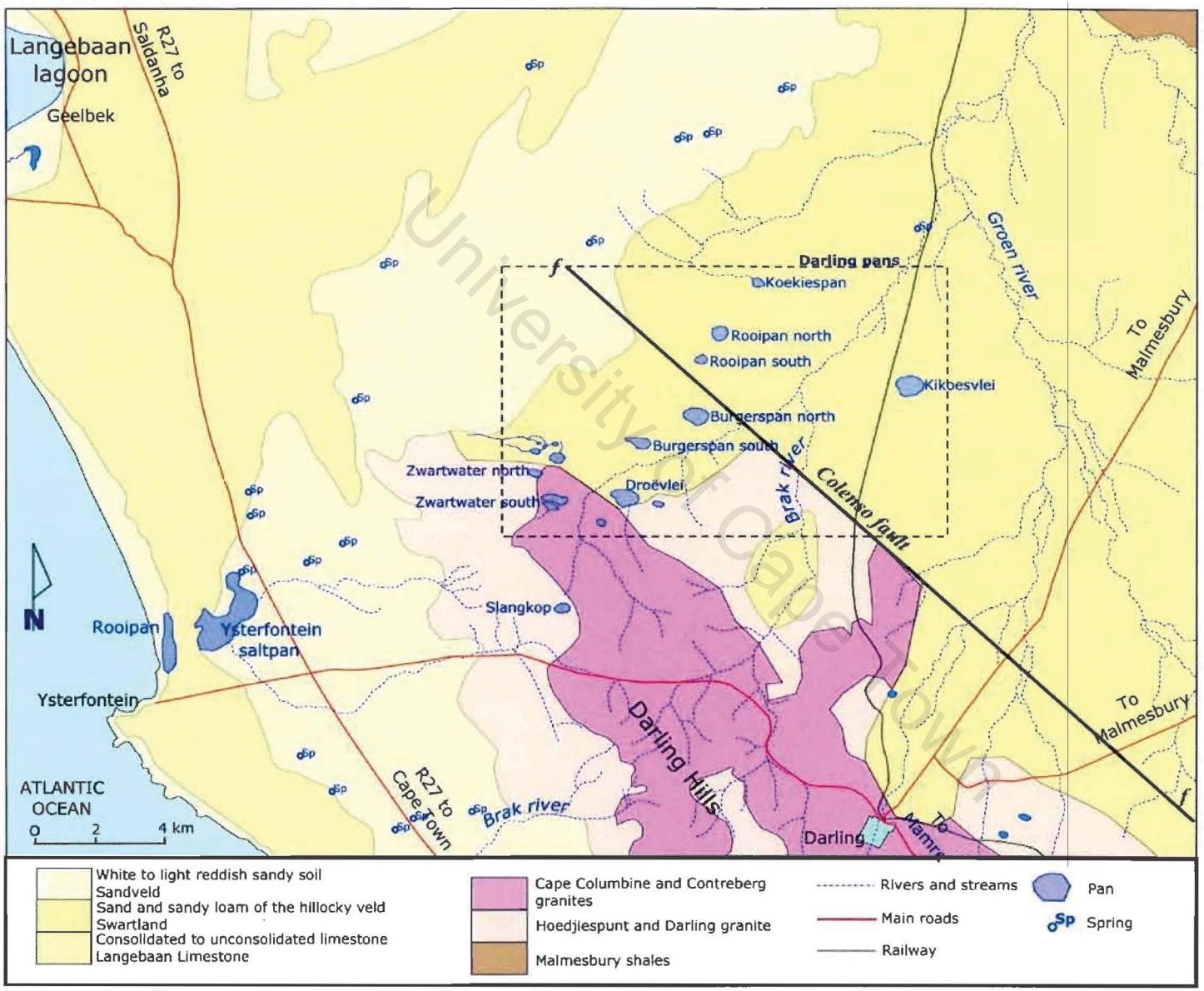


**Figure 1.3: Map of study area showing geology, drainage and pan locations (adapted from Geological Survey, 1972)**

On the western side of the hills a few short streams drain perpendicular to the coast and flow across the Sandveld into the Atlantic. Drainage on the Sandveld is poorly developed due to the high permeability of soils, and low annual rainfall. There are, however, many springs on the Sandveld. To the east, streams drain into the Groen River, which drains northwest into the Salt River, which itself empties into the Berg River, a major river on the coastal lowlands (Figure 1.2). The Brak River, a tributary of the Groen River, drains the area of the Darling pans. Most of the smaller tributaries of the Groen River are ephemeral. In the rainy season they contain fresh water, but in summer only stagnant pools are present, and groundwater is close to the surface. Ysterfontein and Rooipan saltpans, to the west of the Darling Hills, are proximal to the sea. A number of ephemeral streams flow into Ysterfontein saltpan from the Sandveld, but a ridge of calcified dune sand prevents outflow (Visser and Schoch, 1973).

*Climate*

The coastal lowlands experience a moderate Mediterranean climate. Summers, from October to March, are hot, dry and windy, the prevailing summer wind arriving from the south. Cold fronts bring rain in winter, between April and October. The winds associated with fronts are north- and south-westerlies (Visser and Schoch, 1973). The Darling Hills experience greater rainfall than the surrounding plains (Figure 1.4(b)). Darling has an average annual rainfall of about 500 mm, Malmesbury 450 mm and Ysterfontein 330 mm. The rainfall generally decreases to the north, and increases inland (Nieman, 1981).

The cold Benguela current moderates temperatures along the west coast. Temperature increases inland and there is an abrupt change in climatic conditions a short distance away from the sea. Warm, dry berg winds are generated when air drawn off the plateau by a southwards moving offshore low-pressure cell is compressed and heated. During berg wind conditions, transpiration and evaporation are high (Nieman, 1981). In summer, arid conditions exist between Cape Town and the mouth of the Olifants River and evaporation is exacerbated by the wind. Potential pan evaporation varies from 1800 mm per year in the south to 2100 mm per year in the north, and is lowest in June (50-90 mm) and highest in December (280-300 mm) (Nieman, 1981).

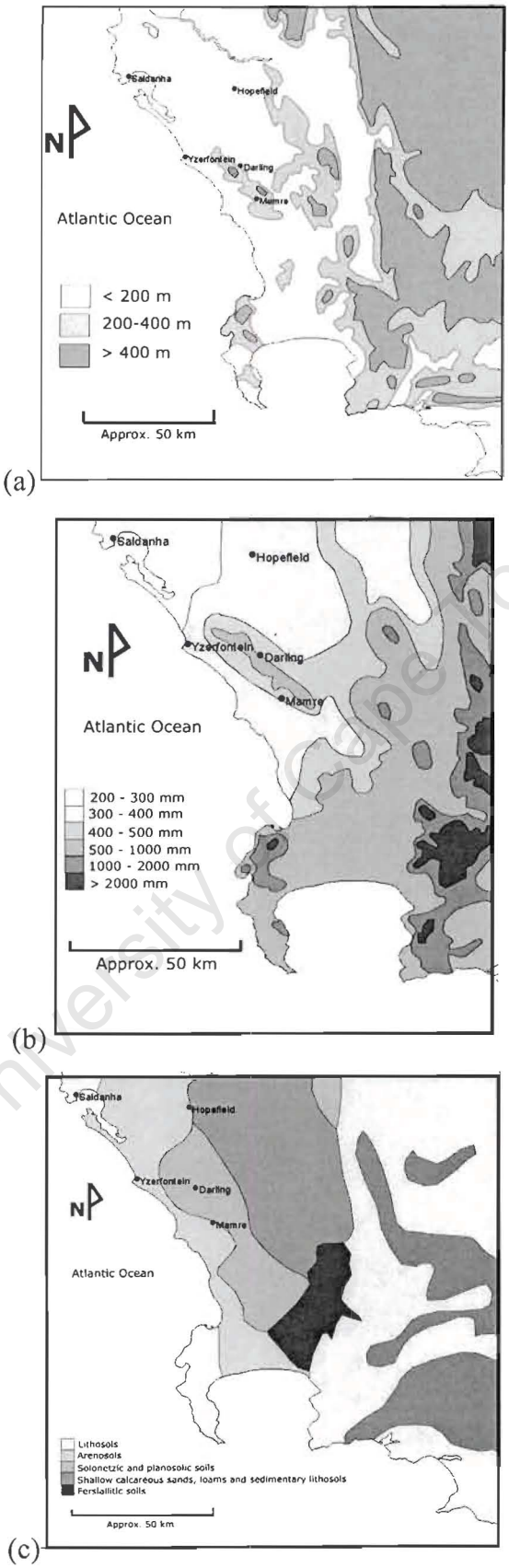




**Figure 1.4: (a) Topography, (b) rainfall and (c) soils of the SW Cape coastal lowlands (adapted from Rogers, 1981, Lambrechts, 1981, Nieman, 1981)**

*Geology*

The Darling Hills are a series of intrusions of Cape Granite into older Malmesbury Group meta-sediments (Figure 1.3). The intrusions are a component of the Saldania belt, which is part of the approximately 550 Ma Pan-African metamorphic event in South Africa (Scheepers, 1995). Schoch (1975) has identified the Darling Granite as the primary intrusion. This granite has large potassium feldspar phenocrysts, with accessory andesine, biotite (sometimes chloritised), cordierite, apatite and clinozoisite. A hybrid granodiorite has formed where Darling Granite reacted with Malmesbury country rocks. It consists of plagioclase, cordierite, biotite and quartz. Schoch (1975) identified a transition zone of porphyritic biotite-rich granite between the Darling Granite and the hybrid granodiorite.

The Malmesbury Group west of the Colenso Fault is part of the Swartland Terrane, and consists of mica schists, fine-grained quartzites, and quartz schists with dolomite and limestone lenses. These sediments have been interpreted as forming in a sea-shelf environment (Hartnady *et al.*, 1974). In the Groen River valley the Malmesbury sediments are deeply weathered and overlain by thick sands (Schoch, 1975). The Groen River depression is postulated to have formed during the Quaternary when a lowering of the erosion base led to active incision to below current base level (Van Niekerk, 1967). A rise in the sea level during the late Pleistocene resulted in the Groen River valley being filled with alluvial and colluvial sands up to 60 m deep (Timmerman, 1986). To the west of the Darling Hills a succession of Cenozoic sediments overlies the deeply weathered Malmesbury Group. Four formations have been identified in this succession, the Elandsfontyn, Saldanha, Varswater and Bredasdorp Formations (Rogers, 1982). The stratigraphy, environment of deposition and ages of the formations are summarised in Table 1.1.



**Table 1.1: Stratigraphy, environment of deposition and age of formations deposited during the Cenozoic near Ysterfontein (from Rogers, 1982)**

| Formation | Environment of deposition | Probable age |
|---|---|---|
| Bredasdorp | Inner shelf – beach – barrier dune – dune plume | Early Pleistocene - Holocene |
| Varswater | Inner shelf and estuary | Early Pliocene |
| Saldanha | Beach and lagoon | Late Miocene |
| Elandsfontein | Meandering fluviatile environment in tropical to subtropical climate | Miocene |

*Soils*

Regional soil distribution is illustrated in Figure 1.4 (c). Swartland soils are shallow calcareous sands and loams, and sedimentary lithosols (shallow soils containing rock fragments, with occasional bedrock exposure). The soils on the granite hills are solonetzic or planosolic. Solonetzic soils consist of thin porous topsoil underlain by a columnar, usually sodic horizon, while planosolic soils have leached surface horizons underlain by clay pans or fragipans (Lambrechts, 1981).

Schloeman (1994) completed a study on the geochemistry of a variety of soils in the Darling area. He grouped soils based on underlying material, for example deep sandy soils derived from recent coastal sands and soils derived from unconsolidated sands of granitic origin. The unconsolidated sands of granitic origin occur between the Darling batholith and the Groen River (Schloeman, 1994).

*Geohydrology*

There are two important aquifers on the coastal lowlands north and west of the Darling Hills – a primary unconfined aquifer in unconsolidated surface sediments of the Bredasdorp Formation and a primary confined aquifer in the sands and gravels of the Elandsfontyn Formation. The two aquifers are separated by an aquitard of clay. These aquifers are recharged by the infiltration of precipitation (Department of Water Affairs and Forestry (DWAF), 1993a).

East of the Darling Hills a primary unconfined aquifer is expected in the alluvial material in the Groen River valley. A thick layer of clay, probably weathered Malmesbury Group sediments, forms a barrier between the primary unconfined aquifer and a secondary aquifer in fractured bedrock (Timmerman, 1986; Visser and Schoch, 1973). Regional groundwater is fresh to brackish, with electrical conductivities (EC) between 1 and 12 milliSiemens/cm (mS/cm) and chloride concentrations greater than 7 mmol/l (Timmerman, 1986). Timmerman (1986) attributes poor groundwater quality and salt in pans to slow movement of groundwater away from the greater flow gradient of the hilly terrain, and connate marine waters remnant from marine transgressions. The conductivity of groundwater increases downslope and is maximum in low points like pans (John Weaver, Geohydrologist, CSIR, pers.comm., June 2000).

*Land use and vegetation*

The Swartland and Sandveld areas are major grain and stock-production areas. Prior to 1946, extensive areas of the Swartland were over-utilised for grain farming, resulting in severe soil erosion (Hall, 1981). The Swartland area is currently utilised for winter cereal (mainly wheat) farming. Dairy cattle farming, ostrich farming and gravel mining are the main businesses in the Darling Hills (Visser and Schoch, 1973). The Western Cape coastal lowlands have been neglected in terms of environmental conservation. The area constitutes only 0.7% of South Africa's area, but lays claim to 14% of the critically rare, threatened or recently extinct plant species (Hall, 1981). Only 14.7% of the vegetation remains in a reasonably natural state (Boucher, 1981). The Swartland (Black land) obtained its name from the dark coloured renosterbos (Rhinoceros bush – *Elytropapps rhinocerotis*), which dominates the natural vegetation of the Swartland. Renosterbos is generally associated with nutrient-rich soils derived from Malmesbury sediments. Much of the natural vegetation has been cleared to exploit these nutrients for wheat farming (Meadows, 1998).

## 1.2. PAN FORMATION AND GEOMORPHOLOGY

### 1.2.1. Definition and General Characteristics

Shaw and Thomas (1989, pg.185) define pans as "arid-zone basins of widely varying size and multivarious origin which, although generally above the present groundwater table, are subject to ephemeral surface water inundation, though the periodicity and extent of inundation is highly variable". This definition is broad, and includes no chemical criteria although most pans contain brackish to saline water. Pans are known by different names in different parts of the world, including playa, salt lake and sabkha. Pans either have no connection to the sea i.e. are athalassic, or are coastal, and in direct continuity with the sea and are known as thalassic pans (Seaman *et al.*, 1991).

Pans always occupy topographic lows, and are generally endorheic, i.e. have no surface outflow. Standing water is periodically found in pans, the extent, frequency and duration of its occurrence being determined by climate and hydrology. Groundwater normally plays an important role in pan formation. The surfaces of pans are often flat and vegetation-free. Sedimentation and erosion both occur in pans. Sediments can be aeolian, fluvial, colluvial, or precipitated as evaporites directly or through microbial mediation. Erosion is primarily through wind deflation (Shaw and Thomas, 1989). A lunette dune is often found on the

downwind shore of the pans, generated by deflational processes. Pans in South Africa are generally small (diameter < 5 km) and seasonally ephemeral (Seaman *et al.*, 1991).

### 1.2.2. PAN FORMATION

There is considerable debate over the mechanism of pan formation. Several processes contributing to the continued existence of pans have been identified, but it is still uncertain what initiates the formation of a pan.

*Requirements for formation*

According to Marshall and Harmse (1991), two basic requirements, apart from an arid environment, need to be satisfied in order for a pan to form. Firstly, the substratum must be susceptible to easy weathering, and must contain a high proportion of leachable salts (Marshall and Harmse, 1991). The substratum is either already unconsolidated or it will easily break down to fine-grained material. Susceptible surfaces typically have a low-angle surface that encourages ponding and limits drainage development (Shaw and Thomas, 1989). In South Africa, pan distribution corresponds to rock and sediment types with most pans on Kalahari sands, and Dwyka tillites and Ecca shales of the Karoo Supergroup (Goudie and Thomas, 1985). Secondly, there must be a mechanism for the disruption of drainage such as river piracy, climatic desiccation, tectonic activity or windblown sands blocking rivers (Marshall and Harmse, 1991). Both the Okavango swamps and Magkadigadi pans in Botswana originated when tectonic uplift diverted headwaters and blocked channels (Goudie, 1991). Pans are also common in areas where integrated drainage systems do not easily develop, for example on very flat, semi-arid land, and in dune systems, where sand is constantly migrating (Shaw and Thomas, 1989).



Pans commonly form on sections of abandoned or choked drainage systems in topographically low areas where rain or surface flow will tend to pond (Goudie, 1991). As the pans deepen, the original watercourses no longer support outflowing water due to the ponding effect of the pans. During drought, the bare pan floors are susceptible to wind erosion, and there is a net removal of sediment (Hugo, 1974). It has been shown that many of the pans in the Northern Cape and Free State Provinces of South Africa formed on relict drainage systems (Goudie, 1991). Pans often exploit geological weaknesses, like joints and dykes. These structures also have a strong control on normal drainage. Subsidence in an area underlain by limestone can also focus pan formation (Marshall and Harmse, 1991).

*Pan maintenance*

Once a pan has formed there must be an ongoing mechanism to maintain it, referred to as maintenance. A number of processes interact to ensure the pan is not obliterated by infilling, namely salt weathering, erosion by animals and deflation. Most pans will be propagated by a combination of processes (Marshall and Harmse, 1991).

Ponding water will evaporate in an arid to semi-arid environment, increasing in salinity and precipitating salts (Marshall and Harmse, 1991). Salts precipitating in cracks of rocks and boulders can build up substantial pressure, leading to cracking and flaking. Changes in volume of crystals can occur by hydration/dehydration and thermal expansion (Goudie, 1989). Salt weathering produces sand and mud-sized material that can easily be blown away, so increasing the size and depth of a pan. A high concentration of salts will also inhibit plant growth that might otherwise prevent soil erosion (Shaw and Thomas, 1989).

Animals are attracted to pans as a source of water in an otherwise water-scarce environment, as well as for salt-licks. By trampling the ground they loosen material, which can subsequently be eroded by the wind. The animals also carry away a substantial amount of mud on their hooves and bodies and they damage vegetation. In the past, herds of tens of thousands of animals were observed at watering holes and they may have played a major role in pan formation and development (Marshall and Harmse, 1991; Verhagen, 1991; Alison, 1899).

Deflation is the removal of material from the pan by aeolian processes. It has been proposed as the main agent of pan formation and maintenance, but it does not adequately explain pan genesis or why pans persist in one location (Verhagen, 1991). Deflation is thought to form lunette dunes downwind of the pan by accretion of windblown fine-grained sand and mud aggregates produced in the pan by desiccation. The size of the dune is a function of the basin size and morphology, and the rate at which sediment is supplied. Some pans have more than one dune due to a change in the palaeoenvironment (Shaw and Thomas, 1989).

Groundwater seepage usually occurs around pan edges because a clay layer or evaporites in the pan centre act as aquitards. In most saltpans, the surface of the brine can be considered as an expression of the regional water table. A permanent pan indicates that groundwater is constantly discharging. The water table and thickness of the capillary zone vary seasonally.

As the water table rises, the vadose (unsaturated soil) zone that was previously dry becomes saturated and the hygroscopic effect of capillary water prevents further erosion. A falling water table will expose sediment to erosion. Deflation can only erode to the level of the water table, forming a flat surface known as a Stokes' surface (Warren, 1999).

*Models of formation*

Many authors subscribe to the saline pan cycle theory (e.g. Warren, 1999; Lowenstein and Hardie, 1985). This is divided into three stages, the flooding stage, the evaporative concentration stage and the desiccation stage (Figure 1.5). During the flooding stage a temporary shallow brackish lake less than 1 m deep forms by ponding of dilute meteoric waters (Lowenstein and Hardie, 1985). The fresh water overlies a lens of saline interstitial water (Warren, 1999). The saline crust that covered the dry surface prior to flooding is partially dissolved and fine-grained clastic sediments are deposited in a thin layer. The dilute inflow gradually becomes more saline by evaporative concentration (Lowenstein and Hardie, 1985). Surface water is only present in a pan at certain times of the year, normally directly after rainfall or during the rainy season. The presence of surface water provides an environment in which organisms like diatoms and algae can survive (Shaw and Thomas, 1989).

During the evaporative concentration or saline lake stage, the shallow water is concentrated by evaporation until it reaches saturation with respect to evaporite minerals, like halite or gypsum (Lowenstein and Hardie, 1985). Further meteoric influx during this stage will form a layer of fresh water overlying the denser brine, and the lake will be stratified. The new fresh water will slowly increase in salinity by evaporation until it is equal in density to the underlying brine. Mixing then occurs. Brines can also become thermally stratified (Warren, 1999).

Eventually the lake dries out completely and enters the desiccation or playa stage (Lowenstein and Hardie, 1985). The dense residual brine will infiltrate into the sediments to replace lost pore water. These brines are not in chemical equilibrium with the surrounding sediments and can react with them. With a prolonged wet spell, the water table will rise up again and form a brine that is the surface expression of the water table, but more saline because of brine infiltration (Warren, 1999). This brine continues to be concentrated through capillary evaporation. When the pan is dry, the water table drops deeper by capillary

evaporation (Warren, 1999). With a new flooding event, the cycle starts again. This cyclical sequence results in recognizable facies in ancient evaporite deposits (Lowenstein and Hardie, 1985).

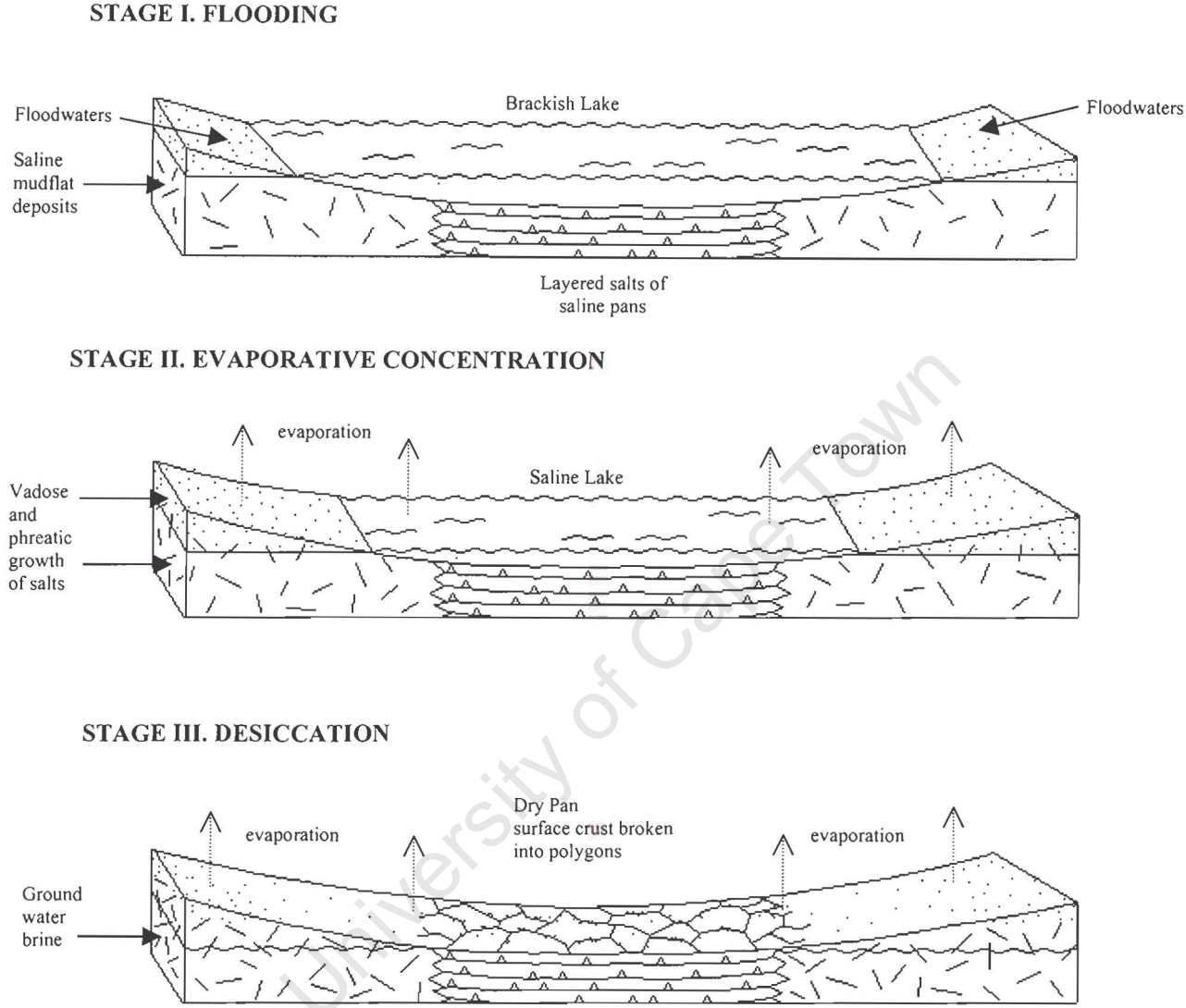


**Figure 1.5: Summary of the basic elements of the saline pan cycle (after Lowenstein and Hardie, 1985).**

Verhagen (1991) has developed an ecological model to explain pans in the Kalahari. This model comes the closest to incorporating the various aspects of pan formation and maintenance. Isolated depressions, formed by disrupted drainage, collect seepage and runoff waters. Clay collecting at the base of the depression will form a locally impermeable zone that prevents water infiltrating rapidly. Perched water tables form below the pan floor as calcretes form local aquitards. The water attracts animals, even in dry periods because water is just below the surface. Animals degrade grass and vegetation in areas where they gather, resulting in excavation and deflation. As the water becomes more saline due to evaporation, animals move on to a new site, and the vegetation slowly recovers. The increase in

vegetation results in more acid waters (increased $pCO_2$, and humic acids), and the calcrete begins to be dissolved. The saline, perched aquifers dissipate, and the pan becomes less saline. When animals return to the hole after their new site has become too saline, the cycle begins again (Verhagen, 1991).

## 1.3. GEOCHEMISTRY OF PAN WATERS AND SEDIMENTS

### 1.3.1. DEFINITION OF SALINITY

Table 1.2 summarises terms used in this study to describe levels of salinity.

**Table 1.2: Definition of terms describing water salinity (adapted from Drever (1997) and Hammer *et al.* (1983))**

| Term | TDS range | Description |
|---|---|---|
| Fresh | <1 g/L | Sufficiently dilute to be potable |
| Brackish | 1-20 g/L | Too saline to be potable but significantly less saline than seawater |
| Saline | 20–50 g/L | Salinities similar to or greater than seawater |
| Brine | >50 g/L | Significantly more saline than seawater |



### 1.3.2. CHEMISTRY OF INFLOW WATERS

The solutes in the dilute inflow into a pan will determine the final composition of the brine, and the mineralogy of the sediments (Eugster, 1980). Solutes originate from a number of sources, and physical processes in the catchment modify the inflow water (Eugster, 1980; Figure 1.6). Salts that originate as sea spray or vapour (cyclic salts) can be deposited by rain in the pan or catchment (Hugo, 1974) resulting in a brine composition similar to the sea. Connate salt originates as saline water trapped in sedimentary rocks that formed in a marine environment, or from the weathering of rocks (Hugo, 1974). Another theory is that the salt is a remnant of seawater isolated in basins following a marine regression and evaporated to dryness (Herczeg and Lyons, 1991). The composition of inflow waters is influenced by the minerals present in the watershed (Eugster, 1980). Reactions and interactions occurring in the ground and the soil zone before the water enters the pan contribute ions to the water (Herczeg and Lyons, 1991).

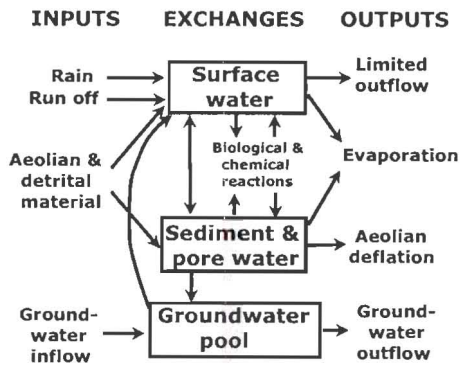


**Figure 1.6: Physical processes affecting the chemical composition of surface and groundwaters in an arid internal drainage basin (from Herczeg and Lyons, 1991)**

### 1.3.3. BRINE CHEMISTRY AND EVOLUTION

*Fractional crystallisation*

The chemistry of a brine is determined by the chemistry of the inflow waters (Eugster, 1980). The inflow waters are concentrated by evaporation until minerals become saturated. As the minerals precipitate out of solution, certain elements are removed from the brine, and remaining elements are residually enriched. This fractionation causes inflow waters of varying chemical composition to all tend towards a similar end product (Eugster and Jones, 1979). Fractional crystallisation implies that once minerals have crystallised, they no longer interact with the brine (Harvie *et al.*, 1980).

Inflow waters all have six primary ions, Na, Mg, Ca, Cl, $SO_4$, and $HCO_3$. The relative proportions of these ions will determine how the brine evolves, according to the Hardie-Eugster model (Figure 1.7). Mineral precipitation causes chemical divides, points at which the brine composition can evolve along a new trend. Elements that behave conservatively throughout the precipitation process will be enriched in the final product. The initial pathway depends on the ratio of bicarbonate to alkali-earth metals. Calcite ($CaCO_3$) is normally the first mineral to reach saturation and precipitate, and therefore defines the first chemical divide. The pathways are described below:

- **Pathway I**: $HCO_3 >> Mg + Ca$.

  Low Ca concentrations limit the amount of calcite that can precipitate. Magnesium is incorporated into high-Mg calcite and dolomite. Once Ca and Mg are depleted, a Na-$CO_3$-$SO_4$-Cl brine remains. The sulphate can be reduced and degassed as $H_2S$, leaving a Na-$CO_3$-Cl brine, as seen at Lake Magadi, Kenya.

➢ **Pathway II**: $HCO_3 << Ca + Mg$

In these waters, Ca concentration usually exceeds Mg concentration. Calcite precipitates. There is now enough Ca remaining to allow gypsum ($CaSO_4 \cdot 2H_2O$) to precipitate, generating another chemical divide. If Ca is the limiting element, then a Na-$SO_4$-Cl brine will form, such as Death Valley. If $SO_4$ is the first ion to be depleted, a Ca-Na-Cl brine will form, for example Bristol Dry Lake.

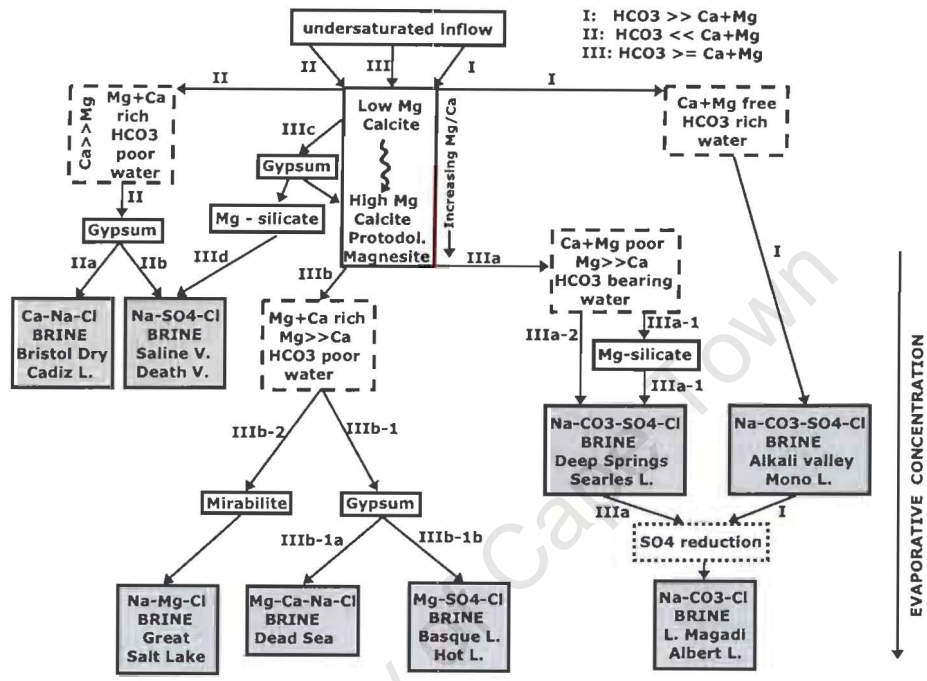


**Figure 1.7: Brine evolution flow diagram, showing critical precipitates (solid rectangles), transitional chemical criteria (dashed rectangles), processes (dotted rectangles) and resulting brines (shaded rectangles). Starting chemical criteria are indicated at top right (from Eugster, 1980).**



➢ **Pathway III**: $HCO_3 \geq Ca + Mg$

This pathway is fairly complicated as there are three possible routes after the precipitation of calcite. Firstly, it could follow a route similar to pathway II by precipitating gypsum, and then a Mg-silicate or carbonate to use the remaining high in solution. Secondly, as calcite precipitates, magnesium is relatively enriched in solution, and high-Mg calcite, aragonite, and dolomite ($CaMg(CO_3)_2$) are precipitated. Following extensive carbonate precipitation the solution is depleted in Ca relative to Mg, and could evolve in 2 ways. If the solution remaining after calcite precipitates has more Mg and Ca than bicarbonate, then either gypsum or mirabilite ($Na_2SO_4 \cdot 10H_2O$) will precipitate, resulting in one of three possible brines – Na-Mg-Cl (e.g. Great Salt Lake), Mg-Ca-Na-Cl (e.g. Dead Sea) or Mg-$SO_4$-Cl (e.g. Basque Lake). A solution with more bicarbonate

than Ca and Mg will form a Na-$CO_3$-$SO_4$-Cl brine, as in Searles Lake. The sulphate can be reduced to form a sulphate-depleted brine (Warren, 1999; Eugster and Jones, 1979).

Mineral precipitation has always been seen as the main process by which the brine composition is changed, but there are a number of other processes occurring in and around pans:

- Degassing of $CO_2$ at springs affects the pH of water, and can result in precipitation or dissolution of minerals (Drever, 1997).
- Precipitation of salts such as calcite and gypsum, causing a change in ionic ratios of water (Herczeg and Lyons, 1991).
- Ion exchange and sorption reactions in the soil zone. Cation ratios in groundwater will change due to different exchange affinities, for example Na will enrich relative to Ca because calcium will be preferentially sorbed onto exchange sites (Herczeg and Lyons, 1991).
- Redox reactions in the saturated soil zone and pan sediments will mainly affect iron and sulphur. In reducing environments sulphur is immobilized while iron becomes more mobile (Herczeg and Lyons, 1991).
- Congruent dissolution of efflorescent crusts. Congruent dissolution occurs when a mineral is completely dissolved (Eugster, 1980). The most soluble minerals in the crust will dissolve first, influencing the major and minor element concentrations of the brine (Herczeg and Lyons, 1991).
- Rock weathering by incongruent dissolution of silicate minerals i.e. the mineral reacts with water to form a new mineral, in the process releasing ions into solution. These reactions often affect feldspars, altering the feldspar to a clay mineral and releasing base cations (Eugster, 1980). Rainwater on its own is not very aggressive but $CO_2$ dissolution in the soil zone decreases the pH and the water can weather more aggressively (Herczeg and Lyons, 1991).

*Equilibrium crystallisation*

Equilibrium crystallisation differs from fractional crystallisation in that precipitating minerals continue to interact with the brine, remaining in equilibrium with the brine (Harvie *et al.*, 1980). The mineral sequence and quantities precipitated in this situation differ from those in fractional crystallisation. This process is more likely to occur when fresh water flows into a pan with a standing body of water than if water flows into a dry pan (Harvie *et al.*, 1980).

Similar processes occur during the desiccation stage of the saline pan cycle, when the remaining dense brine seeps into the pore space of the sediment, and begins to equilibrate with minerals that were precipitated earlier on in the evolution of the brine. This process is known as back-reaction. Back-reaction can occur at the sediment-brine interface and within shallow subsurface brine plumes (Warren, 1999). An example in a seawater system is anhydrite ($CaSO_4$) and gypsum ($CaSO_4 \cdot 2H_2O$) back-reacting with the brine to form glauberite ($CaSO_4 \cdot Na_2SO_4$) and polyhalite ($2CaSO_4 \cdot MgSO_4 \cdot K_2SO_4 \cdot 2H_2O$). The residual brine composition is changed, and new minerals are formed. The new minerals are often compound salts (Warren, 1999).

### 1.3.4. Evaporite, sediment and soil chemistry

*Evaporites*

Evaporites are often zoned around a pan, with the most soluble minerals found in the centre. Carbonates are one of the most abundant products in closed basins. In ephemeral saltpans they are found in the mud flats surrounding the pan where the water is still sufficiently dilute to precipitate Ca- and Mg-carbonates through capillary evaporation (Eugster, 1980). Springs are associated with carbonate precipitates, where the groundwater degasses $CO_2$ and becomes supersaturated with respect to carbonate minerals like calcite (Eugster, 1980). Evaporite crystals precipitating in the sediment cause lateral expansion until the surface of the pan cracks into polygons. Evaporation can occur through the cracks, resulting in the development of a spongy efflorescent crust in the cracks, ultimately pushing up the polygon edges, which become rimmed with ridges of salt. With flooding, dilute inflow water dissolves much of the salt, forming a flat upper surface. A layer of detrital mud settling out of suspension will cover the surface and prevent further dissolution (Lowenstein and Hardie, 1985).

Vertical mineral zonation is also observed, with more soluble minerals closer to the surface due to capillary evaporation. Brine in the sediments is often stratified because the upper layer is subject to capillary evaporation. It becomes denser than underlying water, but there is no tendency for mixing or overturning because of the inhibiting effect of the sediments. Evaporites can be precipitated on the pan surface as a thin monomineralic bed, or interstitially within the sediments (Eugster, 1980). Reactions can occur in the sediment after minerals are deposited, forming double or triple salts and hydrated minerals (Eugster, 1980).

*Sediments and soils*

Soil can form on the various sedimentary inputs, namely aeolian, fluvial and colluvial sediments. Pedogenic processes in pans are regulated by intermittent wet and dry conditions. Little work has been done on the chemistry of sediments underlying pans in South Africa. A review paper by Verster *et al.* (1992) focussing on soils, unconsolidated sediments and duricrusts associated with South African pans concluded that the soil type and chemistry is controlled by the climate, in particular the availability of water and the length of time that the pans are inundated (Table 1.3).

**Table 1.3: Characteristics of pan soils in different climatic regimes in South Africa (after Verster *et al.*, 1992)**

| Climatic regime | Sub-humid to humid | Semi-arid | Arid |
|---|---|---|---|
| **Soil type** | Katspruit | Katspruit | Katspruit/Oakleaf |
| **Soil characteristics** | Gleyed | Gleyed | Gleyed subsoil |
| **Organic matter** | High | Low | Low |
| **Clay content** | High (42%) | Medium (22-54%) | Medium (24%) |
| **EC** | Moderate | Moderate-high | Extremely high |
| **Exchangeable cations** | High $Mg^{2+}$ | Very high conc. | Normal conc. |
| **Clay minerals** | Mica, kaolinite, smectite | Interstratified illite-smectite, kaolinite, sepiolite, palygorskite, quartz, glauconite | Mica, illite-smectite, kaolinite, palygorskite, thenardite, glauconite |
| **Duricrust** | Ferricrete | Ferricrete/calcrete | Calcrete |

Higher concentrations of salts were always found near the pan surface than in the underlying sediments. Although pans often occupy ancient geomorphic surfaces, the soils, duricrusts and sediments found associated with them are usually younger features (Verster *et al.*, 1992).



## 1.4. SUMMARY

Saltpans are complex chemical systems involving interactions of groundwater, surface water and sediments. Although it is not yet fully understood how pans form, it seems likely that drainage disruption on flat surfaces prone to chemical weathering in arid to semi-arid areas leads to ponding of water. Once water ponds, there is a chance for a pan to form. The depression can be made deeper by salt weathering, animal erosion and wind deflation. Pans display cyclical changes due to short-term seasonal variations in rainfall and temperature. The saline pan cycle describes stages of flooding, evaporation and desiccation that are governed by water availability.

The salts in saline pans can be connate, cyclic, or originate as weathering products of the rocks in the catchment. Water from the catchment can be modified by a number of processes before it enters the pan, namely ion exchange, redox reactions and mineral precipitation or dissolution. Water in pans evolves chemically as it is concentrated by evaporation. Mineral precipitation resulting from evaporative concentration removes elements from the brine at different rates depending on their relative concentration in the brine, resulting in a change in solute composition. The Hardie-Eugster model proposes that the final composition of all brines is determined by the composition of the dilute inflow water.

Pans in South Africa have been considered in terms of geomorphology and basic water chemistry. Few pans have been studied in detail and little work has been done on sediments in pans, or on the pathways followed by trace elements in brines. In this study the sediments and brine composition of the Darling and Ysterfontein salt pans will be investigated.

# 2. Sampling

## 2.1. SAMPLING RATIONALE AND NAMING CONVENTION

Sampling was completed over 4 days at the end of July 2000. The first major rains of the winter season fell in the two weeks prior to sampling, but no rain fell during the sampling period. Prior to the rains there was no surface water in the pans. The pans for sampling were selected from a 1:125 000 geological map (Geological Survey, 1972) based primarily on their proximity to each other, ease of access and similar geology. Pans at higher elevation are close to fresh granite outcrop, whereas lower lying pans are formed on colluvial, alluvial and aeolian granitic material. By limiting the area of the study, it is easier to constrain the variables contributing to pan geochemistry. The geological map differentiates between the pans in the Darling area, noting that some of them contain potentially economic quantities of halite, but others do not. Locally, pans are referred to as "vleis" by farmers if no halite is present, and saltpans if halite is present. A selection of both pan types was sampled to ascertain if they are chemically distinct. Two larger pans adjacent to the coastline were included as they were expected to exhibit a strong marine influence, and to provide a useful comparison for the inland pans. The coastal pans both contain economic deposits of gypsum. Throughout this report, pans are grouped according to type, i.e. coastal, vlei or saltpan. Because of possible confusion that may arise by using these terms, the vleis will be referred to as brackish-saline pans and saltpans as brine-type pans.



Sample names are derived from the pan name abbreviations (Table 2.1) and sample type codes (Table 2.2). An example is ZB-WB1:

- The first and second characters (ZB) refer to the pan from which the sample was collected. Pans without local names are named for the farm on which they are located. If two unnamed pans exist on the same farm, they are named alphabetically from the south. In this case the pan is Zwartwater south, the Z after the farm name, and the B because it is the northerly of 2 unnamed pans on the farm.
- The third and fourth characters (WB) refer to the sample type, in this case subsurface water. W as the third character refers to water samples whereas S would indicate a

sediment or soil sample. Combining the third and fourth letters indicates the exact sample type, as indicated in Table 2.2.

**Table 2.1: A summary of pan abbreviations and characteristics**

| Pan type | Pan name | Abbreviation | Long axis (m) | Short axis (m) | Long axis bearing | Approx. size (ha) | Elevation (mamsl) |
|---|---|---|---|---|---|---|---|
| Coastal | Ysterfontein | YF | 2100 | 270 | 044 | 116 | <5 |
| | Rooipan | RP | 900 | 300 | 358 | | <5 |
| Brackish-saline | Slangkop | SK | 400 | 280 | 098 | 4 | 105-110 |
| | Droevlei | DV | 700 | 450 | 104 | 11 | 70-75 |
| | Rooipan north | RB | 330 | 220 | 100 | 2 | 60-65 |
| | Kiekoesvlei | KV | 620 | 800 | 098 | 16 | 60-65 |
| Brine-type | Zwartwater south | ZA | 660 | 80 | 101 | 4 | 70-75 |
| | Zwartwater north | ZB | 310 | 180 | 097 | 2 | 70-75 |
| | Burgerspan south | BA | 670 | 240 | 096 | 7 | 65-70 |
| | Burgerspan north | BB | 650 | 490 | 096 | 10 | 60-65 |
| | Rooipan south | RA | 380 | 260 | 079 | 3 | 60-65 |
| | Koekiespan | KP | 280 | 160 | 080 | 2 | 55-60 |
| Brackish-saline | Brak River | OT | | | | | |

**Table 2.2: Abbreviations of sample type**

| Sample type abbreviation | Sample type |
|---|---|
| WP | Pan water |
| WS | Spring or seep |
| WB | Subsurface water |
| WR | Stream |
| SS | Sediment/soil |
| SE | Evaporite mineral |
| OT | Other |

Three types of water samples were collected. The surface water of each pan was sampled (except Kiekoesvlei, which was dry at the time of sampling), as well as any visible surface water inputs into the pan, such as streams, seeps, and springs. Water seeping from sediments into pits dug for sediment sampling was also sampled, and is referred to as subsurface water. Subsurface water was not collected at every pan.

The number at the end of the sample name differentiates between samples of the same type taken at different locations in the same pan, for example YF-WB1 and YF-WB2. Sediments were collected from different depths at the same location. The letter following the number

indicates the ordering with depth, for example RA-SS3a overlies RA-SS3b. A sediment sample name with a number but no letter is always a surface sample. Many samples that were collected were not analysed due to time constraints, leading to apparent gaps in the sample names.

## 2.2. WATER SAMPLES

Water samples were collected in 250 and 500 mL polyethylene bottles. The bottles were rinsed with the water to be sampled prior to sampling. Four sub-samples were collected from each site

- 500 mL unfiltered sample
- 250 mL filtered through a 0.45 μm cellulose acetate membrane filter
- 250 mL filtered (0.45 μm) and acidified with $HNO_3$ to maintain metals in solution
- 250 mL unfiltered sample for isotope analysis.

Not all samples were filtered in the field due to time constraints, but all were filtered within 12 hours of sampling. Samples were stored in an icebox until returning to the laboratory, when they were placed in a refrigerator at about 4°C. Measurement of pH was completed in the field with a Radiometer PHM201 portable meter. Salinities were also measured in the field with an Atago Hand Refractometer, which can detect salinities below 10 % NaCl. Some samples had salinities exceeding 10% NaCl, and could not be analysed in the field.

## 2.3. SEDIMENT/SOIL SAMPLES

Pits were dug adjacent to most pans but some were omitted due to time constraints (Koekiespan) and difficulties in digging pits through calcrete (Rooipan north, Burgerspan south). Sediment samples were also collected from the pan centres, from beneath the water. These samples will be referred to as subaqueous sediments. The sediment underlying brine-type pans appeared very similar at all localities and was sampled only once, from Rooipan south. It emitted a smell of $H_2S$, indicating a reducing environment. Sediments adjacent to the pans had noticeable layering, but differences in subaqueous sediments were less distinct. Individual layers were sampled separately. Approximately 1 kg of sediment sample was collected using a shovel and placed in a polyethylene bag. On returning to the lab, part of the sample was air-dried and crushed to <2 mm. If the sample was in a reduced state, a portion

was kept wet in an airtight bag. Sediment colours were classified according to the Munsell soil colour charts (Anon, 1992).

## 2.4. SAMPLING LOCALITIES

### 2.4.1. COASTAL PANS

The coastal pans are much larger than the inland pans. They don't have the classical pan morphology as described in the introduction, but appear to have formed perhaps from lagoons or ancient estuaries. Ysterfontein (YF) saltpan has an irregular shape, with a flat pan floor covered by a shallow layer of surface water (5-10 cm deep) (Figure 2.1(a)). It is rarely completely dry. The pan has been mined on a small scale for halite and gypsum for many years, and much of the pan floor has been disturbed by mining operations. The mine overseer indicated an unmined area for sampling. A photograph of sample YF-SS2b is given in Figure 2.2(a), and sample descriptions in Table 2.3. Shells of *Tomichia ventricosa*, a small (±2 mm long), yellow-orange gastropod, were found in large numbers adjacent on the shores of the pan, and appear to have accumulated through aeolian transport. Shells were subsequently found within some of the sediment samples, along with evidence of bioturbation. A band of halophytic plants are found immediately surrounding the portion of the pan that is usually under water. Depth profiles for sampling sites YF-SS1, YF-SS2 and YF-SS3 give an idea of the distribution of layers across Ysterfontein salt pan (Figure 2.3).

Ysterfontein is separated from Rooipan (RP) by a ridge of calcrete and aeolian sediments of the Langebaan Formation. Rooipan is in turn separated from the sea by a ridge of aeolian sand. Rooipan is about 20% the size of Ysterfontein saltpan, and has a more regular shape, elongated north-south at an angle of about 20° from the coastline. Rooipan has been extensively mined and the floor of the pan is cut into irregular trenches filled with water, separated by ridges of removed overburden. These are clearly visible on Figure 2.1(b) and 2.2(b). Many evaporites, including gypsum, halite and calcite, were found on these ridges, but it is not known if they were *in situ* or have been dug up from below. Sample descriptions are given in Table 2.3.

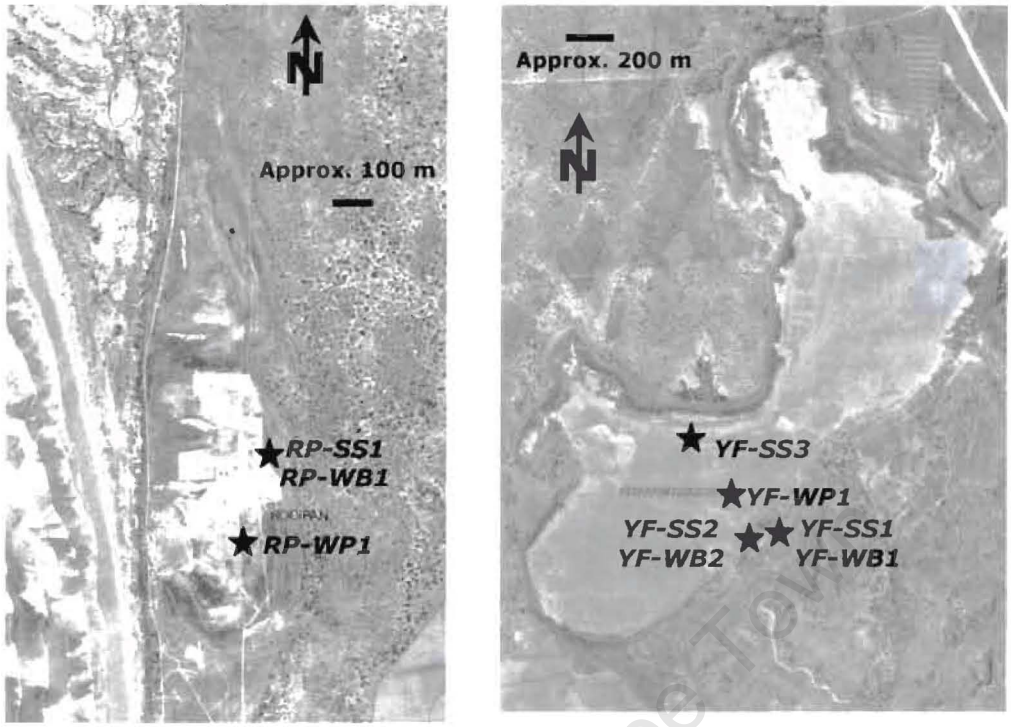


**Figure 2.1: Orthophotos revealing the morphology of and sampling localities at (a) Rooipan and (b) Ysterfontein saltpan.**



(a) (b)

**Figure 2.2: Some features of sampling localities. (a) Sample YF-SS2b – bioturbated blue green gleyed mud with burrows, possibly of *T. ventricosa*. Each chunk is about 10 cm across (b) Rooipan (coast) – note the extremely disturbed nature of the pan.**

**Table 2.3: Descriptions of sediment and water samples collected from coastal pans**

| Sample ID | Description of sample | Munsell colour (Anon, 1992) |
|---|---|---|
| YF-SS1 | Pit dug at edge of Ysterfontein pan, on elevated (20 cm) bench in vegetated zone. Three samples were taken at different depths, a, b and c: | |
| YF-SS1a | Top zone of of fine brown sand with organic detritus. Grades due to bioturbation into underlying white mud. Many shell fragments. Depth 0 – 6 cm | Dry - 2,5Y 6/2 (light brownish grey); Wet - 2,5Y 5/2 (grayish brown). |
| YF-SS1b | White sticky mud. Bioturbated with many *T. ventricosa* shells. Depth 6 – 33 cm. | Dry - 2,5Y 8/1 (white); Wet - 2,5Y 7/2 (light grey). |
| YF-SS1c | Grey brown fine-grained sulphur-smelling sand underlying white mud. Water bearing - water sample (YF-WB1) collected. Depth below 33 cm. | Dry - 10YR 6/2 (light brownish grey); Wet - 10YR 4/2 (dark greyish brown) |
| YF-SS2 | Pit dug on pan floor about 20 m from YF-SS1. Two samples taken at different depths. | |
| YF-SS2a | Mixed bioturbated zone between surface brown sand and underlying green mud. Small granules of sand in fine grained matrix. *T. ventricosa*. Depth 8 - 20 | Wet and dry: 2,5Y 3/1 (Very dark grey) |
| YF-SS2b | Blue green mud directly below YF-SS2a. Contains oyster shells and dark *T. ventricosa* burrows. Depth > 20 cm. | Wet and dry: 5Y 8/1 (white) to 5Y 6/2 (light grey olive) |
| YF-SS3 | Sample intercalated, hard platy gypsum taken from area where mining is currently taking place. Layer also contains very soft fibrous gypsum crystals. Depth 30 - 40 cm. | |
| RP-SE1a | Thin pink and green evaporite crust covering surface in centre of pan. | |
| RP-SE1b | Creamy white blocky gypsum crystals in granular gypsum matrix. | |
| RP-SS1a | Pit dug on periphery of pan. Material appeared to be *in-situ*. | |
| RP-SS1a | Mottled clay at surface. Gypsiferous with soft gypsum nodules and shell fragments. Depth 0 – 26 cm. | Dry-2,5Y 8/2 (pale yellow); Wet - 2,5Y 7/3 (pale yellow) |
| RP-SS1b | Fine grained brown sand which becomes greyer and then orange towards the water seep zone (38 cm). Layer continues 10-15 cm below zone from which water seeped. Water sample taken - RP-WB1. Depth 26 – 50 cm. | Dry- 10YR 6/2 (light brownish grey); Wet - 10YR 4/2 (dark greyish brown). |
| YF-OT1 | Water collected from rain gauge. Not known how long sample was there or how clean the gauge was. | Colourless |
| YF-WB1 | Subsurface water sampled from pit dug at edge of pan (YF-SS1). Water was intersected 50 cm below the pan surface, in brown sand (YF-SS1c). | Very pale yellow |
| YF-WB2 | Pit 2 dug about 20 m from edge, in unvegetated zone. Water table rose to about 20 cm below ground level. | Very pale yellow |
| YF-WP1 | Taken from very shallow water (5cm) about 50 m from the edge of the pan on eastern side, near inflow. | Colourless |
| RP-WB1 | Pit dug on periphery of pan. Water began to seep in from brown sands (38cm below pan surface). | Very pale yellow |
| RP-WP1 | Ponded water in artificial trough. The pan is very disturbed from mining, and there is a lot of algae in the water. | Colourless |

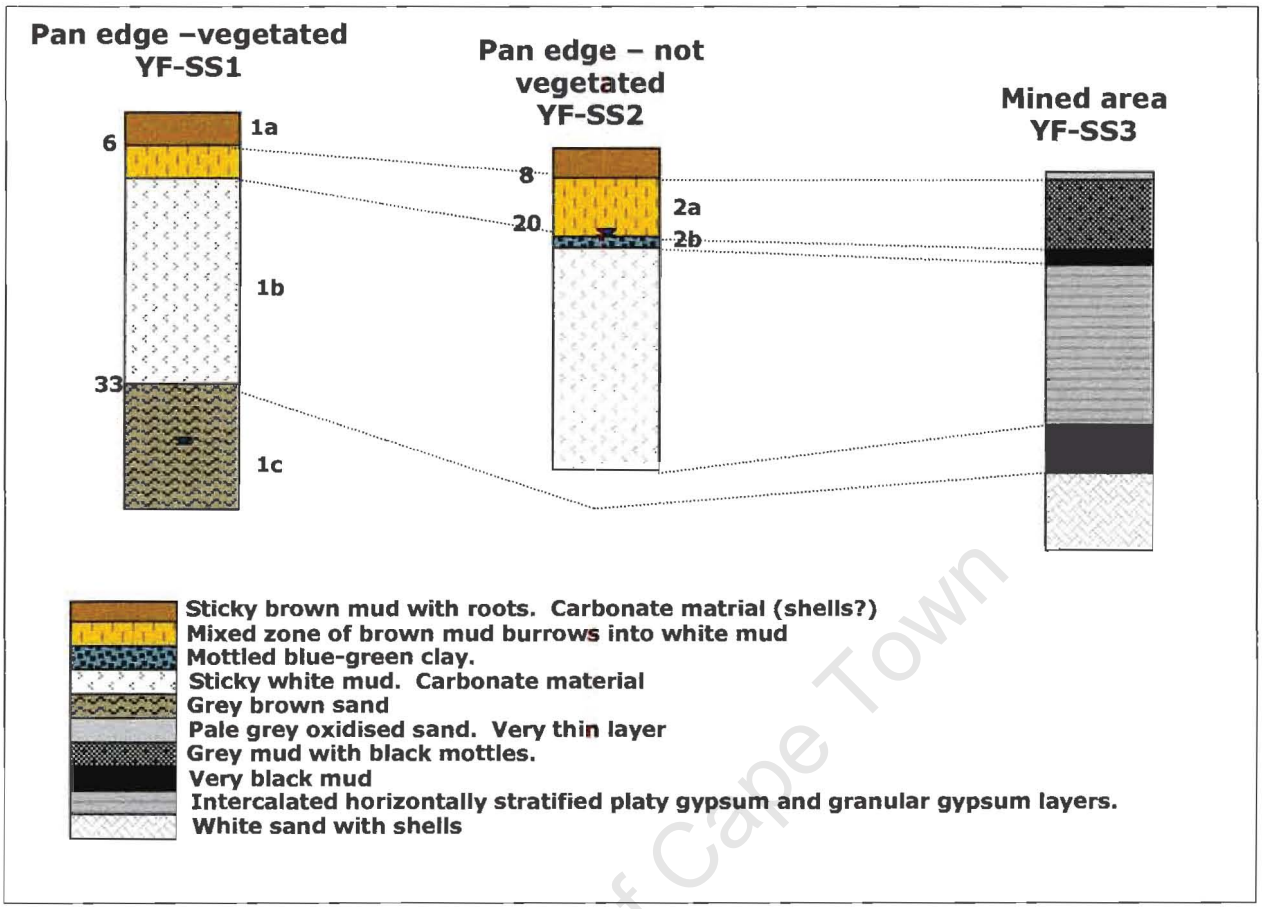


**Figure 2.3: Stratigraphic columns for samples from Ysterfontein saltpan.**



### 2.4.2. BRACKISH-SALINE PANS

Four brackish-saline pans were sampled: Slangkop (SK), Droëvlei (DV), Rooipan north (RB) and Kiekoesvlei (KV). Apart from Kiekoesvlei, the morphology of these pans is not noticeably different from brine-type pans. Both the brackish-saline and brine-type pans differ from the coastal pans in a number of respects. Firstly, they are far smaller. The largest pan in the Darling area is only 18 ha in area, about 10% the size of Ysterfontein saltpan. Secondly, they have a more classical pan morphology – kidney shaped with a steep scarp slope to the south and a raised landform (lunette dune) to the north. The brackish-saline pans differ from the brine-type pans in the lack of a halite crust during the dry months, and in the less reduced sediments below the pan water. Calcrete was found below the pan floor at Droëvlei, Rooipan north and Kiekoesvlei. Shells of *T. ventricosa* were found on the shores of all the brackish-saline pans except Kiekoesvlei. Orthophotographs of the vleis indicating

sampling localities are given in Figure 2.4. Table 2.4 lists the sample descriptions and some features of the pans are illustrated with photographs in Figure 2.5 – 2.7.

*Slangkop (SK)*

Slangkop (Figures 2.4(a) and 2.5) is at a relatively high elevation compared to other pans, in a dip at the foot of the Darling hills. The scarp on the upwind, upslope side is particularly steep and noticeable. A concrete canal feeds into the pan but no water was flowing at the time of sampling. Coarse granitic sand was noted to a depth of 20 cm along the edge of the pan on the eastern side, but the subaqueous sediments are black reducing muds. *T. ventricosa* shells were found on the pan edge. Sediments along the south-western edge of the pan, below the scarp slope, are less sandy than those on the eastern side and water is seeping from the ground. A pit dug into the mud on the western edge revealed a Katspruit soil (Lammermoor family) to a depth of about half a meter, followed by an abrupt transition to water-bearing, clay-free, poorly sorted granitic sand with iron oxide concretions (similar to that observed on the eastern edge of the pan). Katspruit soils of the Lammermoor family are waterlogged and anaerobic, and are commonly associated with pans in South Africa (Verster *et al.*, 1992). They consist of an orthic A horizon underlain by a non-calcareous G horizon. An orthic horizon is a standard A horizon with no special characteristics. A G or gleyed horizon is generally saturated and blue-green in colour (Soil Classification Working Group, 1991).

*Droëvlei (DV)*

Droëvlei (Figure 2.4(b)) is slightly larger than Slangkop and is kidney shaped. The downwind lunette dune is obvious on the orthophotograph. There is an extensive seep zone on the south-western edge of the pan, below the scarp slope. The surface material in this area is very muddy. However, at sampling site DV-SS3, the surface material is sandy and covered by a layer of *T. ventricosa* (Figure 2.6(a)). The water in the pan was very shallow at the time of sampling and the pan floor appeared nodular. Nodules were found to be drier patches of sediment. Sediments sampled from beneath the pan floor were reduced only where there is no bioturbation, an observation clearly illustrated by the zone of oxidation around a burrow in Figure 2.6(b). Sediment samples from Droëvlei encompass three areas, a vegetated zone adjacent to the pan (DV-SS1), an unvegetated beach directly adjacent to the pan (DV-SS3) and a sample from the pan floor (DV-SS2).

*Rooipan north (RB)*

Rooipan north (Figure 2.4(c)) is located about 200 m north of Rooipan south, separated by the lunette dune of Rooipan south. Rooipan north has neither a noticeable lunette dune, nor a steep scarp on the southern side. Calcrete is found around the edge of the pan, as well as below the sediment surface, and prevented digging a pit for subsurface water sampling. Calcrete is not found in a continuous layer, but as large chunks (5-10 cm) in a specific horizon about 5 cm below the sediment surface. The water in the pan was very shallow (<10 cm) at the time of sampling and algae were present as a brown scum below the water surface.

*Kiekoesvlei (KV)*

Kiekoesvlei (Figure 2.4(d)) is very different from all the other pans in this study. The pan floor is an extensive flat grassy surface with no evidence of water (Figure 2.7). The surface has large cracks due to shrinkage of drying clay, but no water could be found even when a pit was dug. A single sediment sample was taken. Subsurface calcrete fragments were found in the pit. Judging from the landing strips visible on the orthophotograph, water is not a common occurrence in the pan.

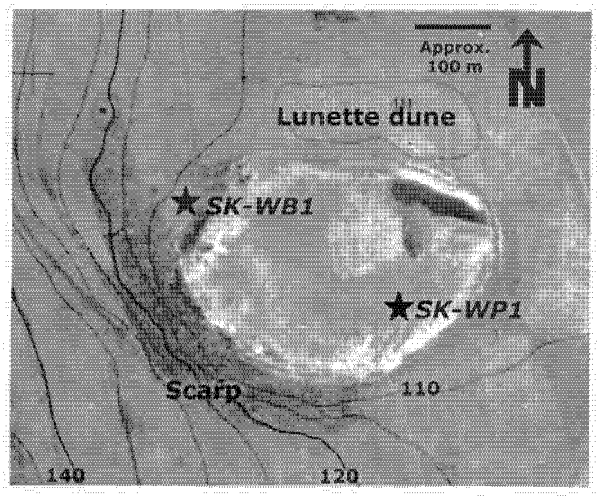


(a)

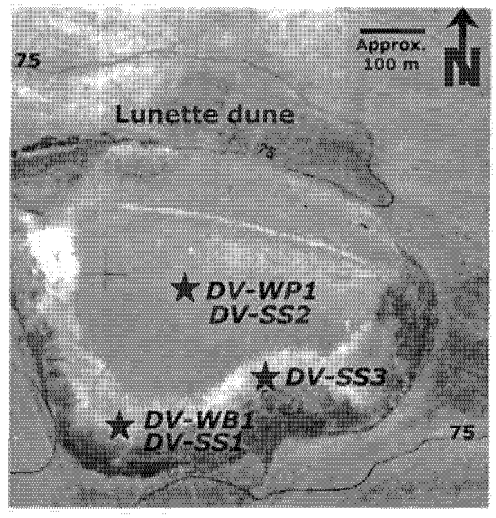


(b)

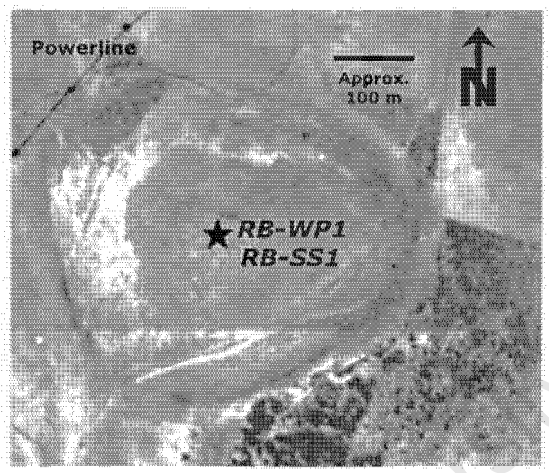


(c)

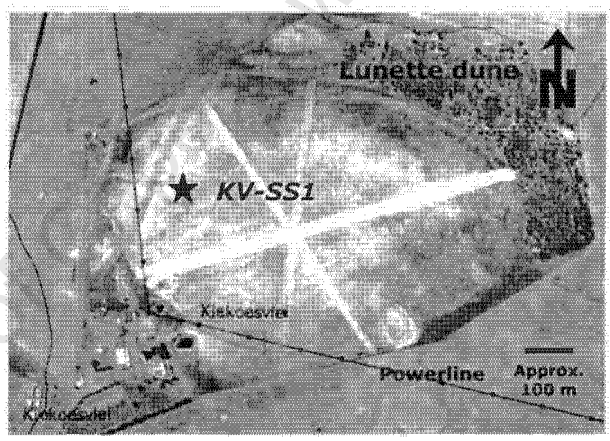


(d)

**Figure 2.4: Orthophotographs revealing the morphology and sample locations for the brackish-saline pans (a) Slangkop, (b) Droëvlei, (c) Rooipan north and (d) Kiekoesvlei. Contour intervals are in metres above mean sea level.**

**Table 2.4: Sample descriptions for sediment and water samples from brackish-saline pans**

| Sample ID | Description of site | Munsell colour (Anon, 1992) |
|---|---|---|
| DV-SS1 | Pit dug in seep zone adjacent to SW edge of pan, at the foot of the scarp. About 50 m from waters edge. | |
| DV-SS1a | Extremely poorly sorted coarse sandy unit with large angular to subrounded pebbles of quartz, feldspar and iron oxide concretions. Water bearing layer (sample DV-WB1). Underlies a grey-brown muddy sand. Depth 15 - 17 cm | Dry and wet: 10YR 5/6 yellowish brown |
| DV-SS1b | Grey brown muddy sand below DV-SS1a. Fine sand with coarse angular-subrounded fragments of quartz, Fe oxides, and feldspar. Layer becomes more clayey with depth and grades into sticky green clay with iron oxides. Depth > 17 cm. | Wet - 5Y 4/3 (olive); Dry - 5Y 6/4 (pale olive) |
| DV-SS2 | Pan floor sediment. Appears nodular but there is no difference in composition between nodules and matrix, the nodules are drier and therefore harder than the matrix. Nodules are 5-10 cm in length. Sediment is bioturbated - burrows of oxidized brown sediment are surrounded by black reduced mud. *T. ventricosa.* | Wet - 5Y 3/2 (dark olive grey); Dry - 5Y 4/2 (olive gray) |
| DV-SS3 | Second pit dug to south of Droëvlei. Sample taken from just below surface. Mixed poorly sorted fine-grained sand with small angular iron oxide concretions. | 5Y 4/3 (olive) |
| RB-SE1 | Calcrete nodules found as discontinuous layer below loamy surface material. | |
| RB-SS1 | Subaqueous sample taken from under water in centre of pan. Pale oxidized layer underlain by brown sand with very sticky clay and iron oxide grains. Poorly sorted sand, fine grained to very coarse angular to subangular pebbles. *T. ventricosa.* | 2,5 8/3 (Very dark grey) |
| KV-SS1b | Pit dug near pan centre - no water. Brown-green clayey sand with calcrete nodules. Also small fragments sub-angular iron oxides and granite (1-5 mm). | Dry - 2,5Y 6/2 (light brownish grey); Wet - 2,5Y 6/3 (light yellowish brown) |
| SK-WB1 | Pit dug on SW edge of pan. Water began seeping in from coarse granitic sand. Water table is at 20 cm below surface. | Turbid yellow |
| SK-WP1 | Water taken about 20 m from pan edge. Water depth at sampling point was about 5-10 cm. | Very pale yellow |
| DV-WB1 | Sampled from pit DV-SS1. Water table approximately 17 cm below surface, water seeping from iron oxide sand (DV-SS1a) | Very pale yellow |
| DV-WP1 | Pan water sampled from about 20 m into Droëvlei. Water very shallow (<10 cm), quite clear. | Pale yellow |
| RB-WP1 | From centre of pan. Pan very shallow. Water is turbid, murky. | Turbid greenish grey |

**Figure 2.5: Slangkop pan from the east, with the Darling Hills in the background. All pans share similar pan morphology. The scarp slope is at the left of the picture, and the lunette dune at the extreme right.**

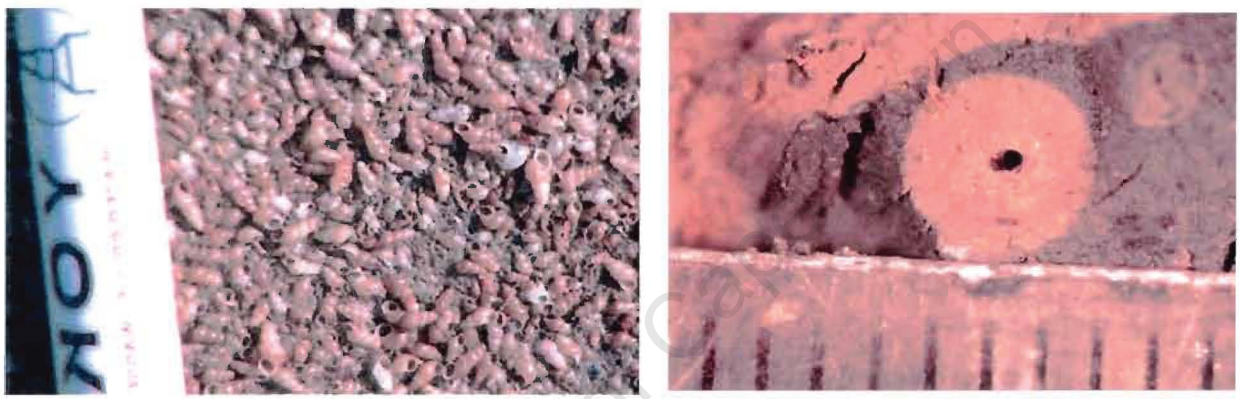

(a) (b)

**Figure 2.6: Features observed during sampling at the brackish-saline pans. (a)*T. ventricosa* shells forming a thin layer on the southern shore of Droëvlei. Marker pen for scale. (b)Close up of *T. ventricosa* burrow in DV-SS2. Note oxidized rim around hole and reduced sediment thereafter. Ruler for scale (oxidized burrow approximately 3 mm in diameter).**

**Figure 2.7: View across Kiekoesvlei with Darling hills in background. Note flat grassy surface and lack of surface water.**

### 2.4.3. BRINE-TYPE PANS

Six brine-type pans were sampled in the Darling area, Zwartwater south (ZA) and north (ZB), Burgerspan south (BA) and north (BB), Rooipan south (RA) and Koekiespan (KP). Brine-type pans are noted for having crusts of halite on their surfaces throughout the year, for the absence of *T. ventricosa*, and for a red tinge to the pan water. Cattle hoof prints were noticed at a number of the pans, both adjacent to the pan and in the salt crust beneath the water.

*Zwartwater south (ZA)*

Zwartwater south (Figure 2.8(a)) has an irregular shape, apparently due to human activities. A small catchment dam has been built upstream of the pan, and the pan itself appears to have been separated into two sections. A seepage zone was found below the scarp to the west (Figure 2.9), and the seepage was sampled (ZA-WS1). The stream flowing into the catchment dam was also sampled. The sediments to the west adjacent to the pan edge consist of a dark reduced mud with *T. ventricosa* burrows, but no *T. ventricosa* shells were found. Unweathered biotite flakes were found in the mud, indicating that fresh granite is nearby. The pan water is extremely salty and a crust of salt 1-2 cm thick exists below the water surface. Below the halite crust is a thin (approximately 1 mm) pale brown oxidized edge to the underlying black sulphurous smelling mud.

*Zwartwater north (ZB)*

Zwartwater north (Figure 2.8(b)) is about half a km north west of Zwartwater south. It is about half the size of Zwartwater south and is kidney-shaped with a steep scarp slope to the west. The pan was visited during April when it was covered by a thick crust of halite with strange halite protuberances (Figure 2.10 and 2.11), and again in July, when it was under about 30 cm of water. A pit dug adjacent to the southern edge of the pan in July penetrated red-brown sand. Nodules of green clay were found in the sand, possibly weathered feldspar. A spring located north of the pan provides a source of relatively fresh surface water inflow. Iron oxide concretions (5-10 cm) were found along the southern edge of the pan, apparently *in situ* at one point as a ferricrete horizon. During April, a small amount of surface water was present due to the spring, but otherwise the pan was dry. Surrounding the halite crust was a non-vegetated zone with desiccation mud cracks.

*Burgerspan south (BA)*

Burgerspan south (Figure 2.8(c)) is currently being exploited for halite for use by agricultural companies. The pan is artificially divided into two sections, both of which were sampled. The smaller pan to the west is far less salty than the main pan. A small spring bubbling up from directly adjacent to the main pan below the scarp slope was sampled. Calcrete and ferricrete horizons were noted outcropping adjacent to the western edge of the pan, and both were sampled. The calcrete directly overlies the ferricrete, as shown in Figure 2.12. The subaqueous sediments are black and reducing. By examining the orthophotograph (Figure 2.8(c)), a dark "plume" can be seen extending to the northeast of the pan, due to aeolian transport of pan material.

*Burgerspan north (BB)*

Burgerspan north (Figure 2.8(d)) is approximately 2 km northwest of Burgerspan south and is not mined. Calcrete was noted adjacent to the pan, and was also found in a pit dug on the northern edge of the pan for a subsurface water sample. The sediments grade from a pale brown sand to a green loamy layer at about 40 cm depth. Below this is a water-bearing sand containing calcrete fragments. Black sulphurous mud and a salt crust are found below the pan water surface. A small stream flowing into Burgerspan north from the north was sampled (Figure 2.13). As with Burgerspan south, a dark "plume" can be seen upwind of the pan on the orthophotograph (Figure 2.8(d)).

*Rooipan south (RA)*

Rooipan south (Figure 2.8(e)) is extremely saline, the water has a pink tinge and in some places a red scum occurs on the water surface. The sediments adjacent to the pan are quite sandy, but the subaqueous sediments are black reducing muds (Figure 2.14). Calcrete outcrops on the unpaved road to the south of the pan. Small crystals of halite were precipitating at the waters edge, and a halite crust existed beneath the water surface at the time of sampling. The halite crust is smooth on the upper surface and jagged on the lower surface. Figure 2.15 illustrates a profile through the pan based on depth profiles at two sites.

*Koekiespan (KP)*

Koekiespan (Figure 2.7(f)) was visited only briefly in order to obtain a surface pan water sample. The pan appears to be worked for halite, but the farm owner was not available to confirm this.

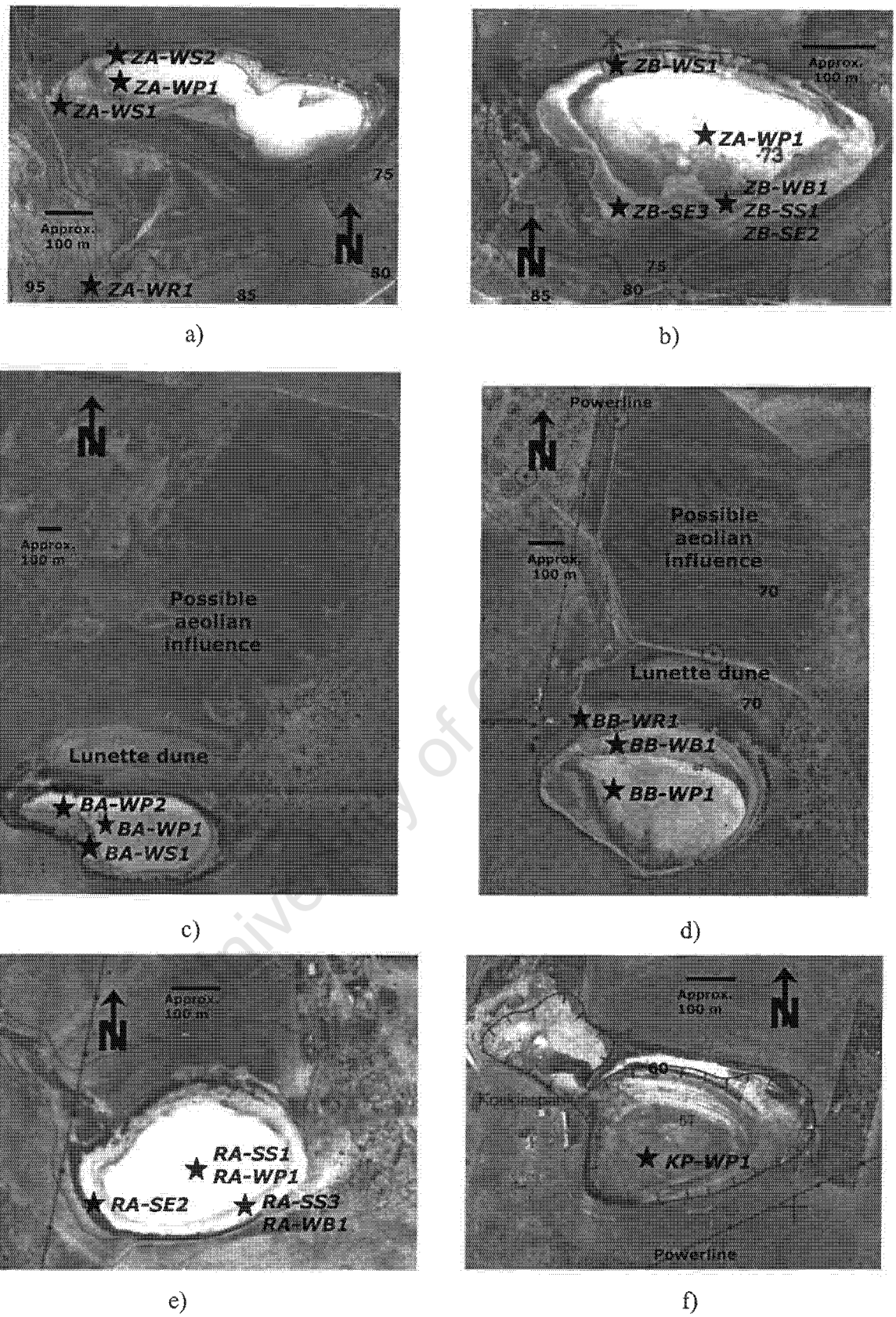


**Figure 2.8: Orthophotographs of saltpans, indicating sample localities. (a) Zwartwater south, (b) Zwartwater north, (c) Burgerspan south, (d) Burgerspan north, (e) Rooipan south, (f) Koekiespan. Contour intervals in metres above mean sea level.**

**Table 2.5: Description of sediment/soil samples collected from brine-type pans**

| Sample ID | Description of site | Colour (Anon, 1992) |
|---|---|---|
| ZB-SE2 | Ferricrete sample from pit dug at pan edge | |
| ZB-SE3 | Ferricrete sample from pan edge, area of outcrop along southern margin. Dark red inside, yellowy on outside, contains small, sandy, angular grains. | |
| ZB-SS1 | Pit dug on southern edge of pan. Mottles of green clay in a reddy brown sand. Depth 30 – 35 cm. | 10YR 6/8 (brownish yellow) and 5GY 5/1 (greenish grey) |
| BA-SE2 | Ferricrete sample from *in situ* position below calcrete on western edge of pan. | |
| BA-SE3 | Calcrete sample from *in situ* position above ferricrete on western edge of pan. | |
| RA-SE2 | Thin crust around edge of pan at vegetation line where water seeps out. | |
| RA-SS1 | Subaqueous sediment samples | |
| RA-SS1a | Black reducing mud, smells of $H_2S$. Sediment contains many seeds, possibly from sedges. The upper surface is a thin layer of oxidized sediment. Depth 0 - 20 cm. | Wet - N 2,5/ (black), Dry - 5GY 4/1 (dark greenish grey) |
| RA-SS1b | Black reducing mud grades into green-grey smelly mud with lobes/nodules of white sand. Depth > 20 cm. | Dry: 5GY 4/1 (dark greenish grey); Wet - 5G 5/1 (greenish grey). |
| RA-SS3 | Pit dug at southern edge of pan. | |
| RA-SS3a | First horizon is pale brown fine to medium sandy layer. Depth 0 – 5 cm. | Wet and dry: 5GY 4/1 (dark greenish grey) |
| RA-SS3b | Second horizon is greenish grey-black mottled fine sand. Depth 5 – 30 cm. | Wet and dry: 5GY 5/1 (greenish grey); N2,5/ (black);10Y 6/8 (brownish yellow) |
| RA-SS3c | Orange-green mottled extremely sticky clay. Depth 30 – 45 cm. | Wet and dry: 5GY 6/1 (greenish grey);2,5Y 6/4 (light yellowish brown). |
| RA-SS3d | Water bearing clean fine-grained white sand below mottled zone. Slightly sticky. Water sample RA-WB1 collected. Depth > 45 cm. | Wet and dry: 5Y 7/2 (white) |

**Table 2.6: Description of water samples collected from brine-type pans**

| Sample ID | Description of site | Colour |
|---|---|---|
| ZA-WP1 | Pan water taken about 20 m from western edge, over a halite crust. Water depth approximately 15-20 cm. | Clear with pink tinge |
| ZA-WR1 | Running stream flowing into catching dam above pan. | Pale yellow |
| ZA-WS1 | Small trickle of spring emanating west of pan below scarp. | Strong yellow but not turbid |
| ZA-WS2 | Water pumped (from underground) into cattle drinking-trough on NW edge of pan. | Colourless |
| ZB-WB1 | Tiny seep of water from pit on southern side of pan. | Turbid |
| ZB-WP1 | Sample taken from about 20 m from pan edge. Water quite deep – 30 cm and turbid with pink algae. | Pink |
| ZB-WS1 | Man-made spring trickling into northern edge of pan. Water clear. A lot of green algae and grass growing in and around spring. | Colourless |
| BA-WP1 | Producing pan. Pan water sample from main section of pan on western edge, away from spring BA-WS1. | Dark orange |
| BA-WP2 | Water sample collected from part of Burgerspan south sectioned off artificially from Burgerspan. | Very pale yellow. |
| BA-WS1 | Small spring bubbling up from pan edge. Difficult to sample without pan contamination. | Pale orange |
| BP-WB1 | Pit dug on northern edge of pan. Water intersected at about 50 cm. | Colourless |
| BP-WP1 | Pan water sample taken from about 20 m from northern edge. | Clear with pinkish tinge |
| BP-WR1 | Stream entering pan from the north, flowing only very slightly. | Yellow |
| RA-WB1 | Water from pit dug at waters edge. Water emanates from clean white sand approximately 50 cm down. | Colourless |
| RA-WP1 | Water sampled about 20 m from pan edge. Water slightly turbid due to algae. | Pink |
| KP-WP1 | Sample taken about 10 m from southern edge. | Pale pink |

**Figure 2.9: Seepage zone to the west of Zwartwater south with scarp in background. Water seeps from the edge of the vegetated zone and collects into the small stream running down centre of photograph.**

**Figure 2.10: Halite crust on surface of Zwartwater north during April 2000. Each spike is approximately 5 cm high.**

**Figure 2.11: Zwartwater north during the dry season. Note the pink halite crust on the surface of the pan and the lack of vegetation immediately around the pan.**

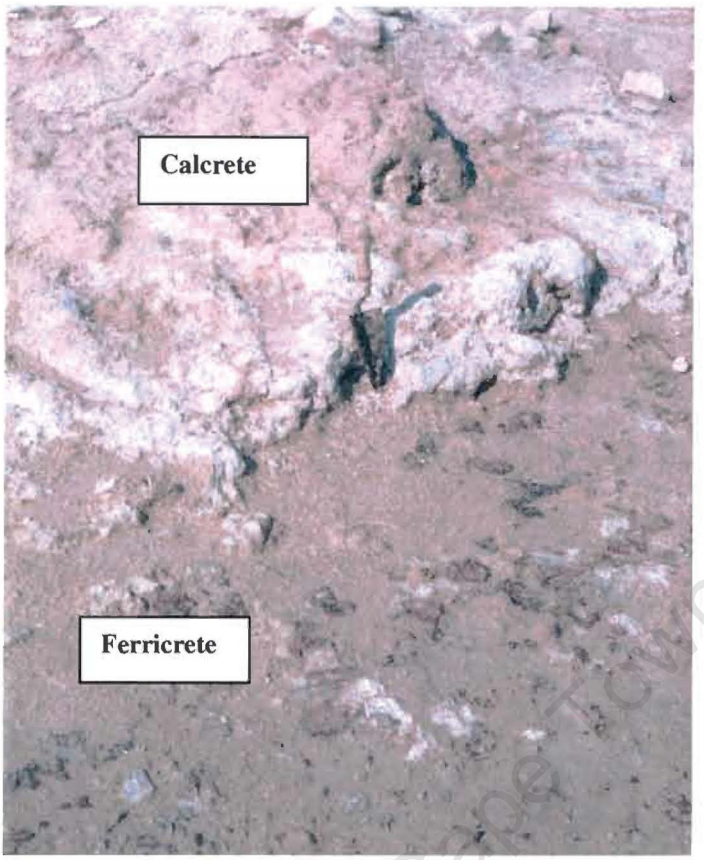


**Figure 2.12: *In-situ* calcrete and ferricrete (dark coloured) horizons at Burgerspan south. Note trowel in centre of photograph for scale.**



**Figure 2.13: Sampling the stream flowing from the north into Burgerspan north.**

Figure 2.14: Section through subaqueous sediment from Rooipan south. Note how basal grey-green mud grades into a black upper sediment.

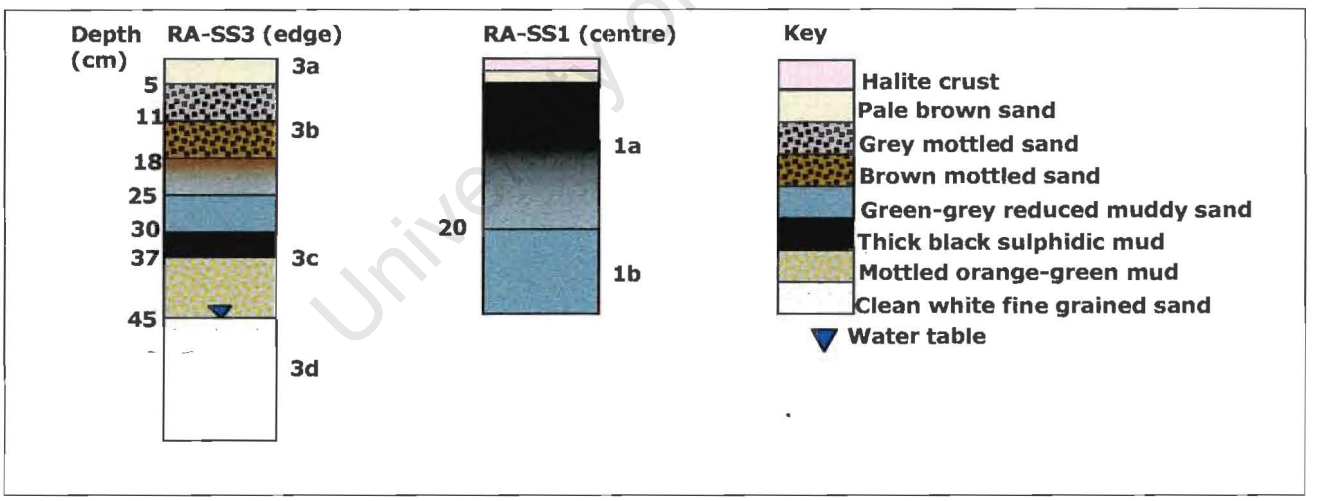


Figure 2.15: Stratigraphic columns of depth profiles of pan edge (RA-SS3) and pan floor (RA-SS1) sediments of Rooipan south.

# 3. Methods

All water samples were stored in a refrigerator at approximately 4°C before and between analyses. Duplicate samples were analysed for all methods, and external standards were analysed where possible. Results for these are given in Appendix A. General measurements as well as major and trace element analyses apply to both water samples and saturated paste extracts. Unless otherwise specified, dilutions were done using distilled water. Reference to a Standard Method indicates a technique given in Eaton *et al.* (1995).

## 3.1. GENERAL MEASUREMENTS

### 3.1.1. pH

The pH of waters was measured in the field with a Radiometer PHM201 portable meter calibrated with pH 7 and pH 10 buffers. Sediment pH was measured in the saturated paste extract (SPE), and in a 1:2.5 suspension of soil in both 1M KCl and distilled water allowed to equilibrate for 30 minutes on a shaker. These measurements were made with a Metrohm 691 pH meter calibrated with standard buffers before use.

### 3.1.2. Electrical conductivity (EC)

Electrical conductivity is a measure of the number of ions in solution and it is a convenient way to approximate the salinity of a solution (Drever, 1997). EC was measured within 24 hours of sampling. Measurements were made using a CRISON microCM 2201 EC meter with conductivity electrode and temperature sensor for temperature correction. The EC values are reported at a reference temperature of 20°C. The upper detection limit of the meter (200 mS/cm) was exceeded on one occasion.

### 3.1.3. Salinity

Salinity was determined in the field where possible. An Atago Hand Refractometer was used to take readings. The refractometer is calibrated up to 10 % NaCl. Samples exceeding 10% NaCl had to be returned to the lab for dilution prior to measurement.

### 3.1.4. DENSITY

Density was determined by weighing a known volume of sample. A 10 mL volume was measured at 20°C using a glass pipette, and weighed on a Scaltec SPO52 balance. Distilled water was used as a standard.

### 3.1.5. ALKALINITY

Alkalinity was determined by potentiometric titration of the sample to a pH of 4.5 with 0.1 N HCl. The procedure outlined in Standard Method 2320 was followed. Analyses were completed in four batches, one after each sampling trip so as to complete analyses within 24 hours of sampling. For each batch of analyses, a sample from the previous batch was re-analysed to ensure consistency. Unfiltered, undiluted samples were used for analysis. The titration was done automatically using a Radiometer TTT85 Titrator and pH meter, and ABU80 Autoburette. Alkalinity was calculated from the volume of acid needed to reduce the pH to 4.5.

### 3.1.6. DISSOLVED ORGANIC CARBON (DOC)

Organic carbon is oxidised to $CO_2$ by persulphate in the presence of UV light. The sample is first acidified to pH of 2 or less using sulphuric acid and heated to 37°C in order to convert all inorganic carbon to $CO_2$. Inorganic $CO_2$ is stripped off with purified $N_2$ gas and organic-derived $CO_2$ is allowed to permeate through a membrane into a buffered alkaline solution with phenolphthalein. The phenolphthalein can be measured colorimetrically (Mike Louw, Laboratory Manager CSIR, pers. comm., 2000). Samples for DOC were submitted to the Council for Scientific and Industrial Research (CSIR) analytical laboratories in Stellenbosch for analysis. The method is calibrated for samples with salinities below that of seawater, consequently only samples with salinities less than seawater were analysed.

### 3.1.7. TOTAL DISSOLVED SOLIDS (TDS) BY OVEN DRYING

TDS was determined by following a method modified from Standard Method 2540 C. The water sample is evaporated to dryness at 180°C and dried at that temperature until constant weight is achieved. TDS is the difference in mass between the sample dish and the dish plus sample. At 180°C, almost all mechanically occluded water should be lost, although some water of crystallisation will remain if sulphates are present. Other losses include some

organic matter, $CO_2$ and some chloride and nitrate salts. TDS by oven drying is expected to be higher than TDS calculated from individual ion concentration data because a significant contributor such as organic matter may not be included in the calculation (Eaton *et al.*, 1995). However, this was not observed. The samples were not analysed within 1 week of collection, as recommended in Eaton *et al.*, (1995) and microbial decay of salts could have occurred. Cellulose acetate filters of smaller pore size than recommended were used, also contributing to a low TDS value. The salts obtained from drying water samples were analysed by X-ray diffraction (XRD).

## 3.2. MAJOR IONS

### 3.2.1. ION CHROMATOGRAPHY (IC)

Major anions (Cl, $NO_3$, $SO_4$) and cations (Na, K, Ca, Mg) in the water and saturated paste extract samples were determined using IC. This technique relies on the variable adsorption of ions to separate them on an exchange separator column. Peak area for each ion are calibrated using solutions of known ion concentrations. Prior to analysis, samples were filtered through 0.45 μm cellulose acetate membrane filters and diluted to below 100 μS/cm. Dilutions ranged from 40 to 10 000 times due to the extreme concentrations of ions in the brines. Immediately prior to analysis, samples were filtered through On-guard-P filters to remove organic colloids. The samples were run separately for anions and cations on Dionex HPIC-AS14A and Dionex HPIC-CS12A exchange columns, respectively. Details of machine settings are given in Appendix A. Dionex API-450 software integrates the area under each conductivity peak, subtracts the background and calculates concentrations of cations and anions based on calibrations.

No major problems were experienced with anion analysis. However, the cation column generated spurious results for certain elements. Initially the problem appeared to be with the software set up. Once this was corrected, all samples were re-analysed and charge balances improved significantly. As the laboratory has no external standard, it was decided to analyse a seawater sample (results in Appendix A). This highlighted Ca and Mg analysis as problematic and it was decided to analyse these by a separate technique. Because of the high dilutions done, ions like F, $NO_3$ and Br were not detected in every sample, and other techniques were used to quantify the concentrations of some of these species.

### 3.2.2. PHOSPHATE BY COLORIMETRY

Phosphate is determined using Standard Method 4500-P E, the ascorbic acid colorimetric method. Only three samples were analysed for phosphate. The samples were filtered on site and stored in glass bottles in a refrigerator at below 4°C until analysis. Fifty mL of sample were reacted with a combined reagent of ammonium molybdate, antimonyl tartrate and ascorbic acid. Any orthophosphate present forms phosphomolybdic acid which is reduced by ascorbic acid to intensely coloured molybdenum blue. The colour of molybdenum blue is proportional to concentration of orthophospate. A set of phosphate standards of concentrations between 0.25 and 1.25 mg/L as well as a blank sample (distilled water) were analysed simultaneously and used to construct a calibration curve. The absorbance at 880 nm was measured using a Sequoia-Turner Model 340 Spectrophotometer. All samples had absorbances equivalent to the blank, and it was decided not to analyse further samples.

### 3.2.3. CALCIUM AND MAGNESIUM BY EDTA TITRATION

Calcium and Mg are determined together using Standard Method 2340C, the EDTA titrimetric method. Both waters and saturated paste extracts were analysed. Calcium and Mg are titrated with ethylenediaminetetraacetic acid (EDTA) using Calmagite as an indicator. At high pH, Calmagite forms a pink solution with the calcium and magnesium. EDTA complexes Ca and Mg, changing the dye colour from pink to blue. The pH is increased to 10 to increase endpoint sharpness without precipitation of calcium carbonate or magnesium hydroxide. All titrations were performed on filtered samples. A portion of sample requiring between 10 and 15 mL of EDTA titrant was diluted to 50 mL. The EDTA titrant was standardised against a standard Ca-carbonate solution. Magnesium concentrations are calculated as the difference between hardness (in mmol/kg) and calcium concentration (determined by atomic absorption spectrometry (AAS); in mmol/kg).

### 3.2.4. CALCIUM BY ATOMIC ABSORPTION SPECTROMETRY(AAS)

Water and saturated paste extract samples were analysed for Ca by AAS at the Department of Chemical Engineering, UCT. AAS determines the amount of radiation from a light source that is absorbed by an atom of an element. The degree of absorption is specific to the element being analysed. The sample is aspirated and mixed with nitrous oxide and combusted, resulting in atomisation (Potts, 1987). A Varian SpectraAA-30 was used for

analysis. The spectrometer is calibrated with Ca standards, and samples diluted to fall within the calibration range.

### 3.2.5. FLUORIDE BY ION-SPECIFIC ELECTRODE (ISE)

Fluoride concentrations were measured using a Corning ion analyser 255 with a Corning fluoride-selective electrode and a calomel reference electrode. The fluoride electrode is a chemically inert body with a sensitive laser-type doped lanthanum fluoride crystal membrane. A potential is established across the crystal by solutions containing fluoride, and the activity of fluoride in solution can be calculated using the Nernst equation. Because the activity of an ion depends on the ionic strength of the solution, the ionic strength of the sample is initially adjusted with a buffer. The buffer also optimises the pH to minimise complexing so that the electrode effectively measures concentration (Eaton *et al.*, 1995; Corning Glass Works, 1984). The electrode was initially calibrated with 5 standard solutions of fluoride concentrations ranging from 0.5 to 10 mg/L. Equal volumes of sample and TISAB (total ionic strength adjustment buffer) were placed into a container with a magnetic stirrer, and the meter was allowed to settle for approximately 5 minutes before a reading was taken. Some of the measurements were below the lowest calibration point, and the meter was recalibrated for concentrations between 0.1 and 2 mg/L to analyse these samples.

## 3.3. TRACE ELEMENTS

### 3.3.1. INDUCTIVELY COUPLED PLASMA MASS SPECTROMETRY (ICP-MS)

The ELAN 6000 ICP-MS housed in the Department of Geological Sciences at UCT was used to determine concentrations of Li, B, Al, Si, Fe, As, Se, Br, Rb, Sr, Ba, and U in both the water samples and saturated paste extracts. ICP-MS operates by ionising a water sample in argon plasma at high temperature and separating the ions by mass for measurement (Potts, 1987). Acidified (with double-distilled $HNO_3$), filtered samples were diluted to acceptable salinities with 2% $HNO_3$. Each sample received an internal standard containing elements not being analysed. The samples were loaded into the autosampler, which was programmed to analyse each sample twice, interspersed with analyses of certified NIST standards and blank samples. The internal standard was used to correct for drift. Limitations of the technique are mainly due to interferences by argon ions produced in the plasma. A well-known interference is between $^{56}Fe$ and $^{40}Ar^{16}O$ (Potts, 1987).

### 3.3.2. IRON BY COLORIMETRY

Iron analyses are notoriously problematic using ICP-MS due to interferences by the argon plasma (Potts, 1987). Iron concentrations were therefore verified by colorimetry, using Standard Method 3500-Fe, the phenanthroline method. Iron in samples preserved with $HNO_3$ was reduced to the ferrous state by boiling with hydroxylamine and HCl. The ferrous atom is chelated by 1-10 phenanthroline to form an orange-red complex, the intensity of which was measured with a Sequoia Turner Model 340 spectrophotometer. Samples that had concentrations of Fe in excess of 15 mg/L (according to ICP-MS) were analysed initially, and when they were found to be below detection limits, no further analyses were done and ICP-MS data were disregarded.

### 3.3.3. SILICA BY COLORIMETRY

Many of the samples analysed by ICP-MS had no detectable Si. These were mainly pan samples which required the greatest dilution (1000 times) prior to analysis. In order to confirm that the low Si concentrations of these samples were valid, and not an artefact of the high dilutions, Si was determined colorimetrically by Standard Methods 4500-Si D and E, the molybdosilicate and heteropoly blue methods. Silica and phosphate react with ammonium molybdate at a pH of approximately 1.2 to form yellow molybdosilicic acid. A reducing agent, aminonaphtholsulphonic acid, added to this solution produces heteropoly blue. Table 3.1 lists methods and absorbance wavelengths used for various Si concentrations. The absorbances were converted to concentrations using calibration curves based on standards of concentrations 0.1, 0.2, 0.5, 1, 2, 4, 5, 7.5, 10, 15 and 20 mg/L.



**Table 3.1: Methods used for Si determination at different concentrations**

| Si range (mg/L) | Method | Absorbance wavelength (nm) |
|---|---|---|
| 0.3-2 | Heteropoly blue | 815 |
| 1-5 | Heteropoly blue | 650 |
| >5 | Molybdosilicic acid | 410 |

The intensity of colour is affected by the ionic strength of the solution, resulting in a 20 to 35% underestimate of Si in seawater using the molybdosilicate method, and a 10-15% overestimate using the heteropoly blue method (Eaton *et al.*, 1995). Because the relative concentrations of Si were of more interest than absolute values, and because of the huge

range in ionic strength, the standards were not prepared in a high ionic strength medium. As the highest ionic strength solutions had the lowest Si concentrations, the overestimation of the heteropoly blue method should not affect interpretation of the data.

## 3.4. STABLE ISOTOPES BY MASS SPECTROMETRY

In order to determine the stable hydrogen isotope ratio, the water is reduced to hydrogen with zinc according to the method of Coleman *et al.* (1982). A 2 µl aliquot of unfiltered, undiluted sample was taken up in a capillary tube and dropped into a 25 cm long, 6 mm diameter oven-dried glass tube. A small amount of "Indiana" zinc was also placed in the tube. The water was frozen using liquid nitrogen and air pumped out of the glass tube. Once a good vacuum was obtained, the tube was sealed with an oxy-acetylene torch. After preparing all samples, they were placed in a furnace at 450°C for 30 minutes to allow the zinc to reduce the water to $H_2$. Because of problems with reduction of very saline samples, samples with salinities greater than seawater were distilled. The sample, taken up into a capillary tube, was placed into a glass oven-dried tube containing no zinc. The water was frozen and the air pumped out. A second tube, containing zinc, was placed on the vacuum line and pumped down, and chilled with liquid nitrogen. Once the system was under a good vacuum, the water was heated with an airgun and frozen into the tube containing zinc. The second tube was then sealed with an oxy-acetylene torch. The remainder of the procedure was identical.

Oxygen samples were prepared by placing approximately 2 mL of sample into a pre-evacuated medical tube, injecting about 0.5 atm of medical grade $CO_2$, and allowing the water and gas to equilibrate while shaking in a water bath at 25°C for 2 hours. The water and $CO_2$ were then separated, the $CO_2$ was trapped into a glass pyrex tube using liquid nitrogen, and the tube was sealed using an oxy-acetylene torch. The isotope ratio of oxygen in water can be calculated by measuring the isotope ratio of oxygen in the $CO_2$ (Socki *et al.*, 1992) assuming a fractionation factor of 1.0412 at 25°C between $CO_2$ and water (Coplen, 1993). The gases are analysed using a Finnegan MAT252 mass spectrometer and the isotope ratios converted to δ–notation, according to the equation (Drever, 1997):

$$\delta = \frac{R_{sample} - R_{SMOW}}{R_{SMOW}} x1000 \text{ where } R = {}^{18}O/{}^{16}O \text{ or } {}^{2}H/{}^{1}H.$$

Oxygen and hydrogen ratios in the sample are reported relative to the international standard SMOW (standard mean ocean water). The departmental standard, CTMP (Cape Town MilliPore) has been calibrated against V-SMOW and SLAP, which can be converted to the SMOW scale using the equations of Coplen (1993). The oxygen and hydrogen ratios in the sample are reported relative to SMOW. The CTMP standard was run with each set of samples and used to correct for drift in the reference gases

The different methods for analysing oxygen and hydrogen isotopes results in data that are not strictly comparable. The equilibration method of oxygen isotope analysis yields a ratio of the activities of the $^{18}O$ and $^{16}O$ isotopes, whereas the method of reducing water with zinc to hydrogen results in concentrations of $^{2}H$ and $^{1}H$ being measured. The main reason for the difference is that water of hydration is taken into account with deuterium analysis, but not with oxygen isotope analysis. In dilute waters, activities and concentrations are virtually equal, however, in saline samples, the activity of ions decreases. The fractionation factor between oxygen in water and $CO_2$ will vary as a function of salinity. Sofer and Gat (1972) measured the deviation of $\delta^{18}O$ values away from their true value as a function of increasing salinity, and noted a linear relationship which varied depending on the solution composition. They developed an empirical correction for $\delta^{18}O$ values measured in brines:

$$\frac{\delta^{18}O_0 - \delta^{18}O_m}{\delta^{18}O_m + 1000} x10^3 = 1.11M_{Mg} + 0.47M_{Ca} - 0.16M_K$$

where $\delta^{18}O_0$ = true value for sample

$\delta^{18}O_m$ = measured value for sample

M = molality of species in solution

The correction should be applied if the concentration of Ca and Mg salts change considerably, or if the distribution of isotopic species between two different phases is being considered (Sofer and Gat, 1972). The conversion is an empirical equation:

$$\frac{\delta_0 - \delta_m}{\delta_m + 1000} \times 10^3 = 1.11M_{Mg} + 0.47M_{Ca} - 0.16M_K$$

where $\delta_0$ is the true $\delta^{18}O$ isotope ratio and $\delta_m$ is the measured ratio, and concentrations are in molalities (Sofer and Gat, 1972). The conversion was applied to the oxygen data, and results are presented in Table 3.2. The difference between activity and concentration of these saline waters is not generally significant because they are Na dominated, and Na does not have a

strong effect on waters of hydration (Sofer and Gat, 1972). The correction does not affect interpretation of the data.

**Table 3.2: $\delta^{18}O$ values corrected to concentrations according to the method of Sofer and Gat (1972).**

| Sample ID | δD (‰) (concentration) | $\delta^{18}O$ (‰) (activity) | Corrected $\delta^{18}O$ (‰) (concentration) |
|---|---|---|---|
| **BA-WP1** | -26 | -1.2 | -0.2 |
| **BA-WP2** | -9 | -2.4 | -1.9 |
| **BA-WS1** | -15 | -2.0 | -0.9 |
| **BB-WB1** | -15 | -3.4 | -3.3 |
| **BB-WP1** | -13 | -1.9 | -1.3 |
| **BB-WR1** | -1 | -1.8 | -1.7 |
| **DV-WB1** | -16 | -2.9 | -2.7 |
| **DV-WP1** | 16 | -1.9 | -1.8 |
| **KP-WP1** | -14 | -1.5 | -0.7 |
| **OT-WR1** | -2 | -2.8 | -2.8 |
| **RA-WB1** | 1 | 3.5 | 4.2 |
| **RA-WP1** | -23 | -3.3 | -2.2 |
| **RB-WP1** | 20 | 0.9 | 0.9 |
| **RP-WB1** | -5 | -2.7 | -2.6 |
| **RP-WP1** | 3 | -0.5 | -0.3 |
| **SK-WB1** | -9 | -4.4 | -4.3 |
| **SK-WP1** | -4 | -1.9 | -1.7 |
| **YF-OT1** | -5 | -3.9 | -3.9 |
| **YF-WB1** | -6 | -0.2 | 0.1 |
| **YF-WB2** | -9 | -0.9 | -0.7 |
| **YF-WP1** | 2 | -0.4 | 0.1 |
| **ZA-WS2** | -9 | -3.7 | -3.6 |
| **ZA-WP1** | -14 | -2.4 | -1.7 |
| **ZA-WR1** | -6 | -3.3 | -3.2 |
| **ZA-WS1** | -5 | -1.7 | -1.6 |
| **ZB-WB1** | 17 | 3.7 | 4.4 |
| **ZB-WP1** | -14 | -1.4 | -0.7 |
| **ZB-WS1** | -10 | -3.4 | -3.3 |



## 3.5. SEDIMENT ANALYSIS

All samples were air dried, hand crushed and sieved to < 2 mm, as required by many analytical methods (e.g. Rhoades, 1982). The < 2 mm fraction was used in all subsequent analyses. Sediment colour was described using Munsell® soil colour charts (Anon, 1992). All samples were analysed for bulk mineralogy. Only a group of samples from each pan type was selected for comprehensive analysis i.e. coastal (Ysterfontein samples), brackish-saline pans (Kiekoesvlei, Rooipan north and Droëvlei) and brine-type pans (Rooipan south). Due to

time constraints it was not possible to examine sediments thoroughly, but it is hoped that the samples chosen will illustrate differences or similarities between the pan types.

### 3.5.1. MINERALOGY BY X-RAY DIFFRACTOMETRY (XRD)

XRD was done on sediment samples to gain a qualitative understanding of the mineralogical composition of samples. Analyses are insufficiently rigorous to quantify the relative amounts of various minerals. The bulk mineralogy of all samples was analysed, and selected samples (mentioned in Section 3.5) were analysed for clay mineralogy. For bulk mineralogy approximately 5 g of sample was crushed by hand with acetone in a mortar and pestle until it no longer felt gritty. The powder was packed into an air-mount and loaded into the machine as a randomly oriented powder. Ferricrete and calcrete samples were also analysed by this method. A small portion of reduced sample from Rooipan south was freeze-dried and analysed by XRD to assess changes of mineralogy with oxidation, if any.

Clays (< 2μm) were separated from bulk sample by dispersion with a Virtis Virsonic 475 ultra-sonicator using $Na_2CO_3$ to increase the pH to aid dispersion. The clay was decanted and NaCl added to increase the ionic strength of the suspension and induce flocculation, so increasing the clay concentration (Moore and Reynolds, 1997). After washing in dialysis tubing, the clay was placed onto a glass slide as a suspension and allowed to dry to obtain preferred orientation. Because many clay minerals have similar d-spacings (i.e. separation between crystal layers), sample treatments are required to aid identification, for example heating or treating with glycerol (Whittig and Allardice, 1986). After the first XRD scan, each slide was treated with glycerol by spraying. Glycerol causes the 14 Å peak of smectite to shift to 18Å. Random smectite-mica interstratification will result in a shift of the peak to a d-spacing between 10 and 18 Å, rather than to exactly 18 Å. Another characteristic of random smectite-mica interstratification is broad shouldered peaks (Knesl, 1996; Bühmann, 1986). Interstratified clays were identified by the change in shape of the curve from convex to concave between 12 and 18 Å, rather than from a particular d-spacing.

The samples were analysed on a Philips PW 1390 XRD in the Department of Geological Sciences at UCT. The instrument utilises a copper K-α X-ray tube generating monochromatic x-rays of wavelength 1.542 Å. Minerals comprising less than 3 weight % of a sample are not detectable. The x-ray generator was set at 40 kV and 25 mA. Bragg angles

between 4° and 75° were scanned for bulk samples, analysing each 0.030° increment for 0.5 s, resulting in an approximately 20 minute long scan. The same settings were used for analysis of clay mounts, except only the first 30° were scanned. Scans were interpreted by comparison to standard reference patterns.

### 3.5.2. SOLUBLE SALTS

Preparing a saturated paste extract (SPE) is a standard method for obtaining a representation of salts in a soil solution. The soil:water ratio used in preparing a SPE is the lowest reproducible ratio for which enough water can be extracted for analysis (Rhoades, 1982). The method described by the Non-affiliated Soil Analysis Work Committee (1990) was used to prepare the saturated pastes. Distilled water was added to the air-dried soil samples to form a paste that conformed to the requirements of a saturated paste, i.e. a shiny surface with no free water, but able to flow slightly. The pastes were allowed to equilibrate for two days, after which the pH was measured, and the water extracted using a vacuum pump. The extract was analysed for EC, major ions (IC, hardness titration), and trace elements (ICP-MS). Because the preparation of a SPE is a subjective method, pastes for three of the samples were prepared in duplicate and subjected to the same analyses to ensure that the data from the pastes could be compared. Only a small amount of extract was obtained from sample RB-SS1 and there was insufficient water to perform many of the analyses.



### 3.5.3. INTERSTITIAL WATER

Saturated paste extracts are intended to be representative of the interstitial water, so a comparison between the two extracts is important to gauge the usefulness of SPE data. Interstitial water is often difficult to obtain from soil samples because there is insufficient water. The subaqueous sediments, however, were saturated, and water was easy to extract. Two subaqueous sediment/soil samples, RA-SS1a and RA-SS1b, were maintained wet, and the water was extracted with a vacuum pump. This water is referred to as interstitial water.

### 3.5.4. ORGANIC CARBON

Organic carbon in sediments is oxidised to $CO_2$ by potassium dichromate and sulphuric acid. Dichromate is reduced to chromic ions ($Cr^{3+}$) in the process, the concentration of which can be determined colorimetrically. Finely ground air-dried samples were reacted with sulphuric acid and potassium dichromate for 30 minutes in a digestor at 150°C. Barium chloride was

added to the reacted samples, and the colour allowed to develop overnight. Absorbance at 600 nm was measured with a Spectronic 20 Genesis spectrophotometer. A calibration curve was prepared from 6 sucrose standards, giving a correlation coefficient of 0.9973 This method is suitable for soils with organic carbon contents greater than 0.2% (Baker, 1976).

# 4. Results

## 4.1. RESULTS FOR WATER ANALYSES

### 4.1.1. General chemical parameters

The general chemical parameters determined are listed in Table 4.1. Data for seawater have been included for comparison. The pH range of subsurface samples is 6.5 to 7.4, surface samples 7.6 to 9.3 and springs and seeps 7.6 to 8.6. Density and EC are highest in brine-type pan surface water samples, reaching a maximum of 1.22 g/cm$^3$ and 324 mS/cm respectively. δD values range from 20 to –26 ‰ and $\delta^{18}O$ from 3.7 to –4.4 ‰.

**Table 4.1. General chemical parameters of water samples**

| Sample ID | pH | EC mS/cm | Density g/cm$^3$ | DOC mg/L | δD ‰ | Measured $\delta^{18}O$ ‰ |
|---|---|---|---|---|---|---|
| Seawater* | 8.1 | 54 | 1.02 | nd | 0.0 | 0.0 |
| BA-WP1 | 7.9 | 163 | 1.15 | nd | -26 | -1.2 |
| BA-WP2 | 8.0 | 137 | 1.09 | nd | -9 | -2.4 |
| BA-WS1 | 8.0 | 147 | 1.12 | nd | -15 | -2.0 |
| BB-WB1 | 7.4 | 29 | 1.01 | nd | -15 | -3.4 |
| BB-WP1 | 7.7 | 197 | 1.18 | nd | -13 | -1.9 |
| BB-WR1 | 8.7 | 36 | 1.02 | nd | -1 | -1.8 |
| DV-WB1 | 7.4 | 51 | 1.02 | nd | -16 | -2.9 |
| DV-WP1 | 8.7 | 32 | 1.01 | 15.4 | 16 | -1.9 |
| KP-WP1 | 8.1 | 183 | 1.16 | nd | -14 | -1.5 |
| OT-WR1 | 8.6 | 11 | 1.00 | 15.0 | -2 | -2.8 |
| RA-WB1 | 6.5 | 161 | 1.11 | nd | 1 | 3.5 |
| RA-WP1 | 7.6 | 324 | 1.19 | nd | -23 | -3.3 |
| RB-WP1 | 9.3 | 2 | 1.00 | nd | 20 | 0.9 |
| RP-WB1 | 7.3 | 37 | 1.01 | 17.8 | -5 | -2.7 |
| RP-WP1 | 8.3 | 92 | 1.05 | nd | 3 | -0.5 |
| SK-WB1 | 6.6 | 23 | 1.01 | nd | -9 | -4.4 |
| SK-WP1 | 8.9 | 80 | 1.04 | nd | -4 | -1.9 |
| YF-WB1 | 7.4 | 102 | 1.05 | nd | -6 | -0.2 |
| YF-WB2 | 7.2 | 93 | 1.04 | nd | -9 | -0.9 |
| YF-WP1 | 7.8 | 130 | 1.07 | nd | 2 | -0.4 |
| ZA-WS2 | 7.6 | 10 | 1.00 | 1.9 | -9 | -3.7 |
| ZA-WP1 | 7.7 | 197 | 1.19 | nd | -14 | -2.4 |
| ZA-WR1 | 8.3 | 24 | 1.01 | 13.9 | -6 | -3.3 |
| ZA-WS1 | 8.4 | 53 | 1.02 | nd | -5 | -1.7 |
| ZB-WB1 | 6.9 | 31 | 1.13 | nd | 17 | 3.7 |
| ZB-WP1 | 7.9 | 182 | 1.14 | nd | -14 | -1.4 |
| ZB-WS1 | 7.7 | 6 | 1.00 | nd | -10 | -3.4 |

* From Faure (1992) nd – analysis not done

### 4.1.2. MAJOR ION RESULTS

Major ion data are given in Table 4.2. TDS was calculated by summation of major ions as indicated in the Appendix A. Seawater is included for comparison. The range in concentrations is large, in some cases extending over 2 orders of magnitude, for example Cl concentration ranges from 17 mmol/kg to 4855 mmol/kg.

**Table 4.2. Major ion chemistry of water samples (concentrations in mmol/kg unless otherwise stated)**

| Sample ID | $Na^+$ | $K^+$ | $Mg^{2+}$ | $Ca^{2+}$ | $F^-$ (μmol/kg) | $Cl^-$ | $Br^-$ | $SO_4^{2-}$ | Alkalinity | TDS (g/L) |
|---|---|---|---|---|---|---|---|---|---|---|
| **Seawater*** | 456 | 10 | 52 | 10.0 | 66 | 534 | 0.84 | 27 | 2.30 | 35 |
| **BA-WP1** | 1787 | 38 | 643 | 5.0 | 38 | 3243 | 5.42 | 211 | 9.27 | 224 |
| **BA-WP2** | 2001 | 17 | 173 | 6.7 | 60 | 2472 | 1.18 | 154 | 4.62 | 168 |
| **BA-WS1** | 2325 | 50 | 514 | 4.7 | 50 | 3063 | 3.89 | 287 | 8.34 | 231 |
| **BB-WB1** | 287 | 3 | 34 | 9.8 | 105 | 331 | 0.13 | 26 | 5.31 | 23 |
| **BB-WP1** | 4283 | 35 | 185 | 18.2 | 11 | 4855 | 1.17 | 330 | 0.87 | 367 |
| **BB-WR1** | 265 | 3 | 32 | 5.1 | 99 | 374 | 0.18 | 25 | 4.70 | 24 |
| **DV-WB1** | 502 | 5 | 56 | 19.1 | 219 | 622 | 0.26 | 40 | 4.79 | 41 |
| **DV-WP1** | 281 | 6 | 43 | 17.1 | 123 | 345 | 0.27 | 43 | 1.12 | 25 |
| **KP-WP1** | 4361 | 25 | 191 | 12.4 | 11 | 4296 | 2.38 | 405 | 2.05 | 349 |
| **OT-WR1** | 83.0 | 2 | 13 | 5.6 | 37 | 117 | 0.06 | 9 | 1.39 | 8 |
| **RA-WB1** | 2713 | 21 | 260 | 18.5 | 7 | 3033 | 2.22 | 215 | 3.26 | 223 |
| **RA-WP1** | 4642 | 27 | 141 | 10.2 | 11 | 4767 | 1.19 | 350 | 0.62 | 379 |
| **RB-WP1** | 25 | 0.4 | 0.3 | 0.1 | 79 | 17 | 0.02 | 1 | 5.06 | 2 |
| **RP-WB1** | 380 | 8 | 33 | 12.4 | 23 | 394 | 0.25 | 45 | 4.16 | 29 |
| **RP-WP1** | 937 | 21 | 104 | 25.2 | 19 | 1102 | 0.81 | 98 | 1.64 | 79 |
| **SK-WB1** | 170 | 2 | 34 | 10.2 | 61 | 244 | 0.07 | 17 | 2.58 | 16 |
| **SK-WP1** | 781 | 12 | 89 | 13.3 | 23 | 957 | 0.55 | 62 | 1.38 | 64 |
| **YF-WB1** | 1041 | 16 | 114 | 39.2 | 19 | 1288 | 0.83 | 90 | 1.32 | 88 |
| **YF-WB2** | 1006 | 17 | 134 | 5.5 | 42 | 897 | 5.99 | 58 | 2.60 | 68 |
| **YF-WP1** | 1844 | 25 | 160 | 37.0 | 17 | 2006 | 1.32 | 186 | 0.97 | 150 |
| **ZA-WS2** | 100 | 1 | 12 | 5.6 | 95 | 140 | 0.07 | 11 | 1.86 | 9 |
| **ZA-WP1** | 3796 | 26 | 186 | 10.2 | 74 | 4574 | 1.16 | 275 | 2.10 | 335 |
| **ZA-WR1** | 193 | 2 | 24 | 9.7 | 69 | 256 | 0.15 | 18 | 2.13 | 17 |
| **ZA-WS1** | 492 | 5 | 60 | 18.4 | 138 | 598 | 0.33 | 33 | 3.79 | 39 |
| **ZB-WB1** | 2256 | 19 | 284 | 13.1 | 48 | 2581 | 0.05 | 141 | 2.58 | 187 |
| **ZB-WP1** | 3655 | 43 | 166 | 13.0 | 30 | 3807 | 1.55 | 373 | 1.45 | 298 |
| **ZB-WS1** | 49 | 0.4 | 6 | 1.7 | 226 | 56 | 0.03 | 4 | 3.24 | 4 |

* From Faure (1992)

### 4.1.3. TRACE ELEMENT CHEMISTRY

Trace element chemistry for water samples is given in Table 4.3. Seawater has been included for comparison. Most trace element concentrations are below 1 mmol/kg.

**Table 4.3. Trace element data for water samples (concentration in μmol/kg unless otherwise stated).**

| Sample ID | Li | B | Al | Si | As | Se | Rb | Sr | Ba | U nmol/kg |
|---|---|---|---|---|---|---|---|---|---|---|
| **Seawater*** | 24 | 416 | 1 | 100 | 1.7 | 0.1 | 0.0 | 87 | 0.1 | 13 |
| **BA-WP1** | 150 | 6610 | 136 | 133 | 9.6 | 42.1 | 7.0 | 82 | 1.7 | 131 |
| **BA-WP2** | 40 | 1462 | 118 | 147 | 3.8 | 9.2 | 1.8 | 74 | <0.1 | 92 |
| **BA-WS1** | 106 | 4652 | 153 | 139 | 6.7 | 31.2 | 5.1 | 63 | 0.8 | 108 |
| **BB-WB1** | 14 | 187 | 5 | 258 | 0.7 | 1.3 | 0.1 | 70 | 0.8 | 59 |
| **BB-WP1** | 24 | 803 | 155 | 7 | 6.7 | 8.7 | 0.8 | 266 | 3.6 | 17 |
| **BB-WR1** | 14 | 393 | 8 | 123 | 0.8 | 1.7 | 0.3 | 50 | 2.1 | 46 |
| **DV-WB1** | 21 | 144 | 1 | 162 | 0.7 | 2.4 | 0.8 | 114 | 1.9 | 538 |
| **DV-WP1** | 8 | 368 | 5 | 1 | 0.6 | 2.0 | 0.4 | 116 | 1.2 | 232 |
| **KP-WP1** | 24 | 3485 | 165 | 9 | 8.3 | 17.9 | 0.6 | 181 | 2.7 | 63 |
| **OT-WR1** | 1 | 51 | 21 | 287 | 0.2 | 0.5 | 0.3 | 29 | 0.6 | 20 |
| **RA-WB1** | 36 | 445 | 474 | 81 | 5.0 | 16.4 | 0.7 | 275 | 3.7 | <10 |
| **RA-WP1** | 23 | 1079 | 138 | 6 | 6.2 | 7.9 | 0.3 | 187 | 0.9 | <10 |
| **RB-WP1** | 2 | 303 | 62 | 122 | 0.2 | 0.1 | 0.1 | 1 | 2.3 | 13 |
| **RP-WB1** | 28 | 499 | 5 | 168 | 0.7 | 1.6 | 1.0 | 103 | 0.2 | 51 |
| **RP-WP1** | 58 | 1438 | 4 | 2 | 1.8 | 5.4 | 2.6 | 334 | 0.2 | <10 |
| **SK-WB1** | 1 | 125 | 7 | 286 | 0.4 | 0.9 | 0.1 | 59 | 2.5 | <10 |
| **SK-WP1** | 1 | 775 | 13 | 2 | 1.6 | 4.4 | 0.8 | 168 | 1.0 | 80 |
| **YF-WB1** | 15 | 312 | 6 | 335 | 2.2 | 6.4 | 2.1 | 272 | 1.0 | <10 |
| **YF-WB2** | 166 | 7309 | 151 | 677 | 10.6 | 46.6 | 7.8 | 91 | 1.9 | 145 |
| **YF-WP1** | 38 | 880 | 217 | 17 | 1.9 | 8.4 | 3.1 | 399 | 0.2 | 51 |
| **ZA-WS2** | 18 | 72 | 5 | 560 | 0.2 | 0.6 | 0.4 | 26 | 0.4 | 269 |
| **ZA-WP1** | 22 | 2630 | 182 | 10 | 7.9 | 7.2 | 0.9 | 245 | 0.6 | 194 |
| **ZA-WR1** | 3 | 131 | 3 | 167 | 0.4 | 1.1 | 0.2 | 48 | 1.0 | 59 |
| **ZA-WS1** | 17 | 315 | 11 | 127 | 1.1 | 2.5 | 0.3 | 118 | 1.2 | 672 |
| **ZB-WB1** | 1 | 45 | 19 | 19 | 0.2 | 0.4 | 0.3 | 25 | 0.5 | 18 |
| **ZB-WP1** | 27 | 1732 | 108 | 5 | 7.1 | 10.5 | 1.5 | 283 | 6.0 | 95 |
| **ZB-WS1** | 4 | 123 | 4 | 168 | 0.1 | 0.6 | 1.4 | 12 | 0.4 | 128 |

* From Faure (1992)

## 4.2. RESULTS FOR SEDIMENT/SOIL SAMPLES

### 4.2.1. GENERAL CHEMICAL PARAMETERS

The general chemical parameters determined on the sediment/soil samples are listed in Table 4.4. The pH is within the same range as for water samples. Organic carbon concentrations are generally low.

**Table 4.4. General chemical parameters of sediment/soil samples**

| Sample ID | pH (SP) | pH ($H_2O$) | pH (KCl) | EC mS/cm | Density g/cm$^3$ | OC % |
|---|---|---|---|---|---|---|
| **DV-SS1a** | 7.6 | 7.8 | 7.5 | 25 | 1.01 | 0.20 |
| **DV-SS1b** | 7.7 | 7.9 | 6.9 | 30 | 1.00 | 0.13 |
| **DV-SS2** | 7.7 | 7.9 | 7.8 | 50 | 1.02 | 1.73 |
| **KV-SS1b** | 8.2 | 8.8 | 7.5 | 4 | 1.00 | 0.29 |
| **RA-SS1a** | 6.9 | 8.1 | 8.0 | 140 | 1.23 | 0.82 |
| **RA-SS1b** | 7.3 | 8.3 | 8.2 | 178 | 1.20 | 0.29 |
| **RA-SS3a** | 7.8 | 8.4 | 8.4 | 164 | 1.13 | 0.33 |
| **RA-SS3b** | 7.9 | 8.2 | 8.2 | 136 | 1.10 | 0.43 |
| **RA-SS3c** | 7.8 | 7.8 | 7.8 | 121 | 1.06 | 0.13 |
| **RA-SS3d** | 7.5 | 7.9 | 7.3 | 136 | 1.11 | bdl |
| **RB-SS1** | 9.0 | 9.7 | 8.2 | 6 | 1.00 | 0.75 |
| **YF-SS1a** | 7.5 | 8.0 | 7.8 | 123 | 1.10 | 1.15 |
| **YF-SS1b** | 7.4 | 7.9 | 7.8 | 98 | 1.06 | 0.39 |
| **YF-SS1c** | 7.9 | 8.1 | 8.3 | 95 | 1.05 | 0.12 |

bdl – below detection limits SP = saturated paste OC=organic C

### 4.2.2. SATURATED PASTE EXTRACT DATA

*Major ion chemistry*

Major ion concentrations determined in the SPE are listed in Table 4.5.

*Trace element chemistry*

Trace element chemistry for the SPE is given in Table 4.6. Silica was not determined colorimetrically in the SPE due to insufficient sample volume and data listed here were determined by ICP-MS.

**Table 4.5. Major ion concentrations in saturated paste extracts (mmol/kg unless otherwise stated).**

| | $Na^+$ | $K^+$ | $Mg^{2+}$ | $Ca^{2+}$ | $Cl^-$ | $Br^-$ | $SO_4^{2-}$ | TDS (g/kg) |
|---|---|---|---|---|---|---|---|---|
| **DV-SS1a** | 229 | 3 | 14 | 7.0 | 271 | <0.01 | 19 | 18 |
| **DV-SS1b** | 241 | 3 | 22 | 7.9 | 291 | <0.01 | 13 | 18 |
| **DV-SS2** | 412 | 9 | 85 | 23.0 | 525 | 0.42 | 67 | 39 |
| **KV-SS1b** | 27.4 | 1 | 1 | 1.7 | 31 | <0.01 | 2 | 2 |
| **RA-SS1a** | 2396 | 46 | 1300 | 2.4 | 4655 | 9.04 | 536 | 307 |
| **RA-SS1b** | 3266 | 33 | 630 | 5.5 | 4604 | 5.42 | 257 | 337 |
| **RA-SS3a** | 2887 | 18 | 204 | 21.4 | 3363 | 0.02 | 160 | 235 |
| **RA-SS3b** | 1859 | 20 | 161 | 12.8 | 2197 | 1.56 | 107 | 150 |
| **RA-SS3c** | 1402 | 9 | 125 | 10.9 | 1658 | 1.24 | 37 | 105 |
| **RA-SS3d** | 2147 | 14 | 218 | 16.7 | 2687 | 2.03 | 103 | 179 |
| **RB-SS1** | 54 | 1 | nd | nd | 34 | 0.02 | 2 | 3 |
| **YF-SS1a** | 1732 | 20 | 190 | 38.7 | 2145 | 1.18 | 119 | 148 |
| **YF-SS1b** | 1129 | 17 | 110 | 47.6 | 1468 | 0.92 | 74 | 96 |
| **YF-SS1c** | 1074 | 14 | 100 | 45.2 | 1340 | 0.71 | 77 | 85 |

nd – analysis not done

**Table 4.6. Trace element chemistry of saturated paste extracts (concentrations in μmol/kg unless otherwise stated).**

| | Li | B | Al | Si | As | Se | Rb | Sr | Ba | U nmol/kg |
|---|---|---|---|---|---|---|---|---|---|---|
| **DV-SS1a** | 1 | 4 | <1 | <10 | <0.1 | 0.1 | <0.1 | <1 | <0.1 | <10 |
| **DV-SS1b** | 1 | 1 | <1 | <10 | <0.1 | <0.1 | <0.1 | <1 | <0.1 | <10 |
| **DV-SS2** | 18 | 911 | <1 | 205 | 0.9 | 3.2 | 0.8 | 151 | 0.9 | 786 |
| **KV-SS1b** | 1 | 162 | 4 | 207 | 0.4 | 0.2 | <0.1 | 8 | 1.0 | 29 |
| **RA-SS1a** | 222 | 6455 | <1 | <10 | 5.6 | 58.8 | 3 | 46 | <0.1 | 4 |
| **RA-SS1b** | 137 | 2041 | 141 | <10 | 4.9 | 38.3 | 2 | 81 | <0.1 | 8 |
| **RA-SS3a** | 1 | 145 | <1 | 223 | 0.3 | 0.3 | 0.1 | 8 | 0.9 | 23 |
| **RA-SS3b** | 35 | 205 | 65 | <10 | 2.1 | 10.4 | 0.8 | 140 | 3.3 | 71 |
| **RA-SS3c** | 20 | 275 | 100 | <10 | 2.2 | 9.0 | 0.5 | 131 | 1.0 | <10 |
| **RA-SS3d** | 25 | 199 | 108 | <10 | 2.8 | 14.3 | 0.3 | 237 | 1.9 | <10 |
| **RB-SS1** | 3 | 948 | 5 | 375 | 1.0 | 0.4 | <0.1 | 1 | 0.3 | 83 |
| **YF-SS1a** | 31 | 575 | 147 | <10 | 4.7 | 8.9 | 2.2 | 384 | 1.4 | <10 |
| **YF-SS1b** | 16 | 262 | <1 | 45 | 1.4 | 5.2 | 1.7 | 290 | 1.2 | <10 |
| **YF-SS1c** | 12 | 608 | <1 | <10 | 1.3 | 7.4 | 1.8 | 262 | 1.8 | 33 |

### 4.2.3. INTERSTITIAL WATERS

Results of analyses completed on interstitial waters extracted from RA-SS1a and RA-SS1b are listed in Table 4.7. The saturated paste extracts for the same samples are included for comparison. Halite precipitated in the interstitial water of RA-SS1a.

**Table 4.7. Comparison between interstitial water and saturated paste extract**

| | Interstitial water | | Saturated paste extract | |
|---|---|---|---|---|
| | RA-SS1a | RA-SS1b | RA-SS1a | RA-SS1b |
| **pH** | 7.0 | 6.5 | 6.9 | 7.3 |
| **Density (g/cm$^3$)** | 1.21 | 1.20 | 1.23 | 1.20 |
| **$Na^+$ (mmol/kg)** | 3670 | 3574 | 2396 | 3266 |
| **$K^+$ (mmol/kg)** | 28 | 32 | 46 | 33 |
| **$Mg^{2+}$ (mmol/kg)** | 583 | 567 | 1300 | 630 |
| **$Ca^{2+}$ (mmol/kg)** | 5.6 | 6.3 | 2.4 | 5.5 |
| **$Cl^-$ (mmol/kg)** | 4565 | 4385 | 4655 | 4604 |
| **$Br^-$ (mmol/kg)** | 9.57 | 8.52 | 9.04 | 5.42 |
| **$SO_4^{2-}$ (mmol/kg)** | 225 | 310 | 536 | 257 |
| **TDS (g/L)** | 304 | 284 | 307 | 281 |
| **Li (µmol/kg)** | 128 | 85 | 222 | 137 |
| **B (µmol/kg)** | 4440 | 2544 | 6457 | 2044 |
| **Al (µmol/kg)** | <1 | 4 | <1 | 141 |
| **Si (µmol/kg)** | 96 | <10 | <10 | <10 |
| **As (µmol/kg)** | 6.0 | 4.4 | 5.6 | 4.9 |
| **Se (µmol/kg)** | 34 | 27 | 59 | 38 |
| **Rb (µmol/kg)** | 1.3 | 1.0 | 3.1 | 1.6 |
| **Sr (µmol/kg)** | 131 | 96 | 46 | 81 |
| **Ba (µmol/kg)** | 0.4 | 2.0 | <0.1 | <0.1 |
| **U (nmol/kg)** | 17 | 27 | <10 | <10 |

### 4.2.4. Department of Water Affairs (DWAF) groundwater data

The Department of Water Affairs maintains a geohydrological database consisting of borehole locations and basic chemical analyses of groundwater. Data from 5 boreholes in the Darling area and 1 at Ysterfontein were obtained from the DWAF database, and have been included in many of the plots. There are limitations to using this data:

- The analytical methods used to obtain this data are not known, and may not be comparable with results from the current study.
- Although borehole coordinates are recorded, the depth of sampling within the borehole is not (Timmerman, 1986). The data can only be considered to represent regional groundwater rather than a particular aquifer.
- The boreholes have been sampled at various times since 1976. There may be seasonal or long-term changes in groundwater chemistry that will influence interpretation.

For these reasons, although groundwater data are plotted on many graphs for comparison, no attempt is made to analyse the data in depth. Data for DWAF boreholes are listed in Table 4.8.

**Table 4.8: Regional groundwater data obtained from the DWAF geohydrological database. All results in mmol/L unless otherwise stated. Sample name derived from farm on which borehole is located.**

| | pH | Na | K | Mg | Ca | F (µmol/L) | Cl | $SO_4$ | Alk | Si (µmol/L) |
|---|---|---|---|---|---|---|---|---|---|---|
| **KV BH** | 8.3 | 59.6 | 0.82 | 5.6 | 3.0 | 136 | 67.3 | 2.9 | 2.2 | 256 |
| **RA BH** | 7.4 | 12.4 | 0.11 | 1.3 | 0.7 | 39 | 14.2 | 0.3 | 0.7 | 231 |
| **KP BH1** | 7.8 | 26.2 | 0.15 | 2.9 | 2.5 | 41 | 33.4 | 0.5 | 1.6 | 231 |
| **KP BH2** | 8.1 | 70.5 | 0.24 | 4.9 | 2.6 | 86 | 70.8 | 3.1 | 5.3 | 499 |
| **SK BH** | 6.8 | 0.6 | 0.02 | 0.1 | 0.3 | 23 | 0.7 | 0.2 | 0.3 | 28 |
| **ZA BH** | 7.6 | 78.0 | 0.69 | 12.3 | 0.1 | 81 | 92.3 | 4.0 | 1.5 | nd |
| **YF BH** | 7.3 | 18.5 | 0.50 | 1.3 | 1.3 | 23 | 21.1 | 0.3 | 2.0 | 30 |

nd = no data BH = borehole

### 4.2.5. MINERALOGY

*Bulk mineralogy*

Bulk mineralogy was determined by both XRD, and observations in the field and laboratory. XRD scans of bulk samples reveal that inland samples are distinguishable by strong quartz peaks while coastal pans are dominated by peaks of secondary precipitates, such as calcite and gypsum. All XRD scans referred to are included in Appendix B. Examination of inland samples under a binocular microscope reveals very fine-grained quartz particles (sometimes Fe-oxides and feldspar) formed into aggregates by clay minerals and secondary precipitates like halite and calcite. Feldspars were detected only at Droëvlei. A summary of mineralogy determined by XRD is given in Table 4.9. Clay mineral peaks in XRD scans of bulk samples are difficult to ascribe to a particular clay mineral, and are described generically as "clay".

Calcite in bulk samples is referred to as either Mg-calcite or as calcite, depending on the position of the 211 peak. There is a linear relationship between the mole fraction of $MgCO_3$ in calcite and the d-spacing (in nm) of the 3 Å peak. This relationship is (Doner and Lynn, 1989):

$$d(211) = 0.3033 - 0.0271 MgCO_3 \quad (r^2 = 0.9905)$$

XRD analyses in this study were not performed with sufficient rigor to apply this equation with any confidence. Instead, calcite is qualitatively classified as either "calcite" if the 211 peak is close to 3.05 Å (no $MgCO_3$) or "Mg-calcite" if the 211 peak is below 3.02 Å (approximately 1 to 20 mole % $MgCO_3$). High-Mg calcite is specifically defined as containing 11-19 mole % $MgCO_3$ by substitution, but Mg contents in calcite are not sufficiently constrained to use this term (Drever, 1997).

Minerals of granitic origin, namely quartz, plagioclase and K-feldspar, were detected in all Droëvlei samples (Figure B.1, Appendix B). The proportion of clay is much greater in the pan floor samples than in any of the pan edge samples. Halite was found only in DV-SS3, where it probably formed by capillary evaporation.

Rooipan south brine-type pan sediments were sampled fairly comprehensively and were all found to contain quartz and halite. Mg-calcite is found only in the top two layers of sediment, and the amount of Mg present in RA-SS3b is less than that in RA-SS3a. The shift in d-spacing is evident on the XRD scan (Figure B.4, Appendix B). Sample RA-SS3c has orange colours indicative of iron oxides, but none were detected. However, a sample collected from the same relative position at Zwartwater north (ZB-SS1) had similar characteristics, and was found to contain goethite (Figure B.5). Minerals present in the subaqueous sediments of Rooipan south (RA-SS1a and b) are quartz, halite, gypsum, high-Mg calcite and epsomite. It is not known whether gypsum, epsomite and halite are present in the sediments or precipitated on air-drying. Epsomite was found only in the surface layer, and only in air-dried sediments. The sulphates may have formed as oxidation products of sulphides in the sediment. A single peak at 2.89 Å could indicate the presence of dolomite.

The presence of iron monosulphides (FeS) in RA-SS1a is indicated by a number of field and laboratory observations:

- Black colour
- Release of $H_2S$ on exposure to dilute HCl
- Fading of black colour on exposure to air due to the extremely unstable nature of monosulphides.
- Once the soil is oxidised, it no longer reacts with HCl (Fanning *et al.,* 1993)

Pyrite does not exhibit these properties. XRD identification of monosulphides was not successful because of their low concentration, small crystal size and poor crystallinity (Fanning *et al.,* 1993).

In contrast to the inland pans, the coastal pans have large volumes of gypsum and little quartz. No black reducing muds were found, and silicate clay contents are low. The dominant minerals are calcite and gypsum. The two samples from Rooipan differ greatly from each other. RP-SS1a contains gypsum and calcite whereas RP-SS1b is pure quartz and has no detectable gypsum, calcite or halite (Figure B.6). The calcite has a low Mg content

(about 1 mole % $MgCO_3$), reflecting the lower Mg:Ca ratio of the water in coastal pans. Depth profiles at both sites YF-SS1 and YF-SS2 illustrate similar mineralogical trends (Figure 2.xx). These trends are clearly visible in the XRD scans of samples from Ysterfontein (Figure 5.30). The gypsum dominates in the surface (a) samples, and calcite peak dominates in the subsurface (b) samples. Underlying these two is clean quartzitic sand similar to RP-SS1b. Halite is the only evaporite identified by XRD in this sand, but it may have formed on air-drying of the sample. Halite concentration decreases down the profile. YF-SS3a is a sample of the laterally extensive economic gypsum horizon currently being mined, with gypsum, halite and calcite.

**Table 4.9: Mineralogy of bulk samples.**

| Sample | Pan type | Mineral (d-spacing of characteristic peak in Å) |
|---|---|---|
| DV-SS1a | Brackish-saline | Quartz (3.34), K-feldspar (3.26) |
| DV-SS1b | Brackish-saline | Quartz (3.34), K-feldspar (3.26), plagioclase (3.19), clay (4.45) |
| DV-SS2 | Brackish-saline | Quartz (3.34), Mg-calcite (3.01), K-feldspar (3.26), plagioclase (3.19), clay (4.45) |
| DV-SS3a | Brackish-saline | Quartz (3.34), halite (2.82), K-feldspar (3.26), clay (4.45) |
| KV-SS1b | Brackish-saline | Quartz (3.34), clay (7.06), Mg-calcite (3.01) |
| RB-SS1 | Brackish-saline | Quartz (3.34), Mg-calcite (3.00), clay (4.45) |
| RA-SS1a | Brine | Quartz (3.34), halite (2.82), Mg-calcite (3.00), epsomite (5.36), gypsum (7.6), dolomite? (2.89) |
| RA-SS1a | Freeze-dried | Quartz (3.34), halite (2.82), Mg-calcite (3.00), gypsum (7.6), dolomite? (2.89) |
| RA-SS1b | Brine | Quartz (3.34), halite (2.82), Mg-calcite (3.02), clay (4.45) |
| RA-SS1b | Freeze-dried | Quartz (3.34), halite (2.82), Mg-calcite (3.02), clay (4.45), gypsum (7.06) |
| RA-SS3a | Brine | Quartz (3.34), Mg-calcite (2.98), halite (2.82) |
| RA-SS3b | Brine | Quartz (3.34), halite (2.82), Mg-calcite (3.02), clay (4.44) |
| RA-SS3c | Brine | Quartz (3.34), halite (2.82), clay (4.44), witherite? (3.72) |
| RA-SS3d | Brine | Quartz (3.34), halite (2.82) |
| ZB-SS1 | Brine | Quartz (3.34), halite (2.82), clay (7.20), goethite (4.18) |
| RP-SS1a | Coastal | Gypsum (7.60), quartz (3.34), Mg-calcite (3.03), halite (2.82) |
| RP-SS1b | Coastal | Quartz (3.34) |
| YF-SS1a | Coastal | Gypsum (7.60), calcite (3.05), halite (2.82), quartz (3.34) |
| YF-SS1b | Coastal | Quartz (3.34), calcite (3.05), halite (2.82) |
| YF-SS1c | Coastal | Quartz (3.34), halite (2.82, calcite (3.05) |
| YF-SS2a | Coastal | Gypsum (7.60), halite (2.82), quartz (3.34), calcite (3.05) |
| YF-SS2b | Coastal | Calcite (3.05), gypsum (7.60), quartz (3.34), halite (2.82) |
| YF-SS3a | Coastal | Gypsum (7.60), halite (2.82), calcite (3.05) |

*Clay mineralogy*

Clay mineralogy from all inland pans is remarkably similar. The coastal pans are distinguished from the inland pans by the presence of carbonate minerals in the clay fraction. Clay mineralogy is summarised in Table 4.10. All samples contain kaolinite, most contain mica, and many have smectite and randomly interstratified smectite-mica (Figure B.8 – B.12). Sepiolite was tentatively identified in RB-SS1 from Rooipan north (Figure B.9). The clay layers beneath pan edges are reddish in colour because of iron oxides.

*Secondary precipitates and soluble salts*

The mineralogy of secondary precipitates and soluble salts is summarised in Table 4.11. Three types of precipitates were scanned, ferricretes, calcretes and soluble salts. Ferricretes contain quartz, haematite, goethite, Mg-calcite and kaolinite. Ferricrete horizons were found adjacent to Zwartwater north and Burgerspan south, and are composed of subrounded to subangular quartz grains and kaolinite gradually being replaced by calcite, goethite and haematite (Figure B.13). Calcretes are made up of quartz, Mg-calcite, K-feldspar, halite and kaolinite. Calcrete was found outcropping adjacent to Rooipan south, Rooipan north and Burgerspan south, and in the pan floor sediments of Rooipan north, Droëvlei and Kiekoesvlei. It is composed of micrite (micro-crystalline calcite) encasing quartz grains. Calcrete samples contain quartz and K-feldspar as cemented grains, Mg-calcite, kaolinite and possibly dolomite in sample RB-SE1 from Rooipan north (Figure B.13).

Two salt samples were analysed, one collected from a salt heap adjacent to the mined pan Burgerspan south (BA-SE1), and another from an *in situ* crust of salt beneath the surface of Rooipan south (RA-SE2). The mined sample consists almost exclusively of halite, but the subaqueous salt sample from Rooipan south contains a small amount of gypsum (Figure B.15).

**Table 4.10: Mineralogy of clay samples**

| Sample | Pan type | Mineral (d-spacing of characteristic peak in Å) |
|---|---|---|
| DV-SS1b | Brackish-saline | Smectite (14.4; glycerol 18.2), mica (10), kaolinite (7.2) |
| DV-SS2 | Brackish-saline | Mica (10), kaolinite (7.2) |
| KV-SS1b | Brackish-saline | Kaolinite (7.3), mica (10.2) |
| RB-SS1 | Brackish-saline | Mica (10.2), kaolinite (7.2), sepiolite? (9.2) |
| RA-SS1a | Brine | Kaolinite (7.2), mica (10), interstratified smectite-mica (shift with glyceration) |
| RA-SS1b | Brine | Kaolinite (7.2), mica (10), interstratified smectite-mica (shift with glyceration) |
| RA-SS3a | Brine | Kaolinite (7.2), mica (10) |
| RA-SS3b | Brine | Kaolinite (7.2), mica (10), interstratified smectite-mica (shift with glyceration) |
| RA-SS3c | Brine | Kaolinite (7.2), mica (10), interstratified smectite-mica (shift with glyceration) |
| RA-SS3d | Brine | Interstratified smectite-mica (shift with glyceration), kaolinite (7.2) |
| YF-SS1a | Coastal | Calcite (3.05), mica (10), gypsum (2.86), kaolinite (7.3) |
| YF-SS1b | Coastal | Calcite (3.05) |
| YF-SS1c | Coastal | Kaolinite (7.3), mica (10), interstratified smectite-mica (shift with glyceration) |

**Table 4.11: Mineralogy of evaporite samples.**

| Sample | Sample type | Mineral (d-spacing of characteristic peak in Å) |
|---|---|---|
| BA-SE3 | Ferricrete | Quartz (3.34), Mg-calcite (3.02), haematite (2.52), kaolinite (7.19), goethite (4.18) |
| ZB-SE2 | Ferricrete | Quartz (3.34), goethite (4.18), haematite (2.52), Mg-calcite (3.01) |
| ZB-SE2 | Clay dispersion | Kaolinite (7.19), goethite (4.18), haematite (2.52) |
| ZB-SE3 | Ferricrete | Quartz (3.34), haematite (2.52), goethite (4.18), kaolinite (7.19) |
| RA-SE2 | Efflorescence | Quartz (3.34), Mg-calcite (3.02) |
| RB-SE2 | Efflorescence | Quartz (3.34), kaolinite (4.45), Mg-calcite (3.02) |
| RB-SE1 | Calcrete | Mg-calcite (3.02), quartz (3.34), kaolinite (7.16), dolomite? (2.89) |
| DV-SE1 | Calcrete | Quartz (3.34), Mg-calcite (3.02), kaolinite (4.45) |
| BA-SE1 | Soluble salts | Halite (2.82) |
| RA-SE1 | Soluble salts | Halite (2.82), gypsum (7.56) |

*Salts obtained from drying water samples*

A variety of salts were identified from salts obtained by drying water samples, although halite dominated in all samples. However, many of the salts have not been identified. The minerals identified are summarised in Table 4.12.

**Table 4.12: Mineralogy of salts obtained from drying water samples.**

| Sample | Pan type | Mineral (d-spacing of characteristic peak in Å) |
|---|---|---|
| BB-WP1 | Brine | Halite (2.82), thenardite ($Na_2SO_4$ (2.78) |
| RA-WB1 | Brine | Halite (2.82), thenardite (2.78) |
| SK-WB1 | Brackish-saline | Halite (2.82) |
| YF-WB1 | Coastal | Halite (2.82), thenardite (2.78) |
| YF-WP1 | Coastal | Halite (2.82), gypsum (7.66) |
| BB-WR1 | Stream | Halite (2.82), epsomite ($MgSO_4$) (4.23) |
| OT-WR1 | Stream | Halite (2.82) |

### 4.2.6. ASSESSMENT OF DATA QUALITY

Full results of duplicate and standard analyses, as well as comparison of methods can be found in Appendix A.

*Charge balance*

A solution is expected to maintain the electrical neutrality of the compounds it dissolves. The charge balance of a solution is the percentage difference between the sum of cations and anions (in $mmol_c/L$), and it gives an indication of the quality of the data. Charge balance calculations were performed on the chemical analyses of waters and saturated pastes according to the method outlined by Eaton *et al.* (1995). The charge balance should not exceed ±5%. Out of 41 analyses of water samples, 17 have charge balances within the 5% limit and only 2 charge balances exceed 10%. Only 4 of the 15 saturated paste extract analyses have charge balances exceeding 5% and none of the charge balances exceed 10%.

*Uncertainty*

Uncertainty is calculated by summing the bias and precision of a measurement. Precision is a measure of the random error of a method, and is calculated as the percentage of the measurement that encompasses 2 standard deviations from the mean. Precision is estimated by completing duplicate analyses of samples. Bias is a measure of the systematic error of a method, and is estimated by calculating the difference between the measured value of a known standard and its true value, as a percentage of the true value (Ramsey, 2000). Precision calculations have been completed on all samples, but standards were not always available and bias for many techniques is not known. The standard used for many techniques was seawater, which does not have certified values, but gives an indication of the bias of a

method. A summary of the precision, bias and uncertainty for all elements by all methods is given in Table 4.13.

**Table 4.13. Precision, bias and analytical uncertainty**

| Method (standard) | Analyte | Units | Precision (%) | Number duplicates | Bias (%) | Number repeats | Analytical uncertainty (%) | Mean ± uncertainty |
|---|---|---|---|---|---|---|---|---|
| Titration | Alkalinity | mmol/kg | 2 | 13 | nd | | 2 | 2.98 ± 0.06 |
| Isotopes | δD | ‰ | 53 | 9 | nd | | 53 | -12 ± 6 |
| | $\delta^{18}O$ | ‰ | 86 | 8 | nd | | 86 | -2.3 ± 2.0 |
| IC | $Na^+$ | mmol/kg | 7 | 13 | 7 | 4 | 14 | 1522 ± 220 |
| (SW*) | $K^+$ | mmol/kg | 30 | 13 | 19 | 4 | 48 | 13 ± 6 |
| | $Ca^{2+}$ | mmol/kg | 71 | 13 | 443 | 4 | 514 | 213 ± 1095 |
| | $Mg^{2+}$ | mmol/kg | 77 | 13 | 35 | 4 | 112 | 208 ± 233 |
| | $Cl^-$ | mmol/kg | 9 | 13 | 14 | 3 | 23 | 1699 ± 389 |
| | $SO_4^{2-}$ | mmol/kg | 26 | 13 | 9 | 3 | 35 | 125 ± 44 |
| ICP-MS | Li | µmol/kg | 53 | 41 | 5 | 8 | 58 | 40 ± 23 |
| (NIST-1643d) | B | µmol/kg | 52 | 41 | -4 | 8 | 48 | 1184 ± 555 |
| | Al | µmol/kg | 196 | 41 | 3 | 8 | 199 | 76 ± 151 |
| | Si | µmol/kg | 54 | 41 | 4 | 8 | 58 | 201 ± 145 |
| | Fe | µmol/kg | 110 | 41 | 47 | 8 | 157 | 93 ± 145 |
| | As | µmol/kg | 40 | 41 | 3 | 8 | 43 | 2.9 ± 1.2 |
| | Se | µmol/kg | 53 | 41 | 3 | 8 | 56 | 9.0 ± 5.1 |
| | Br | µmol/kg | 44 | 41 | nd | 8 | 44 | 2566 ± 1139 |
| | Rb | µmol/kg | 49 | 41 | -5 | 8 | 43 | 1.2 ± 0.5 |
| | Sr | µmol/kg | 13 | 41 | 4 | 8 | 17 | 148 ± 25 |
| | Ba | µmol/kg | 27 | 41 | 4 | 8 | 31 | 1.6 ± 0.5 |
| | U | µmol/kg | 25 | 41 | 5 | 8 | 30 | 0.11 ± 0.03 |
| Titration (SW) | Hardness | mmol/kg | 3 | 13 | 1 | 1 | 4 | 108 ± 5 |
| ISE | F | µmol/kg | 7 | 13 | nd | | 7 | 65.9 ± 4.7 |
| Colorimetry | DOC | mg/kg | 18 | 3 | nd | | 18 | 7.25 ± 1.33 |
| Colorimetry | Si | µmol/kg | 33 | 13 | nd | | 33 | 121 ± 3.9 |
| AA (SW) | $Ca^{2+}$ | mmol/kg | 2 | 12 | 9 | 1 | 11 | 14.8 ± 1.6 |
| Calculation (SW) | $Mg^{2+}$ | mmol/kg | 4 | 13 | 13 | 1 | 16 | 93.4 ± 15.3 |
| Colorimetry | OC (seds) | % | 1 | 2 | nd | | 1 | 0.56 ± 0.008 |

* SW = seawater nd = not done

The uncertainty data presented in the table indicates only analytical uncertainty. Sampling uncertainty, which has not been considered, is often a larger source of uncertainty (Ramsey, 2000). Data for Fe and Al, which have a high level of uncertainty, have not been included in the discussion. Metals are often associated with colloidal-sized Fe and Al hydroxide particles and are consequently overestimated during analysis (Eary, 1999). For analytes analysed by

more than one technique, the results with the lowest uncertainty were used. Comparison between data obtained in two different techniques is included in Appendix A.

# 5. Discussion

## 5.1. INTRODUCTION

Brine evolution studies generally consider chemical changes in saline pan water with time, as the water evaporates (e.g. Camur and Mutlu, 1996; Bryant *et al.*, 1994). In this study, samples from all pans were collected at the same point in the saline pan cycle, during the initial flooding stage prior to extensive evaporative concentration. Only minor evaporation could have occurred between flooding (1-2 weeks prior to sampling) and sampling, and all pans would have been subject to roughly the same degree of evaporation. The data presented in this section represent a "snapshot" of each pan's long-term evolution rather than trends due to seasonal brine evolution.

Different sample types, namely surface, subsurface, streams and saturated paste extracts (SPE) from the three pan types have been distinguished on the graphs. The same symbols are used on all graphs (unless otherwise indicated). SPE data compare very well with interstitial water data for the same samples (Table 4.7) and have been included on the graphs. Samples from the mined pan, Burgerspan south, have also been differentiated. The salt is mined while water is present to prevent mining bitterns, and the chemistry of the remaining water provides useful information about solute behaviour.



## 5.2. GENERAL PARAMETERS

### 5.2.1. Salinity

The salinity of water samples extends from a brackish TDS of 2 g/L (RB-WP1) to a TDS of 379 g/L (RA-WP1). None of the water can be classified as fresh (<1 g/L), but salinities below that of seawater (35 g/L) are found in about one third of samples (Figure 5.1). Brines tend to be found as surface water in pans while subsurface, stream and spring waters tend to be significantly less saline. Evaporated seawater is expected to reach halite saturation at TDS concentrations between 350 and 420 g/L and densities greater than 1.22 g/cm$^3$ (Warren, 1999). The samples from this study appear to be at or below equilibrium with halite, as density and TDS behave linearly, and all densities are below 1.22 (Figure 5.1 (a)). The only exception is sample RA-SS1a, the behaviour of which is not understood.

The relationship between EC and TDS becomes nonlinear at high salt concentrations (Figure 5.1(b)). This is due to electrolytic effects. At infinite dilution, the contribution to conductivity by different ions is additive. However, as the concentrations of ions increase, the conductivity per mole of charge decreases and the conductivity is less than expected by addition of ions (Eaton *et al.*, 1995). For this reason, TDS rather than EC is used to indicate salinity.

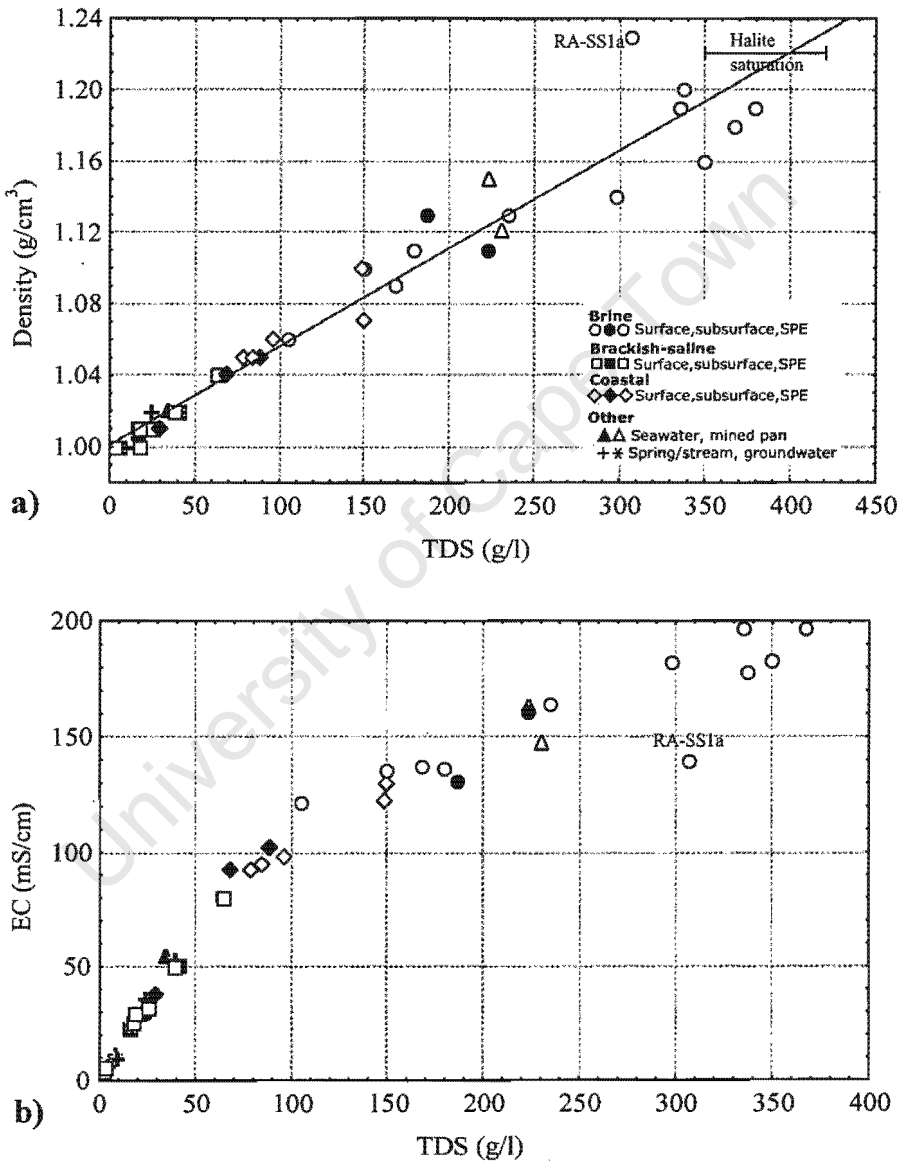


**Figure 5.1 (a) Relationship between density and TDS, (b) Relationship between EC and TDS. Note non-linearity at high salinities.**

The TDS of SPE is generally found to decrease with depth in pan sediments. Salts in sediments originate from the concentration of fresher groundwater by capillary evaporation, resulting in greatest salinities at the surface. Exceptions include a SPE sample (RA-SS3d) which has a higher TDS than overlying sediment samples, and a subsurface water sample from a pit dug adjacent to Droëvlei (DV-WB1), which has a greater salinity than the water in the pan. Greater subsurface salinities may result from accumulation of the remaining brine in the pan sediments following seasonal evaporation. Alternatively, if the saline subsurface water is feeding the pan, the surface water may be diluted by recent rain or runoff.

### 5.2.2. pH

All water samples have neutral to alkaline pH and there is no relationship between pH and TDS (Figure 5.2). Most of the water samples, including brine-type and coastal pan surface waters, deeper groundwater as well as most SPE, are constrained within a narrow range of pH from 7.6 to 8.3. Only subsurface and a few SPE samples have pH below 7.6, while the pH of brackish-saline pans and streams, springs and seeps exceeds 8.3.

The pH of most natural waters is controlled by carbonate reactions. Natural rainwater is expected to have a pH of approximately 5.7 due to equilibrium with atmospheric $CO_2$. Water that is in equilibrium with atmospheric $CO_2$ and calcite at 25°C has a pH of 8.26 (Drever, 1997). The range of pH from 7.6 to 8.3 for the majority of surface water samples is probably due to equilibrium with atmospheric $CO_2$ and calcite. According to McBride (1994), the presence of carbonate minerals buffers pH by the following reaction:

$$H^+ + CaCO_3 \leftrightarrow HCO_3^- + Ca^{2+}$$

An increase in pH will cause precipitation of carbonates and generation of $H^+$, and a decrease in pH will result in dissolution of carbonates and removal of $H^+$ from solution (McBride, 1994).

Low pH in subsurface samples and SPE is probably due to equilibrium with soil $CO_2$. The partial pressure of $CO_2$ ($pCO_2$) is higher in the soil zone due to metabolic activity of plants and soil organisms (McBride, 1994). The more organic matter in the soil, the more $CO_2$ generated. Organic matter in the form of humic acids can also contribute to lower pH. Waters in equilibrium with calcite and soil air have a pH lower than 8.26, and have been found by other authors to have pH between 7.5 and 7.8 (McBride, 1994). In the absence of

calcite a pH lower than 7.5 would be expected, as observed in the subsurface samples in which calcite was not identified. The SPE pH of most samples containing calcite was within this range, but a few exceeded 7.8. Measurements were not taken in the field, so the sediments would have had time to equilibrate to atmospheric $CO_2$, resulting in an increase in pH and an inaccurate pH reading. Calcite is abundant in coastal pan sediments, which will buffer the pH of these sediments. The SPE of brine-type pans may be affected by sulphate reduction and sulphide precipitation, as sulphides were noticed in the sediments (Section 5.7.1). Calculations based on anoxic pore waters in marine sediments by Ben-Yaakov (1973) predict that sulphate reduction will tend to shift pH towards 6.9 while sulphide precipitation will cause the pH to rise to 8.3.

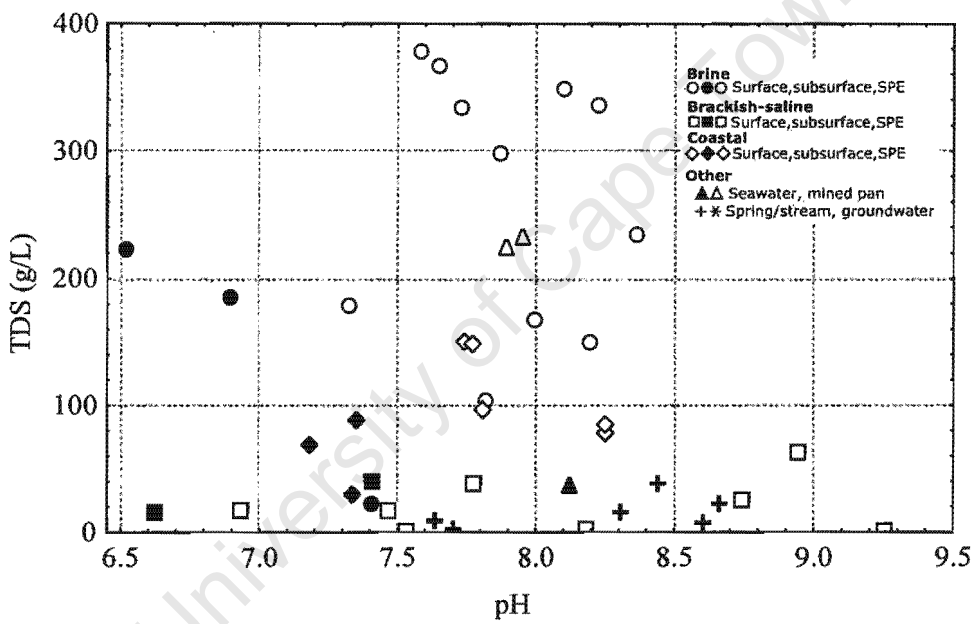


**Figure 5.2: Relationship between pH and TDS**

The high pH in brackish-saline pans and springs indicates they are not in equilibrium with calcite, although calcite was identified in the sediments. Calcite precipitation can be inhibited by high Mg concentrations (Drever, 1997), but the Mg:Ca ratio of these waters is lower than the Mg:Ca ratios of water samples which are in equilibrium with calcite. Calcite precipitation in more saline samples may be initiated by the decrease in solubility and consequent degassing of $CO_2$ at increased salinities (Eugster and Jones, 1979) and temperatures (Hermann *et al.*, 1973). The brackish-saline pan waters may be affected by weathering reactions in the catchment. Faure (1992) states that hydrolysis of primary

silicates like feldspar consumes acidity from the dissociation of $H_2CO_3$, and the pH remains unchanged due to buffering (Faure, 1992). The sediments and waters of the brackish-saline pans and streams/seeps with high pH have higher concentrations of organic carbon than other samples (e.g. DV-SS2 = 1.75%, ZA-WR1 = 14 mg/kg) indicating that the presence of organic matter is not a significant control on pH.

## 5.3. MAJOR ION CHEMISTRY

### 5.3.1. MAJOR ION DOMINANCE

Sodium and Cl are the dominant cation and anion in all water samples (Table 5.1) followed by Mg and $SO_4$. Potassium and Ca contribute roughly equally to the total charge, while Br and alkalinity generally occur as minor species. The order of ion dominance is very similar to seawater. Ion dominance in pan water from Rooipan north (RB-WP1) differs from all other samples in that $HCO_3$ concentration exceeds $SO_4$ concentration. In an extensive review of literature published on saline lakes, Hammer (1986) found that saline lakes dominated by Na and Cl are by far the most common. According to his review, the most common cation equivalence series is Na>Mg>Ca≈K and anion equivalence series is Cl>$SO_4$>$HCO_3$.$CO_3$ (Hammer, 1986). Silberbauer and King (1991) found that Na and Cl are dominant ions in wetlands close to the coast in the Western Cape, but that bicarbonate becomes the dominant anion in panson the plateau that dominates the interior of Southern Africa.

A Piper diagram allows classification of water using major cations and anions. All samples are plotted on both ternary diagrams, one for anions and one for cations. These data points are projected onto the diamond as indicated by the arrows on Figure 5.3 (Faure, 1992). The Piper diagram reveals increasing Na dominance to the detriment of Ca and Mg with increasing salinity. Groundwater has relatively more Ca than surface samples. The mined pans have higher proportions of Mg, and sample RB-WP1 has relatively high Na:Cl compared to other samples. Anion ratios are more consistent than cation ratios, indicating that anions are behaving more conservatively than cations.

**Table 5.1: Ionic dominance as percentage. Cations are % $mmol_c$ of the cation sum, and anions as % $mmol_c$ of the anion sum.**

| | $Na^+$ | $K^+$ | $Mg^{2+}$ | $Ca^{2+}$ | $Cl^-$ | $Br^-$ | $SO_4^{2-}$ | Alkalinity |
|---|---|---|---|---|---|---|---|---|
| **Seawater*** | 78 | 1.7 | 18 | 3.4 | 90 | 0.14 | 9 | 0.39 |
| **BA-WP1** | 57 | 1.2 | 41 | 0.3 | 88 | 0.15 | 12 | 0.25 |
| **BA-WP2** | 84 | 0.7 | 15 | 0.6 | 89 | 0.04 | 11 | 0.17 |
| **BA-WS1** | 68 | 1.5 | 30 | 0.3 | 84 | 0.11 | 16 | 0.23 |
| **BB-WB1** | 76 | 0.7 | 18 | 5.2 | 85 | 0.03 | 13 | 1.37 |
| **BB-WP1** | 91 | 0.7 | 8 | 0.8 | 88 | 0.02 | 12 | 0.02 |
| **BB-WR1** | 78 | 0.8 | 19 | 3.0 | 87 | 0.04 | 12 | 1.09 |
| **DV-WB1** | 76 | 0.7 | 17 | 5.8 | 88 | 0.04 | 11 | 0.68 |
| **DV-WP1** | 69 | 1.5 | 21 | 8.4 | 80 | 0.06 | 20 | 0.26 |
| **KP-WP1** | 91 | 0.5 | 8 | 0.5 | 84 | 0.05 | 16 | 0.04 |
| **OT-WR1** | 68 | 1.7 | 21 | 9.7 | 85 | 0.04 | 14 | 1.01 |
| **RA-WB1** | 82 | 0.6 | 16 | 1.1 | 87 | 0.06 | 12 | 0.09 |
| **RA-WP1** | 93 | 0.5 | 6 | 0.4 | 87 | 0.02 | 13 | 0.01 |
| **RB-WP1** | 95 | 1.5 | 2 | 1.0 | 69 | 0.09 | 10 | 20.21 |
| **RP-WB1** | 79 | 1.7 | 14 | 5.2 | 81 | 0.05 | 18 | 0.85 |
| **RP-WP1** | 77 | 1.7 | 17 | 4.1 | 85 | 0.06 | 15 | 0.13 |
| **SK-WB1** | 65 | 0.9 | 26 | 7.8 | 87 | 0.03 | 12 | 0.92 |
| **SK-WP1** | 78 | 1.2 | 18 | 2.7 | 88 | 0.05 | 11 | 0.13 |
| **YF-WB1** | 76 | 1.2 | 17 | 5.8 | 88 | 0.06 | 12 | 0.09 |
| **YF-WB2** | 77 | 1.3 | 21 | 0.8 | 88 | 0.59 | 11 | 0.25 |
| **YF-WP1** | 82 | 1.1 | 14 | 3.3 | 84 | 0.06 | 16 | 0.04 |
| **ZA-WS2** | 74 | 1.1 | 17 | 8.2 | 86 | 0.04 | 13 | 1.14 |
| **ZA-WP1** | 90 | 0.6 | 9 | 0.5 | 89 | 0.02 | 11 | 0.04 |
| **ZA-WR1** | 74 | 0.7 | 18 | 7.4 | 87 | 0.05 | 12 | 0.72 |
| **ZA-WS1** | 75 | 0.7 | 18 | 5.6 | 89 | 0.05 | 10 | 0.57 |
| **ZB-WB1** | 79 | 0.7 | 20 | 0.9 | 90 | 0.00 | 10 | 0.09 |
| **ZB-WP1** | 90 | 1.1 | 8 | 0.6 | 84 | 0.03 | 16 | 0.03 |
| **ZB-WS1** | 77 | 0.6 | 17 | 5.2 | 84 | 0.04 | 11 | 4.87 |

*from Faure (1992).

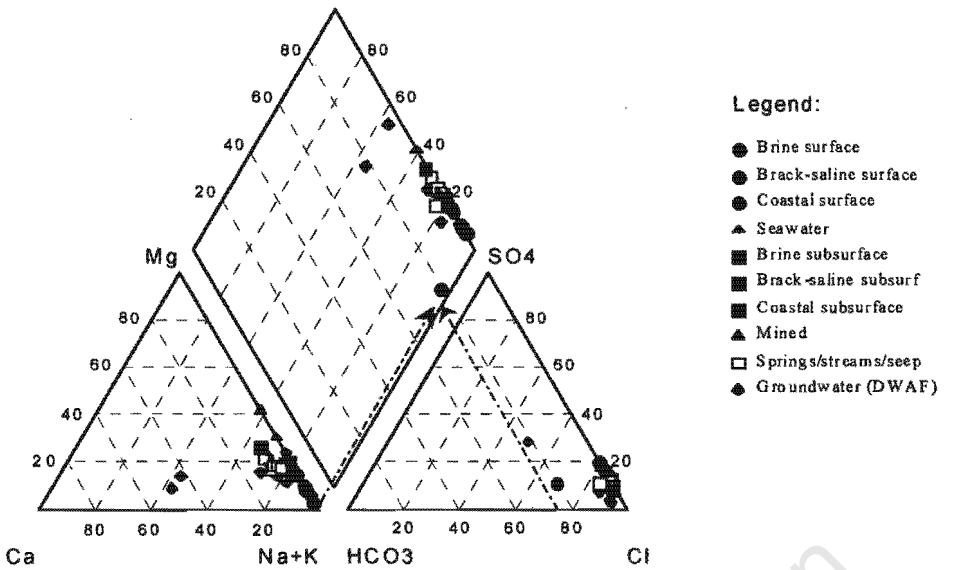


**Figure 5.3: Piper diagram illustrating the relative dominance of major ions in water samples. Arrows indicate projection of a single sample from the ternary diagrams onto the diamond.**



### 5.3.2. SOLUTE TYPES

The various major ions behave differently with increasing concentration of the brine. Eugster and Jones (1979) have identified five basic patterns of solute behaviour in evaporative systems, numbered I through V, as illustrated in Figure 5.4. Each solute is plotted against a conservative element, usually Cl (Eugster and Jones, 1979). Proportions of conservative ions remain constant, but concentrations can vary due to evaporation or dilution. Non-conservative elements do not have a consistent ratio with Cl (Faure, 1992). Conservative behaviour will plot as a straight line through the origin on linear axes, or as a straight line parallel to the 1:1 line on logarithmic axes. A 1:1 line on linear axes will only be observed if the initial solution has equal proportions of the two elements being plotted.

Evidence of ion dominance and ion ratios in waters sampled in the study area indicates that seawater is influencing the chemistry of pan waters. In order to compare elemental ratios of the samples taken in this study with seawater throughout brine evolution, the ratios of elements to Cl were normalised to seawater by the following equation:

$$\text{Enrichment} = \frac{R_{sample} - R_{seawater}}{R_{seawater}} \times 100 \quad \text{where R is the ratio of an element to Cl.}$$

Enrichment factors greater than 0 indicate that the element is enriched in the sample relative to seawater, and negative values indicate depletion of the element relative to seawater.

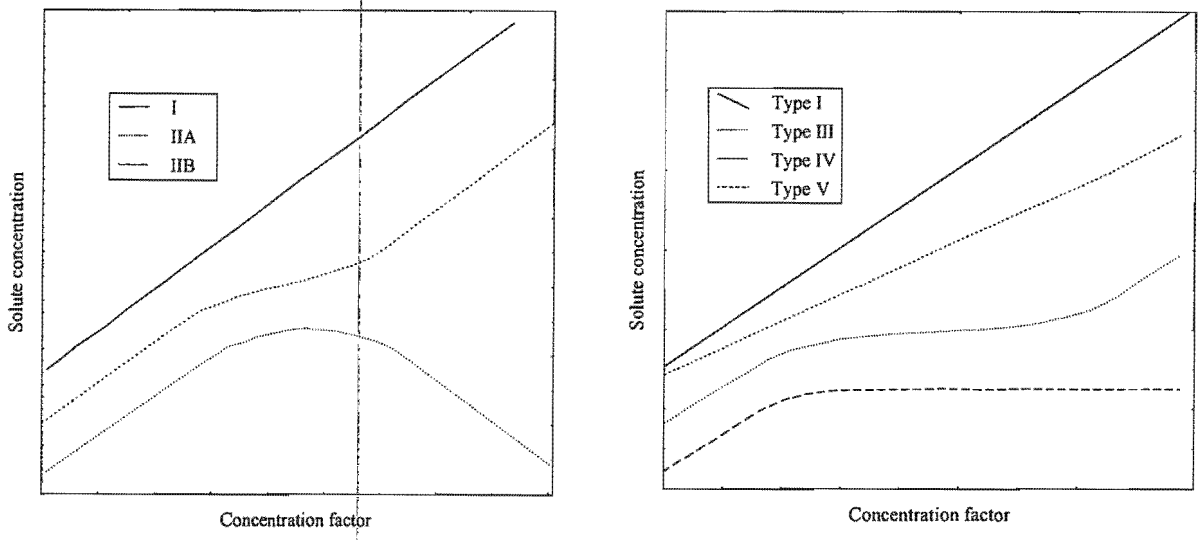


**Figure 5.4: Behaviour of solutes during brine evolution plotted on logarithmic axes (Eugster and Jones, 1979)**

*Alkalinity*

Total alkalinity consists of contributions by $HCO_3^-$, $CO_3^{2-}$, $B(OH)_4^-$, $H_3SiO_4^-$, $HS^-$, organic anions and $OH^-$. In general, bicarbonate and carbonate concentrations greatly exceed the other species and total alkalinity is represented entirely by carbonate alkalinity (Drever, 1997). In this study a plot of B against alkalinity reveals that borate probably contributes to alkalinity (Figure 5.5 (a)). This contribution is in the range of 5 to 10 % based on the percentage of B that occurs as $B(OH)_4^-$ in the pH range encountered in most samples.

The alkalinity of all samples except the surface and spring samples from the mined pan, Burgerspan south, is below 6 mmol/kg (Figure 5.5 (b)). Most of the alkalinity is probably generated by weathering of feldspars (Faure, 1992). The high alkalinity in the samples from Burgerspan south could be due to the high borate levels in these samples. Alkalinity is not correlated to pH or TDS. However, alkalinity is enriched relative to seawater in low-salinity subsurface and spring/stream samples and depleted relative to seawater in surface waters (Figure 5.5 (c)). The rapid decrease of alkalinity in solution is due to removal from solution by carbonate precipitation.

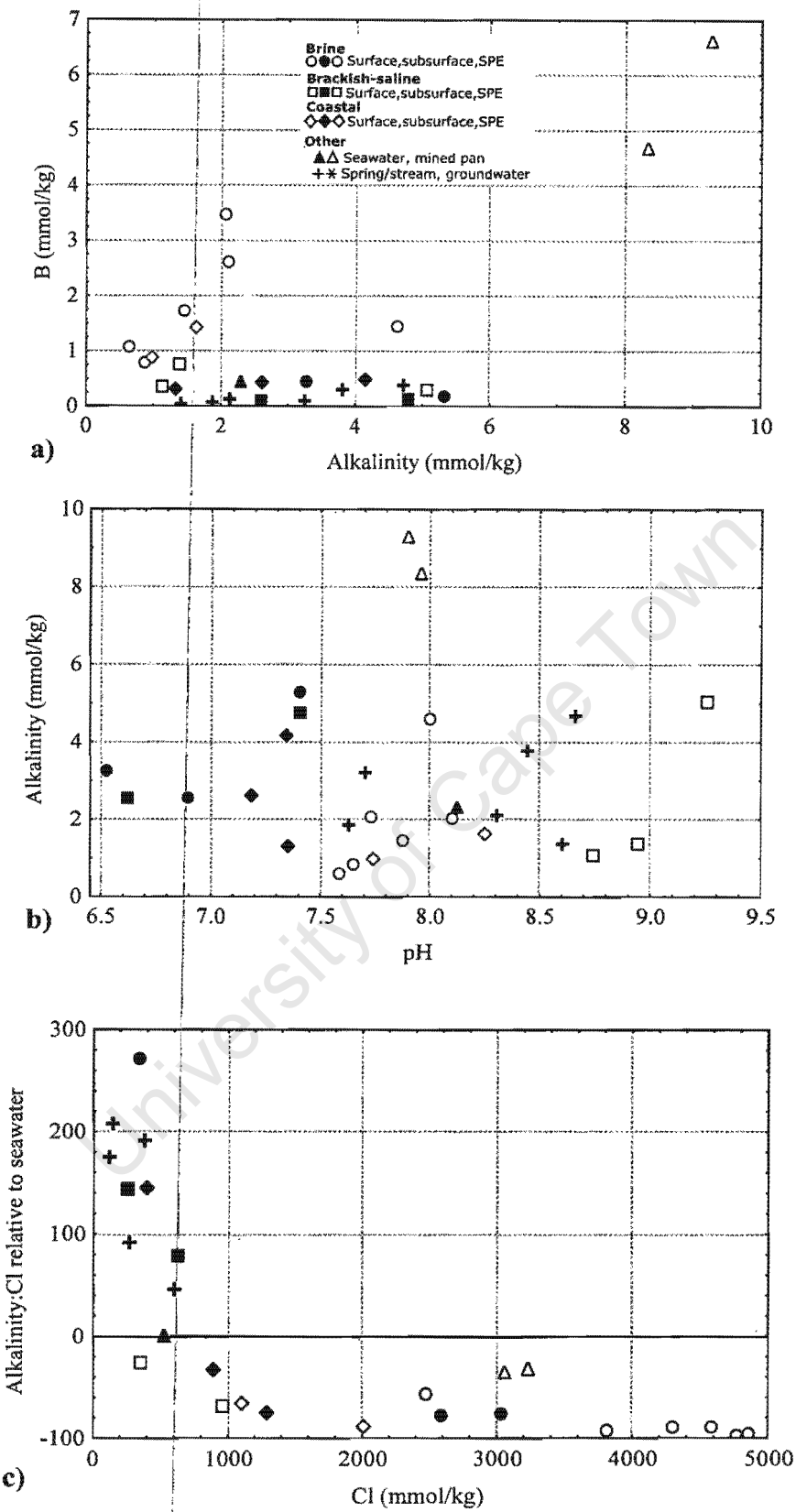


**Figure 5.5: (a) Relationship between B and alkalinity. Note positive correlation in surface water samples, (b) Alkalinity vs pH, illustrating lack of correlation between the two variables (c) Enrichment factor for alkalinity relative to seawater plotted against Cl**

*Sodium*

Sodium behaves as a conservative Type I solute, remaining in solution through most of brine evolution (Figure 5.6 (a)). According to Eugster and Jones (1979), Na is usually removed from solution by crystallisation of the final, most soluble minerals. The corollary is that Na will be one of the first ions to dissolve. Type I solutes are useful for monitoring the concentration of the brine (Eugster and Jones, 1979). There is slightly less Na in solution than Cl, resulting in a slope of 1.18 on Figure 5.6 (a), equivalent to a Na:Cl ratio of 85:100. The molar ratio of Na:Cl in seawater is 86:100 (Grobe *et al.*, 2000). One of the samples from the mined pan is depleted in sodium relative to the trend because removal of halite from the pan results in the remaining brine being residually enriched in Cl.

The three pan types display similar behaviour despite their different salinities, implying similar processes and initial composition of water. RA-SS1a plots off the conservative trend because it may have started precipitating halite. Samples from Rooipan north (RB-SS1 and RB-WP1) are enriched in Na, possibly indicating a different water source. The Na:Cl ratio is plotted against Cl concentration in Figure 5.6 (b). Precipitation of halite would result in a depletion of Na as observed in the SPE of high Cl content, and the sample from the mined pan. Springs and streams are generally depleted in Na relative to seawater.

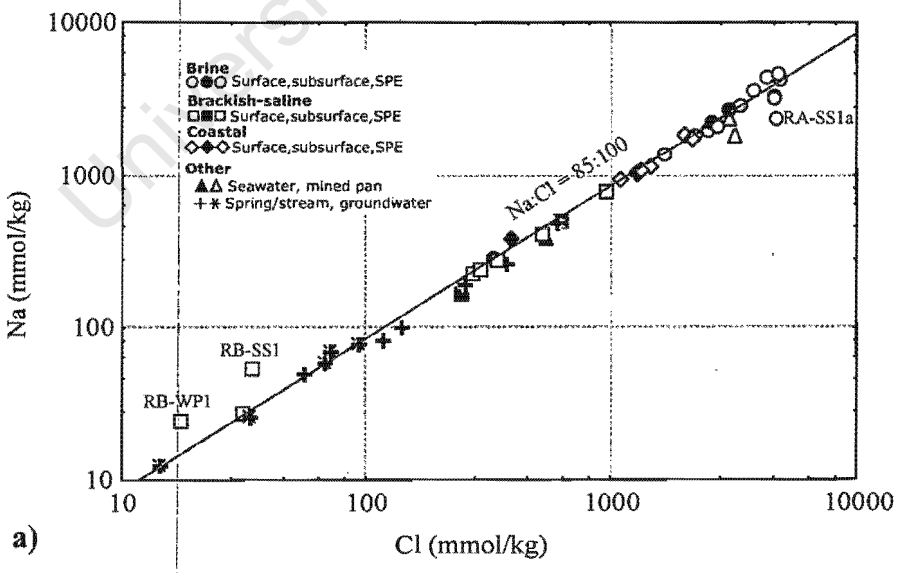


**Figure 5.6 (a): Relationship between Na and Cl. The line is parallel to a 1:1 line and represents a conservative relationship**

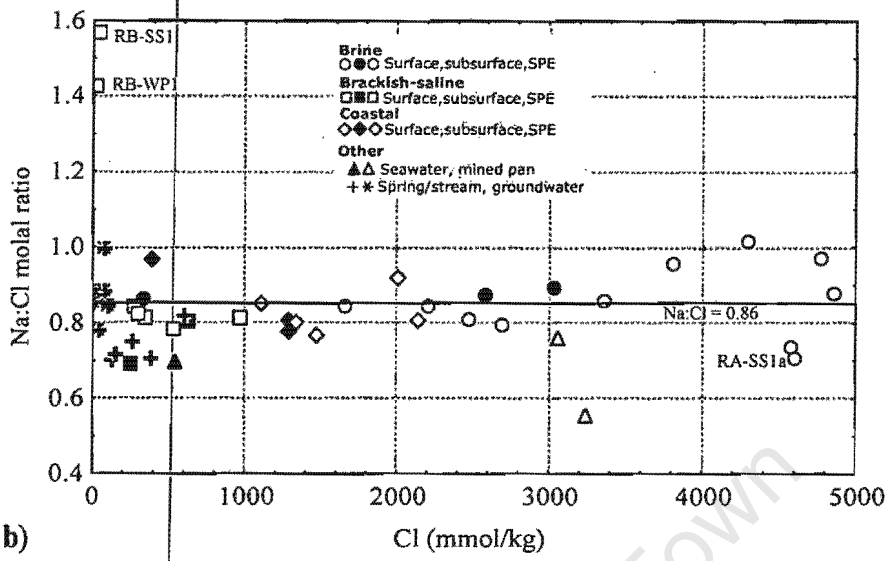


b)

**Figure 5.6 (b): Variation of the Na:Cl ratio with increasing salinity. The line is the Na:Cl ratio in seawater of 0.86.**

*Potassium*

Potassium is commonly found to behave as a type IV solute, being removed from solution by processes that are not strongly concentration related. Eugster and Jones (1979) found that processes like ion exchange, adsorption or biogenic reduction slow the increase in concentration with evaporation, resulting in a sigmoidal curve (Figure 5.4). In their studies, K did not precipitate into any solid phase and generally behaved more conservatively than Cl (Eugster and Jones, 1979). In the current study, K also behaves conservatively (Figure 5.7 (a)). A line parallel to the 1:1 line but with a ratio of K:Cl of 1:100 fits the data. Potassium in the samples from the mined pan is relatively enriched compared to Cl, as would be expected if NaCl was selectively being removed and K remained behind in the pan. Examining the enrichment factors for K (Figure 5.7 (b)) reveals that K is generally depleted with respect to seawater. Assuming a seawater or coastal rainfall origin, K may be removed from solution by ion exchange in soils of the catchment prior to reaching the pans. Sample RP-WP1, from the coastal pan closest to the sea, has K enrichment factors very similar to seawater. Samples from the brackish-saline type pans, Rooipan north and Kiekoesvlei, are K-enriched.

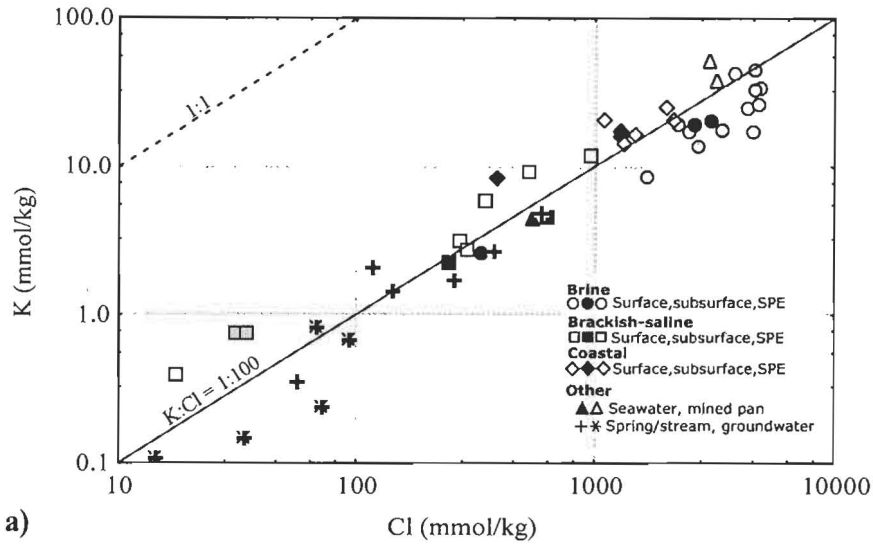


a)

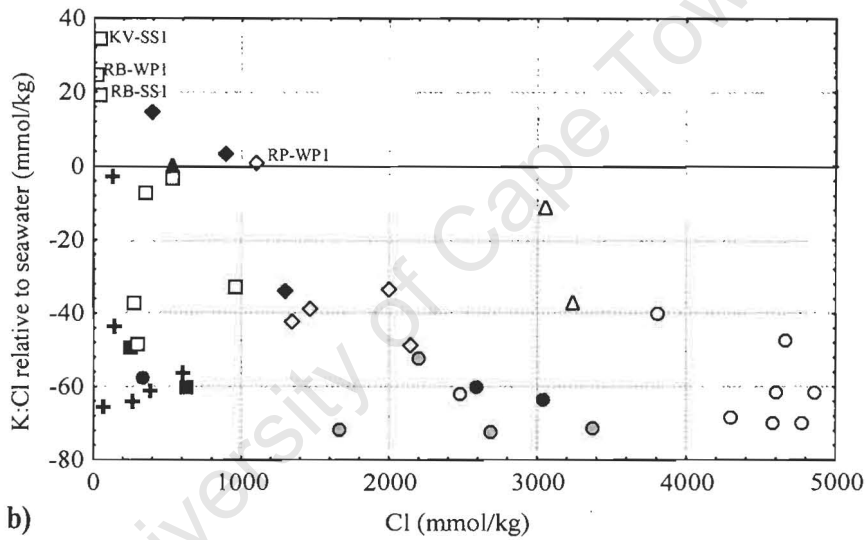


b)

**Figure 5.7: (a) Relationship between K and Cl. The fitted line is parallel to the 1:1 line and represents a conservative relationship, (b) Variation of the K:Cl enrichment factor relative to seawater with increasing salinity.**



*Calcium*

Calcium behaves as a Type IIA solute during precipitation of calcite in streams/seeps and brackish to saline pans because it is limited by availability of bicarbonate, the Type IIB solute (Figure 5.8 (a)). Eugster and Jones (1979) define solutes of type IIA and IIB as an anion and cation removed from solution by precipitation of the same mineral. The solute with the highest initial concentration (A) will continue to concentrate but less rapidly than before, while the other solute (B) will rapidly be removed from solution. Once precipitation of the mineral phase is complete, the concentration of solute (A) will once again increase at the same rate as before precipitation began.

The trend of increasing Ca concentration with increasing Cl is not parallel to a 1:1 line, and Ca is not behaving conservatively. At Cl concentrations above 1000 mmol/kg, Ca is removed from solution, and behaves as a Type IIB solute. Gypsum was found in brine-type pan sediment samples by XRD analysis (Section 5.7). Precipitation of gypsum is limited by Ca concentration so Ca becomes a Type IIB solute while sulphate is the Type IIA solute. The samples from the mined pan, Burgerspan south, are depleted in Ca relative to other samples. Gypsum was found in the subaqueous salt sample from Rooipan south, so Ca is probably being removed from the mined pan as gypsum along with halite. The coastal pans contain more dissolved calcium than the inland pans. The source of this calcium is most likely gypsum dissolution, as saturation index modelling of coastal samples indicates equilibrium with gypsum (Section 5.6.3).

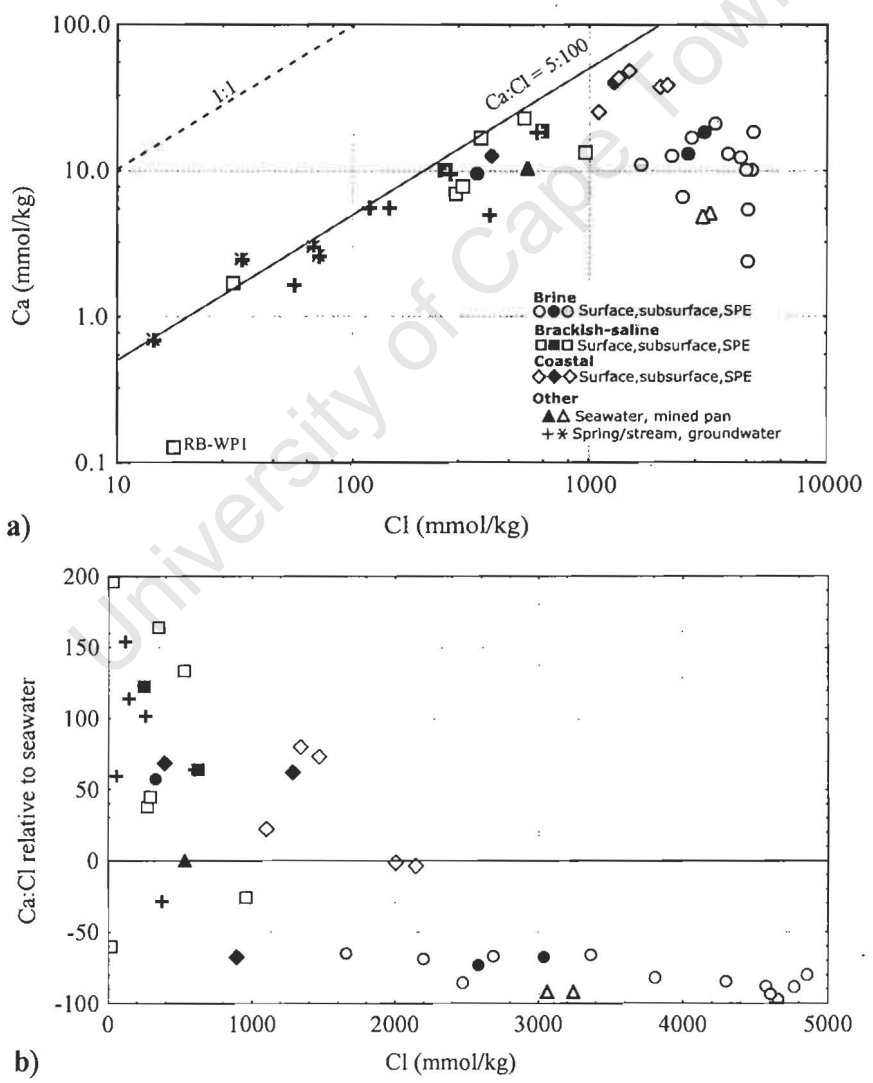


**Figure 5.8: (a) Relationship between Ca and Cl. The fitted line is parallel to the 1:1 line and represents a conservative relationship. Note that the data do not follow a conservative trend (b) Variation of the Ca:Cl enrichment factor relative to seawater with increasing salinity.**

*Magnesium*

Magnesium is found to behave as a conservative Type I solute in coastal and brackish-saline pans, and as a Type IIB solute in brine-type pans (Figure 5.9 (a)). Conservative behaviour is maintained until a Mg concentration of approximately 280 mmol/kg, after which the concentration decreases to 140 mmol/kg. One explanation for Mg removal from solution is precipitation into calcite. The presence of Mg-enriched calcite (Mg-calcite) in brine-type pans was verified by XRD analysis of sediments. High-Mg calcite contains at most 20 mole % $MgCO_3$ (Drever, 1997), but in this study most samples contained about 10 mole % $MgCO_3$. Assuming that all Ca is removed from solution as calcite, 42 mmol of calcite per kg of brine would be expected to form. If the calcite contains 10 mole % of Mg, approximately 4.5 mmol of Mg per kilogram of brine should be removed from solution. The observed decrease of Mg concentration in solution in brine-type pans is 140 mmol/kg, indicating that some other mineral besides high-Mg calcite must be removing Mg from solution. Minerals that have been invoked by previous researchers to explain removal of Mg from brines are sepiolite ($MgSi_3O_6(OH)_2$), dolomite ($CaMg(CO_3)_2$), disordered or proto-dolomite and Mg-rich smectite (Drever, 1997). None of these minerals were detected in significant amounts by XRD. Magnesium is not removed from the pan by mining and is residually enriched in solution. Adsorption of Mg onto clay minerals may also account for its removal from solution, but this should not be limited to high salinity waters. Samples from the brackish-saline pans Rooipan north (RB-WP1) and Kiekoesvlei (KV-SS1b) have low Mg concentrations relative to the general trend.

For any particular ratio of Mg:Ca in solution, there should be a corresponding Mg:Ca ratio in the calcite that precipitates (Drever, 1997). The coastal pan waters have a much lower Mg:Ca ratio than the inland pan waters and are more likely to precipitate low-Mg calcite (Figure 5.9(b)). According to the Hardie-Eugster model, calcite in brines evolves from low to high-Mg calcite (Eugster, 1980). The Mg:Ca ratio increases with increasing salinity due to removal of Ca from solution by precipitation of calcite and the next increment of calcite precipitated will contain a correspondingly higher proportion of Mg. The similarity between Mg:Cl ratios in most low salinity samples and seawater argues that coastal rainwater is primary source of Mg (Figure 5.9 (c)).

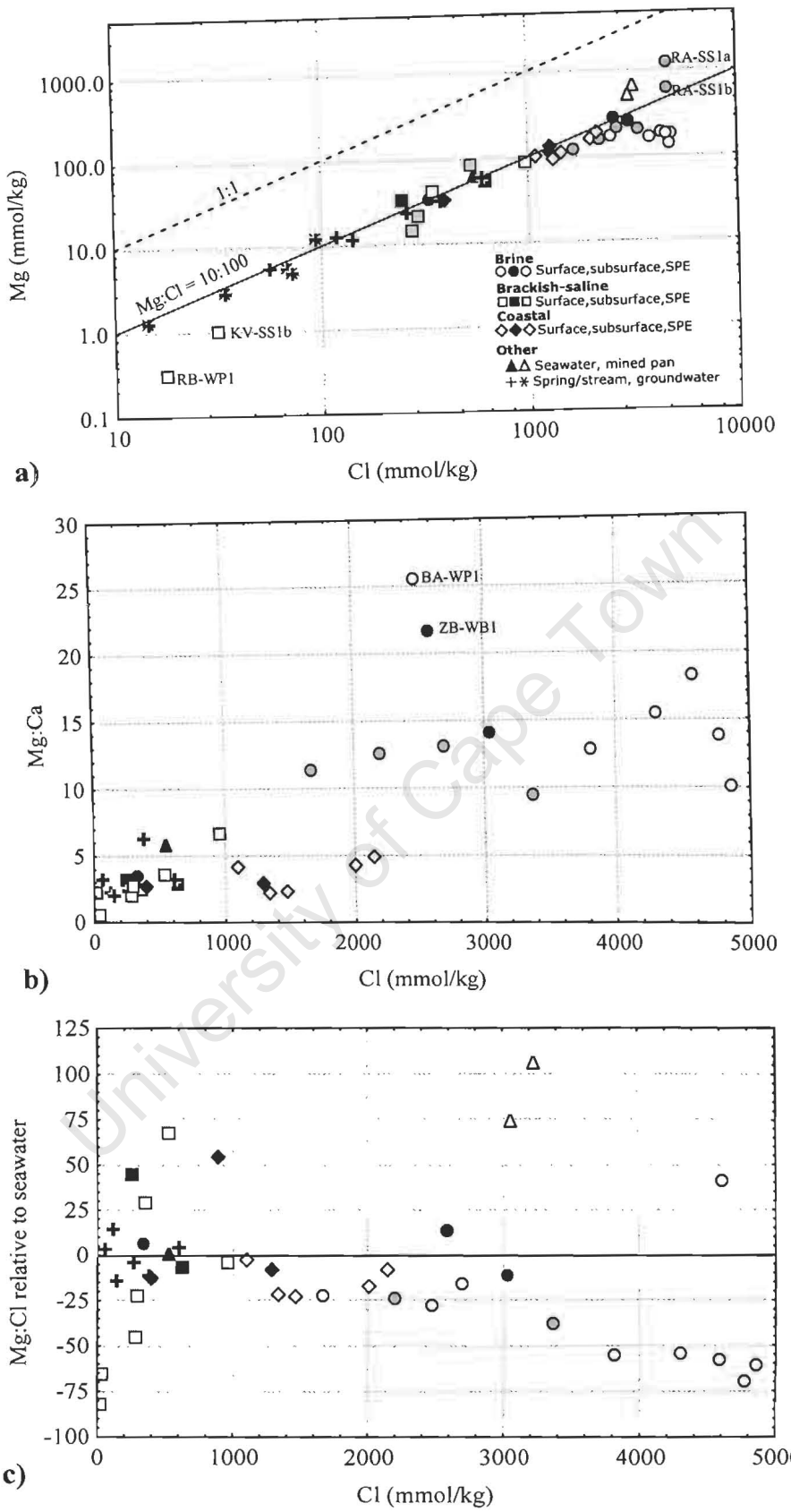


**Figure 5.9: (a) Relationship between Mg and Cl. The fitted line is parallel to the 1:1 line and represents a conservative relationship, (b) Variation of the Mg:Ca ratio with increasing salinity, (c) Variation of the Mg:Cl enrichment factor relative to seawater with increasing salinity**

*Fluoride*

Fluoride concentrations plotted against Cl exhibit a very different trend compared to other major ions, and cannot be classified as any particular solute type (Figure 5.10 (a)). Eugster and Jones (1979) found that fluoride behaved conservatively in pan systems in Kenya (Type I). Knesl (1996) on the other hand, reported fluoride behaving as a Type IIB solute in Barberspan in inland South Africa, being concentrated by evaporation before removal by precipitation of fluorapatite. In this study, however, concentrations are highest at low Cl concentrations and lowest at high Cl concentrations. Samples with high F are mainly spring/seep samples, and surface and subsurface waters from brackish-saline type pans. The decrease in F concentrations relative to Cl in brine-type pans may reflect the removal of F as fluorite ($CaF_2$) or fluorapatite. Neither of these minerals were detected by XRD but they may be present in amounts below the detection limit of 3 weight %.

Calculation of the enrichment factor of F:Cl relative to seawater reveals that F is enriched in low salinity samples, and is rapidly depleted with increasing Cl levels attaining uniform levels for waters with more than 1000 mmol/kg Cl (Figure 5.10 (b)). This pattern is similar to that observed for Ca and alkalinity, suggesting that F is removed during or simultaneous with carbonate precipitation. Enriched F in stream, spring, brackish-saline and subsurface waters is derived from chemical weathering of apatite in the granites. Sample RB-WP1 has an enrichment of 3500 relative to seawater, and was not plotted on the graph.



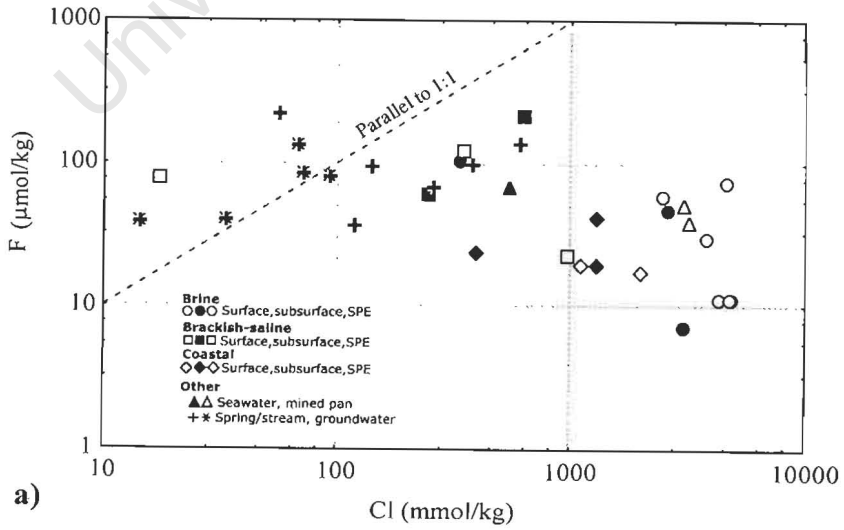


**Figure 5.10 (a): Relationship between F and Cl,**

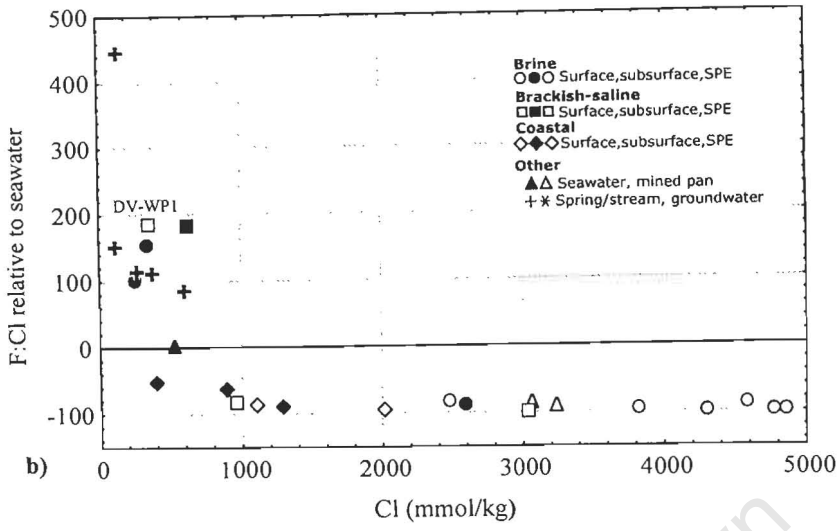


**Figure 5.10 (b): Variation of the F:Cl enrichment factor relative to seawater with increasing salinity.**



*Sulphate*

Sulphate behaves conservatively over the range of chloride concentrations, exhibiting Type I behaviour rather than the Type IV behaviour observed by Eugster (1980). The conservative trend observed in this study becomes quite scattered at higher salinities and it appears that a number of samples from the brine-type pans (especially the SPE) plot below the conservative line, with a lower $SO_4$:Cl ratio (Figure 5.11(a)). This could be due to reduction of sulphate to sulphides in the sediments. Eugster (1980) found that sulphate is often fractionated by redox processes in brines. Sulphate in mined samples is neither depleted nor enriched indicating that $SO_4$ is removed from the pan in the same proportions that it is found in the original inflow waters, due to removal of gypsum. Gypsum precipitation does not affect $SO_4$ concentrations, because the amount of gypsum precipitating is limited by low Ca concentrations. The generally low organic carbon content of brine-type pan sediments (0.07 – 0.82 wt %) may limit reduction of sulphate. Sources of organic carbon to pan sediments include algae, particulate matter washed into the pan and animal faeces (e.g. birds and cattle).

Sulphate is enriched relative to seawater with the exception of a few SPE extracts (Figure 5.11 (b)). Sulphate probably originates primarily from coastal rainwater, but the enrichment suggests an additional minor source. One possibility is oxidation of sulphide minerals in

granites, which would release sulphate into solution. Sulphate is depleted in the SPE from brine-type pans and in groundwaters due to sulphate reduction.

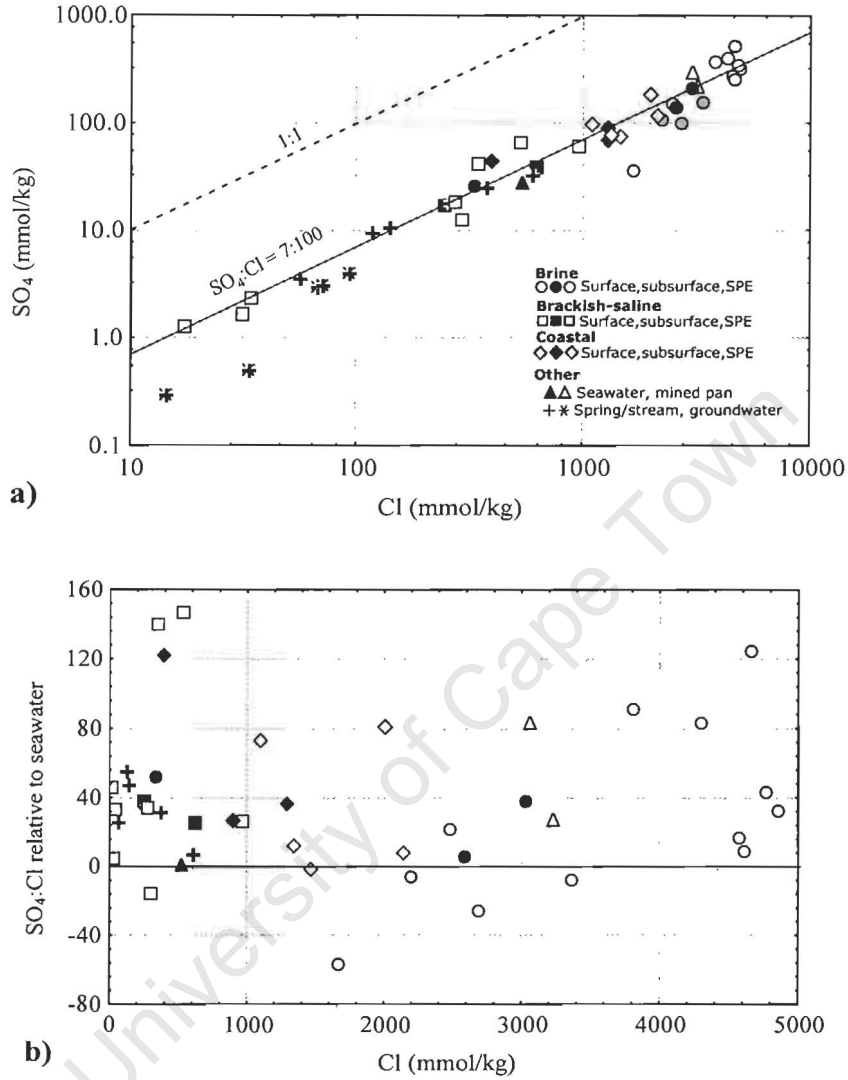


**Figure 5.11: (a) Relationship between $SO_4$ and Cl. The fitted line is parallel to the 1:1 line and represents a conservative relationship (b) Variation of the $SO_4$: Cl enrichment factor relative to seawater with increasing salinity.**

*Bromine*

Bromine displays Type I behaviour over virtually the entire range of chloride concentrations (Figure 5.12 (a)). A similar trend of conservative behaviour was found by Eugster and Jones (1979). The mined pans are enriched in Br, because Br does not precipitate into any minerals that are removed by mining. According to Herczeg and Lyons (1991), Br tends to partition into halite but this does not seem to be the case. The behaviour of Br is similar to Mg, i.e. concentrating in the mined pan water and in brine-type pan floor sediments (RA-SS1a and b),

but generally depleted in brine-type pan surface waters Br may be removed by clay minerals. Two samples (ZB-WB1, RA-SS3a) have very low Br concentrations, but it is not known why. The Br:Cl ratio relative to seawater is depleted except in mined samples (Figure 5.12 (b)). If coastal rainwater is the source, which is likely, then Br is being removed by a process such as ion exchange.

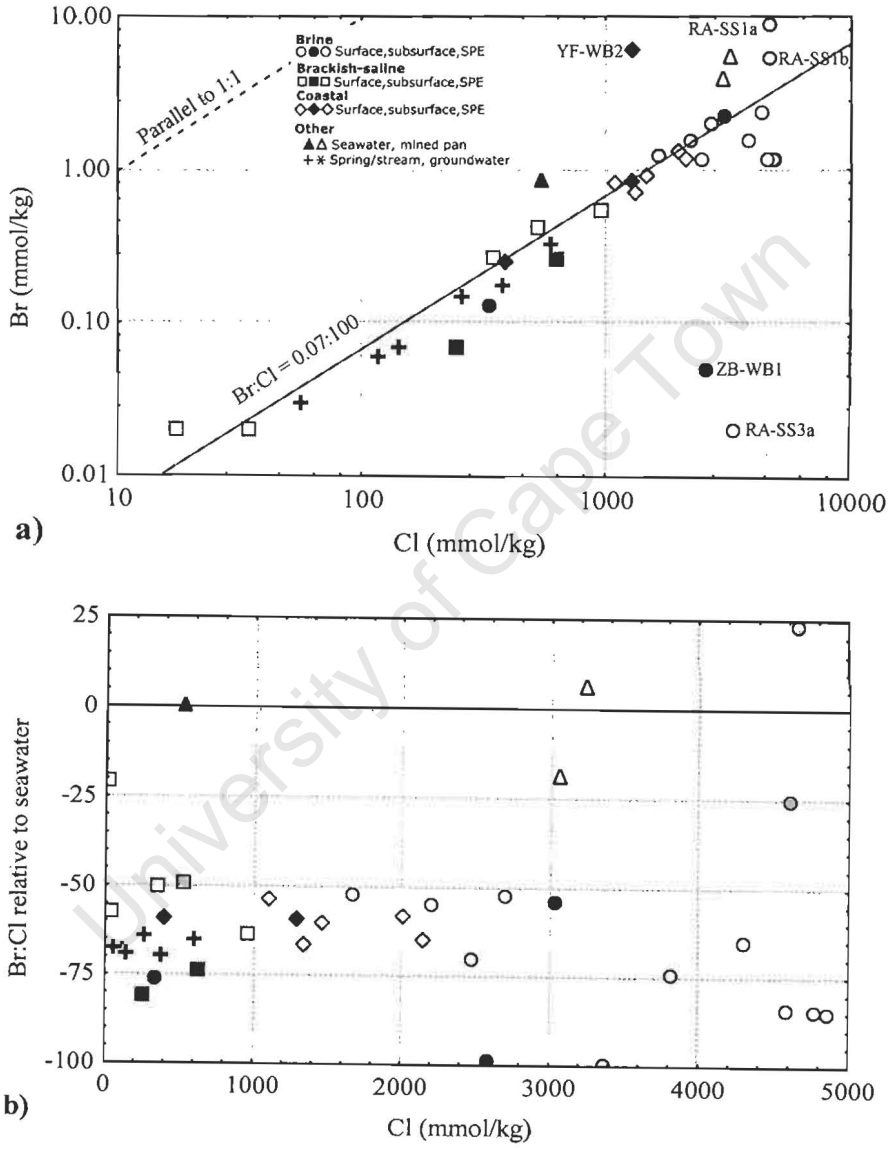




**Figure 5.12: (a) Relationship between Br and Cl. The fitted line is parallel to the dashed 1:1 line and represents a conservative relationship (b) Variation of the Br: Cl enrichment factor relative to seawater with increasing salinity.**

### 5.3.3. ORIGIN OF MAJOR IONS

Possible sources of major solutes in the pans are seawater, rain, marine aerosols, groundwater and dissolution of minerals in the catchment. Seawater is dominated by $Na^+$ and $Cl^-$, and has lesser amounts of $SO_4^{2-}$, $Mg^{2+}$, $Ca^{2+}$, $K^+$, $CO_3^{2-}$ and $HCO_3^-$. Darling and Ysterfontein are near the coast and the pans are expected to be influenced by the sea, either by previous inflow or from marine aerosols.

The marine influence on continental brines is via aerosols brought in by precipitation, or blown in by wind. Rainwater in coastal regions is dominated by Na and Cl, but the concentrations of these ions decrease rapidly away from the coast (Faure, 1992). In Australia, even continental brines are dominated by Na and Cl (Warren, 1999). An approximation of the inflow water composition normalised to Cl can be made for this study from the slope of the conservative portion of the plots of elements against Cl (from previous section). Using this method, the ratios of elemental dominance to Cl in inflow waters have been calculated and compared to seawater and global average coastal rainfall (Table 5.2). Alkalinity cannot be estimated graphically because it does not behave conservatively, but it is present only in low concentrations. Na:Cl and K:Cl ratios of rain in coastal regions are very similar to seawater, but rain is enriched in Ca and $SO_4$ relative to the sea (Faure, 1992). The inflow water composition in this study reflects the Ca and $SO_4$ enrichments of coastal rainwater, rather than the lower ratios expected from a direct seawater source.



**Table 5.2: Comparison of ionic concentrations normalised to Cl for this study, seawater and global average coastal rainfall.**

| Element normalised to Cl (%) | Estimated graphically for inflow waters | Regional groundwater (DWAF, pers. comm., 2000) | Seawater (Faure, 1992) | Global average coastal rainfall (Faure, 1992) |
|---|---|---|---|---|
| **Na** | 85 | 87 | 85 | 89 |
| **K** | 1 | 0.8 | 2 | 2.6 |
| **Mg** | 10 | 9 | 10 | 11 |
| **Ca** | 5 | 4.6 | 2 | 4.3 |
| **Cl** | 100 | 100 | 100 | 100 |
| **$SO_4$** | 7 | 2 | 5 | 9 |
| **Br** | 0.07 | n.d. | 0.2 | nd |

nd = no data

Mineral weathering is another major source of ions. Water travelling through a weathered aquifer or soil accumulates ions released by weathering reactions. Incongruent dissolution of feldspars to clay releases Na and Ca, while chemical weathering of biotite, olivine, pyroxene

and amphibole release K, Fe and Mg. Oxidation of sulphide minerals contributes $SO_4$ to water (Faure, 1992; Eugster, 1980). Very little Mg is contributed to waters from weathering of granite, most is retained at the source by ion exchange, so the source of Mg is more likely to be rain (Nesbitt *et al.*, 1980). Silica is released by weathering of silicate minerals, and quartz dissolution. Equilibrium with $CO_2$, carbonate minerals and hydrolysis of silicates determines the bicarbonate concentration of water (Faure, 1992). Congruent dissolution of soluble minerals like gypsum or carbonates can also be a source of Ca, $HCO_3$ and $SO_4$ (Faure, 1992; Eugster, 1980).

Ion concentrations in rain or soil water can further be affected by processes in the soil zone, like ion exchange, sorption, co-precipitation, salt dissolution and solution-mineral reactions (Herczeg and Lyons, 1991). Ion exchange can immobilise elements released by weathering (Nesbitt *et al.*, 1980). Cation ratios in the groundwater will change due to different exchange affinities, for example Na will enrich relative to Ca because calcium will be preferentially sorbed onto exchange sites (Herczeg and Lyons, 1991).

In summary, the primary source of major ions in pan waters is coastal rainfall, as indicated by the chemical signature of inflow water. Chemical weathering of granite in the catchment contributes minor amounts of Na, Ca and K, and a significant amount of alkalinity to the runoff waters. Congruent dissolution of gypsum enriches the coastal pans in Ca relative to the inland pans. Ion exchange within the catchment depletes K and Br from the waters before they enter the pans.



### 5.3.4. Spatial variation

The major element concentrations in depth profiles and from different sites at a pan vary considerably. Spatial variations in concentration tend to be consistent between pans. Sodium, K, Mg, Ca, Cl, $SO_4$, organic carbon and Br usually decrease in concentration with depth down the profile due to capillary evaporation concentrating salts at the surface. Exceptions are:

- Increase in Na from RA-SS1a to RA-SS1b, due to precipitation of halite in RA-SS1a and removal of Na from solution.
- Organic carbon is greatest in RA-SS3b, rather than RA-SS3a. RA-SS3a is very sandy.

- RA-SS3d for all elements, most likely because it is the recipient of saline evaporated reflux waters from the pan.
- Bromine in RA-SS3 increases with increasing depth.
- Calcium at Ysterfontein is most concentrated in YF-SS1b, probably due to dissolution of gypsum in the sediment. In the pan floor sample at Rooipan south (RA-SS1), calcium increases with depth. It is probably removed from solution in RA-SS1a by precipitation of gypsum.

Concentrations of almost all elements increase markedly from sediments adjacent to the pan to sediments of the pan floor. There are two reasons for this. Firstly, as the lowest topographical point, all leachable elements will ultimately concentrate in the pan floor sediments. Secondly, the proportion of clay under the pan surface is greater than adjacent to the pan, and the sediments will have a higher cation exchange capacity. An exception in the case of Rooipan south is Ca, which is more concentrated in the SPE of pan edge sediments. Calcium is removed from pan floor interstitial water by precipitation of calcite and gypsum.

## 5.4. TRACE ELEMENTS

Trace elements in brines have not been extensively studied. In theory they are able to provide as much information about the origin of salts and brine evolution as major elements, but they tend to have low concentrations in the inflow, making them difficult to study Trace element concentrations are often regulated by coprecipitation into minerals and ion exchange (Eugster, 1980).

### 5.4.1. SOLUTE TYPES

*Boron*

Boron behaves conservatively over most of the salinity range, but there is considerable scatter in the data (Figure 5.13 (a)). Eugster and Jones (1979) observed that boron behaves as a Type I solute, and that appears to be the case here. The SPE and surface water samples for brine-type pans are significantly off the trend and appear to have lost B. The curve may be flattening out, perhaps like a Type V solute. The samples from the mined pan are enriched relative to the remaining data, suggesting that B remains in solution and is not removed from the pan during the mining process. Sediment samples from the most dilute pans, Rooipan north (RB-SS1), Kiekoesvlei (KV-SS1b) and Droëvlei (DV-SS1a and b) are enriched in B.

Boron is adsorbed most effectively in the pH 8 to 9 range, on to oxides and silicate minerals. According to McBride (1994), a large fraction of total B is water extractable in some soils. The enrichment of B in brackish-saline pan sediments may be due to release of B from exchange sites into the SPE. Why B should be released from exchange sites of these sediments only is not known.

Boron is enriched relative to seawater in a few samples, but in general it is depleted relative to seawater (Figure 5.13 (b)). This indicates that the source of B is not from coastal rainfall, or that B is removed from solution by a mechanism like ion exchange.

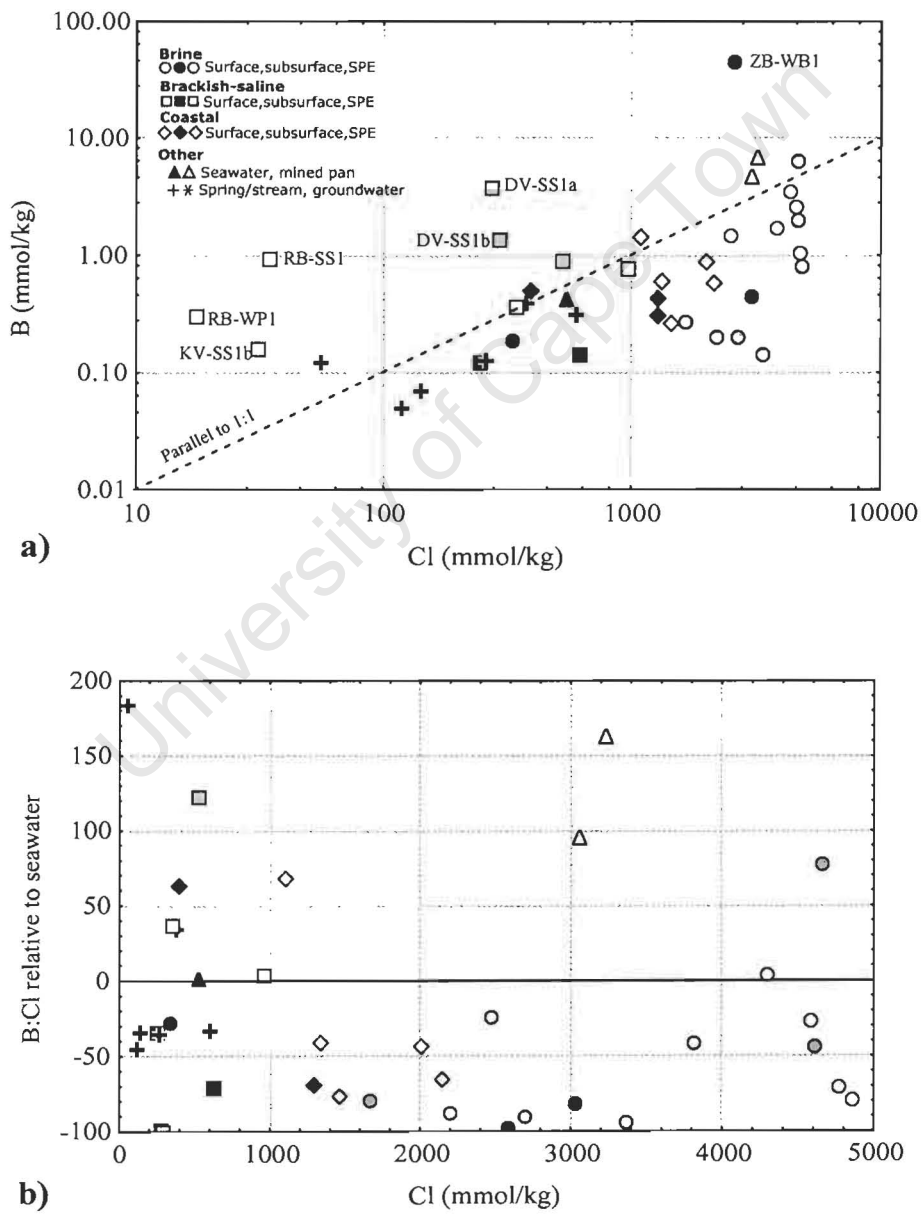


**Figure 5.13: (a) Relationship between B and Cl. Samples falling off the trend are labelled, (b) Variation of the B:Cl ratio relative to seawater with increasing salinity**

*Arsenic*

Arsenic behaves conservatively over most of the range of Cl concentrations (Figure 5.14 (a)). The mined pans are enriched in As indicating that As remains in solution even after halite precipitation. Brine-type and coastal pan SPE appear to be slightly depleted in As due to sorption of arsenate ($AsO_4^{3-}$) by calcite, loss of arsenic by volatilisation under reducing conditions (McBride, 1994), or coprecipitation with sulphides in the sediments (O'Neill, 1995). Arsenate adsorbs on oxides and clays effectively between pH 7 and 9, rendering it virtually immobile in oxidizing environments. Under anaerobic conditions arsenic is converted to sulphides (McBride, 1994).

Arsenic can be concentrated by evaporative concentration (O'Neill, 1995), and this seems to be the most likely mechanism for increasing As concentrations with increasing salinity in the pans. There are a number of outliers. Samples from Rooipan north and Kiekoesvlei are relatively enriched in As compared to the conservative trend, while sediment samples from the vegetated zone adjacent to Droëvlei, as well as RA-SS3a and ZB-WB1 are depleted relative to the general trend. Low values in Droëvlei samples could be due to leaching, as these samples were sampled from an area slightly above the pan, and above the water table. The Droëvlei samples are sandy compared to other samples, and would have low cation exchange capacity. Arsenic is highly enriched relative to seawater in most samples (Figure 5.14 (b)). This is a strong indication that As is not of marine origin and is probably derived by weathering of sulphide minerals in the granite.

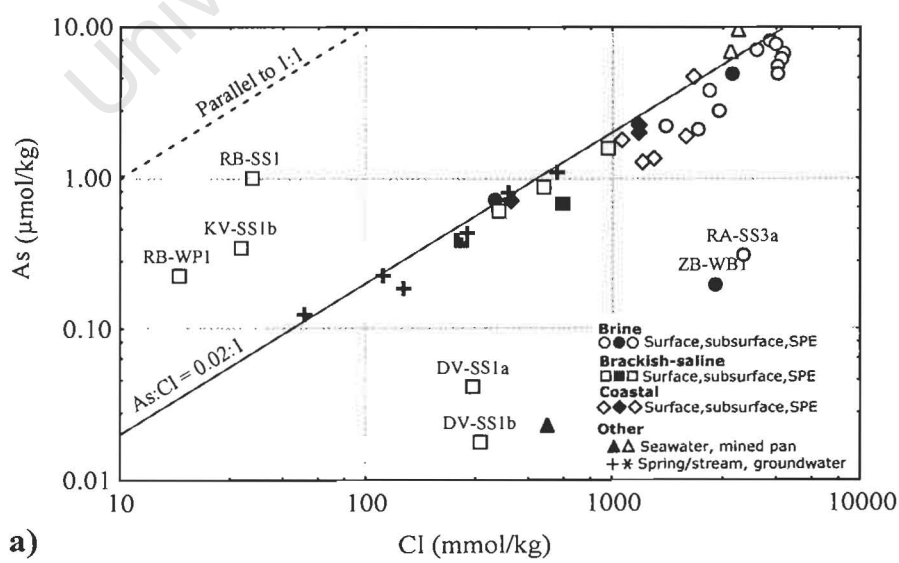


a)

**Figure 5.14: (a) Relationship between As and Cl. Samples falling off the trend are labelled. The fitted line is parallel to a 1:1 line and represents conservative behaviour,**

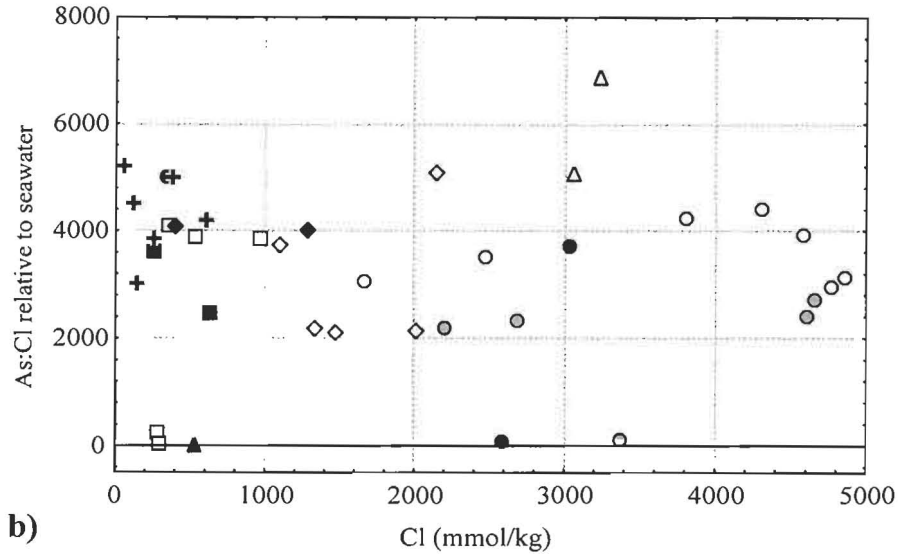


**Figure 5.14: (b) Variation of the As:Cl ratio relative to seawater with increasing salinity**

*Rubidium*

Although there is considerable scatter, Rb appears to be following the trend of a Type IIB solute, initially behaving conservatively and then being removed from solution in the brine-type pans (Figure 5.15 (a)), reminiscent of Ca behaviour (see Figure 5.8 (a)). Rubidium is enriched in the mined pan samples, so it is not precipitating into halite or gypsum. Rubidium is expected to behave most like K (McBride, 1994). Nesbitt *et al.* (1980) found that Rb is preferentially adsorbed onto clays over K, and Schloeman (1994) observed that Rb was retained in weathered granite and was particularly associated with soils of high clay content in the Darling area. These observations indicate that Rb behaviour is likely to be controlled by ion exchange. Concentrations of Rb are higher in the coastal pans, perhaps due to a lower proportion of silicate clay available for cation exchange (Section 5.7.2). Low Rb concentrations are found in samples DV-SS1a and DV-SS1b. As mentioned before, these samples are probably subject to leaching rather than capillary evaporation, resulting in depletion in trace elements. Rubidium is removed from the solution preferentially to K resulting in a gradual increase in the K:Rb ratio (Figure 5.15(b)), possibly due to the selectivity of ion exchange sites for Rb (Nesbitt *et al.*, 1980). Why Rb should only be removed from solution at high salinities is not known. A possibility is that Rb substitutes for K in clays that precipitate in brine-type pans, or that these clays provide a fresh sink of exchange sites for Rb. The depletion of Rb relative to seawater is due to ion exchange at the site of granite weathering which removes Rb from solution (Figure 5.15 (c)).

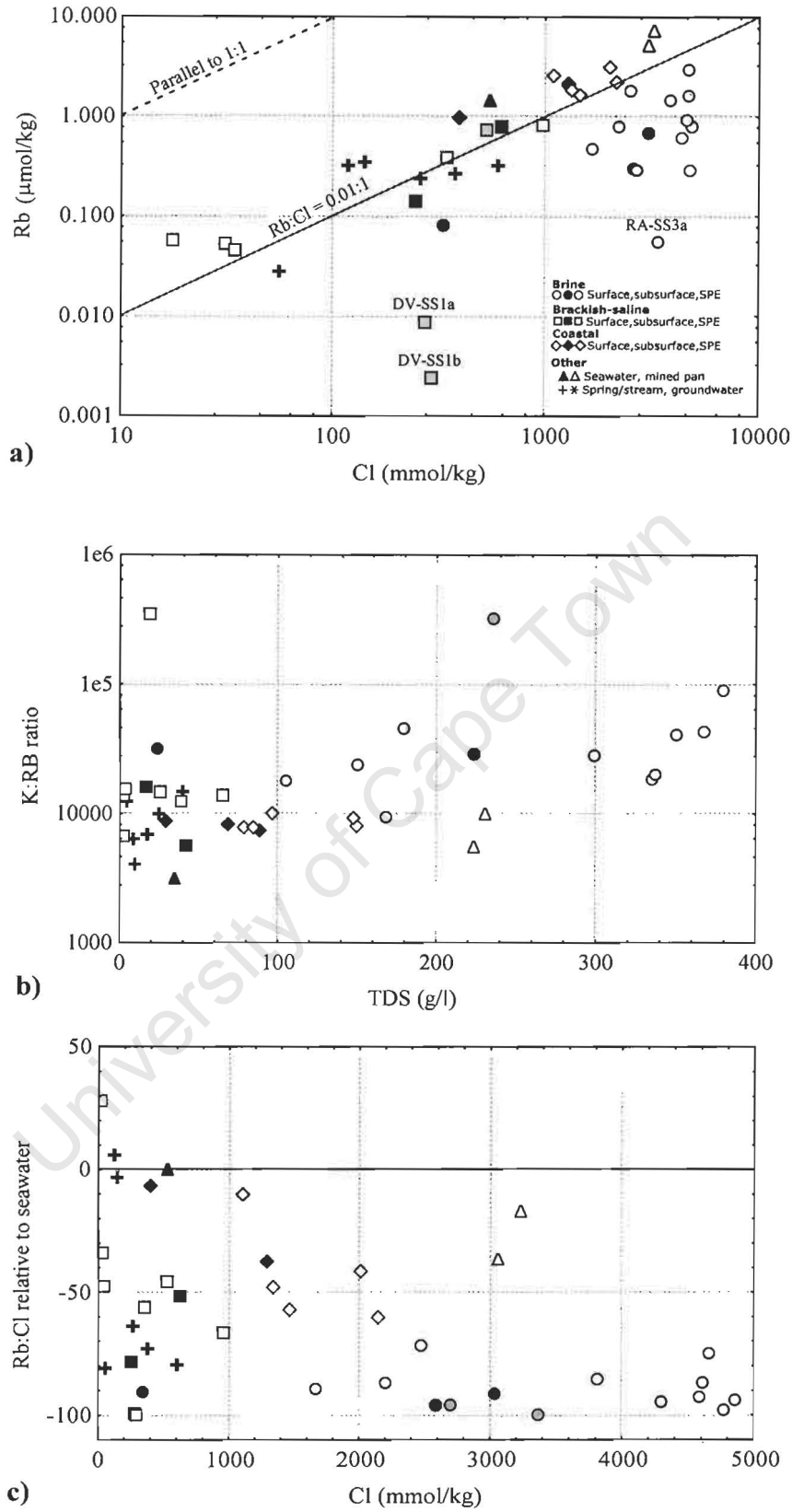


**Figure 5.15: (a) Relationship between Rb and Cl. Samples falling off the trend are labelled. The fitted line is parallel to a 1:1 line and represents conservative behaviour (b) K:Rb trend plotted against salinity. Note gradual increase in ratio, (c) Variation of the Rb:Cl ratio relative to seawater with increasing salinity**

*Strontium*

Strontium behaves similarly to Ca, as a Type IIB solute (Figure 5.16 (a)). It exhibits conservative behaviour in the dilute waters of streams and in the coastal and brackish-saline pans, but is depleted in the brine-type pan samples. The mined pan samples are depleted suggesting that Sr is removed from the pans with halite, probably as associated gypsum. According to Herczeg and Lyons (1991), Sr tends to partition into gypsum. Samples from Droëvlei and Rooipan north again plot off the trend. The Sr:Ca ratio increases with increasing TDS but the slope appears to flatten out after a TDS of about 200 g/L (Figure 5.16 (b)). Removal of Ca by calcite precipitation will increase the Sr:Ca ratio over the entire salinity range, but precipitation of gypsum and removal of Sr only occurs at salinities above 200 g/L. A small amount of Sr is removed by calcite, but most is incorporated into gypsum.

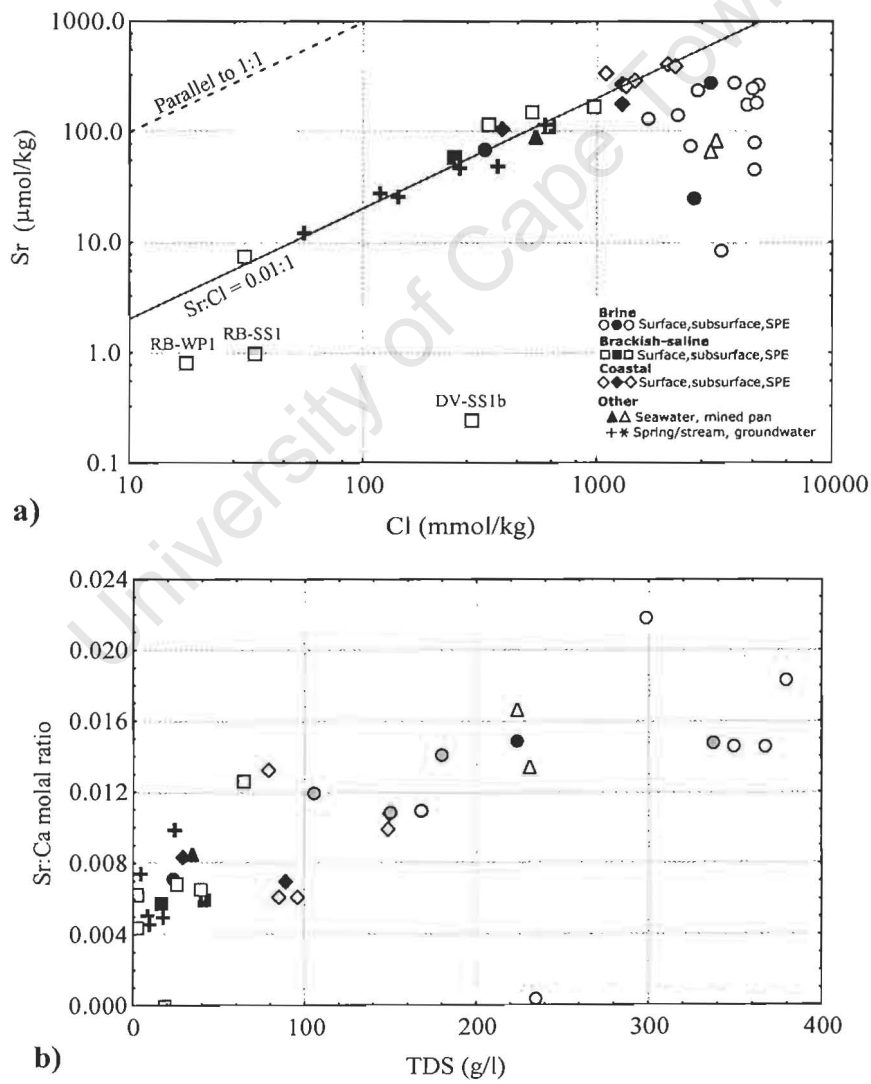


**Figure 5.16: (a) Relationship between Sr and Cl. Samples falling off the trend are labelled. The fitted line is parallel to a 1:1 line and represents conservative behaviour, (b) Sr:Ca trend plotted against salinity. Note gradual increase in ratio.**

**Table A.9. cont.**

| | Sample | | Duplicate | | | | |
|---|---|---|---|---|---|---|---|
| **Aluminium** | **Repeat 1** | **Repeat 2** | **Repeat 1** | **Repeat 2** | **Average** | **Std Dev** | **Precision (%)** |
| BA-WP1 | 4713 | 3736 | | | 4224 | 691 | 16 |
| BA-WP2 | 3710 | 3785 | 3069 | 3290 | 3463 | 341 | 10 |
| BA-WS1 | 4815 | 4425 | | | 4620 | 276 | 6 |
| BB-WB1 | 188 | 194 | 96 | 94 | 143 | 55 | 39 |
| BB-WP1 | 4861 | 4801 | 5052 | 5071 | 4946 | 136 | 3 |
| BB-WR1a | 130 | 143 | 290 | 282 | 211 | 86 | 41 |
| DV-WB1 | 13 | 31 | 34 | 23 | 25 | 9 | 38 |
| DV-WP1 | 165 | 106 | | | 135 | 42 | 31 |
| KP-WP1a | 5737 | 5735 | 4929 | 4196 | 5149 | 741 | 14 |
| OT-WR1 | 577 | 559 | | | 568 | 12 | 2 |
| RA-WB1 | 14755 | 13657 | | | 14206 | 776 | 5 |
| RA-WP1 | 2968 | 2899 | 6399 | 5399 | 4416 | 1760 | 40 |
| RB-WP1b | 2386 | 2225 | 1051 | 1066 | 1682 | 723 | 43 |
| RP-WB1 | 124 | 159 | | | 141 | 25 | 18 |
| RP-WP1a | 101 | 102 | 155 | 152 | 127 | 30 | 24 |
| SK-WB1 | 200 | 198 | 188 | 198 | 196 | 6 | 3 |
| SK-WP1 | 78 | 78 | 641 | 668 | 366 | 333 | 91 |
| YF-OT1 | 1922 | 1583 | | | 1752 | 240 | 14 |
| YF-WB1a | 98 | 84 | 235 | 246 | 166 | 87 | 52 |
| YF-WB2 | 121 | 134 | | | 128 | 9 | 7 |
| YF-WP1 | 6125 | 6422 | | | 6274 | 210 | 3 |
| ZA-WS2 | 132 | 140 | | | 136 | 5 | 4 |
| ZA-WP1 | 5843 | 5814 | | | 5828 | 20 | 0 |
| ZA-WR1 | 91 | 82 | | | 86 | 6 | 7 |
| ZA-WS1 | 536 | 465 | 115 | 125 | 310 | 221 | 71 |
| ZB-WP1 | 3325 | 3294 | | | 3309 | 22 | 1 |
| ZB-WS1 | 96 | 100 | | | 98 | 3 | 3 |
| KV-SS1b | 47 | 106 | 100 | | 84 | 32 | 38 |
| RA-SS1b | 4470 | 4669 | | | 4569 | 141 | 3 |
| RA-SS1b IW | 208 | 59 | | | 134 | 105 | 78 |
| RA-SS3b | 1871 | 2002 | | | 1937 | 93 | 5 |
| RA-SS3c | 2783 | 2954 | | | 2868 | 121 | 4 |
| RA-SS3d | 3108 | 3365 | | | 3237 | 182 | 6 |
| RB-SS1 | 109 | 107 | 155 | 149 | 130 | 26 | 20 |
| YF-SS1a | 4263 | 4488 | | | 4375 | 159 | 4 |

*Selenium*

Selenium behaves as a Type IIb solute (Figure 5.17 (a)). It displays conservative behaviour for most of the salinity range, but is removed from solution at high salinity. Selenium is enriched in both the samples from the mined pan, Burgerspan south, and the SPE from subaqueous samples at Rooipan south (RA-SS1a, RA-SS1b). In general, Se is found to behave like sulphur – it exists in the same oxidation states, and the oxidised form is more mobile than the reduced form (McNeal and Balistrieri, 1989). Selenate ($SeO_4^{2-}$), the predominant ion in oxidised soils (McBride, 1994), would be expected to follow sulphate.

Selenium could be removed from solution by ion sorption or by incorporation into sulphide minerals. Ion sorption is not effective under alkaline conditions because adsorption surfaces are negatively charged and adsorption is minimised. Some sorption will occur at more neutral pH (Eary, 1999). A redox control is more likely as the behaviour of Se is critically dependent on redox (McBride, 1994). Selenite ($SeO_3^-$) is the most stable form of Se in mildly reducing environments (McNeal and Balistrieri, 1989). In studies of evaporation ponds in California, it was found that only 2% of Se occurred as selenite in inflow waters, but within the pond waters, 20-30% occurred as selenite (Ohlendorf, 1989). Further reduction of Se to selenide ($Se^{2-}$) at the onset of sulphate reduction would allow Se to be concentrated by coprecipitation with iron monosulphides. This would concentrate Se in brine-type pan sediments, while depleting Se from the pan waters, as is observed. Mayland *et al.* (1989) found that Fe controls Se concentrations due to the association of Se with sulphides and adsorption onto iron oxides. Saturated paste extracts that plot off the trend (RA-SS3a, DV-SS1a, DV-SS1b) are all from oxidizing environments subject to leaching where soluble selenate would be washed down profile. Selenium is transported in a soluble oxidized form like selenate, concentrated by evaporation in the pans and some is immobilized into the sediments by reduction.

Magnesium exhibits a conservative relationship with Se (Figure 5.17 (b)). These elements are not expected to be incorporated into a single mineral phase, and the strong correlation between the variables is surprising and not understood. Selenium is highly enriched relative to seawater (Figure 5.17 (c)), indicating that Se does not have a marine origin. Selenium is also significantly more enriched in the sediment SPE than in water, indicating that sediments are acting as a sink for Se.

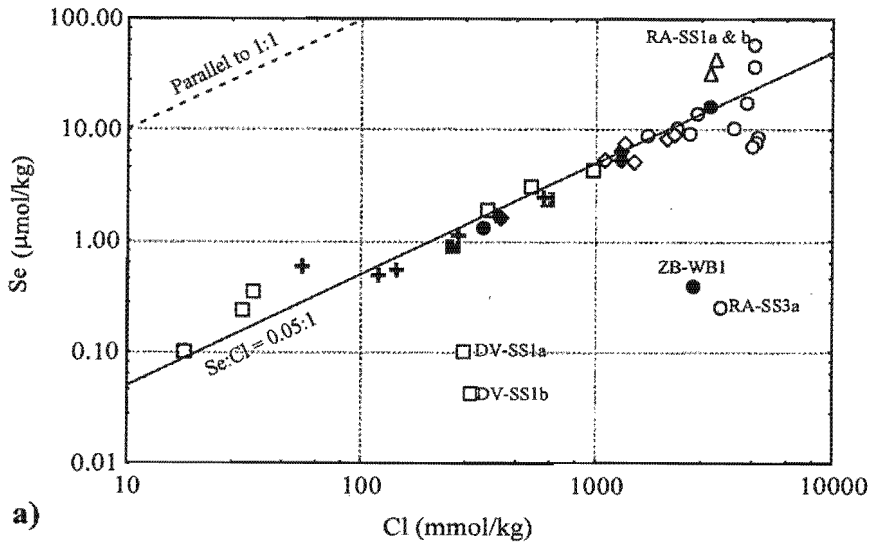


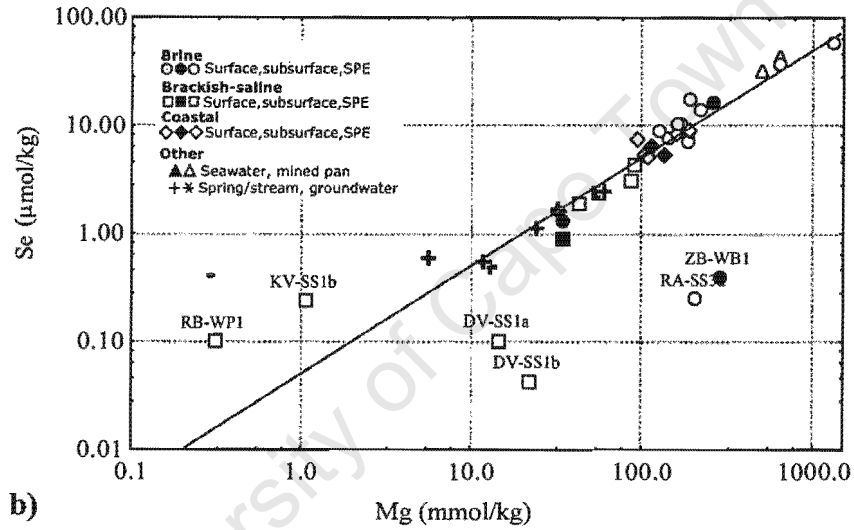


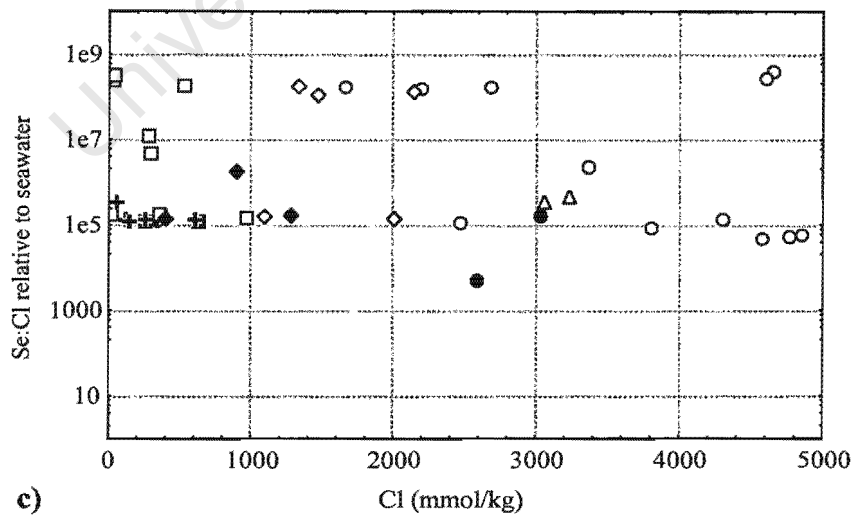


**Figure 5.17: (a) Relationship between Se and Cl. Samples falling off the trend are labelled. The fitted line is parallel to a 1:1 line and represents conservative behaviour, (b) Relationship between Se and Mg. The fitted line is parallel to a 1:1 line and represents conservative behaviour, (c) Enrichment factors for Se relative to seawater**

*Barium*

Barium displays a general increase in concentration with increasing salinity, but there is a large degree of scatter (Figure 5.18 (a)). Ion exchange may be the controlling variable. Barium and K have similar ionic radii, so Ba can substitute readily for K. Clays and humus exchange Ba selectively over Ca and Mg, so it is quite immobile (McBride, 1994). The mined pan samples do not exhibit an enrichment of Ba, so it may follow Ca into gypsum, or form very small quantities of barite ($BaSO_4$). Barium is enriched relative to seawater and probably originates from granites (Figure 5.18 (b)). It becomes depleted as it is removed from solution by ion exchange. The ratio of K:Ba initially increases sharply, indicating Ba is removed from solution selectively over K (Figure 5.18 (c)). The ratio levels out in the brine-type pans, indicating that Ba and K are being removed at the same rate. Samples from the mined pan are enriched in K relative to Ba, possibly because Ba is being removed from the pan as gypsum or as trace quantities of barite.



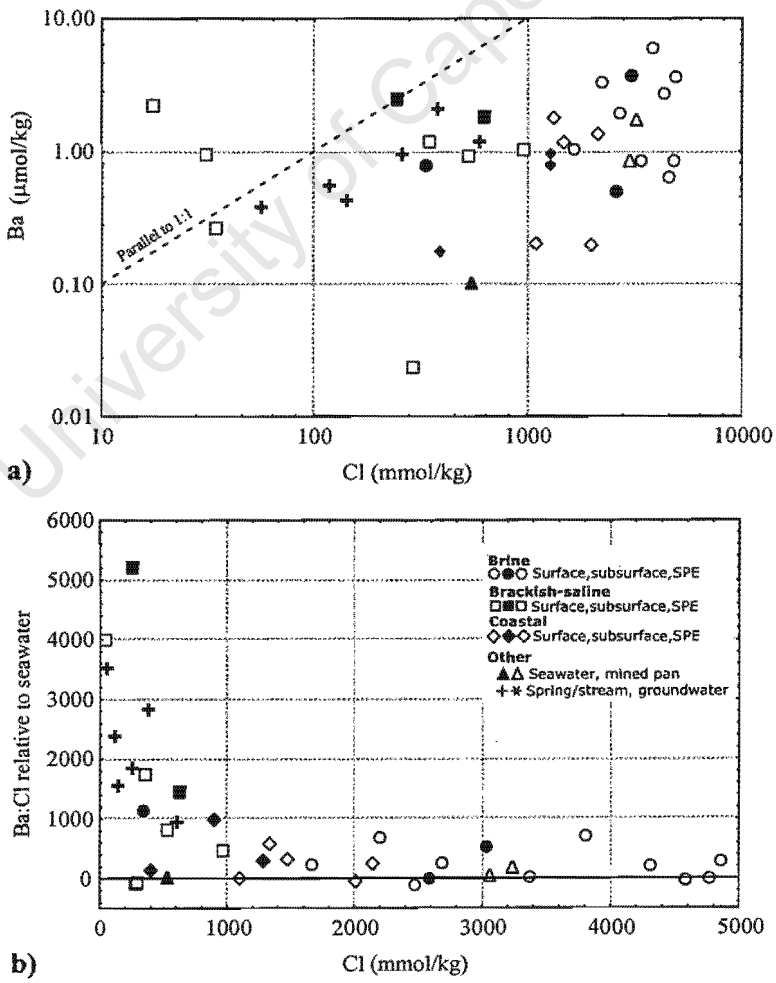


**Figure 5.18: (a) Relationship between Ba and Cl, (b) Enrichment factors for Ba relative to seawater.**

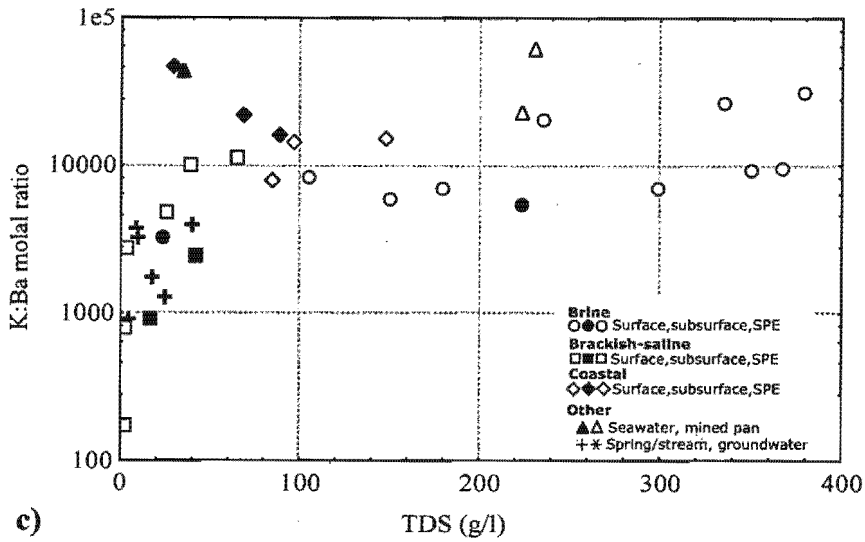


**Figure 5.18: (c) Variation in the K:Ba ratio with increasing salinity**



*Uranium*

Uranium behaves differently from most ions, exhibiting non-conservative behaviour with Cl (Figure 5.19 (a)). It behaves most like F and Si. Subsurface waters of low salinity have the highest U concentrations whereas surface waters from brine-type pans have virtually no detectable U. The reason for this could be that subsurface, spring and stream waters have all spent time in contact with the granite or granite-derived soils of the area. Granite is a known source of U (Drever, 1997) and the waters percolating through the granites may dissolve U and transport it to the pans. Pans with higher concentrations of U probably have a higher proportion of subsurface water entering the pans. Uranium is immobilised in reducing environments (Drever, 1997), and the subsurface sediments of all the brine-type pans were found to be reducing, which would remove U from solution. Low concentrations of U in coastal samples reflect distance from the source. The high concentrations of U in less saline waters could be because colloidal material can remain suspended if the salt concentration is not too high. If this material was not removed by filtering, the sample will appear to have high U concentration. In highly saline water, clays flocculate and are not sampled along with the water. Uranium is up to 10 000 times enriched relative to seawater in subsurface and stream water samples due to the granitic influence (Figure 5.19 (b)). Pan waters from two of the brackish-saline pans, Rooipan north and Droëvlei, are enriched in U.

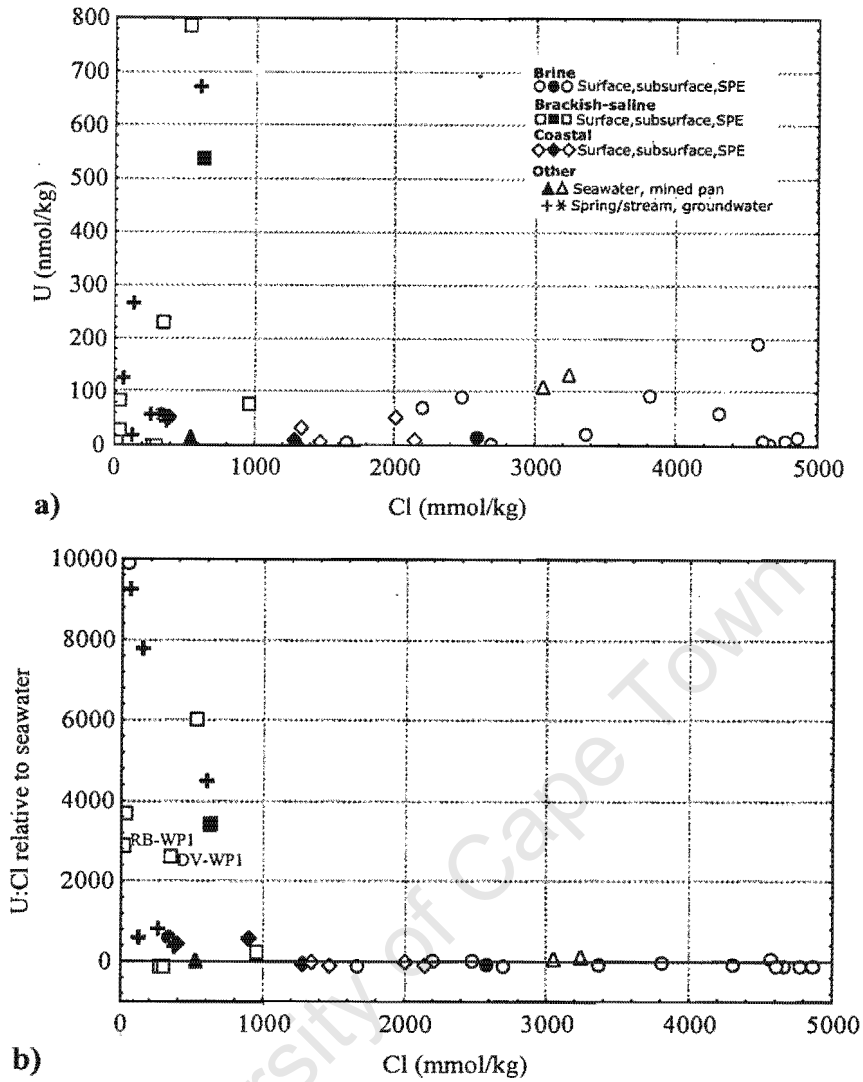


**Figure 5.19: (a) Relationship between U and Cl, (b) Enrichment factors for U relative to seawater**



*Silicon*

In many studies of brines, Si has been found to behave as a Type V solute, initially increasing in concentration with increasing salinity, and then maintaining a constant concentration with further increases in salinity (Eugster and Jones, 1979). This was not the case in the current study. Almost without exception, concentrations in low salinity subsurface, spring and groundwaters are higher than in the pan surface waters (Figure 5.20). Again, this pattern could be due to colloidal effects, but the high Si in the subsurface water versus low Si in the surface water of the coastal pans (of approximately the same salinity) suggests that it is a real effect. Silica appears most concentrated in subsurface and groundwaters, and is probably derived from weathering of granites. Silicon in samples from the mined pans is residually enriched. Diatoms can be important for its removal from solution (Eugster and Jones, 1979), but no evidence of diatoms was found. The low Si concentrations argue against formation of

clay as a sink for Mg, and many of the trace elements. However, Si concentrations in the SPE are generally higher than those found in the surface waters, and precipitation of clay may be possible within the sediments.

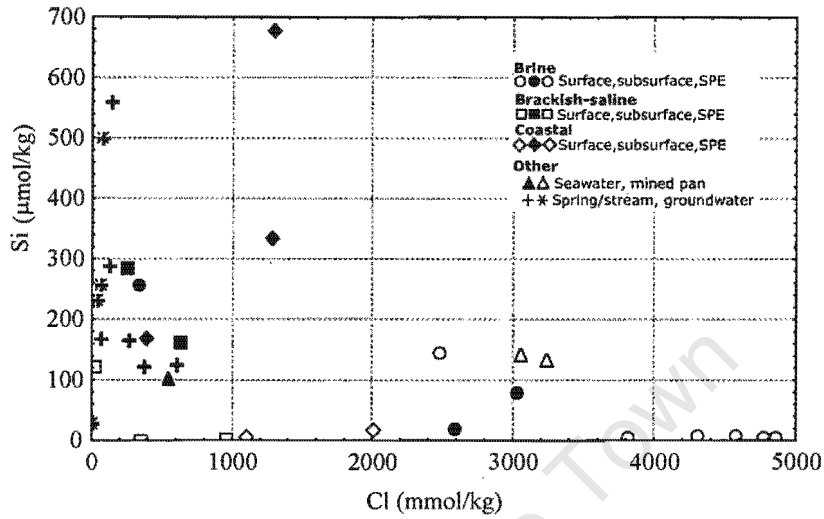


**Figure 5.20: Changes in concentration of Si with increasing Cl concentration**

*Lithium*

Lithium behaves slightly less than conservatively over most of the salinity range (Figure 5.21), but is depleted in the brine-type pan surface water samples, and enriched in the mined pan water samples and subaqueous sediments from Rooipan north. The enrichment in the mined pan water samples suggests it is not precipitating into a mineral, but it does seem to be removed from solution over the whole range of salinities, perhaps by ion exchange. In his study of soils of the Darling area, Schloeman (1994) noticed that Li concentrates from weathered granite into soil, but it does not appear to leach from the soil. Lithium is noticed to concentrate in fine-textured and Fe-oxide enriched soils, as would be expected if it was involved in ion exchange (Schloeman, 1994). The depletion of Li in brine-type pan samples is probably related to the similar depletions of Mg, Rb, Br and K.

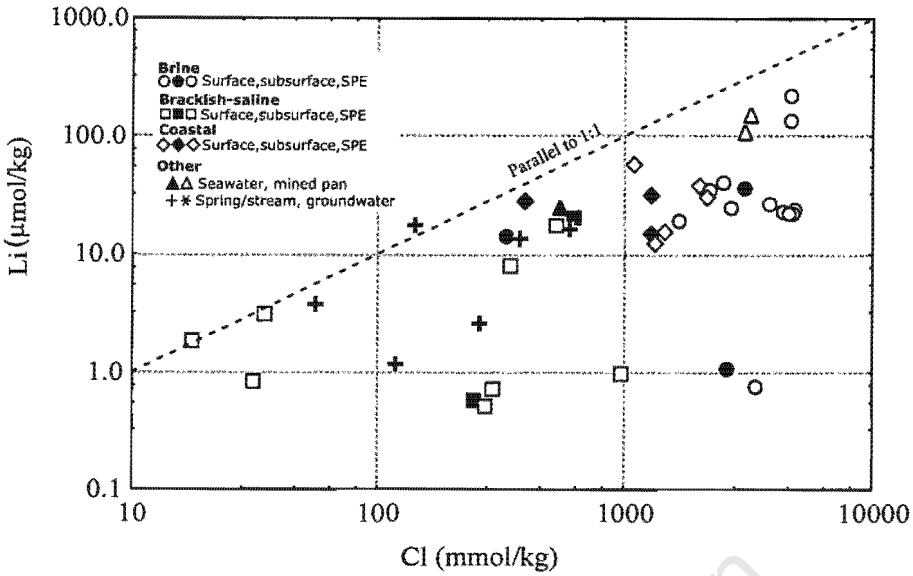


**Figure 5.21: Changes in concentration of Li with increasing Cl concentration**



### 5.4.2. ORIGIN OF TRACE ELEMENTS

Trace elements, like the major elements, probably originate either as weathering products, or as solutes in coastal rain and groundwater. Trace element concentrations in weathered Klipberg granite, a typical unweathered granite and seawater are listed in Table 5.3. Klipberg is a granitic hill found 8 km to the south of the pans, and provides representative data for trace element concentrations of granites in the study area (Schloeman, 1994).

Many trace elements originate as coprecipitates in feldspars and micas in granite – they rarely form their own minerals. Boron probably originates from coastal rainfall as it is the fourth most abundant ion in seawater (Hammer, 1986), but it is also present in granite. Arsenic and Se are easily weathered from sulphides in granite, and are significantly enriched in soils formed from granite. Selenium concentrations in the sea are very low, and granite therefore seems a likely source (Schloeman, 1994). Weathering oxidises insoluble reduced selenides in sulphide minerals to more soluble selenites and selenates (McBride, 1994). Bromine originates from the atmospheric aerosols and coastal rainfall (Schloeman, 1994). An appreciable amount of Rb is found in biotite and K-feldspar (Nesbitt *et al.*, 1980), but it is retained on exchange sites in weathered granite and not released into the soil, unless the soil has large percentages of clay (Schloeman, 1994). Strontium released by weathering of granite mimics Ca, and is released from granite at the same rate as Ca (Nesbitt *et al.*, 1980).

Potassium feldspars, plagioclase and biotite are important sources of Ba (Schloeman, 1994; Nesbitt *et al.*, 1980).

**Table 5.3: Trace element concentrations in the Klipberg granite, a typical unweathered granite and seawater**

| | Weathered Klipberg granite (mg/kg) (Schloeman, 1994) | Typical granite (mg/kg) (Drever, 1997) | Ocean (mg/kg ) (Drever, 1997) |
|---|---|---|---|
| **Li** | 16 | 30 | 0.17 |
| **B** | nd* | 10 | 4.45 |
| **F** | 404 | 800 | 1.30 |
| **Al** | Major | Major | 0.001 |
| **Fe** | Major | Major | 0.002 |
| **As** | 1.3 | 2 | 0.003 |
| **Se** | <0.7 | 0.05 | 0.0001 |
| **Br** | 1.0 | 4 | 67.3 |
| **Rb** | 357 | 150 | 0.12 |
| **Sr** | 7.7 | 250 | 8.1 |
| **Ba** | nd | 600 | 0.01 |
| **U** | 4.9 | 3 | 0.003 |

*no data



### 5.4.3. SPATIAL VARIATION

Like major elements, trace elements in saturated paste extracts display variation with depth and between pan edge and pan floor sediments. These variations are due to a number of factors, namely capillary evaporation, proportion of clay, redox conditions and mineralogy. Clay content increases from the edge to the centre of pans. At Rooipan south, RA-SS3b and RA-SS3c have a significantly higher proportion of clay than RA-SS3a or RA-SS3d, while YF-SS1c is the only sample at Ysterfontein with silicate clay. Sample YF-SS1a and YF-SS1b contain a large proportion of clay-sized material but it is predominantly calcite, which has low cation exchange capacity (McBride, 1994). Elements with concentrations that vary as a function of clay content are Li, Ba, Rb and U. These elements are found in greatest concentrations in samples with higher clay contents. Schloeman (1994) noted that these elements associate with the fine fraction and that their behaviour may be ion exchange controlled.

Sediments are more reducing with longer periods of water saturation, and the brine-type pan sediments are waterlogged year round. Pan floor sediments are more reducing than pan edge sediments. Selenium and As show increased concentration in more reduced sediments, but in

the absence of reducing conditions, capillary evaporation concentrates these elements at the surface. Strontium is found to behave like Ca, due to precipitation into gypsum.

## 5.5. STABLE ISOTOPES

Isotope ratios of rainwater are affected by latitude, continentality and temperature. There is a strong correlation between $\delta^{18}O$ and $\delta D$ of meteoric water worldwide. The best fit line of this relationship is known as the global meteoric water line (MWL) (Craig, 1961):

$$\delta D = 8\delta^{18}O + 10$$

The exact slope and intercept of the MWL varies from place to place due to local conditions. The MWL for the Western Cape is (Diamond and Harris, 1997):

$$\delta D = 6.1\delta^{18}O + 8.6$$

Latitude, altitude and temperature should be fairly consistent over the area considered, so variations in isotope ratios are due to evaporation and mixing. During evaporation, isotopically lighter molecules are preferentially evaporated, resulting in residual enrichment of the heavy isotopes in the water body. Evaporated water plots on a line with a lower slope than the MWL on a graph of $\delta D$ against $\delta^{18}O$. The gradient of an evaporation line depends on the humidity of an area (Drever, 1997).

Isotopic data do not indicate significant evaporation of pan water, although slight evaporation has occurred, as indicated by the high $\delta^{18}O$ of pan waters relative to the weighted average of rainfall for Cape Town airport (Figure 5.22 (a)). Coastal pan water is evaporated relative to inland pan water. The position of coastal pans between rainwater and seawater could be explained by mixing of the two waters or by evaporation of rainwater. Evaporation of the coastal pans is likely to be greater than the inland pans because the water is shallow (< 10 cm) and covers a large surface area. The most evaporated waters are two subsurface waters sampled from holes dug directly adjacent to the brine-type pans (ZB-WB1; RA-WB1). No other subsurface water is more evaporated than the corresponding surface water. There are two possible explanations for the enrichment of subsurface waters:

- Capillary evaporation from adjacent to the pan is an important process. Based on a number of laboratory experiments, Zimmerman *et al.* (1967) concluded that transpiration does not fractionate isotopes in soil water and that capillary evaporation from bare soil can only cause deuterium enrichments of 10 ‰. Capillary evaporation as a mechanism

of fractionation cannot be discounted as the subsurface samples with enriched isotope ratios were taken in unvegetated areas.

- Dense evaporated pan water is stored in the pan floor sediments.

All spring and seep waters plot in the vicinity of present-day weighted annual average Cape Town airport meteoric water, implying recharge by recent rain. The weighted average is likely to be the best approximation of the isotope composition of recharge water (Diamond and Harris, 1997). It is therefore not possible to distinguish between groundwater and meteoric water in order to determine relative contributions of each to the pans. However, water from the brackish-saline type pans Rooipan north and Droëvlei exhibit deuterium-enriched isotope ratios which are distinctly different from the bulk of the samples, representing a different source water.

If evaporation is the only process contributing to high salinities, there should be a positive correlation between $\delta^{18}O$ and TDS. An evaporative trend is noticed from meteoric water to the subsurface samples (Figure 5.22 (b)), including streams, brackish-saline pans and coastal pans. The surface waters of brine-type pans are not as isotopically heavy as would be expected if high salinity was due to evaporation. The high salinity is probably due to dissolution of soluble salts by dilute inflow water.



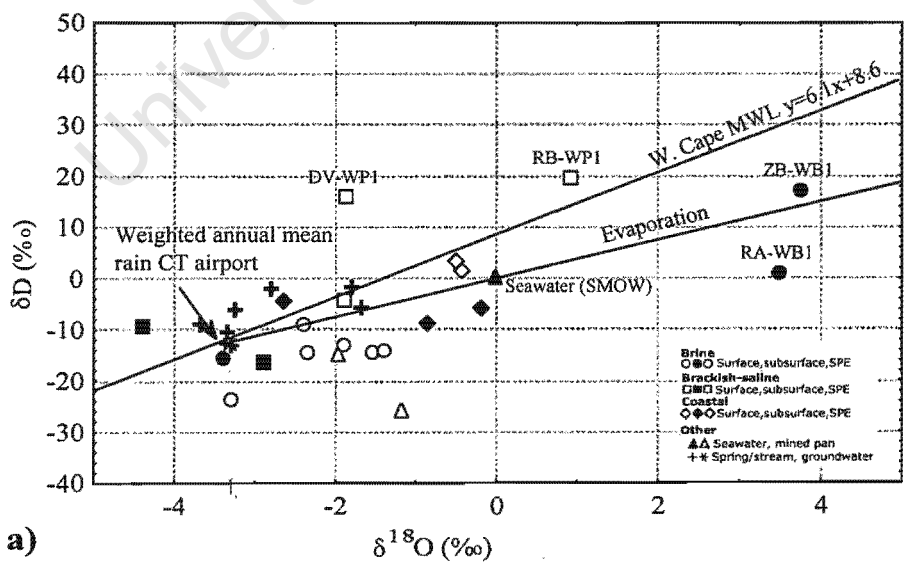


**Figure 5.22: (a) Plot of δD vs $\delta^{18}O$ showing the MWL for the Western Cape and evaporation trend**

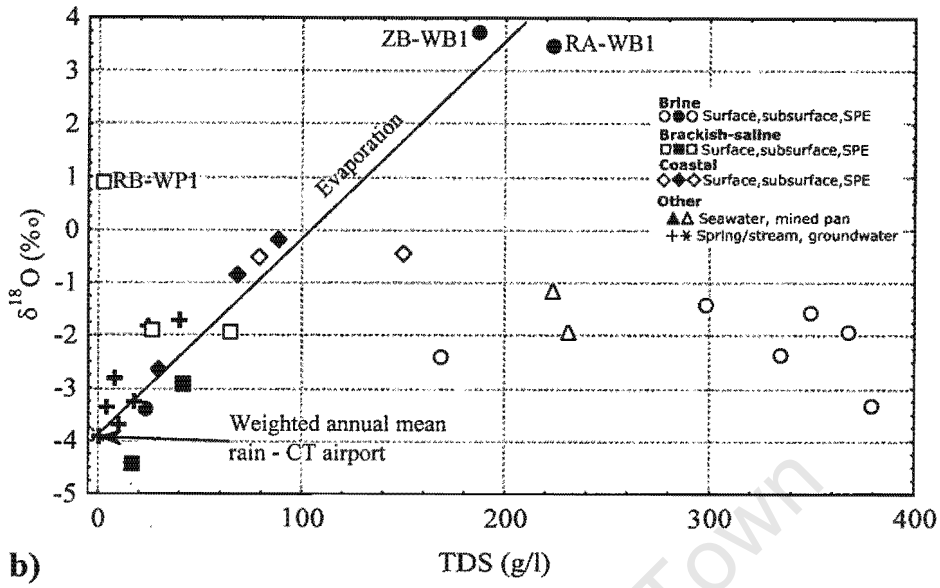


**Figure 5.22: (b) Evaporation illustrated by increasing $\delta^{18}O$ with increasing salinity. Note that the most saline samples are not evaporated.**

## 5.6. MODELLING

### 5.6.1. PHRQPITZ AND PHREEQC

Modelling of saturation and speciation of solutions was completed using the PHRQPITZ and PHREEQC geochemical modelling codes (Parkhurst and Appelo, 1999). Electrostatic interactions between ions in solution and the ordering of water around ions in hydration shells results in the free energy of a solution differing from that of an ideal solution. Ion activity, or effective concentration in solution, is generally less than the true concentration because of these interactions. Prediction of the extent to which a solution behaves non-ideally is possible using models (Drever, 1997).

PHRQPITZ makes use of specific-interaction theory, or the Pitzer model, to predict non-ideal behaviour. This is a complex expansion of the Debye-Hückel theory that includes coefficients for interactions between every pair and triplet combination of aqueous species. Mean activity coefficients are calculated for chemical reactions. This semi-empirical approach is applicable to mixed solutions of all ionic strengths (Drever, 1997; Parkhurst and Plummer, 1993). PHRQPITZ is designed for geochemical modelling in brines with ionic

strengths greater than that of seawater (Plummer *et al.*, 1988). PHRQPITZ software uses a database of interaction parameters for the system Na-K-Mg-Ca-H-Cl-$SO_4$-OH-$HCO_3$-$CO_3$-$CO_2$-$H_2O$, as well as B, Fe(II), Mn(II), Sr, Ba, Li, and Br (USGS, 1997). Limitations to PHRQPITZ are as follows:

- It doesn't account for the removal of water from solution by precipitation of hydrous minerals.
- Redox reactions cannot be modelled.
- Data in the database for Fe(II), Mn(II), Sr, Ba, Li, and Br have not been verified.
- Aluminosilicate calculations cannot be modelled because of a lack of interaction coefficients for aqueous aluminium and silicate species (USGS, 1997).

Calculations in PHRQPITZ are based on the modelling of Harvie and Weare (1980), Harvie *et al.* (1984) and Felmy and Weare (1986). The Pitzer model has been used successfully for ionic strengths up to 20 molar (USGS, 1997; Felmy and Weare, 1986; Harvie *et al.*, 1984; Harvie and Weare, 1980). The use of PHRQPITZ is outlined in Appendix C, along with the database and examples of input and output files.

Many of the limitations of PHRQPITZ are not shared by PHREEQC. In order to gain an understanding of aluminosilicate mineral behaviour and effects of redox, PHREEQC was used to model speciation and determine mineral saturation indices for solutions with salinity less than seawater. It was used in conjunction with the WATEQ4F database (Ball and Nordstrom, 1991). PHREEQC uses ion association theory to predict non-ideal behaviour of aqueous solutions, accounted for by the formation of ion complexes in solution. Activity coefficients are calculated using extensions of the Debye-Hückel equation which are only valid up to ionic strengths approaching seawater (Parkhurst and Appelo, 1999; Parkhurst and Plummer, 1993). Limitations shared by PHREEQC and PHRQPITZ include the assumptions that systems reach thermodynamic equilibrium and that alkalinity is assumed to represent carbonate species only.

### 5.6.2. SPECIATION

The speciation, or chemical form of an element, can affect bioavailability, toxicity, chemical equilibrium and adsorption of the element (Drever, 1997; McBride, 1994). PHRQPITZ does not calculate comprehensive speciation for elements. Speciation calculations for all elements for low salinity samples (i.e. less than seawater) were performed using PHREEQC. As the

redox potential of the system is not known, the default redox potential (pe = 4) was accepted, and speciation of elements that are redox dependent disregarded. Literature consensus was used to predict possible speciation for redox-dependent elements. A significant exclusion from calculations is organic carbon. Organic complexes can affect solubility of elements and adsorption of trace metals (Drever, 1997).

Sodium, Rb, K, Ba and Li are predicted to occur dominantly as monovalent ions, they do not form ion pairs at low salinities. Complexes of Mg, Na and Ca should begin to form with $SO_4$ at increased salinities, but the $SO_4^{2-}$ ion is expected to dominate at all salinities investigated with PHREEQC (< seawater). At high pH (> 9) carbonate complexes may begin to form. Sulphate is redox affected but reducing conditions sufficient for the formation of sulphides were only noticed in the sediments of the brine-type pans. The interface between the reducing sediments and water had an oxidised edge, indicating the water is not highly reducing, so most S in water would occur as sulphate. Fluorine in solution should occur either as the fluoride ion, or as a $MgF^+$ complex. Fluoride has a particular affinity for Al, forming stable complexes which increase the solubility and mobility of both ions in solution, but probably reduce the toxicity of high concentrations of Al (McBride, 1994). Between pH 6.5 to 7.5, boric acid ($B(OH)_3$) is predicted to dominate, but borate ($B(OH)_4^-$) should become dominant at pH 9. The borate anion is noted for adsorbing to soil organic matter, iron oxides and silicate minerals strongly at pH between 8 and 9. The solubility of B can be increased by the formation of Na borate salts, but these are not predicted to form by PHREEQC (McBride, 1994). Barium is calculated to occur mostly as $Ba^{2+}$ in all samples modelled. However, a significant proportion (10-40%) should occur as $BaSO_4^0$ in solution. Silicic acid ($H_4SiO_4$) is expected to dominate over the whole range of pH and salinity, but should form $H_3SiO_4^-$, a more soluble form of silica, at higher pH. If the pH were to increase further (> 9), silica concentrations in solution would be expected to increase (McBride, 1994). Strontium is predicted to occur as $Sr^{2+}$, with a small amount of complexation to $SO_4^{2-}$ (10%). The relationship is independent of both pH and TDS.

Arsenic, Se and U are redox affected elements and their speciation could not be modelled. It is possible to make some predictions based on knowledge of their behaviour. In conditions as found in the pans, As may be found as the arsenate species ($HAsO_4^{2-}$ ) under oxidizing conditions above pH 7. Under the more reducing conditions that occur in the brine-type pan sediments, $As(OH)_3$ should be the dominant species. However, the change from oxidised to

reduced species and vice versa is not rapid and the speciation may not be in equilibrium with current conditions (O'Neill, 1995). Selenium is affected by redox conditions and pH. Under oxidizing conditions, $HSeO_3^-$ will dominate up to pH of approximately 8 and then selenite $SeO_3^{2-}$ will become dominant (McBride, 1994). Brine-type pan waters may be slightly reduced due to the decrease in oxygen solubility in water with increasing salinity (Hermann *et al.*, 1973). In this case, selenite is expected to be the more common species. In the black muds underlying the brine-type pans, the conditions are sufficiently reducing for sulphate reduction and selenium is likely to be reduced. Uranium is mobile in oxidised environments and immobile in reduced environments, so the black reducing muds underlying the brine-type pans may be an important sink for U. PHREEQC predicts that in oxidizing waters, uranyl carbonate ($UO_2(CO_3)_3^{4-}$) and to a lesser extent $UO_2(CO_3)_2^{2-}$ will be the dominant dissolved species.

### 5.6.3. Mineral saturation indices

Saturation indices indicate the saturation state of a mineral with respect to a solution composition. The saturation index (SI) is defined as:

$$SI = \log_{10}\left(\frac{IAP}{K_{sp}}\right)$$

where IAP is the ion activity product as defined by the mass action equation and $K_{sp}$ is the solubility-product constant for the mineral. Saturation indices greater than 0 imply super-saturation of the water with respect to that mineral, if the SI is 0, the water is in equilibrium (saturated) with the mineral, and if it is less than 0, the solution is undersaturated with respect to the mineral. It is important to note that the SI gives no indication of the kinetics of mineral precipitation or dissolution. Minerals that are not kinetically favoured may only precipitate extremely slowly, for example dolomite and magnesite (Parkhurst and Plummer, 1993). Equilibrium with respect to a solid phase is the simplest process that might control the concentration of trace elements in solution (Drever, 1997).

Uncertainties in modelling of saturation indices arise particularly from uncertainty in pH and redox data (Parkhurst and Plummer, 1993). Measurements of pH in this study are fairly confident. However, no measurement of redox potential (Eh) was done and an attempt to calculate Eh from the relative proportions of $Fe^{2+}$:$Fe^{3+}$ in the system failed as iron concentration was below detection limits. However, even measurement of Eh is no guarantee

of confidence, as redox species in solution are commonly not in equilibrium with each other (Drever, 1997). Most waters sampled are expected to be well aerated and oxidizing, except the interstitial waters from subaqueous sediments. Most minerals modelled by PHRQPITZ are not redox dependent.

Halite is the most likely mineral to control Na and Cl concentrations (and salinity) of the solution. It was mentioned in Section 5.2.1 that no TDS greater than 373 g/L was measured and the limiting factor was probably halite saturation. Halite saturation has not yet been reached (Figure 5.23 (a)) but it is expected to become saturated at a TDS concentration of about 400 g/L. Gypsum solubility controls the concentrations of Ca and $SO_4$ in solution (Figure 5.23 (b)). Gypsum is the least soluble of the common sulphate minerals (which include epsomite ($MgSO_4 7H_2O$) and mirabilite ($Na_2SO_4 10H_2O$)) and as such is the first to reach saturation, precipitate and control solubility. Sulphate concentration is limited only by gypsum precipitation in many aqueous systems (Drever, 1997). Calcite solubility is controlled by pH, but calcite is supersaturated in most solutions, indicating that gypsum is the phase regulating Ca concentrations (Figure 5.23 (c)). Calcite often appears oversaturated in natural aqueous systems due to slow precipitation kinetics, the solubility of $CO_2$ (g) and rate of $CO_2$ (g) loss or gain by solution (Eary, 1999). It is due to the slow precipitation of calcite that gypsum controls Ca solubility. The SI of common Mg-phases are plotted on Figure 5.23 (d). All samples are supersaturated with respect to dolomite and magnesite and undersaturated with respect to epsomite. Magnesium concentrations are not regulated by dolomite and magnesite because of kinetic limitations to their precipitation (Drever, 1997).



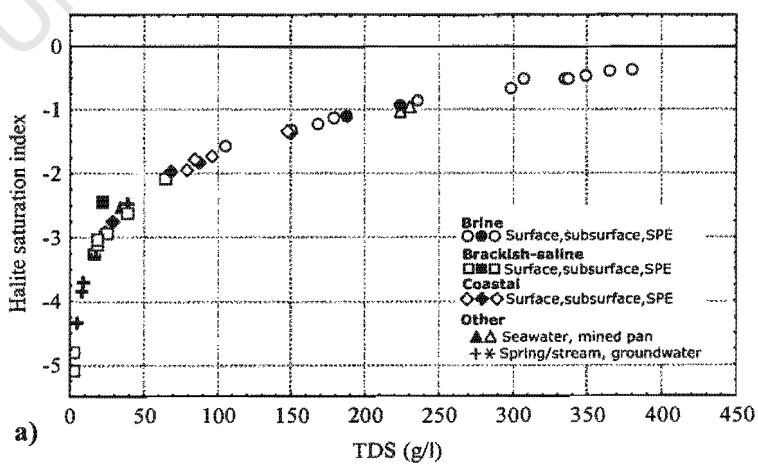


**Figure 5.23: (a) Saturation index of halite as a function of TDS**

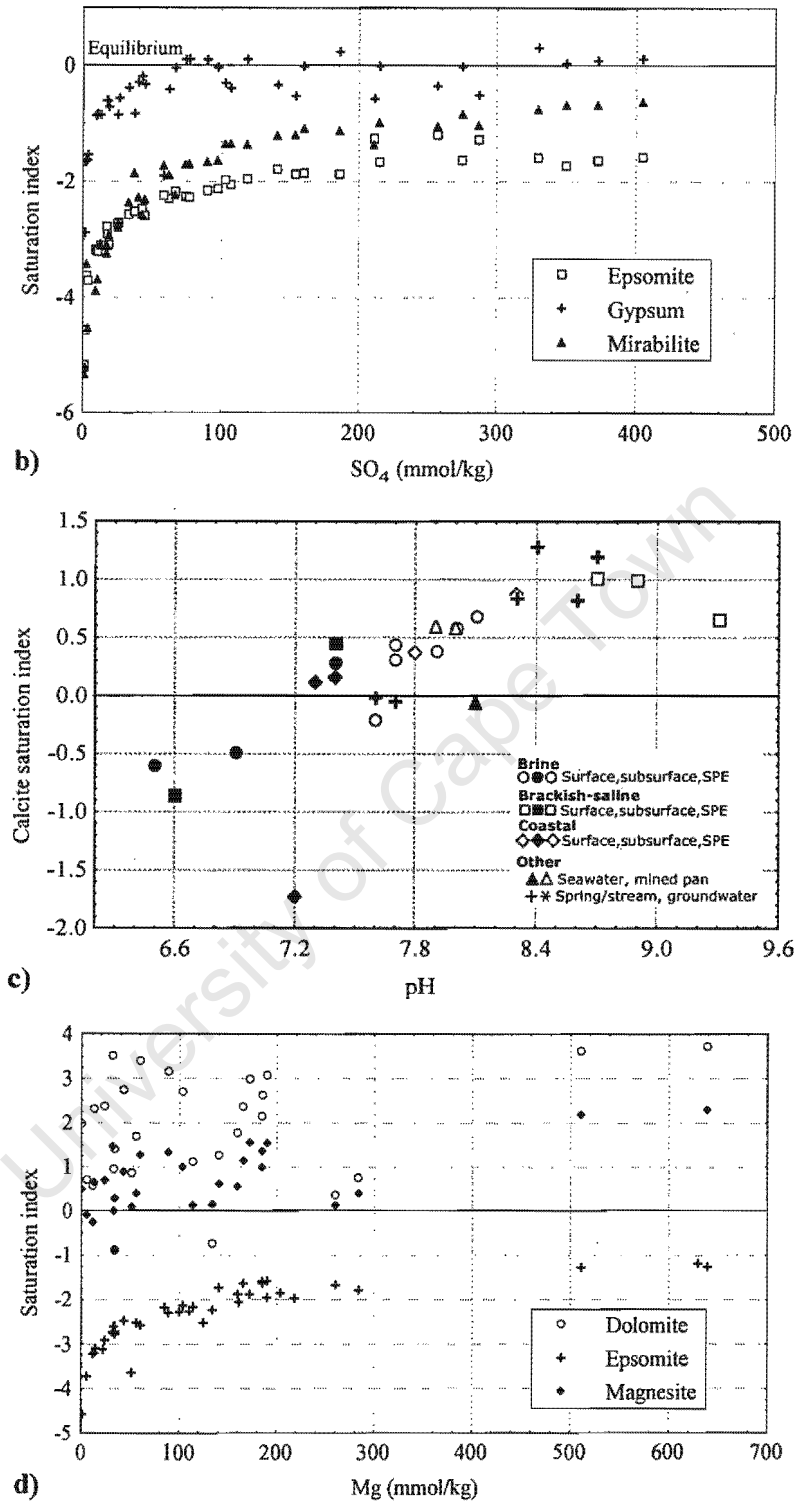


**Figure 5.23: (b) Relationship between the saturation indices of epsomite, gypsum and mirabilite and sulphate concentration, (c) Calcite SI as a function of pH (d) Saturation indices of common Mg minerals (dolomite, epsomite, magnesite) as a function of Mg concentrations**

Strontianite ($SrSO_4$), celestite ($SrCO_3$), barite ($BaSO_4$) and witherite ($BaCO_3$) thermodynamic data from the WATEQ4F database (Ball and Nordstrom, 1991) were added to the PHRQPITZ database in order to assess the controls on Sr and Ba concentration. Eary (1999) found that in water where sulphate exceeds bicarbonate, Ca, Ba and Sr concentrations are controlled by the sulphate mineral phase, whereas in bicarbonate-dominated solutions, the carbonate phase dominates. The samples are oversaturated with respect to barite, and undersaturated with respect to witherite (Figure 5.24 (a)). No barite was detected by XRD, but barite may only be precipitating in trace amounts. Precipitation of barite is substantiated by the apparent depletion of Ba in mined pans as discussed in Section 5.4.1. Nordstrom *et al.* (1992) found that barite is often supersaturated up to half an order of magnitude, and suggested that this is due to kinetic limitations on precipitation. However, in the current study the SI index for barite continues to increase and does not appear to level out. A combination of barite precipitation and ion exchange may regulate Ba concentration in the pans. Strontium concentration does appear to be regulated by the sulphate Sr-phase, celestite (Figure 5.24 (b)).



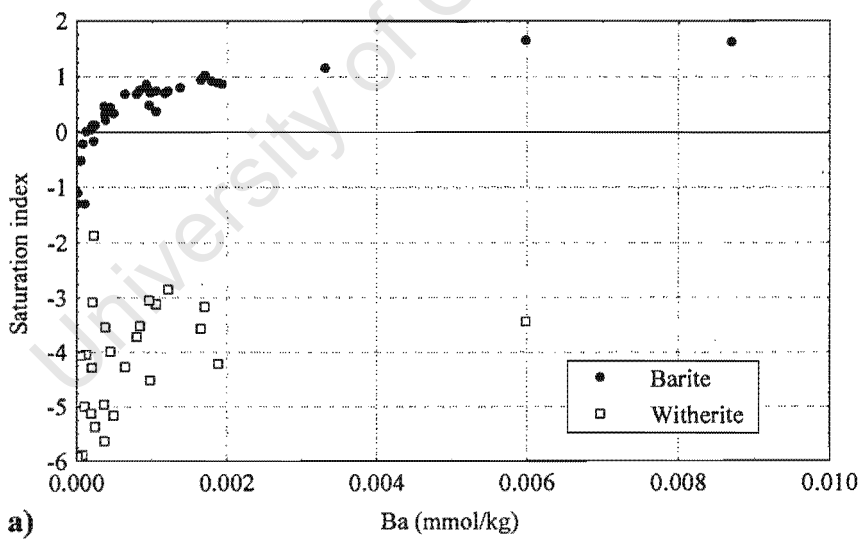


**Figure 5.24: (a) Saturation indices of barite and witherite as a function of Ba concentration**

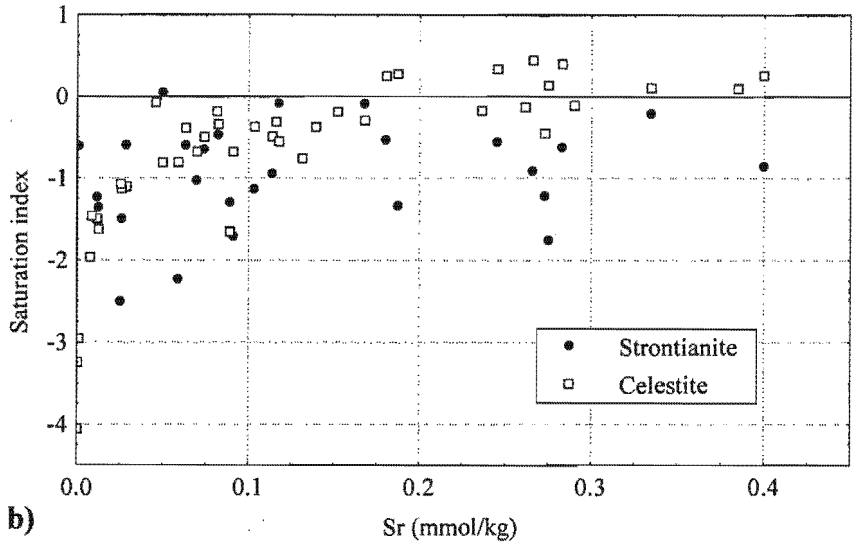


**Figure 5.24 (b) Saturation indices of strontianite and celestite as a function of Sr concentration.**

Samples with TDS values below that of seawater were modelled on PHREEQC to determine silicate mineral saturation. These samples are mainly subsurface, spring and stream samples, as well as pan water samples from Droëvlei and Rooipan north. It must be remembered that Al determination by ICP-MS was fairly uncertain and may be overestimated due to the presence of colloids. Modelling of albite and quartz saturation indices reveals that most of the less saline samples appear to be in equilibrium with these common granitic minerals (Figure 5.25 (a)). Kaolinite, a common alteration product of feldspar, is supersaturated in all samples. The low silica concentration of brine-type pan waters suggests that they are not in equilibrium with quartz. The hypothesis of precipitation of a clay mineral to remove Mg from solution in brine-type pan waters cannot be tested as PHRQPITZ is incapable of modelling clay mineral saturation indices. Many of the high pH low-salinity samples are found to be supersaturated with respect to sepiolite (Figure 5.25 (b)). Sepiolite was tentatively identified in Rooipan north, and saturation indices for RP-WP1 do indicate precipitation is possible. However, the low Si concentration of more saline brine-type waters argue against equilibrium with sepiolite.

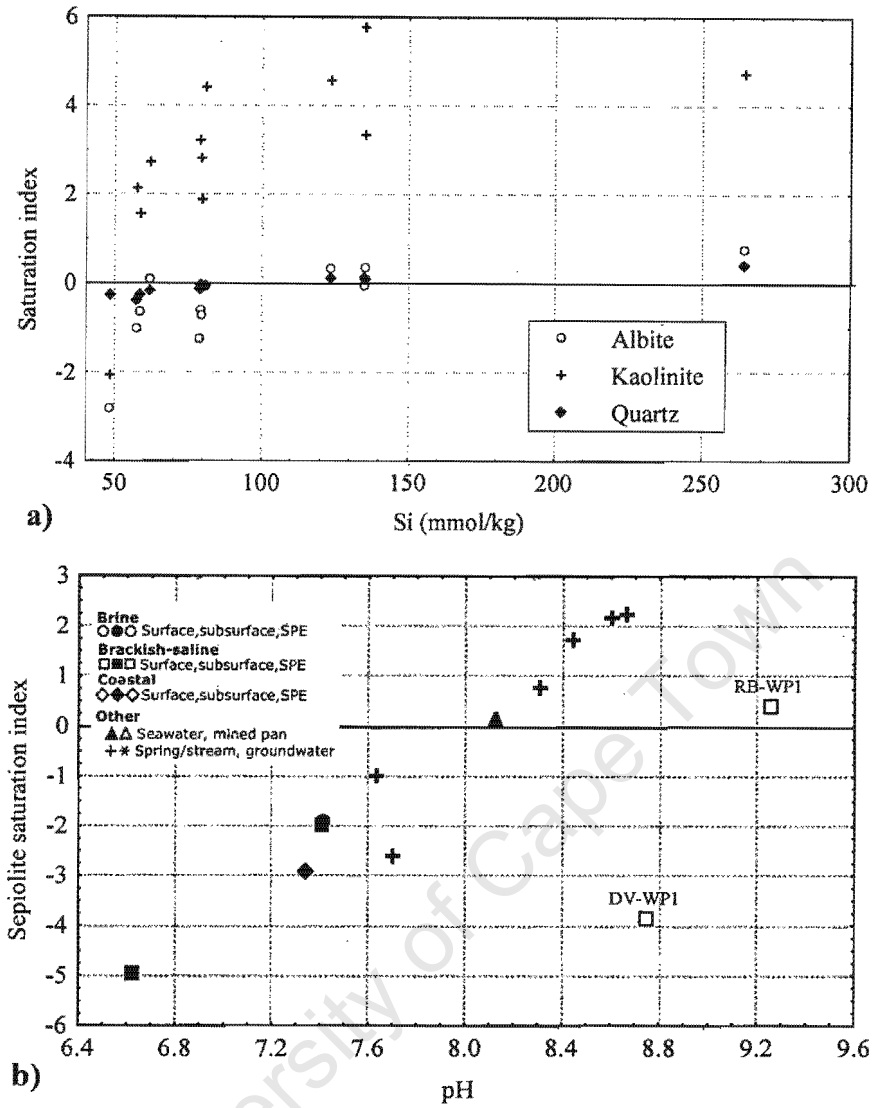


**Figure 5.25: (a) Saturation indices for common granitic minerals as a function of Si concentration, (b) Saturation indices for sepiolite as a function of pH.**

Fluoride solubility is commonly limited in pan systems by fluorite ($CaF_2$), the least soluble F-containing mineral that can form in low-temperature systems (Eary, 1999, Edmunds and Smedley, 1996). In this study, the solution is undersaturated with respect to fluorite in most of the less saline samples, reaching saturation in just one sample, DV-WB1 (Figure 5.26). Fluoride concentrations are highest at low salinities, and lowest at high salinities, so it is unlikely that brine-type and coastal pan waters will be saturated with fluorite. It is not known what controls F solubility.

Both As and Se have been found to accumulate in alkaline (pH > 7.5) lakes because there is no mechanism limiting their concentrations in solution. The most likely control on solubility of both elements is adsorption, which decreases significantly at higher pH (Eary, 1999).

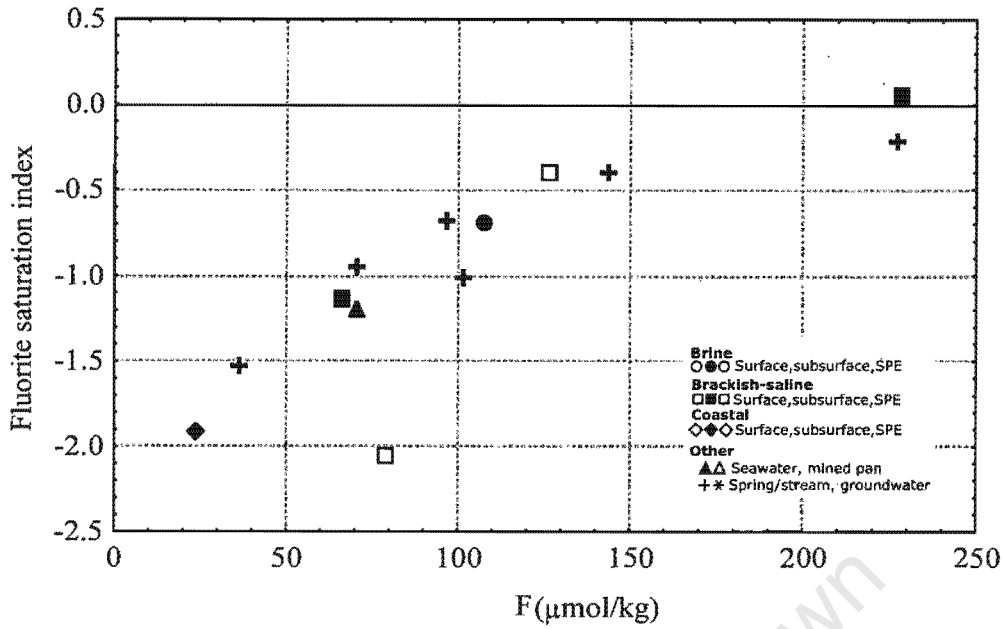


**Figure 5.26: Relationship between fluorite saturation indices and F concentration**



### 5.6.4. ROOIPAN NORTH

Throughout the preceding sections, samples from Rooipan north have been found to plot off the general trends. It is thought that water from Rooipan north may represent a deeper or older groundwater in equilibrium with granite, that has mixed with shallower groundwater with a seawater-like composition. In order to test this hypothesis, PHREEQC was used to equilibrate meteoric water with common granite minerals, namely quartz, albite (Na-feldspar), adularia (K-feldspar), K-mica, and the weathering product, kaolinite. This water was then mixed with shallow groundwater, as represented by ZA-WS1. The results, normalised to Cl, are given in Table 5.4. A mixture of 20% granite-equilibrated rainfall with 80% shallow groundwater yield pH, Na:Cl, Mg:Cl, $SO_4$:Cl and alkalinity:Cl ratios that are very similar to RB-WP1. Calcium in RB-WP1 may be affected by calcite precipitation while K appears to be derived from an additional source. The elevated trace element concentrations (B, As, Rb, Ba, U and Si) observed for this sample confirm a greater granitic influence on the water.

**Table 5.4: Results for modelling of possible origin of water of composition RB-WP1 (all results normalised to Cl)**

| Element normalised to Cl | Global average coastal rainfall (Faure, 1992) | Rainfall equilibrated with common granite minerals | Shallow groundwater (ZA-WS1) | Mixture (20:80) | RB-WP1 |
|---|---|---|---|---|---|
| pH | 5.7 | 9.2 | 8.4 | 9.1 | 9.3 |
| Na | 89 | 581800 | 82 | 122 | 143 |
| K | 2.6 | 0.002 | 0.08 | 0.08 | 2.3 |
| Ca | 11 | 4.3 | 3.1 | 3.6 | 0.1 |
| Mg | 4.3 | 11 | 10 | 10 | 10 |
| Cl | 100 | 100 | 100 | 100 | 100 |
| $SO_4$ | 9 | 9 | 6 | 6 | 8 |
| Alkalinity | 7.7 | 408700 | 0.6 | 28 | 29 |

## 5.7. SEDIMENT MINERALOGY

### 5.7.1. BULK MINERALOGY

According to the Hardie-Eugster model, calcite in brines evolves from low to high-Mg calcite as the Mg:Ca ratio increases (Eugster, 1980). There is evidence for this in a number of samples. Mg-calcite is found in the subaqueous sample (DV-SS2) consistent with the relatively high Mg:Ca ratio of the waters from this pan (Figure 5.9 (b)). The calcite in RA-SS3b, with a d-spacing of 3.02 (approximately 5 mole % $MgCO_3$) appears to have precipitated earlier in the evolution of water than calcite in RA-SS3a, which has a d-spacing of 2.98 (approximately 20 mole % $MgCO_3$). Watson (1983) found that if salts are leached down a soil profile and minerals precipitate, calcite would be found at the surface, underlain by gypsum and then halite. The sediments at Rooipan south show a reverse order, indicating that water movement is upwards. These observations are consistent with concentration of water due to capillary evaporation, which exerts an upward pull on water. The same phenomonen is seen in the subaqueous sediments of Rooipan south (RA-SS1a and b). Calcite in the surface layer contains a higher proportion of Mg than the underlying layer, implying upwards movement of water and recharge from below.

A single peak at 2.89Å in sample RA-SS1a indicates the presence of dolomite. Dolomite and magnesite are both supersaturated in all samples according to saturation index modelling. Precipitation of primary dolomite does not occur without microbial mediation, even if a solution is supersaturated with respect to dolomite because reaction kinetics are too slow:

$Ca^{2+} + Mg^{2+} + 2(CO_3^{2-}) = CaMg(CO_3)_2$ (Warren, 2000).

Dolomite is thought to form at low temperatures by the dolomitisation reaction:

$2CaCO_3 + Mg^{2+} = CaMg(CO_3)_2 + Ca^{2+}$ (Drever, 1997).

This reaction is slow, and rare unless the Mg:Ca ratio is much greater than 1 (Drever, 1997). Baker and Kastner (1981) report that the presence of dissolved $SO_4^{2-}$, even at concentrations of less than 5 % of seawater $SO_4^{2-}$ (approx. 1.4 mmol/kg), can inhibit dolomitisation under experimental conditions. Microbial reduction of $SO_4^{2-}$ to sulphides is an effective mechanism for removal of sulphate from sediments, allowing the formation of dolomite (Baker and Kastner, 1981). In contrast, Vasconcelos and McKenzie (1997) propose that the precipitation of dolomite is microbially mediated by sulphate-reducing bacteria, and that sulphate is an essential component for the formation of dolomite. They found dolomite precipitating in a black sludge layer under hypersaline anoxic conditions in association with Mg-calcite, a setting reminiscent of the Darling pans. Bacterial mediation can overcome the kinetic barrier to dolomite precipitation. Mediation is thought to be through the creation of favourable microenvironments for dolomite precipitation immediately surrounding the bacterial cell (Vasconcelos *et al.*, 1995).

Lippman (1973) suggests that a factor which may inhibit dolomite precipitation and dolomitisation is the strength of the electrostatic bond of Mg for water. Carbonate ions cannot overcome the strong Mg hydration shell to form a bond. Extremely high Mg concentrations, such as those found in hypersaline brines, make it easier for dolomite to form, but only in a disordered Ca-dolomite form (Lippmann, 1973). Dolomite that precipitates initially (protodolomite) is poorly crystalline and disordered, and gradually "ages" to a more highly-ordered form (Warren, 2000). The conditions required for dolomite formation, i.e. high Mg/Ca ratio, high concentration of Mg, and sulphate reduction, are all met in the brine-type pans. However, low organic matter content of sediments in Rooipan south will limit the extent of sulphate reduction and consequent dolomite formation. A poorly crystalline form of dolomite may explain why so little dolomite is detected by XRD in these sediments. The amount of sulphide present is probably also limited by the low organic matter contents of the brine-type pan floor sediments.

Teller *et al.* (1982) report finding sediments similar to those observed in the brine-type pans in Lake Tyrrell, Australia. A black monosulphide-rich mud is found immediately below a salt crust, and it grades downwards into a grey to greenish-grey mud. Iron found in the monosulphides probably originates from goethite, or from phyllosilicates like illite, chlorite

or biotite. Bacterial reduction of gypsum is the source of sulphide, predominantly by the bacteria *Desulfovibrio* by the following reaction (Teller *et al.*, 1982):

$$CaSO_4 2H_2O + 2 \text{ lactate} \xrightarrow{\text{Desulfovibrio}} 2 \text{ acetate} + H_2O + CO_2 + S^{2-} + Ca^{2+}$$

Iron monosulphides form soon after this reaction has liberated elemental S. The most favourable environment for *Desulfovibrio* is within 20 cm of the sediment-water interface. As sediment accumulates, the bacteria furthest from the sediment-water interface die, and the black monosulphide-rich zone remains near the surface (Teller *et al.*, 1982). The black mud from Rooipan south (RA-SS1a) has probably been subject to similar processes. Sedimentation in Rooipan south may continue with the sulphide-rich zone migrating upwards.

The transition from reddish oxidised muds and sands adjacent to the pan to black reduced muds in the pan floor is abrupt. It is likely that the material is the same, but that the pan floor sediments have been exposed to more reducing conditions. Reducing conditions would be favoured in pan floor sediments by the greater degree of waterlogging, and by the presence of more organic matter than in the sediments adjacent to the pan. The absence of the monosulphide layer in the less saline pans is possibly due to biological activity aerating the sediments. The high salinity of the brine-type pans renders them toxic to most species, including burrowing organisms. For example, the small gastropod *T. ventricosa* and its burrows were observed in the brackish-saline and coastal pans, but are absent in brine-type pans (Figure 2.5 (a) and (b)).



*Coastal pans*

In contrast to the inland pans, the coastal pans have large volumes of gypsum and little quartz. A mineralogical trend is detected in the depth profiles of these sediments, with gypsum dominating in the surface (a) samples, and calcite dominating in the subsurface (b) samples. The calcite is low-Mg calcite (about 1 mole % $MgCO_3$), reflecting the lower Mg:Ca ratio of the coastal pans. The variation of mineralogy with depth mirrors the sequence expected from evaporation of seawater, and may represent the complete evaporation of a body of seawater during late Pleistocene sea level highstands.

### 5.7.2. CLAY MINERALOGY

Clays commonly originate as weathering products of feldspars but may also precipitate in the pans. It is possible that a clay like glauconite may be forming in the pan floor sediments of the brine-type pans. Glauconite :

$$(K,Na,Ca)_{1.2\text{-}2.0}(Fe^{3+},Al,Fe^{2+},Mg)_{4.0}[Si_{7\text{-}7.6}Al_{1\text{-}0.4}O_{20}](OH)_4.n(H_2O)$$

has been reported from a number of pans in South Africa (Verster *et al.*, 1992). It is a ferric-ferrous mica known to form under moderately reducing conditions induced by microbial sulphate reduction, and is particularly associated with shallow water marine diagenesis during periods of slow or negative sedimentation (Deer *et al.*, 1970). Mica was identified in clay mounts of both RA-SS1a and b, but positive identification of glauconite was not possible. Glauconite may be the cause of the green colour of RA-SS1b, but its colour may be hidden by the black sulphide pigmentation in RA-SS1a. The formation of glauconite could account for removal of K and Mg from solution at high salinities. Trace elements like Rb, Li and Ba may be removed by substitution for K in the clay structure, or by adsorption onto negatively charged surfaces on the clay. Bromine also exhibits similar behaviour to Mg in pan waters, and may substitute for OH. Low silica concentrations may however limit or inhibit glauconite formation. It is not known if any clays are forming *in situ* or if all are detrital. The high clay content and presence of smectite will impart a large cation exchange capacity (CEC) to pan floor sediments.

YF-SS1a and b have a high proportion of clay-sized particles, but most is carbonate material. Clay-sized gypsum was detected only in trace quantities, but gypsum could have been dissolved out of the sediment during preparation of clay mounts. According to Eugster (1980), carbonates are often precipitated as a soft micritic carbonate mud in wet mudflats as was found in this case. Substantial deposits can build up if the water table remains constant over a long time (Eugster, 1980). Sediments in the coastal pans will have a much lower CEC than inland pans, as calcite does not have a high capacity for ion exchange.

### 5.7.3. SECONDARY PRECIPITATES AND SOLUBLE SALTS

*Calcretes*

Calcrete is powdery to nodular to highly indurated calcium carbonate which displaces and replaces soil, rock or weathered material in the vadose zone (Goudie, 1983a). Calcrete was found associated with many of the pans. Calcrete is generally forming by focussing of calcite

precipitation by the seasonal change in level of the water table. In the case of the brackish-saline pans, it may be a relict feature, or it may be forming currently because these pans are not protected by a halite crust in the dry season, and capillary evaporation can result in significant draw down of the water table. Water is present immediately below the salt crust in the brine-type pans. Calcrete outcrop adjacent to the pans is more likely to be a relict feature that now affects pan hydrology by acting as an aquitard.

*Ferricretes*

The ferricrete associated with pans in the Darling area appear to have formed by replacement of calcite by iron oxides. The calcite initially replaced kaolinite, which probably originates as a weathering product of feldspar. The replacement of calcite by iron oxides may be due to change in redox or pH. At Burgerspan south, a ferricrete horizon was found directly below a calcrete horizon (Figure 2.11). An increase in pH due to degassing of $CO_2$ and precipitation of carbonates may cause Fe to precipitate as iron oxide, because it is immobile in high pH environments (Faure, 1992). It is not known if the ferricretes are continuing to form, or if they are relict features.

*Salt crusts*

Watson (1983) observed that salt crusts can be destroyed by an influx of fresh water but if the amount of salt dissolved is less than that precipitated, thick salt layers can develop. Fluctuations in groundwater chemistry and leaching by meteoric waters inhibit the formation of thick halite crusts (Watson, 1983). Despite the thick layers of salt observed on the brine-type pans in the dry season, salt layers are not preserved in the pan floor sediments. A similar observation was made at Lake Tyrrell where up to 10 cm of salt are precipitated each year in the lake, but no permanent salt is formed (Teller *et al.*,1982). During the field visit, a thin layer of detrital material was observed to have settled on the salt crust. Once the salt crust has fully dissolved this material will be incorporated into the existing sediments. The formation of the salt crust during the dry season will prevent deflation of underlying material. The subaqueous halite crusts observed are probably remnants from the dry season that have not yet fully dissolved. Unlike halite, calcite does appear to accumulate in the pans. The very low Ca concentrations in brine-type pans compared to brackish-saline pans is evidence of the permanent removal of Ca from solution by precipitation and accumulation of calcite.

## 5.8. PAN FORMATION AND EVOLUTION

### 5.8.1. CHEMICAL EVOLUTION

Evolution of pans occurs on two timescales – the seasonal evolution of brine due to evaporative concentration, and the lifetime evolution of the pan due to accumulation of salts. The chemistry of the pan waters defines trends although all pans were sampled at the same point in the saline pan cycle. This indicates that the various pans are in different stages of evolution and are therefore probably different ages. The trends observed are residual trends i.e. chemical signatures inherited from accumulation of salts over a long time period.

*Hardie-Eugster model*

According to the Hardie-Eugster model, the chemistry of inflow waters determines the final composition of the brine. The brine evolves via various chemical divides (Eugster, 1980). The first chemical divide of the Hardie-Eugster model is based on the relative proportions of Ca, Mg and $HCO_3$ (Figure 1.8). In the streams, springs and seeps, and in average coastal rainwater, Ca + Mg >> $HCO_3$. Dilute inflow of this composition is expected to follow pathway II, with initial calcite precipitation limited by bicarbonate availability, followed by gypsum precipitation. According to Eugster and Jones (1979), Ca concentration in such brines usually exceeds Mg concentration. This is not the case in the Darling or coastal pans. The mineralogy of the pans, as well as the increasing Mg:Ca ratio with brine evolution, is more suggestive of a slightly modified pathway III, as illustrated in Figure 5.31. According to this model, calcite begins to precipitate before the water enters the pan, and continues to precipitate throughout brine evolution. At high salinities, a number of precipitates form concurrently. Gypsum removes Ca and $SO_4$ from solution, a Mg-phase, possibly a clay mineral or dolomite provides a sink for Mg, and sulphate reduction removes S and some trace elements from solution. The formation of a clay mineral may account for removal of K, Rb, Li and Ba from solution. Although the current brine in the pans is a Na-Mg-Cl-$SO_4$ brine, this could change when saturation points of other minerals, like halite or mirabilite, are encountered. This model does not apply to Rooipan north in which alkalinity exceeds Ca + Mg and Na > Cl. Rooipan north will probably follow pathway IIIa-1 with evaporation (Figure 1.8), precipitating calcite and then sepiolite.

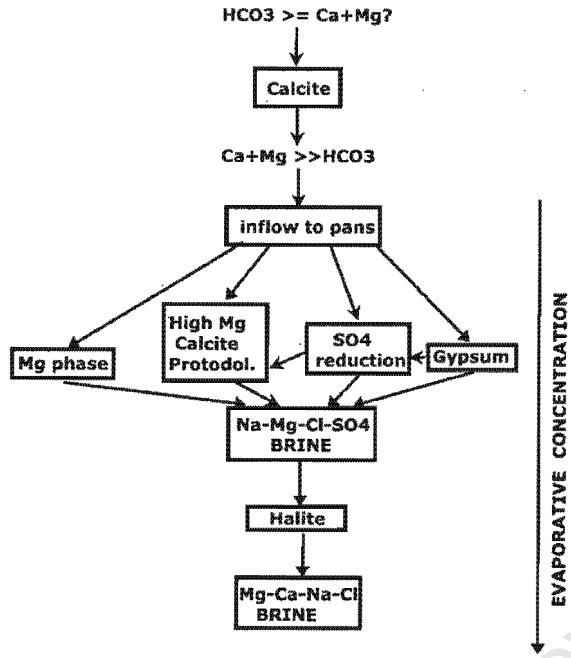


**Figure 5.27: Chemical evolution of water in the Darling pans.**

The coastal pans do not show the same range in concentrations as the inland pans. Although in general the chemistry of the coastal pans appears to follow the geochemical trends of the inland pans, there is insufficient spread in the data to define trends exclusively for the coastal pans. Calcium behaves quite differently in the coastal pans. Calcium is involved in many of the chemical divides during brine evolution, and it is likely that the coastal pans will follow a different evolutionary pathway over the season. The mineralogical sequence from calcite to gypsum to halite in sediments suggests that the pans will follow pathway II.

The principles of the Hardie-Eugster model are obeyed in the pans, with mineral precipitation causing changes in ionic dominance in the water, but the inland pans do not follow one of the simplified pathways.

*Origin of salts*

Salt input into the pans is from a number of sources:

- coastal rainfall
- runoff, both surface and subsurface, will accumulate salts in the catchment from chemical weathering of granite weathering and dissolution of soluble salts
- regional groundwater (DWAF samples)
- some pans may be affected by deep or old groundwater and aerosols and windblown dust

The contribution of each is difficult to estimate with the limited information available. Water leaves the pan by evaporation and seepage into pan floor sediments. Isotopically heavy water sampled from sediments adjacent to Rooipan south and Zwartwater north also indicates dense evaporated waters are stored in sediments.

Modelling of evaporation of rain, stream water and groundwater was done using PHREEQC to determine the extent of evaporation required for halite saturation and the likely mineral assemblages. An example of an input file is given in Appendix C (Section C.6.1). Evaporation was modelled by removing moles of water from the solution as described by Parkhurst and Appelo (1999). Following removal of water, the concentrated solution was equilibrated with calcite, gypsum, halite, fluorite and atmospheric $CO_2$. Dolomite was not included as it is not kinetically favoured, a factor which PHREEQC does not take into account. Average coastal rainwater equilibrated with atmospheric $CO_2$ requires 50 000 times concentration through evaporation before halite precipitates (Figure 5.32 (a)). Calcite does not precipitate because of the low pH, and gypsum becomes saturated and removes Ca. Sulphate is affected slightly by gypsum precipitation but recovers rapidly. The pH remains low throughout precipitation. Precipitation of halite at high salinities removes Na and Cl, but Mg, K and $HCO_3$ are perfectly conserved throughout the evaporative concentration process.



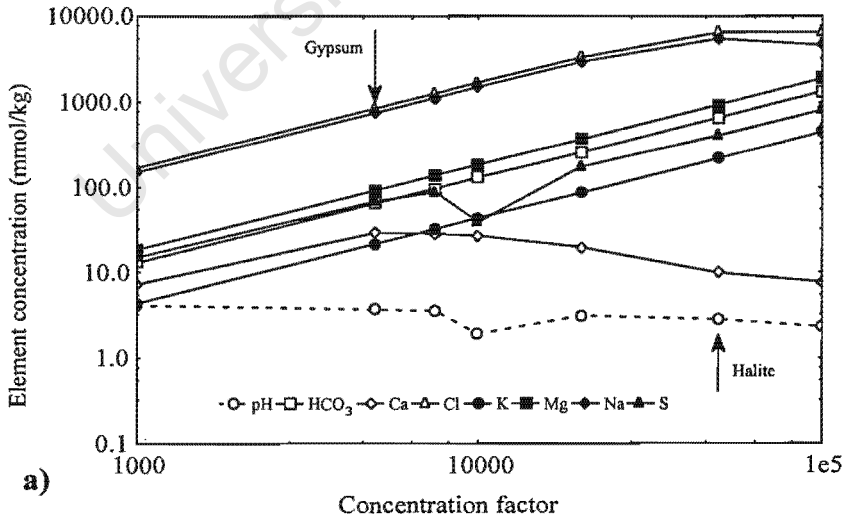


**Figure 5.28: Chemical evolution of solutes with evaporative concentration for starting solutions of the composition of (a) global average coastal rainwater**

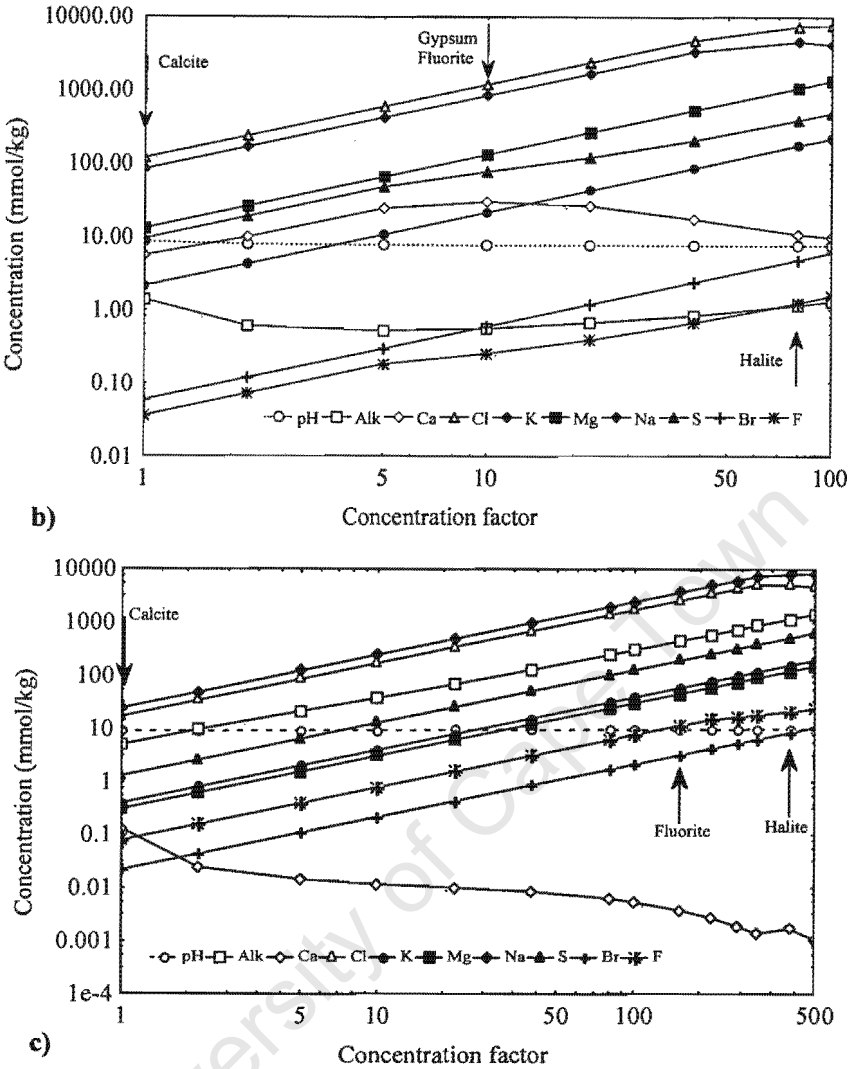


**Figure 5.28: Chemical evolution of solutes with evaporative concentration for starting solutions of the composition of (b) stream water (OT-WR1) and (c) Rooipan north pan water (RB-WP1).**

Sample OT-WR1 is stream water from a tributary of the Brak River and is chosen to represent inflow water composition. Halite reaches saturation once the solution has been concentrated 80-fold (Figure 5.32 (b)). The solution is saturated with respect to calcite from the beginning, and precipitation of calcite is limited by alkalinity. Once gypsum begins to precipitate, Ca is removed from solution, but sulphate is not strongly affected. Magnesium, K and Br behave conservatively throughout. Based on the F concentrations of OT-WR1, the solution should become saturated with fluorite, but the fluoride concentration will continue to increase as Ca is the limiting element. This model is more effective than evaporation of rainwater in explaining observed trends. The pH is buffered throughout by precipitation of calcite. The evaporation of a mixture of stream water (OT-WR1) and global average coastal

rainfall was also modelled. This mixture is strongly affected by the chemistry of the stream water and shows the same solute trends as for OT-WR1. The only difference is that a greater degree of evaporation is required to reach saturation due to dilution by rainwater.

Sample RB-WP1 from Rooipan north has a very different chemical makeup from other pan water samples, as previously discussed. Evaporative concentration of water of this type yields calcite and no gypsum (Figure 5.32 (c)). Calcium is the limiting element for calcite precipitation, rather than alkalinity as was the case in other samples. Halite begins to precipitate after 200 times concentration. A consequence of the severely depleted Ca concentrations is dramatically increased F concentrations due to the fluorite solubility control. Water of the composition of RB-WP1, i.e. water strongly influenced by granite, is unlikely to be a major contributor to other pan waters.

The reason for the seawater signature in all waters may be explained by Drever and Smith's (1978) cyclic wetting and drying theory. In arid climates, rainfall is most likely to evaporate before it infiltrates. This leads to a build up of salts in or on the soil. A heavy period of rain will infiltrate and dissolve all salts in the soil, leading to recharge by a relatively salty solution, enriched in Cl and $SO_4$ relative to $HCO_3^-$, and $Na^+$ and $K^+$ relative to $Ca^{2+}$ and $Mg^{2+}$ (Drever and Smith, 1978). The water should have the signature of coastal rainfall, which is similar to seawater. Evidence for the origin of salt by cyclic wetting and drying comes from Schloeman's (1994) observation of the process of throughflow on granite slopes in the Darling area. Throughflow is "lateral subsurface soil-water movement" (Conacher, 1975, pg.34). Throughflow occurs commonly on granitic terrain, where rainfall infiltrates the sandy colluvium at the base of weathering granite domes (tops of hills) and flows within soil layers downslope. This water forms a saturated zone at the base of a hill. Movement of water along the soil profile dissolves a greater quantity of salts than water passing through the soil vertically or flowing over the surface, due to greater exposure (Conacher, 1975). Seepage at the base of the slope would occur because the soil zone is intersected by a more resistant layer, perhaps a calcrete or ferricrete horizon. Seepage water is often yellow (eg. sample ZA-WS1), probably due to dissolution of organic acids as it flows through the soil.

### 5.8.2. MODEL OF PAN EVOLUTION

Figure 5.33 illustrates the general characteristics of inland brine-type pans. The pans receive water inputs from a number of sources, including rainfall, surface runoff and throughflow. Throughflow will maintain reducing conditions at the base of the slope during the wet season (Schloeman, 1994), while the salt crust will limit capillary evaporation and prevent drying out during the dry season. The inflow waters contain salts that accumulated in the soils of the catchment during the dry season, modified by contributions from the chemical weathering of granite. The rising water table in the wet season can also contribute water to the pan. The relatively fresh water arriving in the pan at the beginning of the wet season dissolves a significant proportion of salts already accumulated in the pan, the most soluble first. Evaporation from the pan, and capillary evaporation from adjacent to the pan leads to concentration of salts. Not all the water is evaporated, and a subsurface brine remains, where it can be further concentrated by capillary evaporation until the next flooding cycle.

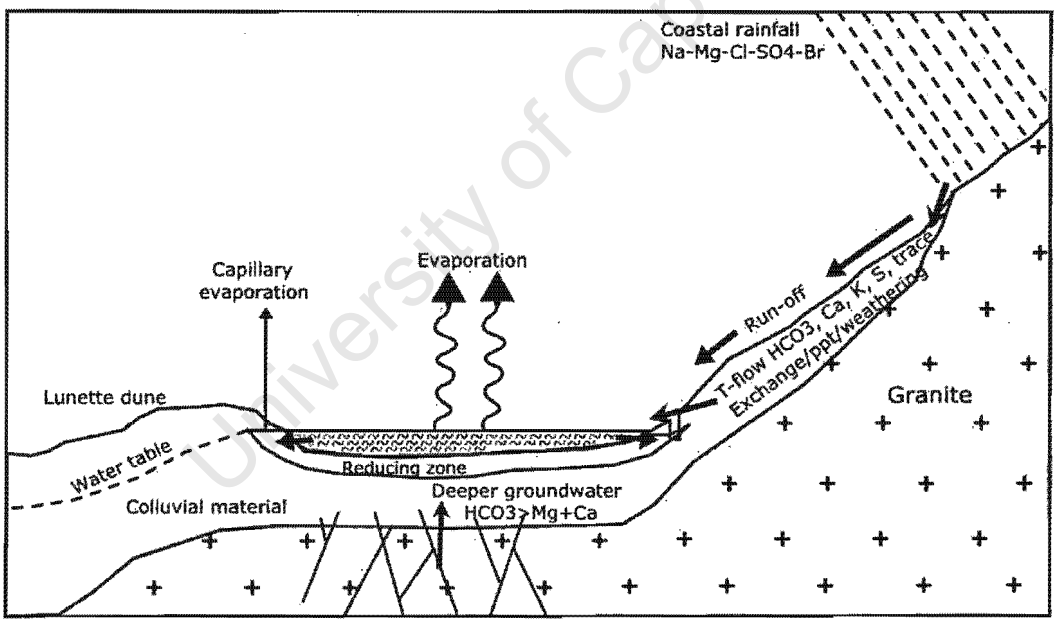


**Figure 5.29: Model of processes occurring in Darling pans**

As can be seen in the orthophotographs (Chapter 2), the long axes of inland pans are oriented roughly west-northwest east-southeast, and the lunette dune is usually north-northwest of the pan. The scarp slope is not exactly opposite the lunette dune but rather to the southwest of the pans. On a regional scale, many of the pans occur in a distinct line, trending northwest. Exceptions are the Zwartwater pans and Kiekoesvlei. The linear trend of the pans indicates a geological control in their formation. No faults have been identified, and the significant

Colenso Fault that transects the area appears affect neither the individual pan orientations nor the overall trend. The pans may have formed in an abandoned drainage system. Because the wind direction and drainage direction coincide, wind activity could have built up dunes in the floor of the drainage system which would have acted as a downslope dam to trap runoff.

The coastal pans may have formed originally as lagoons or estuaries cut off from the sea by the formation of dunes, or by a drop in sea level. Seawater in the lagoons was evaporated to form calcite, gypsum and halite evaporite deposits during late Pleistocene sea-level highstands 120 000 to 440 000 years ago. These relict evaporites are now cut off from the sea and are affected more by surface runoff and groundwater from the Darling Hills.

The age of the pans is very difficult to estimate with the limited information available. A ballpark figure can be calculated based on accumulation of salt. If all the salt in the pans precipitated in a thick layer on the surface (rather than interstitially in the sediments), and salt originated from rainfall in a catchment of 100 ha at 500 mm per year, a layer of pure halite 5 cm thick (as observed at Zwartwater north during the dry season) would take approximately 1500 years to accumulate.



## 5.9. ENVIRONMENTAL CONSIDERATIONS

### 5.9.1. WATER QUALITY

Table 5.5 lists the water quality guidelines for irrigation water, livestock drinking water and domestic use as set out by the Department of Water Affairs (Department of Water Affairs and Forestry, 1993b). Industrial use is not considered because the water is highly corrosive due to the high Cl content. The irrigation guidelines are sufficient for Class IV fitness for use, i.e. yield losses of 20% or more will be recorded even if special management practices are implemented (Department of Water Affairs and Forestry, 1993b). Included for comparison are the minimum and maximum of each parameter recorded in all samples, and three representative samples. RA-WP1 is the most saline of all samples, ZA-WS2 represents groundwater, and RB-WP1 is least saline and represents potentially useable water.

**Table 5.5: Irrigation, livestock and domestic water quality guidelines (Department of Water Affairs and Forestry, 1993b) compared to minimum and maximum values in all samples, and representative samples. Values exceeding the maximum in all classes are in bold.**

| | Min | Max | RB-WP1 | ZA-WS2 | RA-WP1 | Class IV Irrigation | Livestock (Dairy) | Domestic |
|---|---|---|---|---|---|---|---|---|
| **TDS (g/L)** | 1.6 | **379** | 2 | 9 | **379** | 0-3.5 | 0-5 | 0-0.45 |
| **pH** | 6.5 | **9.3** | **9.3** | 8.4 | 7.6 | 6.5-8.4 | ng | 6-9 |
| **Sodicity (SAR)** | **18** | **378** | nd | **23** | **378** | 10 | ng | ng |
| **Na (mmol/kg)** | 25 | **4642** | 25 | **100** | **4642** | 9 | 87 | ng |
| **Ca (mmol/kg)** | 0.1 | **39.2** | 0.1 | 5.6 | 10.2 | ng | 25 | ng |
| **Mg (mmol/kg)** | 5.6 | **643** | 0.3 | 12 | **141** | ng | 21 | ng |
| **Cl (mmol/kg)** | 17 | **4855** | 17 | **140** | **4767** | 10 | 85 | ng |
| **$SO_4$ (mmol/kg)** | 1.3 | **405** | 1 | **11** | **350** | ng | 0-10 | ng |
| **F (µmol/kg)** | 7 | 226 | 79 | 95 | 11 | 790 | 316 | 53 |
| **Li (µmol/kg)** | 0.6 | 166 | 2 | 18 | 23 | 360 | ng | ng |
| **B (µmol/kg)** | 45 | **7310** | 303 | 72 | **1079** | 278 | 463 | ng |
| **As (µmol/kg)** | 0.2 | 11 | 0.2 | 0.2 | 6.2 | 27 | 6.7 | ng |
| **Se (µmol/kg)** | 0.1 | **47** | 0.1 | 0.6 | **7.9** | 0.6 | 0.6 | ng |
| **U (nmol/kg)** | 9 | **672** | 13 | 269 | 8 | 420 | ng | ng |

*ng = no guideline nd = no data

Water of the quality of RA-WP1 (and probably the brine-type pans in general) is too saline for any use. Many of the major and trace elements exceed toxic levels. At the other extreme, water from Rooipan north is virtually acceptable for domestic use, although pH and fluoride levels are slightly high. Sample ZA-WS2 was water being pumped into a dairy cattle drinking trough. While most livestock can tolerate TDS up to 15 000 to 17 000 g/L, their health and consequently production will be affected. Livestock must be adapted to saline waters or they will drink large quantities and die (Department of Water Affairs and Forestry, 1993b). High levels of chloride become unpalatable before becoming toxic, resulting in a reduction in the animal's water and food intake. Levels of sulphate above 10 mmol/kg lead to decreased health and production of dairy cattle. High concentrations of Na can cause sodium toxicity, characterised by nervous disorders and hypertension (Department of Water Affairs and Forestry, 1993b). While the water being consumed by the dairy cattle in the Darling area is not toxic, it may be affecting production.

Most farmers in the area regard the pans as wasteland, and were not using the water. A couple of farmers mined salt from the pans. However, wildlife was commonly observed in the vicinity of the pans, particularly birdlife. Grysbok and Cape Fox were seen around the pans, and numerous bird species in the pans. An element in the pans that is of concern for

wildlife is Se. Selenium toxicity in livestock results in diseases known as alkali disease and blind staggers. Symptoms of alkali disease in livestock are dullness, lack of vitality, emaciation, rough coat and loss of hair, hoof changes and lameness and loss of reproductive performance. Alkali disease is so-called because the disease is associated with high-salt waters from saline seeps. Symptoms of blind staggers are impaired vision, anorexia, weakened legs, paralysis of the tongue, laboured respiration, abdominal pain, salivation, emaciation and ultimately death. The role of Se in blind staggers has not yet been verified. High concentrations of Mg-sulphate in waters can produce the same symptoms as blind staggers (James *et al.*, 1989).

The average Se concentration in water is usually less than 0.02 μmol/L. It can be concentrated in waters by leaching from soil. Ohlendorf (1989) describes the situation in the San Joaquin Valley in California where Se has concentrated up to 53 μmol/L in agricultural return flow. Selenium in water has been concentrated into aquatic organisms, providing an important link to the foodchain. Bird embryos are particularly sensitive to Se toxicity, resulting in high rates of embryo mortality and developmental abnormalities in the valley (Ohlendorf, 1989). A number of bird carcasses were observed in the vicinity of the pans near Darling, but without analysis their deaths cannot be attributed to Se toxicity.



### 5.9.2. Effects of mining and agriculture

*Mining*

Mining of Burgerspan south has noticeable effects on the chemistry of the water. Elements that are removed from the pan as part of the mining operation, namely Na and Cl, in halite and Ca, $SO_4$ and Sr in gypsum, are depleted in this pan compared with other pans in the area. The implication is that mining is not sustainable over a long period as salt is not being replaced as rapidly as it is being removed. Elements not removed during mining namely K, Mg, Br, B, As, Rb, Se, U, Si and Li are residually enriched in the remaining brine. This enrichment leads to some of the highest concentrations in any pan of Se (42 μmol/kg), As (9.6 μmol/kg), Li (150 μmol/kg), and B (6610 μmol/kg). In an examination of trace element contamination of evaporites in agricultural evaporation ponds in California, Ong *et al.* (1997) warn against the concentration of trace elements into the brine by mining of evaporites. They suggest that the remaining brine be isolated and specially treated to minimise exposure to birds.

*Agriculture*

Clearing of the indigenous Swartland vegetation to make way for wheat and pasture affects the regional hydrology. With a change from natural vegetation to crops, there is more infiltration of water and less surface runoff during the wet season, and less transpiration during the dry season. The combined effect is to raise the water table, and dissolve salts stored in the soil zone. These salts are transported to low points in the landscape, like pans. Salinisation of non-irrigated agricultural land and groundwater in Australia has been attributed to the clearing of natural vegetation to plant wheat (Conacher, 1975). Although the Darling pans formed naturally, the change in land use over the last few hundred years may have increased the rate of salinisation.

# 6. Conclusions

The Darling and Ysterfontein pans were studied and compared in order to understand the processes and source of salts that render much of the surface and groundwater on the semi-arid coastal lowlands unpalatable due to high salinities. This chapter will summarise the main findings of the geochemical investigation, and will attempt to answer the questions posed in the introduction, namely:

- What is the origin of salts in the brines?
- What are the relative contributions of groundwater, rainfall and surface run-off to the pans?
- Are there potentially harmful trace elements in the salt pans?
- Do the Darling and Ysterfontein salt pans follow the Hardie-Eugster model of brine evolution?



## 6.1. PHYSICAL CHARACTERISTICS OF THE SALT PANS

The Darling and Ysterfontein saltpans can be classified geographically into two main groups, the inland pans and the coastal pans. The large (50-116 ha), irregularly shaped coastal pans are remnants of lagoons that have become isolated from the sea by marine regressions and the formation of dune ridges. The smaller (2-16 ha), rounded inland pans were found to have a lunette dune downwind, and a scarp slope upwind, features not seen in the coastal pans. The inland pans define a linear trend across the Groen River valley and probably formed by deflation in an abandoned drainage system. An important determinant of pan chemistry is the hydrology of the pans. The climate of the coastal lowlands is semi-arid, and annual evaporation significantly exceeds annual precipitation. Persistent southwesterly winds during the dry summer season increase the amount of evaporation. Water found in the pans during the wet winter season is contributed by direct rainfall, surface and subsurface runoff (throughflow), unconfined groundwater (by raising of the water table) and deeper or older groundwater. Water is removed from the pans by evaporation. Evaporated subsurface waters of high salinities found in pits dug adjacent to the pans provide evidence for storage of dense brines within pan floor sediments.

## 6.2. GEOCHEMICAL CHARACTERISTICS OF THE SALT PANS

Salinities of pans vary between 2 and 379 g/L total dissolved solids (TDS), the most saline approaching halite saturation. The inland pans can be divided into brine-type (168 – 379 g/L TDS) and brackish-saline pans (2 – 64 g/L) based on the salinity of water. These two classes can be distinguished in the field by physical differences, namely brine-type pans have a salt crust in the dry season, whereas brackish-saline pans have no salt crust and show evidence of the presence of the gastropod *Tomichia ventricosa*. The pH of all waters is neutral to alkaline and constrained within a narrow range from 6.5 to 9.2. Important controls on the pH of water are the partial pressure of $CO_2$, carbonate precipitation and weathering of granite. Where carbonate precipitation is the dominant reaction, pH is between 7.6 and 8.3. Lower pH is due to greater $pCO_2$ generated by microbial activity in the soil zone, while higher pH is associated with alkalinity generated by weathering of granite.

The behaviour of different elements across the range of salinities was used to identify the processes occurring in pans. Major element behaviour is controlled primarily by precipitation of minerals. Samples from a mined pan proved very useful in identifying element sinks, as elements removed by mining of the *in situ* subaqueous salt crust (Na, Cl, Ca, $SO_4$ and Sr), are depleted in this pan relative to other pans. Elements not removed by mining are residually enriched in the surface brine. With the exception of Ca and F, all elements behave conservatively in the brackish-saline and coastal pans, as well as in all streams and springs. Although the behaviour of F is not well understood, it may precipitate as fluorite ($CaF_2$), or into carbonate such as calcite. Calcium is gradually removed from solution in all samples by the precipitation of calcite. Bicarbonate is rapidly depleted from solution and limits calcite precipitation. Calcite evolves from low-Mg to high-Mg calcite as the Mg:Ca ratio increases with removal of Ca from solution. The coastal pans contain relatively more Ca than inland pans because they have equilibrated with an older deposit of gypsum, and calcite has a low Mg content relative to inland pans. In the brine-type pans Ca is removed by precipitation of gypsum. Although gypsum is found in the sediments of the coastal pans, gypsum is not currently precipitating.

Sodium and Cl are both conserved in all pans at this stage in the saline pan cycle. It is expected that halite will precipitate in the brine-type pans following seasonal evaporation, and Na, the limiting element, will be depleted in the remaining solution. Precipitation of Mg

into high-Mg calcite cannot account for the quantity of Mg removed from solution in the brine-type pans, and it is hypothesised that another mineral is forming, perhaps a Mg-rich clay mineral or dolomite, or that Mg is adsorbed onto clay. Dolomite was tentatively identified in the pan floor sediments of a brine-type pan, as well as mica and smectite in the clay fraction. Although there is no direct evidence, precipitation of glauconite could also explain the removal of K and a number of trace elements (Rb, Li, Ba, Br) from solution, as would ion exchange. Sulphate is involved in both gypsum precipitation and sulphide reduction in the pan floor sediments of brine-type pans. However, gypsum precipitation is limited by the low Ca concentrations and sulphide reduction is limited by low organic matter content, such that only trace quantities of sulphate are removed and it behaves essentially conservatively.

Trace element concentrations are controlled by substitution into minerals, ion exchange and redox. All trace elements except Si and U behave conservatively in springs, streams and coastal pans. Brackish-saline pans often plot off the conservative trend. Depletions in brackish-saline pan saturated paste extracts are due to leaching in some sediments, while enrichments are due to contributions from a deeper groundwater that is in equilibrium with granite. Rubidium, Ba, Li, Br, Se and Mg all show similar trends relative to Cl, i.e. they are depleted in the brine-type pan waters but enriched in the brine-type pan sediments. A sink for these elements may be precipitation of a clay mineral or ion exchange. Rubidium, Ba and Li are thought to be controlled primarily by ion exchange because of their association with sediments, particularly clay-rich sediments. In addition, Ba may be precipitating as trace quantities of barite, undetectable by XRD. The behaviour of Se is either redox controlled, because it precipitates into the sulphides forming in surface sediments of brine-type pans, or it could be removed from solution by adsorption onto clay surfaces. Arsenic behaves conservatively throughout and is concentrated by evaporation. Unlike Se, As is not incorporated into sulphides or involved in ion exchange. Strontium is removed from solution in brine-type pans by precipitation into gypsum or as trace quanitites of celestite with gypsum. Silicon and U display very similar non-conservative behaviour which is not fully understood. Both elements are found to be enriched in subsurface waters due to equilibration with quartz and U-phases, but are virtually undetectable in pan waters. Uranium is immobilised by the reducing conditions found in pan-floor sediments.

Minerals are zoned within the pan sediments. Capillary evaporation draws water upward through the sediments of the inland pans and concentrates it, resulting in a mineralogical evolution from depth to surface. Halite occurs as a 1 – 2 cm thick crust on the floor of all inland brine-type pans. Calcite is found in the top 20 – 30 cm of sediment, grading from low-Mg calcite at depth to high-Mg calcite closer to the surface, reflecting the increase in the Mg:Ca ratio with brine evolution. Minerals like calcite, clay, gypsum and sulphides provide a permanent sink for elements within the sediments whereas halite and gypsum in the salt crust are dissolved on a seasonal basis with influx of fresh water. Gypsum was found in the halite crust and pan floor sediments of the brine-type pans. The brine-type pan floor consists of a thick black reduced mud containing iron monosulphides. The absence of this black mud in brackish-saline pans is interpreted to be due to the presence of burrowing *T. ventricosa*, which aerate the subsurface sediments. These gastropods cannot survive in the highly saline environment of the brine-type pans. Evaporation to dryness of seawater would produce the mineral sequence observed in coastal pans. Gypsum dominates in the upper 10 – 20 cm. Below 20 cm, low-Mg calcite becomes the dominant mineral. This sequence is interpreted to be relict, having formed during Late Pleistocene sea-level highstands. Aeolian dunes now isolate the pans from the sea and the inflow waters are terrestrial runoff.

Modelling with PHRQPITZ and PHREEQC was found to be a useful tool in predicting element speciation, mineral precipitation and evaporative mineral sequences. Most waters are predicted to be supersaturated with respect to calcite, dolomite and magnesite. Dolomite and magnesite do not precipitate due to kinetic limitations. Sulphate and Ca concentrations are found to be limited by gypsum saturation, but no phase could be identified to explain removal of Mg, Rb, Br or Li from solution. Both celestite and barite, the sulphate phases of Sr and Ba, are predicted to be at equilibrium or supersaturated in solution. Subsurface water reaches equilibrium with quartz, albite and fluorite, but these phases are undersaturated in most of the surface waters. Modelling of mineral sequences expected by evaporation of a selection of source waters, namely coastal rainwater, stream water and water from the pan influenced by deeper groundwater, indicates that the source of water most likely to precipitate the correct mineral sequence is stream water, which has strong seawater signature modified by chemical weathering of granite

## 6.3. ORIGIN OF SALTS

Salts are contributed to the pans by various water sources, namely coastal rainwater, marine aerosols, regional groundwater, deeper groundwater, direct and subsurface runoff (throughflow), and spring and stream water. The major ion signature of all these waters except deeper groundwater is similar to seawater. The order of cation dominance is Na>>Mg>>Ca≈K, while anion dominance is Cl>>$SO_4$>>$HCO_3$, and the Na:Cl ionic ratio of inflow waters (0.86) is very similar to seawater. The seawater signature is inherited by dissolution of salts precipitated and concentrated in the soil zone by evaporation of coastal rainwater, which is chemically similar to seawater. Runoff water will dissolve precipitates and chemically weather granite in the Darling hills, adding salts directly to the pans and recharging regional groundwater. Weathering of granite modifies the chemical signature of water slightly, contributing most of the trace elements and $HCO_3$.

Salts accumulate within the pans over centuries. Stable isotope data indicate that the salinity of water in brine-type pans is primarily due to dissolution of these accumulated salts by meteoric water, not due to evaporation. Groundwater and throughflow will add salts to the pan on an annual basis but only in small amounts relative to the quantity of salt already accumulated. Permanent removal of some elements by precipitation of minerals like calcite and gypsum has changed the chemical signature of brine-type pan waters. Deeper groundwater is chemically influenced by granite and differs from seawater in that Na>Cl and $HCO_3$ > Mg + Ca. The chemistry of the brackish-saline pan Rooipan north is significantly affected by this deeper groundwater. The deeper groundwater is chemically and isotopically distinct from regional groundwater

## 6.4. RELATIVE CONTRIBUTIONS OF DIFFERENT WATER SOURCES

Because of the similarity of all water entering the pans, both chemically and isotopically, it is difficult to determine the relative contributions of each type of water to the pan. One case in which two separate water sources were identified is Rooipan north, where a different geochemical signature is due to mixing of regional groundwater and deeper groundwater in equilibrium with granite. Modelling of a mixture of 20% deeper groundwater and 80% regional groundwater yields the correct ionic ratios for Rooipan north pan water.

## 6.5. ACCUMULATION OF POTENTIALLY HARMFUL TRACE ELEMENTS

Although only a selection of trace elements was analysed, most were found to be at or near toxic levels in the pans. Selenium is the element of most concern, because it is potentially hazardous for livestock and wildlife, particularly birds. Concentrations of Se range from 0.1 to 47 μmol/kg, the highest concentration exceeding guideline limits for livestock by almost 10 fold. High concentrations of trace elements are not of human concern as the high salinity results in the surface water being unfit for any human related use. However, similar brines generated by human activities would be of environmental concern. As most potentially harmful trace elements partition into the liquid phase, the salt that is mined is not expected to contain high levels of trace elements. However, mining results in residual enrichment of trace elements in the brine posing a risk to livestock and birds using the pan as a source of water or salt.

## 6.6. BRINE EVOLUTION

Evidence of mineral zonation and solute patterns suggest that the saltpans evolve according to the principles of the Hardie-Eugster model, i.e. that the chemistry of inflow waters does determine the final composition of the brine, and that precipitation of minerals define the pathways along which the brines evolve. However, evolution of these brines cannot be classed into one of the simplified pathways defined by Eugster (1980). The inflow water composition in inland pans contains Ca and Mg in excess of $HCO_3$ and would be expected to evolve along a Type II pathway. However, based on the observed mineralogy and final brine composition, it is more likely that the brine is evolving along a modified Type III pathway. The first mineral to precipitate is calcite, and based on saturation index modelling and the non-conservative behaviour of Ca, calcite precipitation probably begins prior to the inflow water reaching the pan. Once in the pan, calcite continues to precipitate, increasing the Mg:Ca ratio, resulting in the evolution of calcite from low Mg to high Mg form. Later in brine evolution, gypsum, calcite and a Mg-phase, possibly protodolomite, precipitate concurrently. A Na:Mg:Cl:$SO_4$ brine results. With precipitation of halite later in the season, the brine will evolve to a Mg:Na:Cl:$SO_4$ form.

# References


Alison, M.S. 1899. On the origin and formation of pans, *Trans. Geol. Soc.S.A.*, 4 (7), 159-161.

Anon 1992. *Munsell® Soil Color Charts*, Macbeth division of Kolmorgen Instruments Corp, New York.

Baker, K.F. 1976. *The determination of organic carbon in soil using a probe-colorimeter, Laboratory Practice*, 25, 82-83.

Baker, P.A. and Kastner, M. 1981. Constraints on the formation of sedimentary dolomite, *Science*, 213, 214-216.

Ball, J.W. and Nordstrom, D.K. 1991. *User's manual for WATEQ4F, with revised thermodynamic database and test cases for calculating speciation of major, trace, and redox elements in natural waters*, Open-File Report 91-183, U.S. Geological Survey, Menlo Park, California.

Ben-Yaakov, S. 1973. pH buffering of pore water of recent anoxic marine sediments, *Limnology and Oceanography*, 18(1), 86-94.

Boucher, C. 1981. Floristic and structural features of the coastal foreland vegetation south of the Berg River, Western Cape Province, South Africa., in Moll, E.(ed) *Proceedings of a Symposium on Coastal Lowlands of the Western Cape*, University of the Western Cape, Cape Town.

Branford, W. (ed) 1987. *The South African Pocket Oxford Dictionary*, Oxford University Press, Cape Town.

Bryant, R.G., Drake, N.A., Millington, A.C. and Sellwood, B.W. 1994. The chemical evolution of the brines of Chott el Djerid, Southern Tunisia, after an exceptional rainfall event in January 1990, in Renaut, R.W. and Last, W.M. *Sedimentology and Geochemistry of Modern and Ancient Saline Lakes*, SEPM Special Publication No. 50, Tulsa, USA.

Bühmann, C 1986. *The Investigation of 2:1 Layer Silicate Clays in Selected Southern African Soils*, Unpublished PhD Thesis, University of Natal, Pietermaritzburg.

Camur, M.Z. and Mutlu, H. 1996. Major-ion geochemistry and mineralogy of the Salt Lake (Tuz Gölü) basin, Turkey, *Chemical Geology*, 127, 313-329.

Coleman, M.L., Shephard, T.J., Rouse, J.E. and Moore, G.M. 1982. Reduction of water with zinc for hydrogen isotope analysis, *Analytical Chemistry*, 54, 993-995.

Conacher, A.J. 1975. *Throughflow as a mechanism responsible for excessive soil salinisation in non-irrigated, previously arable lands in the Western Australian wheatbelt: A field study,* Catena, 2, 31-68.

Coplen, T.B. 1988. Normalisation of oxygen and hydrogen isotope data, *Chemical Geology (Isotope Geoscience Section)*, 72, 293-297.

Corning Glass Works 1984. *Fluoride Electrode - Operating Instructions/Technical Specifications*, Corning Glass Works, Medfield.

Craig, H. 1961. Isotopic variations in natural waters, *Science*, 133, 1702-1703.

Day, J.A. 1993. The major ion chemistry of some southern African saline systems, *Hydrobiologia*, 267, 37-59.

Deer, W.A., Howie, R.A. and Zussman, J. 1970. *An Introduction to the Rock Forming Minerals*, Longman Group Ltd, London.

Department of Water Affairs and Forestry, 1993a. *A Review of the Groundwater Resources of the Western Cape*, DWAF report no. P G000/00/2591, Prepared by G Dyke of Ninham Shand Inc. in association with BKS Inc. as part of the Western Cape System Analysis.

Department of Water Affairs and Forestry, 1993b. *South African Water Quality Guidelines, Volume 4: Agricultural Use.*

Diamond, R.E. and Harris, C. 1997. Oxygen and hydrogen isotope composition of Western Cape meteoric water, *South African Journal of Science*, 93, 371-374.

Drever, J.I. 1997. *The Geochemistry of Natural Waters: Surface and Groundwater Environments (3rd ed.)*, Prentice-Hall, New Jersey.

Drever, J.I. and Smith, C.L. 1978. Cyclic wetting and drying of the soil zone as an influence on the chemistry of ground water in arid terrains, *American Journal of Science*, 278, 1448-1454.

Eary, L.E. 1999. Geochemical and equilibrium trends in mine pit lakes, *Applied Geochemistry*, 14, 963-987.

Eaton, A.D., Clesceri, L. and Greenberg, A.E. 1995. *Standard Methods for the Examination of Water and Wastewater (19th ed.)*, American Public Health Association, Washington DC.

Edmunds, W.M. and Smedley, P.L. 1996. Groundwater geochemistry and health: an overview, in Appleton, J.D., Fuge, R. and McCall, G.J.H. (eds) *Environmental Geochemistry and Health*, Geological Society Special Publication No.113.

Eugster, H.P. 1980. Geochemistry of evaporitic lacustrine deposits, *Ann. Rev. Earth. Planet. Sci.*, 8, 35-63.

Eugster, H.P. and Jones, B.F. 1979. Behaviour of major solutes during closed-basin brine evolution, *American Journal of Science*, 279 (June), 609-631.

Fanning, D.S., Rabenhorst, M.C. and Bigham, J.M. 1993. Colors of acid sulfate soils, in Bigham, J.M. and Ciolkosz, E.J. (eds) *Soil Color*, SSSA Special Publication Number 31, Madison.

Faure, G. 1992. *Principals and Applications of Inorganic Geochemistry*, Macmillan Publishing Company, New York.

Felmy, A.R. and Weare, J.H. 1986. The prediction of borate mineral equilibria in natural waters: Application to Searles Lake, California, *Geochimica et Cosmochimica Acta*, 50, 2771-2783.

Geological Survey 1972. *Geological Map of Southern Africa: 3217D & 3218C - St. Helena Bay and 3317B & 3318A - Saldanha Bay*, Government Printer, Pretoria.

Goudie, A.S. 1983. Calcrete, in Goudie, A.S. and Pye, K. (eds), *Chemical Sediments and Geomorphology: Precipitates and Residua in the Near Surface Environment*, Academic Press, London, 93-132.

Goudie, A.S. 1989. Weathering processes, in Thomas, D.S.G. (ed) *Arid Zone Geomorphology*, Belhaven Press, London.

Goudie, A.S. 1991. Pans, *Progress in Physical Geography*, 15(3), 221-237.

Goudie, A.S. and Thomas, D.S.G. 1985. Pans in southern Africa with particular reference to South Africa and Zimbabwe, *Z. Geomorph. N. F.*, 29(1), 1-19.

Grobe, M., Machel, H.G. and Heuser, H. 2000. Origin and evolution of saline groundwater in the Münsterland Cretaceous Basin, Germany: oxygen, hydrogen, and strontium isotope evidence, *Journal of Geochemical Exploration*, 69-70, 5-9.

Hall, A.V. 1981. Conservation status of the vegetation of the Western Cape coastal lowlands, in Moll, E.(ed) *Proceedings of a Symposium on Coastal Lowlands of the Western Cape*, University of the Western Cape, Cape Town.

Hammer, U.T. 1986. *Saline Lake Ecosystems of the World*, Dr W. Junk Publishers, Dordrecht.

Hammer, U.T., Shamess, J. and Haynes, R.C. 1983. The distribution and abundance of algae in saline lakes of Saskatchewan, Canada, in Hammer, U.T. (ed) *Saline Lakes - Proc. 2nd Int. Symp. Athalassic (Inland) Saline Lakes*, Dev. Hydrobiologia., Junk, The Hague.

Hardie, L.A. and Eugster, H.P. 1970. The evolution of closed-basin brines, *Mineral. Soc. Am. Spec. Publ.*, 3, 273-290.

Hartnady, C.J.H., Newton, A.R. and Theron, J.N. 1974. *The stratigraphy and structure of the Malmesbury Group in the southwestern Cape*, Bulletin Precambrian Research Unit, University of Cape Town, 15, 193-123.

Harvie, C.E., Møller, N. and Weare, J.H. 1984. The prediction of mineral solubilities in natural waters: The Na-K-Mg-Ca-H-Cl-SO4-OH-HCO3-CO3-CO2-H2O system to high ionic strengths at 25°C, *Geochimica et Cosmochimica Acta*, 48, 723-751.

Harvie, C.E. and Weare, J.H. 1980. The prediction of mineral solubilities in natural waters: the Na-K-Mg-Ca-Cl-SO4-H2O system from zero to high concentration at 25°C, *Geochimica et Cosmochimica Act*, 44, 981-997.

Harvie, C.E., Weare, J.H., Hardie, L.A. and Eugster, H.P. 1980. Evaporation of seawater: Calculated mineral sequences, *Science*, 208, 498-500.

Herczeg, A.L. and Lyons, W.B. 1991. A chemical model for the evolution of Australian sodium chloride lake brines, *Palaeogeography, Palaeoclimatology, Palaeoecology*, 84, 43-53.

Hermann, A.G., Knake, D., Schneider, J. and Peters, H. 1973. Geochemistry of modern seawater and brines from salt pans: Main components and bromine distribution, *Contr. Mineral. and Petrol.*, 40, 1-24.

Hugo, P.J.(ed.) 1974. *Salt in the Republic of South Africa*, Memoir 65, Dept. of Mines, Geological Survey, Pretoria.

James, L.F., Panter, K.E., Mayland, H.F., Miller, M.R. and Baker, D.C. 1989. Selenium poisoning in livestock: A review and progress, in Jacobs, L.W. (eds) *Selenium in Agriculture and the Environment*, SSSA Special Publication No.23, Madison.

Knesl, O. 1996. *A Geochemical Investigation of the Water and Sediments of Barber's Pan, North West Province*, M.Sc. Thesis, University of Cape Town, Cape Town.

Kruzic, A.P. 1994. Natural treatment systems, *Water Environment Research*, 66(4), 357-361.

Lambrechts, J.J.N. 1981. Soils of the coastal lowlands of the Western Cape, in Moll, E.(ed) *Proceedings of a Symposium on Coastal Lowlands of the Western Cape*, University of the Western Cape, Cape Town.

Lippman, F. 1973. *Sedimentary Carbonate Minerals*, Springer, New York.

Lowenstein, T.K. and Hardie, L.A. 1985. Criteria for the recognition of salt-pan evaporites, *Sedimentology*, 32, 627-644.

Marshall, T.R. and Harmse, J.T. 1991. A review of the origin and propogation of pans, *SA Geographer*, 19(1/2), 9-21.

Mayland, H.F., James, L.F., Panter, K.E. and Sonderegger, J.L. 1989. Selenium in seleniferous environments, in Jacobs, L.W. (eds) *Selenium in Agriculture and the Environment*, SSSA Special Publication No.23, Madison.

McBride, M.B. 1994. *Environmental Chemistry of Soils*, Oxford University Press, New York.

McNeal, J.M. and Balistrieri, L.S. 1989. Geochemistry and occurrence of selenium: an overview, in Jacobs, L.W. (eds) *Selenium in Agriculture and the Environment*, SSSA Special Publication No.23, Madison.

Meadows, M.E. 1998. The southwestern Cape of South Africa, in Conacher, A.J. and Sala, M. *Land Degradation in Regions of Mediterranean Climate*, Wiley, London.

Moore, D.M. and Reynolds, R.C. Jr. 1997. *X-Ray Diffraction and the Identification and Analysis of Clay Minerals 2nd ed.*, Oxford University Press, Oxford.

Nesbitt, H.W., Markovics, G. and Price, R.C. 1980. Chemical processes affecting alkalis and alkaline earths during continental weathering, *Geochimica et Cosmochimica Acta*, 44, 1659-1666.

Nieman, W.A. 1981. Climate of the coastal lowlands of the Western Cape, in Moll, E.(ed) *Proceedings of a Symposium on Coastal Lowlands of the Western Cape*, University of the Western Cape, Cape Town.

Non-Affiliated Soil Analysis Work Committee 1990. *Handbook of Standard Soil Testing Methods for Advisory Purposes*, 34/1-34/2, Soil Science Society of S.A., Pretoria.

Ohlendorf, H.M. 1989. Bioaccumulation and effects of selenium in wildlife, in Jacobs, L.W. (eds) *Selenium in Agriculture and the Environment*, SSSA Special Publication No.23, Madison, 133-178.

O'Neill, P. 1995. Arsenic, in Alloway, B.J. (ed) *Heavy Metals in Soils (2nd edition)*, Blackie Academic and Professional, London.

Ong, C.G., Herbel, M.J., Dahlgren, R.A. and Tanji, K.K. 1997. Trace element (Se, As, Mo, B) contamination of evaporites in hypersaline agricultural evaporation ponds, *Environ. Sci. Technol.*, 31, 831-838.

Oremland, R.S., Dowdle, P.R., Hoeft, S., Sharp, J.O., Schaefer, J.K., Miller, L.G., Blum, J.S., Smith, R.L., Bloom, N.S. and Wallschlaeger, D. 2000. Bacterial dissimilatory reduction of arsenate and sulfate in meromictic Mono Lake, California, *Geochimica et Cosmochimica Acta*, 64(18), 3073-3084.

Parker, S.P. (ed). 1989. *McGraw-Hill Dictionary of Scientific and Technical Terms (4th ed.)*, McGraw Hill Book Company, New York.

Parkhurst, D.L. and Appello, C.A.J. 1999. *User's Guide to PHREEQC (Version 2)- A computer program for speciation, batch reaction, one dimensional transport, and inverse geochemical calculations*, Water Resources Investigations Report 99-4259, US Geological Survey, Colorado.

Parkhurst, D.L. and Plummer, L.N. 1993. Geochemical models, in Alley, W.M. (ed) *Regional Ground-water Quality*, Van Nostrand Reinhold, New York.

Plummer, L.N., Parkhurst, D.L., Flemming, G.W. and Dunkle, S.A. 1988. *Computer Program Incorporating Pitzer's Equations for Calculation of Geochemical Reactions in Brines*, Water-Resources Investigations Report 88-4153, USGS.

Potts, P.J. 1987. *Handbook of Silicate Rock Analysis*, Blackie, Glasgow, 575-586.

Ramsey, M. 2000. *Environmental Sampling: Estimating the Uncertainty. A One Day Workshop*, Centre for Environmental Research.

Rhoades, J.D. 1982. Soluble salts, in Page, A.L., Miller, R.H. and Keeney, D.R. (eds) *Methods of Soil Analysis: Part 2 - Chemical and Microbiological Properties (2nd Ed.)*, Agronomy Monograph no.9, Wisconsin.

Rogers, J. 1982. Lithostratigraphy of Cenozoic sediments between Cape Town and Eland's Bay, *Palaeo-ecology of Africa*, 15, 121-137.

Rowell, D.L. 1988. Soil acidity and alkalinity., in Wild, A.(ed) *Russell's Soil Conditions and Plant Growth*, Longman Scientific & Technical, Essex.

Scheepers, R. 1995. Geology, geochemistry and petrogenesis of the Late Precambrian S-, I-, and A-type granitoids in the Saldania belt, Western Cape Province, *Journal of African Earth Sciences*, 21(1), 35-58.

Schloeman, H. 1994. *The Geochemistry of Some Common Western Cape Soils (South Africa) with Emphasis on Toxic and Essential Elements*, Unpublished PhD Thesis, UCT, Cape Town.

Schoch, A.E. 1975. The Darling granite batholith, *Ann. Univ. Stell.*, Ser. A1 (Geol.) Vol. 1, 1-104.

Seaman, M.T., Ashton, P.J. and Williams, W.D. 1991. Inland salt waters of southern Africa, *Hydrobiologia*, 210, 75-91.

Shaw, P.A. and Thomas, D.S.G. 1989. Playas, pans and salt lakes, in Thomas, D.S.G. (ed) *Arid Zone Geomorphology*, Belhaven Press, London.

Silberbauer, M.J. and King, J.M. 1991. Geographical trends in the water chemistry of wetlands in the south-western Cape Province, South Africa, *Sth. Afr. J. aquat. Sci.*, 17(1/2), 82-88.

Socki, R.A., Karlsson, H.R. and Gibson, E.K. 1992. Extraction technique for the determination of oxygen-18 in water using preevacuated glass vials, *Analytical Chemistry*, 64, 829-831.

Sofer, Z and Gat, J.R. 1972. Activities and concentrations of oxygen-18 in concentrated aqueous salt solutions: Analytical and geophysical implications, *Earth and Planetary Science Letters*, 15, 232-238.

Soil Classification Working Group (SCWG) 1991. *Soil Classification: A Taxonomic System for South Africa*, Memoirs on the Agricultural Natural Resources of South Africa No. 15, Department of Agricultural Development, Pretoria.

Tanner, R., Glenn, E.P. and Moore, D. 1999. Food chain organisms in hypersaline industrial evaporation ponds, *Water Environment Research*, 71(4), 494-505.

Teller, J.T., Bowler, J.M. and Macumber, P.G. 1982. Modern sedimentation and hydrology in Lake Tyrrell, Victoria, *Journal of Geological Society of Australia*, 29, 159-175.

Timmerman, K.M.G. 1986. *Hydrocensus in the Area Between Darling, Malmesbury and Mamre*, Technical Report GH3477, Department of Water Affairs, Cape Town.

USGS 1997. *Summary of PHRQPITZ*, World Wide Web, http://water.usgs.gov\cgi-bin\man_wrdapp?phrqpitz.

Van Niekerk, B.J. 1967. *The Soils of the Darling Area*, Unpublished MSc Thesis, University of Stellenbosch.

Vasconcelos, C. and Mackenzie, J.A. 1997. Microbial mediation of modern dolomite precipitation and diagenesis under anoxic conditions (Lagoa Vermelha, Rio de Janeiro, Brazil), *Journal of Sedimentary Research*, 67(3), 378-390.

Vasconcelos, C., Mackenzie, J.A., Bernasconi, S., Grujic, D. and Tien, A.J. 1995. Microbial mediation as a possible mechanism for natural dolomite formation at low temperatures, *Nature*, 377(6546), 220-222.

Verhagen, B.Th. 1991. On the nature and genesis of pans - A review and an ecological model, *Palaeoecology of Africa*, 21, 179-194.

Verster, E., van Deventer, P.W. and Ellis, F. 1992. Soils and associated materials of some pan floors and margins in southern Africa: a review, *SA Geographer*, 19(1/2), 35-47.

Visser, H.N. and Schoch, A.E. 1973. *The Geology and Mineral Resources of the Saldanha Bay Area*, Memoire No. 63, 10-13, 98-135, Dept. of Mines Geological Survey, Pretoria.

Warren, J. 1999. *Evaporites - Their Evolution and Economics*, Blackwell Science, Oxford.

Warren, J. 2000. Dolomite: occurrence, evolution and economically important associations, *Earth-Science Reviews*, 52, 1-81.

Watson, A. 1983. Evaporite sedimentation in non-marine environments, in Goudie, A.S. and Pye, K. *Chemical Sediments and Geomorphology: Precipitates and Residua in the Near-Surface Environment*, Academic Press, London.

Weiss, J. 1986. *Handbook of Ion Chromatography*, Dionex Corporation, California.

Whitten, D.G.A. and Brooks, J.R.V. 1972. *The Penguin Dictionary of Geology*, Penguin, London.

Whittig, L.D. and Allardice, W.R. 1986. X-ray diffraction techniques, in Klute, A. (ed) *Methods of Soil Analysis, Part I. Physical and Mineralogical Methods*, Soil Science Society of America, Madison, Wisconsin.

Williams, W.D. 1996. What future for saline lakes?, *Environment*, 38(9), 12-20.

Zimmerman, U., Ehhalt, D. and Munnich, K. O. 1967. *Soil-water movement and evapotranspiration: Changes in the isotopic composition of the water, Proceedings of the Symposium on Isotopes in Hydrology, 14-18 November 1966*, 567-585, IAEA, Vienna.

# A. Method Appraisal

## A.1. WATER ANALYSIS

### A.1.1. ALKALINITY

Eight samples were analysed in duplicate. For each batch of analyses, a sample from the previous batch was reanalysed to ensure consistency. The results of duplicate analyses are given in Table A.1. No standards were analysed.

**Table A.1: Duplicate alkalinity analyses**

| | Result 1(mmol/kg) | Result 2 (mmol/kg) | Difference | Mean | Std. Dev. | %RSD |
|---|---|---|---|---|---|---|
| **BA-WP2** | 4.65 | 4.58 | 0.07 | 4.62 | 0.05 | 1.09 |
| **BB-WB1** | 5.35 | 5.26 | 0.09 | 5.31 | 0.07 | 1.23 |
| **BB-WP1** | 0.88 | 0.86 | 0.02 | 0.87 | 0.01 | 1.30 |
| **DV-WB1** | 4.80 | 4.77 | 0.03 | 4.79 | 0.02 | 0.38 |
| **RA-WP1** | 0.65 | 0.65 | 0.00 | 0.65 | 0.00 | 0.19 |
| **SK-WB1** | 2.63 | 2.58 | 0.05 | 2.60 | 0.03 | 1.28 |
| **SK-WP1** | 1.42 | 1.42 | 0.00 | 1.42 | 0.00 | 0.19 |
| **ZA-WS1** | 3.79 | 3.78 | 0.01 | 3.78 | 0.00 | 0.13 |
| **BB-WR1** | 4.69 | 4.71 | 0.02 | 4.70 | 0.01 | 0.27 |
| **KP-WP1** | 2.06 | 2.04 | 0.02 | 2.05 | 0.01 | 0.73 |
| **RB-WP1** | 5.07 | 5.06 | 0.01 | 5.06 | 0.01 | 0.14 |
| **RP-WP1** | 1.64 | 1.64 | 0.00 | 1.64 | 0.00 | 0.12 |
| **YF-WB1** | 1.33 | 1.31 | 0.02 | 1.32 | 0.01 | 0.90 |
| | | **Std. Dev.** | **0.03** | | | |
| | | **Mean** | **2.98** | | | |
| | | **Precision (%)** | **1.87** | | | |

### A.1.2. DISSOLVED ORGANIC CARBON (DOC)

Detection limits depend on the amount of sample used, the buffering capacity of the alkaline solution, thickness of the colorimetry cell and the sensitivity of the colorimeter. Concentrations between 1 and 25 ppm can be easily detected (Mike Louw, Laboratory Manager, CSIR, pers. comm., 2000). Three duplicates were sent to ensure repeatability of analysis. The results are given in Table A.2.

**Table A.2: Results for duplicate analysis for DOC.**

| DOC | Result (mg/kg) | Result (mg/kg) | Difference | Mean | Std. Dev | % RSD |
|---|---|---|---|---|---|---|
| **BB-WB1** | 3.17 | 3.17 | 0.00 | 3.17 | 0.0 | 0.0 |
| **BB-WR1** | 12.75 | 14.02 | 1.27 | 13.39 | 0.9 | 6.7 |
| **SK-WB1** | 5.05 | 5.35 | 0.30 | 5.20 | 0.2 | 4.1 |

### A.1.3. MAJOR IONS BY ION CHROMATOGRAPHY

Dionex API-450 software integrates the area under each conductivity peak, subtracts the background and calculates concentrations of cations and anions based on calibrations. Instrument parameters are listed in Table A.3.

**Table A.3: Instrument parameters for IC**

| | Anions | Cations |
|---|---|---|
| Sample loop capacity | 50 :l | 25 :l |
| Separator Column | AS14 | CS12A |
| Guard Column | AG4A | CG12A |
| Eluant | 3.5 mM $Na_2CO_3$ + 1mM $NaHCO_3$ | 22N $H_2SO_4$ |
| Eluant flow rate | 1.2 mL/min | 1.0 mL/min |
| Suppressor | ASRS-I-4mm | CSRS-I-4mm |

Problems were experienced with the computer software definition of background values, and initial analyses had to be discarded. Eight of the samples were run in duplicate, and seawater standard was run with each analysis. Results for the duplicate analyses for each element are given in Table A.4 and repeat analyses of the standard and seawater are given in Table A.5. A charge balance was performed for the cation and anion concentrations or each sample, based on the principle that ions in solution are derived from dissolution of electrically neutral compounds. The solution is expected to maintain the electrical neutrality of the parent compounds. The sum of cations and anions in mmols of charge per litre ($mmol_c/L$) is determined, and the percentage difference between them calculated according to the formula: $$\%\ difference = 100 * \frac{\sum cations - \sum anions}{\sum cations + \sum anions}$$

Ions that could contribute to more anionic charge are dissolved organic matter and bicarbonate. According to Eaton *et al.* (1995), samples with anion sums of 10.0 to 800 meq/L should have a charge balance below 5%. The anion sum of samples in this study varies from 20 to 6500 meq/L. Most charge balances are below 5%, as can be seen in Table A.6.

**Table A.4: Duplicate IC analyses for all elements**

| Sodium | Result (mmol/kg) | Result (mmol/kg) | Difference | Mean | Std. Dev | % RSD |
|---|---|---|---|---|---|---|
| **BA-WP2** | 2 013 | 1 989 | 23.9 | 2 001 | 16.9 | 0.8 |
| **BB-WB1** | 282 | 291 | 9.0 | 287 | 6.4 | 2.2 |
| **BB-WP1** | 4 283 | 4 283 | 0.0 | 4 283 | 0.0 | 0.0 |
| **DV-WB1** | 491 | 513 | 22.2 | 502 | 15.7 | 3.1 |
| **RA-WP1** | 4 638 | 4 646 | 7.3 | 4 642 | 5.2 | 0.1 |
| **SK-WB1** | 164 | 175 | 10.7 | 170 | 7.6 | 4.5 |
| **SK-WP1** | 815 | 748 | 67.2 | 781 | 47.5 | 6.1 |
| **ZA-WS1** | 494 | 490 | 3.8 | 492 | 2.7 | 0.5 |
| **BB-WR1** | 254 | 277 | 22.9 | 265 | 16.2 | 6.1 |
| **KP-WP1** | 4260 | 4463 | 203.0 | 4 361 | 143.5 | 3.3 |
| **RB-WP1** | 24.9 | 24.5 | 0.4 | 25 | 0.3 | 1.1 |
| **RP-WP1** | 978 | 897 | 80.8 | 937 | 57.1 | 6.1 |
| **YF-WB1** | 1053 | 1029 | 24.6 | 1 041 | 17.4 | 1.7 |
| **Potassium** | **Result (mmol/kg)** | **Result (mmol/kg)** | **Difference** | **Mean** | **Std. Dev** | **% RSD** |
| **BA-WP2** | 17.8 | 16.9 | 0.9 | 17 | 0.7 | 3.8 |
| **BB-WB1** | 2.66 | 2.53 | 0.1 | 3 | 0.1 | 3.4 |
| **BB-WP1** | 36.8 | 32.5 | 4.3 | 35 | 3.1 | 8.8 |
| **DV-WB1** | 4.61 | 4.61 | 0.0 | 5 | 0.0 | 0.0 |
| **RA-WP1** | 23.6 | 30.1 | 6.4 | 27 | 4.6 | 17.0 |
| **SK-WB1** | 3.44 | 1.22 | 2.2 | 2 | 1.6 | 67.6 |
| **SK-WP1** | 13.3 | 10.6 | 2.7 | 12 | 1.9 | 16.0 |
| **ZA-WS1** | 5.01 | 4.81 | 0.2 | 5 | 0.1 | 2.9 |
| **BB-WR1** | 2.76 | 2.65 | 0.1 | 3 | 0.1 | 2.9 |
| **KP-WP1** | 24.3 | 26.6 | 2.3 | 25 | 1.6 | 6.5 |
| **RB-WP1** | 0.399 | 0.389 | 0.0 | 0 | 0.0 | 1.8 |
| **RP-WP1** | 21.9 | 19.2 | 2.7 | 21 | 1.9 | 9.2 |
| **YF-WB1** | 17.0 | 14.6 | 2.4 | 16 | 1.7 | 10.9 |

**Table A.4: cont.**

| Calcium | Result (mmol/kg) | Result (mmol/kg) | Difference | Mean | Std. Dev | % RSD |
|---|---|---|---|---|---|---|
| **BA-WP2** | 235 | 221 | 14.6 | 228 | 10.4 | 4.5 |
| **BB-WB1** | 43.8 | 56.2 | 12.4 | 50 | 8.7 | 17.5 |
| **BB-WP1** | 622 | 550 | 71.9 | 586 | 50.8 | 8.7 |
| **DV-WB1** | 78.9 | 71.0 | 7.8 | 75 | 5.5 | 7.4 |
| **RA-WP1** | 543 | 826 | 283.0 | 685 | 200.1 | 29.2 |
| **SK-WB1** | 35.8 | 42.1 | 6.3 | 39 | 4.5 | 11.5 |
| **SK-WP1** | 81.9 | 89.3 | 7.5 | 86 | 5.3 | 6.2 |
| **ZA-WS1** | 52.6 | 76.5 | 23.9 | 65 | 16.9 | 26.1 |
| **YF-WB1** | 191 | 123 | 68.2 | 157 | 48.2 | 30.8 |
| **RP-WP1** | 101 | 97.7 | 3.1 | 99 | 2.2 | 2.2 |
| **RB-WP1** | 3.37 | 4.31 | 0.9 | 4 | 0.7 | 17.3 |
| **BB-WR1** | 20.5 | 35.2 | 14.6 | 28 | 10.3 | 37.1 |
| **KP-WP1** | 652 | 685 | 33.1 | 668 | 23.4 | 3.5 |
| **Magnesium** | **Result (mmol/kg)** | **Result (mmol/kg)** | **Difference** | **Mean** | **Std. Dev** | **% RSD** |
| **BA-WP2** | 316 | 332 | 16.6 | 324 | 11.7 | 3.6 |
| **BB-WB1** | 39.7 | 51.5 | 11.8 | 46 | 8.4 | 18.3 |
| **BB-WP1** | 293 | 300 | 7.0 | 296 | 4.9 | 1.7 |
| **DV-WB1** | 120 | 112 | 8.1 | 116 | 5.7 | 4.9 |
| **RA-WP1** | 878 | 578 | 300.9 | 728 | 212.7 | 29.2 |
| **SK-WB1** | 46.0 | 61.8 | 15.8 | 54 | 11.2 | 20.8 |
| **SK-WP1** | 157 | 151 | 6.0 | 154 | 4.2 | 2.7 |
| **ZA-WS1** | 103 | 76.8 | 25.8 | 90 | 18.3 | 20.3 |
| **BB-WR1** | 46.4 | 47.6 | 1.2 | 47 | 0.9 | 1.9 |
| **KP-WP1** | 500 | 545 | 44.9 | 523 | 31.8 | 6.1 |
| **RB-WP1** | 2.27 | 1.58 | 0.7 | 2 | 0.5 | 25.4 |
| **RP-WP1** | 175 | 154 | 21.2 | 164 | 15.0 | 9.1 |
| **YF-WB1** | 142 | 174 | 31.3 | 158 | 22.1 | 14.0 |
| **Chloride** | **Result (mmol/kg)** | **Result (mmol/kg)** | **Difference** | **Mean** | **Std. Dev** | **% RSD** |
| **BA-WP2** | 2 488 | 2 511 | 23.2 | 2 500 | 16.4 | 0.7 |
| **BB-WB1** | 334 | 335 | 0.8 | 335 | 0.6 | 0.2 |
| **BB-WP1** | 4 809 | 5 013 | 204.3 | 4 911 | 144.5 | 2.9 |
| **DV-WB1** | 644 | 614 | 30.1 | 629 | 21.3 | 3.4 |
| **RA-WP1** | 4 833 | 4 810 | 22.8 | 4 821 | 16.1 | 0.3 |
| **SK-WB1** | 246 | 249 | 3.2 | 247 | 2.3 | 0.9 |
| **SK-WP1** | 949 | 987 | 37.6 | 968 | 26.6 | 2.8 |
| **ZA-WS1** | 604 | 606 | 1.8 | 605 | 1.3 | 0.2 |
| **BB-WR1** | 374 | 374 | 0.3 | 374 | 0.2 | 0.1 |
| **KP-WP1** | 4196 | 4397 | 200.8 | 4 296 | 142.0 | 3.3 |
| **RB-WP1** | 17.1 | 17.5 | 0.4 | 17 | 0.3 | 1.6 |
| **RP-WP1** | 1151 | 1052 | 99.4 | 1 102 | 70.3 | 6.4 |
| **YF-WB1** | 1317 | 1258 | 58.6 | 1 288 | 41.4 | 3.2 |

**Table A.4: cont.**

| Sulphate | Result (mmol/kg) | Result (mmol/kg) | Difference | Mean | Std. Dev | % RSD |
|---|---|---|---|---|---|---|
| **BA-WP2** | 154 | 155 | 0.2 | 154 | 0.1 | 0.1 |
| **BB-WB1** | 25.6 | 26.1 | 0.5 | 26 | 0.3 | 1.3 |
| **BB-WP1** | 359 | 300 | 58.7 | 330 | 41.5 | 12.6 |
| **DV-WB1** | 40.1 | 40.0 | 0.1 | 40 | 0.1 | 0.2 |
| **RA-WP1** | 346 | 353 | 6.8 | 350 | 4.8 | 1.4 |
| **SK-WB1** | 17.4 | 17.1 | 0.3 | 17 | 0.2 | 1.4 |
| **SK-WP1** | 61.9 | 62.6 | 0.7 | 62 | 0.5 | 0.8 |
| **ZA-WS1** | 33.3 | 32.7 | 0.6 | 33 | 0.4 | 1.3 |
| **BB-WR1** | 22.6 | 27.8 | 5.2 | 25 | 3.6 | 14.5 |
| **KP-WP1** | 396 | 413 | 17.1 | 405 | 12.1 | 3.0 |
| **RB-WP1** | 1.25 | 1.25 | 0.0 | 1 | 0.0 | 0.0 |
| **RP-WP1** | 98.3 | 96.8 | 1.4 | 98 | 1.0 | 1.0 |
| **YF-WB1** | 97.4 | 82.4 | 15.0 | 90 | 10.6 | 11.8 |

**Table A.5: Repeat analysis of seawater standard by IC**

| SEAWATER | Li | Na | NH4 | K | Mg | Ca |
|---|---|---|---|---|---|---|
| 11/9/00 | 0.00 | 18.16 | 0.00 | 0.66 | 3.71 | 3.48 |
| 12/9/00 | 0.00 | 14.49 | 0.00 | 0.28 | 2.37 | 3.47 |
| 15/9/00 | 0.00 | 17.90 | 0.00 | 0.62 | 2.62 | 4.81 |
| 19/9/00 | 0.00 | 13.38 | 0.00 | | 2.46 | 2.58 |
| **Average** | 0.00 | 15.98 | 0.00 | 0.52 | 2.79 | 3.59 |
| **Expected** | 0.00 | 17.22 | 0.00 | 0.64 | 2.06 | 0.66 |
| **Bias** | 0.00 | -1.23 | 0.00 | -0.12 | 0.73 | 2.92 |
| **Relative bias** | | -7.16 | | -18.55 | 35.17 | 442.52 |

**Table A.6: Charge balance of samples**

| Sample | Charge balance | Sample | Charge balance | Sample | Charge balance |
|---|---|---|---|---|---|
| **BA-WP1** | -8.26 | **KP-WP1a** | -3.75 | **SK-WP1-a1** | -2.01 |
| **BA-WP2-a1** | -7.44 | **KP-WP1b** | -3.87 | **SK-WP1-a2** | -6.80 |
| **BA-WP2-a2** | -8.41 | **OT-WR1** | -6.06 | **YF-WB1a** | -5.14 |
| **BA-WS1** | -3.79 | **RA-SS1a** | -6.47 | **YF-WB1b** | -3.04 |
| **BB-WB1-a1** | -2.40 | **RA-WB1** | -3.04 | **YF-WB2** | *11.80* |
| **BB-WB1-a2** | -1.49 | **RA-WP1-a1** | -5.42 | **YF-WP1** | -3.05 |
| **BB-WP1-a1** | -7.88 | **RA-WP1-a2** | -5.22 | **ZA-WS2** | -9.34 |
| **BB-WP1-a2** | -8.19 | **RB-WP1a** | 2.87 | **ZA-WP1** | -9.77 |
| **BB-WR1a** | *-12.29* | **RB-WP1b** | 1.89 | **ZA-WR1** | -6.05 |
| **BB-WR1b** | *-10.68* | **RP-WB1** | -1.12 | **ZA-WS1-a1** | -0.83 |
| **DV-WB1-a1** | -5.60 | **RP-WP1a** | -3.42 | **ZA-WS1-a2** | -1.21 |
| **DV-WB1-a2** | -1.78 | **RP-WP1b** | -3.46 | **ZB-WB1** | 0.06 |
| **DV-WP1** | -3.29 | **SK-WB1-a1** | -4.79 | **ZB-WP1** | -5.80 |
| **ZB-WS1** | -2.81 | **SK-WB1-a2** | -3.19 | | |

### A.1.4. CALCIUM AND MAGNESIUM BY EDTA TITRATION

Eight samples were run in duplicate to determine the repeatability of hardness titrations. A known standard was run, as well as a seawater sample. A sample of distilled water was run to determine background concentrations. Results are given in Table A.7.

**Table A.10: Results for duplicate analysis of hardness**

| Sample | Result (mmol/kg) | Result (mmol/kg) | Difference | Mean | Std. Dev | % RSD |
|---|---|---|---|---|---|---|
| BA-WP2 | 180 | 179 | 0.7 | 180 | 0.5 | 0.3 |
| BB-WB1 | 44.0 | 43.8 | 0.2 | 44 | 0.1 | 0.3 |
| BB-WP1 | 201 | 204 | 3.0 | 203 | 2.1 | 1.1 |
| DV-WB1 | 75.2 | 75.3 | 0.1 | 75 | 0.1 | 0.1 |
| RA-WP1 | 152 | 150 | 2.4 | 151 | 1.7 | 1.1 |
| SK-WB1 | 44.5 | 45.3 | 0.8 | 45 | 0.6 | 1.3 |
| SK-WP1 | 100 | 104 | 3.9 | 102 | 2.7 | 2.7 |
| ZA-WS1 | 79.0 | 78.7 | 0.3 | 79 | 0.2 | 0.3 |
| BA-WR1 | 37.4 | 36.7 | 0.6 | 37 | 0.5 | 1.2 |
| KP-WP1 | 206 | 200 | 6.0 | 203 | 4.2 | 2.1 |
| RB-WP1 | 0.403 | 0.454 | 0.1 | 0 | 0.0 | 8.3 |
| RP-WP1 | 131 | 128 | 3.1 | 129 | 2.2 | 1.7 |
| YF-WB1 | 153 | 153 | 0.1 | 153 | 0.1 | 0.0 |

### A.1.5. FLUORIDE BY ION-SELECTIVE ELECTRODE

Eight samples were analysed in duplicate and an independent standard was analysed to ensure the calibration was correct. Results for duplicate analyses are given in Table A.8. It is not possible to compare the data obtained by ion-selective electrode with data from ion chromatography as fluoride was only detected in a few samples by IC and then only at the limits of detection.

**Table A.8. Results for duplicate fluoride analysis**

| Sample | Result (µmol/kg) | Result (µmol/kg) | Difference | Mean | Std. Dev | % RSD |
|---|---|---|---|---|---|---|
| BP2-WP2 | 59.9 | 59.9 | 0.0 | 60 | 0.0 | 0.0 |
| BP-WB1 | 100.6 | 109.4 | 8.8 | 105 | 6.2 | 5.9 |
| BP-WP1 | 11.2 | 11.2 | 0.0 | 11 | 0.0 | 0.0 |
| DV-WB1 | 219.3 | 218.8 | 0.5 | 219 | 0.4 | 0.2 |
| RA-WP1 | 10.6 | 11.9 | 1.3 | 11 | 0.9 | 8.2 |
| SK-WB1 | 61.0 | 62.0 | 1.0 | 62 | 0.7 | 1.1 |
| SK-WP1 | 22.9 | 22.9 | 0.0 | 23 | 0.0 | 0.0 |
| ZA-WS1 | 139.3 | 136.7 | 2.6 | 138 | 1.8 | 1.3 |
| BP-WR1 | 99.6 | 98.5 | 1.1 | 99 | 0.8 | 0.8 |
| KP-WP1 | 11.3 | 11.4 | 0.1 | 11 | 0.1 | 0.6 |
| RB-WP1 | 79.5 | 77.9 | 1.6 | 79 | 1.1 | 1.4 |
| RP-WP1 | 19.5 | 19.0 | 0.5 | 19 | 0.4 | 1.8 |
| YF-WB1 | 19.5 | 19.0 | 0.5 | 19 | 0.4 | 1.8 |

### A.1.6. TRACE ELEMENTS BY ICP-MS

Along with the repeat analyses performed by the autosampler, duplicate samples were also run. The data for repeat and duplicate analyses are given in Table A.9 and analysis of certified standards in Table A.10.

**Table A9: Results for repeat and duplicate analysis of samples by ICP-MS**

| | Sample | | Duplicate | | | | |
|---|---|---|---|---|---|---|---|
| **Lithium** | **Repeat 1** | **Repeat 2** | **Repeat 1** | **Repeat 2** | **Average** | **Std Dev** | **Precision (%)** |
| BA-WP1 | 1290 | 1102 | | | 1196 | 133 | 11 |
| BA-WP2 | 309 | 329 | 283 | 303 | 306 | 19 | 6 |
| BA-WS1 | 734 | 914 | | | 824 | 127 | 15 |
| BB-WB1 | 107 | 106 | 94 | 97 | 101 | 6 | 6 |
| BB-WP1 | 120 | 199 | 232 | 230 | 195 | 52 | 27 |
| BB-WR1 | 97 | 110 | 93 | 92 | 98 | 8 | 8 |
| DV-WB1 | 143 | 148 | 158 | 140 | 147 | 8 | 5 |
| DV-WP1 | 55 | 57 | | | 56 | 1 | 2 |
| KP-WP1 | 189 | 203 | 161 | 208 | 190 | 21 | 11 |
| OT-WR1 | 7 | 9 | | | 8 | 1 | 17 |
| RA-WB1 | 246 | 315 | | | 281 | 49 | 17 |
| RA-WP1 | 197 | 204 | 183 | 161 | 186 | 19 | 10 |
| RB-WP1 | 9 | 14 | 13 | 16 | 13 | 3 | 21 |
| RP-WB1 | 193 | 200 | | | 197 | 5 | 3 |
| RP-WP1 | 442 | 443 | 393 | 404 | 420 | 26 | 6 |
| SK-WB1 | 1 | 5 | 6 | 6 | 4 | 2 | 58 |
| SK-WP1 | 7 | 8 | 6 | 9 | 7 | 2 | 21 |
| YF-OT1 | 2 | 2 | | | 2 | 0 | 10 |
| YF-WB1 | 101 | 107 | 105 | 113 | 107 | 5 | 5 |
| YF-WB2 | 220 | 227 | | | 224 | 5 | 2 |
| YF-WP1 | 275 | 291 | | | 283 | 11 | 4 |
| ZA-WS1 | 131 | 135 | 103 | 108 | 119 | 16 | 14 |
| ZA-WS2 | 129 | 124 | | | 127 | 3 | 3 |
| ZA-WP1 | 181 | 185 | | | 183 | 3 | 2 |
| ZA-WR1 | 15 | 22 | | | 19 | 5 | 28 |
| ZB-WP1 | 191 | 243 | | | 217 | 37 | 17 |
| ZB-WS1 | 26 | 27 | 23 | 25 | 25 | 2 | 7 |
| DV-SS1a | 84 | 89 | | | 86 | 4 | 4 |
| DV-SS1b | 86 | 94 | | | 90 | 5 | 6 |
| DV-SS2 | 130 | 126 | | | 128 | 3 | 2 |
| KV-SS1b | 8 | 6 | 6 | 6 | 6 | 1 | 20 |
| RA-SS1a | 2117 | 1668 | | | 1893 | 317 | 17 |
| RA-SS1b | 1184 | 1104 | | | 1144 | 57 | 5 |
| RA-SS1b IW | 801 | 615 | | | 708 | 131 | 19 |
| RA-SS3b | 266 | 269 | | | 267 | 2 | 1 |
| RA-SS3c | 142 | 147 | | | 144 | 3 | 2 |
| RA-SS3d | 185 | 198 | | | 191 | 9 | 5 |
| RB-SS1 | 22 | 22 | 21 | 22 | 22 | 1 | 3 |
| YF-SS1a | 245 | 224 | | | 235 | 15 | 6 |
| YF-SS1b | 113 | 124 | 113 | 111 | 115 | 6 | 5 |
| YF-SS1c | 77 | 92 | | | 85 | 10 | 12 |

**Table A.9 cont.**

| | Sample | | Duplicate | | | | |
|---|---|---|---|---|---|---|---|
| **Boron** | **Repeat 1** | **Repeat 2** | **Repeat 1** | **Repeat 2** | **Average** | **Std Dev** | **Precision (%)** |
| BA-WP1 | 94547 | 69806 | | | 82176 | 17495 | 21 |
| BA-WP2 | 16671 | 17045 | 16881 | 18296 | 17223 | 732 | 4 |
| BA-WS1 | 55334 | 56900 | | | 56117 | 1107 | 2 |
| BB-WB1 | 2004 | 1963 | 2116 | 2100 | 2046 | 74 | 4 |
| BB-WP1 | 7386 | 8627 | 12531 | 12442 | 10246 | 2636 | 26 |
| BB-WR1 | 4298 | 4567 | 4322 | 4117 | 4326 | 185 | 4 |
| DV-WB1 | 1582 | 1680 | 1682 | 1399 | 1586 | 133 | 8 |
| DV-WP1 | 4096 | 3935 | | | 4015 | 113 | 3 |
| KP-WP1 | 41493 | 41721 | 49167 | 42005 | 43596 | 3720 | 9 |
| OT-WR1 | 525 | 568 | | | 546 | 30 | 6 |
| RA-WB1 | 5320 | 5366 | | | 5343 | 32 | 1 |
| RA-WP1 | 14765 | 14772 | 13997 | | 14511 | 445 | 3 |
| RB-WP1 | 3127 | 3228 | 3404 | 3324 | 3271 | 120 | 4 |
| RP-WB1 | 5328 | 5559 | | | 5444 | 163 | 3 |
| RP-WP1 | 16853 | 16935 | 16161 | 15324 | 16318 | 748 | 5 |
| SK-WB1 | 1310 | 1384 | 1366 | 1409 | 1367 | 42 | 3 |
| SK-WP1 | 9103 | 8634 | 8757 | 8242 | 8684 | 355 | 4 |
| YF-OT1 | 39 | 35 | | | 37 | 3 | 9 |
| YF-WB1 | 3861 | 3340 | 3416 | 3531 | 3537 | 230 | 6 |
| YF-WB2 | 4933 | 4876 | | | 4904 | 40 | 1 |
| YF-WP1 | 9986 | 10385 | | | 10185 | 282 | 3 |
| ZA-WS2 | 761 | 794 | | | 777 | 23 | 3 |
| ZA-WP1 | 34403 | 33092 | | | 33748 | 927 | 3 |
| ZA-WR1 | 1401 | 1451 | | | 1426 | 35 | 2 |
| ZA-WS1 | 3489 | 3139 | 3589 | 3691 | 3477 | 240 | 7 |
| ZB-WP1 | 21030 | 21664 | | | 21347 | 448 | 2 |
| ZB-WS1 | 1348 | 1321 | 1243 | 1255 | 1292 | 51 | 4 |
| DV-SS1a | 1743 | 1802 | | | 1772 | 42 | 2 |
| DV-SS1b | 1256 | 1277 | | | 1267 | 15 | 1 |
| DV-SS2 | 10352 | 9732 | | | 10042 | 438 | 4 |
| KV-SS1b | 1741 | 1772 | 1722 | | 1745 | 25 | 1 |
| RA-SS1a | 92900 | 78765 | | | 85832 | 9995 | 12 |
| RA-SS1b | 27477 | 25465 | | | 26471 | 1422 | 5 |
| RA-SS1b IW | 36966 | 29141 | | | 33053 | 5533 | 17 |
| RA-SS3b | 2497 | 2389 | | | 2443 | 76 | 3 |
| RA-SS3c | 3106 | 3207 | | | 3157 | 71 | 2 |
| RA-SS3d | 2215 | 2558 | | | 2386 | 242 | 10 |
| RB-SS1 | 10523 | 10788 | 9745 | 9947 | 10251 | 487 | 5 |
| YF-SS1a | 6847 | 6830 | | | 6838 | 12 | 0 |
| YF-SS1b | 2566 | 2519 | 3380 | 3539 | 3001 | 534 | 18 |
| YF-SS1c | 6705 | 6437 | | | 6571 | 189 | 3 |

**Table A.9. cont.**

| | Sample | | Duplicate | | | | |
|---|---|---|---|---|---|---|---|
| Iron | Repeat 1 | Repeat 2 | Repeat 1 | Repeat 2 | Average | Std Dev | Precision (%) |
| BA-WP1 | 36015 | 30800 | | | 33408 | 3687 | 11 |
| BA-WP2 | 4457 | 151 | 1014 | | 1874 | 2278 | 122 |
| BA-WS1 | 24177 | 27127 | | | 25652 | 2086 | 8 |
| BB-WB1 | 1871 | 1346 | 488 | | 1235 | 698 | 57 |
| BB-WP1 | 5498 | 10743 | 11697 | 5510 | 8362 | 3323 | 40 |
| BB-WR1 | 902 | 16 | 1965 | 1308 | 1048 | 816 | 78 |
| DV-WB1 | 2575 | 2533 | 3388 | 2307 | 2701 | 473 | 18 |
| DV-WP1 | 3251 | 2752 | | | 3001 | 353 | 12 |
| KP-WP1 | 2862 | | 24618 | 25982 | 17820 | 12972 | 73 |
| OT-WR1 | 519 | 870 | | | 695 | 248 | 36 |
| RA-WB1 | 4766 | 6792 | | | 5779 | 1433 | 25 |
| RA-WP1 | 3358 | | 2193 | | 2775 | 824 | 30 |
| RB-WP1 | 2221 | 2527 | 639 | 177 | 1391 | 1158 | 83 |
| RP-WB1 | 811 | 125 | | | 468 | 485 | 104 |
| RP-WP1 | 3417 | 2586 | 4678 | 3626 | 3577 | 861 | 24 |
| SK-WB1 | 8259 | 8126 | 7845 | 7671 | 7975 | 266 | 3 |
| SK-WP1 | 2937 | 2330 | 2575 | 2851 | 2673 | 276 | 10 |
| YF-OT1 | 694 | 575 | | | 634 | 84 | 13 |
| YF-WB1 | 8239 | 6094 | 6045 | 5766 | 6536 | 1144 | 18 |
| YF-WB2 | 2029 | 1309 | | | 1669 | 509 | 30 |
| YF-WP1 | 8804 | 4209 | | | 6507 | 3249 | 50 |
| ZA-WP1 | 15524 | 12220 | | | 13872 | 2336 | 17 |
| ZA-WR1 | 1856 | 2107 | | | 1981 | 178 | 9 |
| ZA-WS1 | 3542 | 2673 | 1414 | 1843 | 2368 | 941 | 40 |
| ZB-WS1 | 212 | 205 | | | 209 | 5 | 3 |
| DV-SS1a | 1025 | 857 | | | 941 | 119 | 13 |
| DV-SS1b | 1621 | 1433 | | | 1527 | 133 | 9 |
| DV-SS2 | 3797 | 3163 | | | 3480 | 448 | 13 |
| KV-SS1b | 175 | 109 | 194 | | 159 | 45 | 28 |
| RA-SS1a | 19301 | 3387 | | | 11344 | 11253 | 99 |
| RA-SS1b | 9801 | 4425 | | | 7113 | 3802 | 53 |
| RA-SS3c | 8851 | 2872 | | | 5862 | 4228 | 72 |
| RA-SS3d | 7956 | 2811 | | | 5384 | 3638 | 68 |
| RB-SS1 | 124 | 50 | 155 | 37 | 91 | 57 | 62 |
| YF-SS1a | 9352 | 4469 | | | 6911 | 3453 | 50 |
| YF-SS1b | 8544 | 3365 | | | 5954 | 3662 | 61 |

**Table A.9. cont.**

| Arsenic | Sample Repeat 1 | Repeat 2 | Duplicate Repeat 1 | Repeat 2 | Average | Std Dev | Precision (%) |
|---|---|---|---|---|---|---|---|
| BA-WP1 | 952 | 696 | | | 824 | 181 | 22 |
| BA-WP2 | 359 | 288 | 316 | 282 | 311 | 35 | 11 |
| BA-WS1 | 562 | 562 | | | 562 | 0 | 0 |
| BB-WB1 | 57 | 56 | 50 | 53 | 54 | 3 | 6 |
| BB-WP1 | 559 | 517 | 621 | 673 | 592 | 69 | 12 |
| BB-WR1 | 61 | 63 | 64 | 60 | 62 | 2 | 3 |
| DV-WB1 | 55 | 52 | 57 | 46 | 52 | 5 | 9 |
| DV-WP1 | 50 | 44 | | | 47 | 4 | 9 |
| KP-WP1 | 708 | 584 | 873 | 707 | 718 | 118 | 16 |
| OT-WR1 | 18 | 17 | | | 17 | 1 | 5 |
| RA-WB1 | 426 | 399 | | | 413 | 19 | 5 |
| RA-WP1 | 662 | 690 | 478 | 379 | 552 | 149 | 27 |
| RB-WP1 | 20 | 17 | 17 | 14 | 17 | 2 | 15 |
| RP-WB1 | 48 | 57 | | | 53 | 7 | 12 |
| RP-WP1 | 133 | 141 | 153 | 135 | 141 | 9 | 7 |
| SK-WB1 | 31 | 29 | 28 | 30 | 30 | 1 | 4 |
| SK-WP1 | 130 | 118 | 130 | 125 | 126 | 6 | 4 |
| YF-OT1 | 1 | 1 | | | 1 | 0 | 19 |
| YF-WB1 | 206 | 161 | 173 | 165 | 176 | 20 | 12 |
| YF-WB2 | 151 | 160 | | | 155 | 6 | 4 |
| YF-WP1 | 159 | 146 | | | 153 | 10 | 6 |
| ZA-WS2 | 16 | 12 | | | 14 | 3 | 18 |
| ZA-WP1 | 712 | 684 | | | 698 | 19 | 3 |
| ZA-WR1 | 32 | 33 | | | 33 | 1 | 3 |
| ZA-WS1 | 96 | 80 | 77 | 82 | 84 | 9 | 10 |
| ZB-WP1 | 654 | 553 | | | 603 | 72 | 12 |
| ZB-WS1 | 8 | 11 | 8 | 7 | 9 | 1 | 17 |
| DV-SS1a | 30 | 26 | | | 28 | 3 | 11 |
| DV-SS1b | 30 | 28 | | | 29 | 1 | 5 |
| DV-SS2 | 70 | 67 | | | 68 | 2 | 3 |
| KV-SS1b | 27 | 25 | 26 | | 26 | 1 | 4 |
| RA-SS1a | 588 | 444 | | | 516 | 102 | 20 |
| RA-SS1b | 452 | 429 | | | 440 | 16 | 4 |
| RA-SS1b IW | 447 | 349 | | | 398 | 70 | 17 |
| RA-SS3b | 178 | 175 | | | 176 | 2 | 1 |
| RA-SS3c | 181 | 174 | | | 178 | 5 | 3 |
| RA-SS3d | 234 | 233 | | | 233 | 1 | 0 |
| RB-SS1 | 76 | 77 | 77 | 75 | 76 | 1 | 1 |
| YF-SS1a | 379 | 400 | | | 390 | 15 | 4 |
| YF-SS1b | 104 | 101 | 109 | 121 | 108 | 9 | 8 |
| YF-SS1c | 93 | 101 | | | 97 | 6 | 6 |

**Table A.9. cont.**

| | Sample | | Duplicate | | | | |
|---|---|---|---|---|---|---|---|
| **Bromine** | **Repeat 1** | **Repeat 2** | **Repeat 1** | **Repeat 2** | **Average** | **Std Dev** | **Precision (%)** |
| BA-WP1 | 1148035 | 843129 | | | 995582 | 215601 | 22 |
| BA-WP2 | 213861 | 214236 | 215695 | 220470 | 216066 | 3041 | 1 |
| BA-WS1 | 694522 | 694014 | | | 694268 | 359 | 0.05 |
| BB-WB1 | 30142 | 30054 | 30328 | 30798 | 30330 | 332 | 1 |
| BB-WP1 | 198033 | 202880 | 266455 | 265417 | 233196 | 37859 | 16 |
| BB-WR1 | 39098 | 39600 | 39830 | 39082 | 39402 | 373 | 1 |
| DV-WB1 | 52311 | 51166 | 57441 | 48357 | 52319 | 3797 | 7 |
| DV-WP1 | 43766 | 43801 | | | 43783 | 25 | 0 |
| KP-WP1 | 421576 | 420017 | 526767 | 437637 | 451499 | 50807 | 11 |
| OT-WR1 | 9463 | 9340 | | | 9402 | 87 | 1 |
| RA-WB1 | 399027 | 387792 | | | 393410 | 7944 | 2 |
| RA-WP1 | 235831 | 236968 | 256130 | 222080 | 237752 | 13996 | 6 |
| RB-WP1 | 1813 | 1709 | 1744 | 1655 | 1730 | 66 | 4 |
| RP-WB1 | 40514 | 41260 | | | 40887 | 527 | 1 |
| RP-WP1 | 135573 | 137899 | 136052 | 131178 | 135175 | 2848 | 2 |
| SK-WB1 | 21874 | 21705 | 22454 | 22588 | 22155 | 432 | 2 |
| SK-WP1 | 102351 | 99405 | 100853 | 103280 | 101472 | 1703 | 2 |
| YF-OT1 | 154 | 133 | | | 143 | 15 | 11 |
| YF-WB1 | 168931 | 141624 | 141647 | 144047 | 149062 | 13294 | 9 |
| YF-WB2 | 137057 | 140484 | | | 138770 | 2423 | 2 |
| YF-WP1 | 224310 | 227560 | | | 225935 | 2298 | 1 |
| ZA-WG1 | 10767 | 11045 | | | 10906 | 196 | 2 |
| ZA-WP1 | 219916 | 218601 | | | 219259 | 930 | 0.4 |
| ZA-WR1 | 23759 | 23514 | | | 23637 | 173 | 1 |
| ZA-WS1 | 63134 | 54439 | 57999 | 59826 | 58850 | 3628 | 6 |
| ZB-WP1 | 281712 | 282183 | | | 281948 | 333 | 0.1 |
| ZB-WS1 | 4544 | 4584 | 4590 | 4681 | 4600 | 58 | 1 |
| DV-SS1a | 21187 | 21064 | | | 21125 | 87 | 0.4 |
| DV-SS1b | 25727 | 25655 | | | 25691 | 51 | 0.2 |
| DV-SS2 | 69063 | 68016 | | | 68540 | 741 | 1 |
| KV-SS1b | 3548 | 3556 | 4317 | | 3807 | 441 | 12 |
| RA-SS1a | 1895881 | 1657321 | | | 1776601 | 168687 | 9 |
| RA-SS1b | 1067739 | 1009265 | | | 1038502 | 41348 | 4 |
| RA-SSb IW | 899712 | 734869 | | | 817290 | 116562 | 14 |
| RA-SS3b | 277537 | 270524 | | | 274031 | 4959 | 2 |
| RA-SS3c | 211648 | 209361 | | | 210504 | 1617 | 1 |
| RA-SS3d | 359309 | 360997 | | | 360153 | 1193 | 0.3 |
| RB-SS1 | 3612 | 3673 | 3647 | 3675 | 3652 | 30 | 1 |
| YF-SS1a | 205089 | 209026 | | | 207058 | 2783 | 1 |
| YF-SS1b | 151704 | 148398 | 160841 | 162230 | 155793 | 6790 | 4 |
| YF-SS1c | 113828 | 113712 | | | 113770 | 82 | 0.07 |

**Table A.9. cont.**

| | Sample | | Duplicate | | | | |
|---|---|---|---|---|---|---|---|
| **Selenium** | **Repeat 1** | **Repeat 2** | **Repeat 1** | **Repeat 2** | **Average** | **Std Dev** | **Precision (%)** |
| BA-WP1 | 4552 | 3098 | | | 3825 | 1028 | 27 |
| BA-WP2 | 819 | 835 | 787 | 728 | 792 | 47 | 6 |
| BA-WS1 | 2653 | 2841 | | | 2747 | 133 | 5 |
| BB-WB1 | 105 | 103 | 111 | 101 | 105 | 4 | 4 |
| BB-WP1 | 725 | 689 | 990 | 853 | 814 | 137 | 17 |
| BB-WR1 | 127 | 136 | 140 | 152 | 139 | 11 | 8 |
| DV-WB1 | 195 | 182 | 216 | 194 | 197 | 14 | 7 |
| DV-WP1 | 145 | 168 | | | 156 | 16 | 10 |
| KP-WP1 | 1490 | 1433 | 1938 | 1696 | 1639 | 229 | 14 |
| OT-WR1 | 39 | 39 | | | 39 | 1 | 1 |
| RA-WB1 | 1426 | 1447 | | | 1436 | 15 | 1 |
| RA-WP1 | 745 | 786 | 736 | 690 | 739 | 39 | 5 |
| RB-WP1 | 1 | 9 | 12 | 9 | 8 | 5 | 58 |
| RP-WB1 | 132 | 128 | | | 130 | 2 | 2 |
| RP-WP1 | 450 | 435 | 466 | 429 | 445 | 17 | 4 |
| SK-WS1 | 62 | 76 | 73 | 78 | 72 | 7 | 10 |
| SK-WP1 | 353 | 323 | 388 | 365 | 357 | 27 | 8 |
| YF-WB1 | 619 | 506 | 486 | 511 | 530 | 60 | 11 |
| YF-WB2 | 452 | 438 | | | 445 | 9 | 2 |
| YF-WP1 | 680 | 741 | | | 710 | 43 | 6 |
| ZA-WS2 | 45 | 41 | | | 43 | 3 | 7 |
| ZA-WP1 | 685 | 670 | | | 677 | 10 | 1 |
| ZA-WR1 | 92 | 90 | | | 91 | 1 | 1 |
| ZA-WS1 | 239 | 208 | 179 | 182 | 202 | 28 | 14 |
| ZB-WP1 | 961 | 937 | | | 949 | 17 | 2 |
| ZB-WS1 | 54 | 42 | 59 | 59 | 54 | 8 | 15 |
| DV-SS1a | 89 | 100 | | | 94 | 8 | 9 |
| DV-SS1b | 101 | 106 | | | 103 | 3 | 3 |
| DV-SS2 | 266 | 246 | | | 256 | 14 | 6 |
| KV-SS1b | 14 | 17 | 22 | | 18 | 4 | 23 |
| RA-SS1a | 6155 | 5275 | | | 5715 | 623 | 11 |
| RA-SS1b | 3860 | 3404 | | | 3632 | 323 | 9 |
| RA-SS1b IW | 2752 | 2390 | | | 2571 | 256 | 10 |
| RA-SS3b | 967 | 848 | | | 907 | 85 | 9 |
| RA-SS3c | 805 | 695 | | | 750 | 77 | 10 |
| RA-SS3d | 1275 | 1229 | | | 1252 | 33 | 3 |
| RB-SS1 | 28 | 30 | 28 | 27 | 28 | 1 | 5 |
| YF-OT1 | 1 | 1 | | | 1 | 0 | 1 |
| YF-SS1a | 805 | 749 | | | 777 | 40 | 5 |
| YF-SS1b | 419 | 434 | 427 | 461 | 435 | 18 | 4 |
| YF-SS1c | 579 | 592 | | | 586 | 9 | 2 |

**Table A.9. cont.**

| | Sample | | Duplicate | | | | |
|---|---|---|---|---|---|---|---|
| **Rubidium** | **Repeat 1** | **Repeat 2** | **Repeat 1** | **Repeat 2** | **Average** | **Std Dev** | **Precision (%)** |
| BA-WP 1 | 801.0 | 584.4 | | | 693 | 153.2 | 22.1 |
| BA-WP 2 | 172.8 | 172.0 | 174.2 | 170.8 | 173 | 1.4 | 0.8 |
| BA-WS 1 | 490.7 | 481.0 | | | 486 | 6.9 | 1.4 |
| BB-WB 1 | 7.2 | 7.3 | 7.3 | 7.4 | 7 | 0.1 | 1.3 |
| BB-WP 1 | 88.1 | 80.8 | 77.2 | 73.1 | 80 | 6.4 | 8.0 |
| BB-WR 1A | 22.9 | 23.0 | 23.2 | 23.1 | 23 | 0.1 | 0.5 |
| DV-WB1 | 68.0 | 68.1 | 76.0 | 64.0 | 69 | 5.0 | 7.3 |
| DV-WP 1 | 34.8 | 34.4 | | | 35 | 0.2 | 0.7 |
| KP-WP 1A | 64.3 | 62.3 | 62.7 | 51.8 | 60 | 5.7 | 9.5 |
| OT-WR 1 | 28.0 | 28.0 | | | 28 | 0.0 | 0.0 |
| RA-WB 1 | 70.2 | 63.3 | | | 67 | 4.9 | 7.4 |
| RA-WP 1 | 30.3 | 28.7 | 31.2 | 28.6 | 30 | 1.3 | 4.3 |
| RB-WP 1B | 6.4 | 6.4 | 3.8 | 4.0 | 5 | 1.5 | 28.3 |
| RP-WB 1 | 83.1 | 82.9 | | | 83 | 0.1 | 0.1 |
| RP-WP 1A | 232.3 | 234.0 | 237.2 | 228.0 | 233 | 3.8 | 1.7 |
| SK-WB 1 | 11.7 | 11.7 | 11.5 | 11.6 | 12 | 0.1 | 0.9 |
| SK-WP 1 | 73.0 | 72.4 | 76.4 | 76.0 | 75 | 2.0 | 2.7 |
| YF-OT1 | 4.8 | 4.2 | | | 5 | 0.4 | 9.0 |
| YF-WB 1A | 215.5 | 182.5 | 180.1 | 181.0 | 190 | 17.2 | 9.1 |
| YF-WB 2 | 183.4 | 181.9 | | | 183 | 1.1 | 0.6 |
| YF-WP1 | 276.3 | 286.4 | | | 281 | 7.1 | 2.5 |
| ZA-WG 1 | 30.6 | 30.7 | | | 31 | 0.1 | 0.2 |
| ZA-WP 1 | 96.1 | 92.1 | | | 94 | 2.8 | 3.0 |
| ZA-WR 1 | 21.1 | 21.3 | | | 21 | 0.1 | 0.6 |
| ZA-WS 1 | 30.9 | 26.9 | 27.4 | 27.6 | 28 | 1.8 | 6.5 |
| ZB-WP 1 | 145.5 | 141.7 | | | 144 | 2.7 | 1.9 |
| ZB-WS 1 | 2.4 | 2.5 | 2.6 | 2.8 | 3 | 0.2 | 6.9 |
| DV-SS1A | 33.6 | 34.7 | | | 34 | 0.8 | 2.3 |
| DV-SS1B | 37.9 | 38.2 | | | 38 | 0.2 | 0.6 |
| DV-SS2 | 66.8 | 64.1 | | | 66 | 1.9 | 2.9 |
| KV-SS1B | 3.8 | 3.8 | 5.4 | | 4 | 0.9 | 21.6 |
| RA-SS1A | 344.7 | 302.4 | | | 324 | 29.9 | 9.3 |
| RA-SS1B | 175.5 | 160.5 | | | 168 | 10.6 | 6.3 |
| RA-SS1B IW | 115.6 | 94.3 | | | 105 | 15.1 | 14.4 |
| RA-SS3B | 74.5 | 75.5 | | | 75 | 0.7 | 0.9 |
| RA-SS3C | 42.1 | 43.6 | | | 43 | 1.1 | 2.5 |
| RA-SS3D | 28.2 | 27.8 | | | 28 | 0.3 | 1.1 |
| RB-SS1 | 3.6 | 3.7 | 4.5 | 4.3 | 4 | 0.4 | 10.6 |
| YF-SS1A | 208.6 | 209.6 | | | 209 | 0.7 | 0.3 |
| YF-SS1B | 150.0 | 145.0 | 155.8 | 151.2 | 151 | 4.4 | 2.9 |
| YF-SS1C | 156.0 | 157.1 | | | 157 | 0.8 | 0.5 |

**Table A.9. cont.**

| | Sample | | Duplicate | | | | |
|---|---|---|---|---|---|---|---|
| **Strontium** | **Repeat 1** | **Repeat 2** | **Repeat 1** | **Repeat 2** | **Average** | **Std Dev** | **Precision (%)** |
| BA-WP1 | 9627 | 6925 | | | 8276 | 1910.9 | 23.1 |
| BA-WP2 | 6984 | 7123 | 7150 | 6972 | 7057 | 92.6 | 1.3 |
| BA-WS1 | 6190 | 6172 | | | 6181 | 12.8 | 0.2 |
| BB-WB1 | 6104 | 6262 | 6223 | 6021 | 6152 | 110.4 | 1.8 |
| BB-WP1 | 23665 | 23958 | 30985 | 31565 | 27543 | 4317.5 | 15.7 |
| BB-WR1 | 4452 | 4281 | 4547 | 4470 | 4438 | 112.3 | 2.5 |
| DV-WB1 | 10159 | 9966 | 11192 | 9301 | 10154 | 783.1 | 7.7 |
| DV-WP1 | 10179 | 10394 | | | 10286 | 152.0 | 1.5 |
| KP-WP1 | 17082 | 17391 | 21139 | 17617 | 18307 | 1900.3 | 10.4 |
| OT-WR1 | 2510 | 2486 | | | 2499 | 17.2 | 0.7 |
| RA-WB1 | 26959 | 26657 | | | 26808 | 213.8 | 0.8 |
| RA-WP1 | 20097 | 19730 | 20589 | 17531 | 19487 | 1350.6 | 6.9 |
| RB-WP1 | 72 | 71 | 69 | 71 | 71 | 1.4 | 2.0 |
| RP-WB1 | 9358 | 8948 | | | 9153 | 290.2 | 3.2 |
| RP-WP1 | 30701 | 30036 | 31503 | 30622 | 30716 | 603.2 | 2.0 |
| SK-WB1 | 5154 | 5143 | 5365 | 5191 | 5213 | 103.2 | 2.0 |
| SK-WP1 | 15480 | 15341 | 15209 | 15008 | 15259 | 200.6 | 1.3 |
| YF-OT1 | 35 | 31 | | | 33 | 3.1 | 9.3 |
| YF-WB1 | 27837 | 23440 | 24279 | 24678 | 25056 | 1922.7 | 7.7 |
| YF-WB2 | 16645 | 16168 | | | 16409 | 337.4 | 2.1 |
| YF-WP1 | 37399 | 37547 | | | 37473 | 104.6 | 0.3 |
| ZA-WS2 | 2304 | 2217 | | | 2261 | 61.8 | 2.7 |
| ZA-WP1 | 25122 | 25827 | | | 25476 | 498.3 | 2.0 |
| ZA-WR1 | 4277 | 4303 | | | 4290 | 18.1 | 0.4 |
| ZA-WS1 | 11213 | 9857 | 10617 | 10387 | 10519 | 561.8 | 5.3 |
| ZB-WP1 | 28162 | 28463 | | | 28313 | 212.5 | 0.8 |
| ZB-WS1 | 1111 | 1078 | 1079 | 1079 | 1089 | 16.4 | 1.5 |
| DV-SS1a | 3694 | 3698 | | | 3696 | 2.6 | 0.1 |
| DV-SSb | 4288 | 4318 | | | 4303 | 21.6 | 0.5 |
| DV-SS2 | 13645 | 13389 | | | 13517 | 180.6 | 1.3 |
| KV-SS1b | 505 | 501 | 825 | | 610 | 185.7 | 30.4 |
| RA-SS1a | 5340 | 4468 | | | 4904 | 616.7 | 12.6 |
| RA-SS1b | 8870 | 8228 | | | 8549 | 454.5 | 5.3 |
| RA-SSb IW | 11369 | 8786 | | | 10078 | 1827.0 | 18.1 |
| RA-SS3b | 13724 | 13172 | | | 13448 | 390.0 | 2.9 |
| RA-SS3c | 12226 | 12112 | | | 12169 | 80.7 | 0.7 |
| RA-SS3d | 23134 | 22876 | | | 23005 | 182.5 | 0.8 |
| RB-SS1 | 78 | 79 | 98 | 97 | 88 | 10.8 | 12.4 |
| YF-SS1a | 36769 | 37319 | | | 37044 | 389.3 | 1.1 |
| YF-SS1b | 26741 | 26108 | 27421 | 27366 | 26909 | 616.6 | 2.3 |
| YF-SS1c | 22905 | 22954 | | | 22930 | 34.9 | 0.2 |

**Table A.9. cont.**

| | Sample | | Duplicate | | | | |
|---|---|---|---|---|---|---|---|
| **Barium** | **Repeat 1** | **Repeat 2** | **Repeat 1** | **Repeat 2** | **Average** | **Std Dev** | **Precision (%)** |
| BA-WP1 | 331 | 206 | | | 269 | 89.0 | 33.2 |
| BA-WS1 | 140 | 117 | | | 129 | 15.8 | 12.3 |
| BB-WB1 | 137 | 138 | 83 | 81 | 110 | 32.1 | 29.3 |
| BB-WP1 | 643 | 604 | 561 | 540 | 587 | 46.1 | 7.9 |
| BB-WR1 | 336 | 342 | 254 | 239 | 293 | 53.6 | 18.3 |
| DV-WB1 | 266 | 252 | 294 | 233 | 261 | 25.8 | 9.9 |
| DV-WP1 | 171 | 168 | | | 169 | 1.8 | 1.1 |
| KP-WP1 | 559 | 554 | 349 | 258 | 430 | 151.0 | 35.1 |
| OT-WR1 | 79 | 75 | | | 77 | 2.8 | 3.7 |
| RA-WB1 | 594 | 548 | | | 571 | 33.2 | 5.8 |
| RA-WP1 | 145 | 134 | | | 140 | 8.2 | 5.9 |
| RB-WP1 | 292 | 283 | 327 | 336 | 309 | 26.0 | 8.4 |
| RP-WB1 | 25 | 25 | | | 25 | 0.2 | 0.7 |
| RP-WP1 | 49 | 48 | 12 | 9 | 30 | 22.1 | 74.5 |
| SK-WB1 | 350 | 343 | 343 | 342 | 345 | 3.8 | 1.1 |
| SK-WP1 | 148 | 142 | 157 | 148 | 149 | 6.1 | 4.1 |
| YF-OT1 | 8 | 6 | | | 7 | 1.0 | 14.5 |
| YF-WB1 | 139 | 107 | 160 | 156 | 141 | 24.1 | 17.2 |
| YF-WB2 | 113 | 113 | | | 113 | 0.4 | 0.4 |
| YF-WP1 | 28 | 30 | | | 29 | 1.6 | 5.6 |
| ZA-WS2 | 61 | 61 | | | 61 | 0.1 | 0.2 |
| ZA-WP1 | 109 | 101 | | | 105 | 5.7 | 5.4 |
| ZA-WR1 | 138 | 128 | | | 133 | 7.0 | 5.3 |
| ZA-WS1 | 179 | 142 | 180 | 179 | 170 | 18.7 | 11.0 |
| ZB-WP1 | 930 | 945 | | | 938 | 10.4 | 1.1 |
| ZB-WS1 | 52 | 54 | 69 | 67 | 61 | 8.7 | 14.4 |
| DV-SS1a | 60 | 58 | | | 60 | 1.1 | 1.9 |
| DV-SS1b | 139 | 134 | | | 137 | 3.2 | 2.4 |
| DV-SS2 | 131 | 128 | | | 130 | 2.2 | 1.7 |
| KV-SS1b | 131 | 125 | 135 | | 130 | 5.1 | 3.9 |
| RA-SSb IW | 348 | 306 | | | 327 | 29.6 | 9.1 |
| RA-SS3b | 499 | 497 | | | 498 | 1.1 | 0.2 |
| RA-SS3c | 154 | 151 | | | 153 | 1.9 | 1.2 |
| RA-SS3d | 295 | 294 | | | 294 | 0.7 | 0.3 |
| RB-SS1 | 33 | 31 | 42 | 42 | 37 | 5.5 | 15.0 |
| YF-SS1a | 204 | 210 | | | 207 | 4.4 | 2.1 |
| YF-SS1b | 141 | 143 | 197 | 202 | 171 | 32.9 | 19.2 |
| YF-SS1c | 243 | 249 | | | 246 | 4.7 | 1.9 |

**Table A.9. cont.**

| | Sample | | Duplicate | | | | |
|---|---|---|---|---|---|---|---|
| **Uranium** | **Repeat 1** | **Repeat 2** | **Repeat 1** | **Repeat 2** | **Average** | **Std Dev** | **Precision (%)** |
| BA-WP1 | 42 | 29 | | | 35.9 | 9.0 | 25.2 |
| BA-WP2 | 23 | 24 | 23 | 25 | 23.6 | 0.8 | 3.4 |
| BA-WS1 | 29 | 28 | | | 28.6 | 0.4 | 1.3 |
| BB-WB1 | 14 | 14 | 14 | 14 | 14.1 | 0.2 | 1.6 |
| BB-WP1 | 5 | 5 | 5 | 5 | 5.0 | 0.2 | 4.5 |
| BB-WR1 | 11 | 11 | 11 | 11 | 11.2 | 0.2 | 1.8 |
| DV-WB1 | 130 | 129 | 145 | 118 | 130.7 | 11.2 | 8.6 |
| DV-WP1 | 56 | 56 | | | 55.7 | 0.2 | 0.3 |
| KP-WP1 | 16 | 16 | 20 | 16 | 16.9 | 1.8 | 10.8 |
| OT-WR1 | 5 | 5 | | | 4.8 | 0.0 | 0.9 |
| RA-WB1 | 9 | 10 | | | 9.7 | 0.5 | 4.7 |
| RA-WP1 | 2 | 2 | 2 | 2 | 2.0 | 0.3 | 13.7 |
| RB-WP1 | 3 | 3 | 2 | 2 | 2.5 | 0.1 | 5.2 |
| RP-WB1 | 12 | 13 | | | 12.3 | 0.5 | 4.3 |
| RP-WP1 | 10 | 10 | 10 | 10 | 10.1 | 0.3 | 2.6 |
| SK-WB1 | 3 | 3 | 2 | 3 | 2.5 | 0.1 | 3.1 |
| SK-WP1 | 19 | 19 | 20 | 20 | 19.4 | 0.7 | 3.5 |
| YF-OT1 | 0 | 0 | | | 0.0 | 0.0 | 11.0 |
| YF-WB1 | 3 | 2 | 2 | 2 | 2.2 | 0.3 | 13.6 |
| YF-WB2 | 1 | 1 | | | 1.0 | 0.0 | 1.1 |
| YF-WP1 | 13 | 13 | | | 13.1 | 0.5 | 3.5 |
| ZA-WS2 | 63 | 65 | | | 64.1 | 1.9 | 3.0 |
| ZA-WP1 | 55 | 54 | | | 54.7 | 0.8 | 1.4 |
| ZA-WR1 | 15 | 14 | | | 14.1 | 0.6 | 4.5 |
| ZA-WS1 | 185 | 153 | 155 | 159 | 162.9 | 14.8 | 9.1 |
| ZB-WP1 | 26 | 26 | | | 25.9 | 0.2 | 0.8 |
| ZB-WS1 | 30 | 31 | 32 | 33 | 31.6 | 1.6 | 4.9 |
| DV-SS1a | 44 | 44 | | | 44.1 | 0.3 | 0.7 |
| DV-SS1b | 10 | 10 | | | 10.4 | 0.0 | 0.2 |
| DV-SS2 | 197 | 185 | | | 190.7 | 8.6 | 4.5 |
| KV-SS1b | 8 | 8 | 6 | 6 | 6.8 | 1.0 | 14.6 |
| RA-SS1a | 1 | 1 | | | 1.2 | 0.2 | 17.0 |
| RA-SS1b | 2 | 2 | | | 2.4 | 0.0 | 0.8 |
| RA-SSb IW | 9 | 7 | | | 7.6 | 1.5 | 20.1 |
| RA-SS3b | 19 | 19 | | | 18.7 | 0.1 | 0.5 |
| RA-SS3c | 2 | 2 | | | 1.6 | 0.0 | 2.9 |
| RA-SS3d | 1 | 0 | | | 0.5 | 0.1 | 13.6 |
| RB-SS1 | 20 | 20 | 20 | 20 | 19.8 | 0.3 | 1.3 |
| YF-SS1A | 2 | 2 | | | 2.4 | 0.0 | 0.6 |
| YF-SS1B | 1 | 1 | 1 | 2 | 1.3 | 0.4 | 29.3 |
| YF-SS1C | 8 | 8 | | | 7.8 | 0.1 | 1.8 |

**Table A.9. cont.**

| | Sample | | Duplicate | | | | |
|---|---|---|---|---|---|---|---|
| **Silicon** | **Repeat 1** | **Repeat 2** | **Repeat 1** | **Repeat 2** | **Average** | **Std Dev** | **Precision (%)** |
| BA-WP1 | 14135 | 3264 | | | 8700 | 7687 | 88 |
| BA-WP2 | 5267 | 3320 | 5132 | 5226 | 4736 | 946 | 20 |
| BA-WS1 | 8826 | 4879 | | | 6853 | 2791 | 41 |
| BB-WB1 | 9917 | 9851 | 9688 | 9859 | 9829 | 98 | 1 |
| BB-WR1 | 2960 | 3087 | 3094 | 2805 | 2987 | 136 | 5 |
| KP-WP1 | 282 | 5719 | | | 3000 | 3845 | 128 |
| OT-WR1 | 9518 | 9140 | | | 9329 | 267 | 3 |
| RB-WP1 | 8596 | 8370 | 4519 | 4355 | 6460 | 2339 | 36 |
| RP-WB1 | 6582 | 7354 | | | 6968 | 546 | 8 |
| RP-WP1 | 24 | 2 | 42 | | 22 | 20 | 90 |
| SK-WB1 | 11657 | 10720 | 10340 | 10854 | 10893 | 554 | 5 |
| YF-OT1 | 3049 | 2465 | | | 2757 | 414 | 15 |
| YF-WB1 | 10399 | 10628 | 10260 | | 10429 | 185 | 2 |
| YF-WB2 | 8535 | 8742 | | | 8638 | 147 | 2 |
| ZA-WS2 | 14194 | 14990 | | | 14592 | 563 | 4 |
| ZA-WR1 | 7082 | 6425 | | | 6753 | 464 | 7 |
| ZA-WS1 | 4594 | 3194 | 3462 | 3268 | 3630 | 653 | 18 |
| ZB-WS1 | 5661 | 5913 | | | 5787 | 178 | 3 |
| DV-SS1a | 5715 | 5479 | | | 5597 | 166 | 3 |
| DV-SS1b | 6838 | 6649 | | | 6743 | 133 | 2 |
| DV-SS2 | 5808 | 5915 | | | 5862 | 76 | 1 |
| DV-WB1 | 6093 | 5784 | 7075 | 5183 | 6034 | 790 | 13 |
| KV-SS1b | 4727 | 4410 | 7083 | | 5407 | 1461 | 27 |
| RB-SS1 | 12472 | 11864 | 8507 | 9332 | 10544 | 1921 | 18 |
| YF-SS1b | 1305 | 766 | 1830 | 1421 | 1331 | 438 | 33 |

**Table A.10: Results for repeat analysis of the NIST-1643d standard**

| | Li | B | Al | Si | Fe | As | Se | Rb | Sr | Ba |
|---|---|---|---|---|---|---|---|---|---|---|
| **NIST-1643d** | 18.0 | 144.9 | 134.9 | 2881.3 | 119.5 | 59.1 | 11.8 | 12.7 | 308.6 | 553.6 |
| **NIST-1643d** | 17.8 | 143.2 | 131.4 | 2756.3 | 154.5 | 58.9 | 12.8 | 12.3 | 307.9 | 528.1 |
| **NIST-1643d** | 17.4 | 140.6 | 130.9 | 2691.2 | 55.0 | 57.6 | 11.1 | 12.3 | 312.8 | 539.2 |
| **NIST-1643d** | 17.2 | 138.4 | 131.0 | 2789.6 | | 59.3 | 12.1 | 12.4 | 303.5 | 534.1 |
| **NIST-1643d** | 17.4 | 135.0 | 131.1 | 2893.2 | 187.8 | 57.2 | 11.9 | 12.2 | 309.8 | 514.0 |
| **NIST-1643d** | 17.0 | 132.4 | 127.1 | 2819.0 | 166.3 | 57.1 | 11.7 | 12.1 | 302.8 | 515.4 |
| **NIST-1643d** | 17.1 | 136.1 | 131.9 | 2794.2 | 149.5 | 57.5 | 11.2 | 12.2 | 307.9 | 508.8 |
| **NIST-1643d** | 17.3 | 136.1 | 133.8 | 2794.2 | 103.5 | 56.8 | 11.6 | 12.3 | 305.4 | 529.7 |
| **Average** | 17.4 | 138.3 | 131.5 | 2802.4 | 133.7 | 57.9 | 11.8 | 12.3 | 307.4 | 527.9 |
| **Std dev** | 0.35 | 4.28 | 2.30 | 64.95 | 44.68 | 1.01 | 0.54 | 0.17 | 3.33 | 14.84 |
| **Certified** | 16.5 | 144.8 | 127.6 | 2700.0 | 91.2 | 56.0 | 11.4 | 13.0 | 294.8 | 506.5 |
| **Bias** | 0.9 | -6.5 | 3.9 | 102.4 | 42.5 | 1.9 | 0.3 | -0.7 | 12.6 | 21.4 |
| **% bias** | 5.4 | -4.5 | 3.1 | 3.8 | 46.6 | 3.4 | 3.0 | -5.3 | 4.3 | 4.2 |

### A.1.7. SILICA BY COLORIMETRY

Results for repeat analyses are given in Table A.11. Results from colorimetric analysis are compared with data from ICP-MS in Table A.12.

**Table A.11: Results for repeat analyses of samples for Si**

| Sample | Result (mg/kg) | Result (mg/kg) | Difference | Mean | Std. Dev | % RSD |
|---|---|---|---|---|---|---|
| BP2-WP2 | 4.12 | 4.11 | 0.0 | 4 | 0.0 | 0.2 |
| BP-WB1 | 6.69 | 7.81 | 1.1 | 7 | 0.8 | 10.9 |
| BP-WP1 | 0.19 | 0.18 | 0.0 | 0 | 0.0 | 3.8 |
| DV-WB1 | 4.58 | 4.54 | 0.0 | 5 | 0.0 | 0.6 |
| RA-WP1 | 0.15 | 0.16 | 0.0 | 0 | 0.0 | 3.6 |
| SK-WB1 | 8.93 | 7.12 | 1.8 | 8 | 1.3 | 15.9 |
| SK-WP1 | 0.04 | 0.06 | 0.0 | 0 | 0.0 | 32.1 |
| ZA-WS1 | 3.53 | 3.62 | 0.1 | 4 | 0.1 | 1.8 |
| BP-WR1 | 3.68 | 3.21 | 0.5 | 3 | 0.3 | 9.6 |
| KP-WP1 | 0.26 | 0.26 | 0.0 | 0 | 0.0 | 0.0 |
| RB-WP1 | 3.39 | 3.49 | 0.1 | 3 | 0.1 | 2.1 |
| RP-WP1 | 0.04 | 0.06 | 0.0 | 0 | 0.0 | 23.7 |
| YF-WB1 | 9.06 | 9.78 | 0.7 | 9 | 0.5 | 5.4 |

**Table A.12: Comparison between Si data determined by ICP-MS and colorimetry.**

| | ICP-MS (mg/kg) | Colorimetry (mg/kg) | Difference |
|---|---|---|---|
| BP2-WP1 | 7.57 | 3.73 | 3.83 |
| BP2-WP2 | 4.14 | 4.12 | 0.03 |
| BP2-WS1 | 6.14 | 3.92 | 2.22 |
| BP-WB1 | 9.73 | 7.25 | 2.48 |
| BP-WP1 | bdl | 0.19 | |
| BP-WR1 | 2.94 | 3.44 | -0.51 |
| DV-WB1 | 5.92 | 4.56 | 1.36 |
| DV-WP1 | 0.07 | 0.03 | 0.05 |
| KP-WP1 | 2.60 | 0.26 | 2.34 |
| OT-WR1 | 9.33 | 8.07 | 1.26 |
| RA-WB1 | 2.97 | 2.26 | 0.71 |
| RA-WP1 | bdl | 0.16 | |
| RB-WP1 | 6.46 | 3.44 | 3.02 |
| RP-WB1 | 6.90 | 4.71 | 2.19 |
| RP-WP1 | 0.03 | 0.05 | -0.02 |
| SK-WB1 | 10.79 | 8.02 | 2.76 |
| SK-WP1 | 0.30 | 0.05 | 0.25 |
| YF-WB1 | 10.75 | 9.42 | 1.32 |
| YF-WB2 | 8.37 | 19.03 | -10.66 |
| YF-WP1 | bdl | 0.49 | |
| ZA-WG1 | 14.59 | 15.73 | -1.14 |
| ZA-WP1 | bdl | 0.27 | |
| ZA-WR1 | 6.69 | 4.69 | 2.00 |
| ZA-WS1 | 3.56 | 3.57 | -0.01 |
| ZB-WB1 | 8.26 | 0.53 | 7.73 |
| ZB-WP1 | 0.47 | 0.13 | 0.34 |
| ZB-WS1 | 5.79 | 4.71 | 1.08 |
| | **Average difference** | | 0.98 |
| | **Mean** | | 4.94 |
| | **Bias (%)** | | 19.90 |

### A.1.8. STABLE ISOTOPES BY MASS SPECTROMETRY

The CTMP standard was run with each set of samples and used to correct for drift in the reference gases. A number of duplicate analyses were also completed, and the results are given in Table A.6.

**Table A.13: Repeat isotope analyses of water samples**

| Delta-18O | Result (mmol/kg) | Result (mmol/kg) | Difference | Mean | Std. Dev | % RSD |
|---|---|---|---|---|---|---|
| **BA-WP2** | -2.9 | -1.8 | -1.13 | -2.4 | 0.8 | -33.6 |
| **BB-WB1** | -3.9 | -2.9 | -0.92 | -3.4 | 0.7 | -19.1 |
| **BB-WP1** | -2.0 | -1.9 | -0.02 | -1.9 | 0.0 | -0.8 |
| **DV-WB1** | -2.9 | -2.9 | -0.06 | -2.9 | 0.0 | -1.5 |
| **RA-WP1** | -3.2 | -3.3 | 0.13 | -3.3 | 0.1 | -2.8 |
| **RP-WP1** | -0.5 | -0.5 | -0.02 | -0.5 | 0.0 | -2.8 |
| **SK-WB1** | -5.9 | -2.9 | -3.06 | -4.4 | 2.2 | -49.2 |
| **SK-WP1** | -2.0 | -1.9 | -0.04 | -1.9 | 0.0 | -1.5 |
| **ZA-WS1** | -1.8 | -1.6 | -0.20 | -1.7 | 0.1 | -8.5 |
| **RP-WP1** | -0.5 | -0.5 | -0.02 | -0.5 | 0.0 | -2.8 |

| Delta-D | Result (mmol/kg) | Result (mmol/kg) | Difference | Mean | Std. Dev | % RSD |
|---|---|---|---|---|---|---|
| **BA-WP2** | -6 | -12 | 6.00 | -9 | 4.2 | -47.8 |
| **BB-WB1** | -13 | -17 | 4.06 | -15 | 2.9 | -18.8 |
| **BB-WP1** | -13 | -13 | 0.40 | -13 | 0.3 | -2.2 |
| **DV-WB1** | -17 | -15 | 1.53 | -16 | 1.1 | -6.7 |
| **RA-WP1** | -24 | -23 | 1.37 | -23 | 1.0 | -4.1 |
| **SK-WB1** | -8 | -10 | 1.90 | -9 | 1.3 | -14.5 |
| **SK-WP1** | -4 | -4 | 0.66 | -4 | 0.5 | -11.8 |
| **ZA-WS1** | -10 | -0.60 | 9.37 | -5 | 6.6 | -125.4 |

## A.2. SEDIMENT ANALYSIS

### A.2.1. SOLUBLE SALTS

Because the preparation of a SPE is a subjective method, three pastes were prepared in duplicate and subjected to the same analyses to ensure that the data from the all the pastes could safely be compared. Results of the duplicate analyses for all the three pastes are given in Table A.14. Only a small amount of extract was obtained from sample RB-SS1 and there was insufficient to perform many of the analyses.

**Table A.14: Comparison of SPE prepared in duplicate**

| | Na | K | Mg | Ca | Cl | $SO_4$ | Hardness |
|---|---|---|---|---|---|---|---|
| **KV-SS1b-a1** | 24.8 | 0.7 | 3.6 | 4.9 | 27.2 | 1.6 | 2.8 |
| **KV-SS1b-a2** | 29.9 | 0.8 | 4.1 | 3.1 | 35.2 | 1.8 | 3.8 |
| **RSD (%)** | **13.1** | **9.4** | **9.3** | **30.8** | **18.1** | **8.2** | **22.3** |
| **RB-SS1-a1** | 53.4 | 0.8 | 1.2 | 4.0 | 34.1 | 2.4 | nd |
| **RB-SS1-a2** | 53.7 | 0.7 | 2.0 | 3.9 | 34.9 | 2.2 | nd |
| **RSD (%)** | **0.5** | **10.6** | **38.3** | **1.1** | **1.6** | **5.3** | nd |
| **YF-SS1b-a1** | 1184 | 17.9 | 156 | 143 | 1587 | 80 | 158 |
| **YF-SS1b-a2** | 1210 | 17.4 | 244 | 201 | 1561 | 77 | 157 |
| **RSD (%)** | **1.5** | **2.0** | **31.1** | **23.8** | **1.2** | **2.3** | **0.5** |

### A.2.2. ORGANIC CARBON

Three samples were analysed in duplicate. One was of the duplicates was unfortunately contaminated by soil and the results were discarded. Data for the remaining two are given in Table A.16.

**Table A.15: Duplicate analyses of organic carbon**

| OC (%) | Repeat 1 | Repeat 2 | Difference | Average | Stdev | RSD (%) |
|---|---|---|---|---|---|---|
| **RB-SS1** | 0.75 | 0.74 | 0.01 | 0.74 | 0.01 | 1.36 |
| **YF-SS1b** | 0.38 | 0.39 | 0.01 | 0.39 | 0.01 | 1.58 |

### A.2.3. SOIL PH

The pH of a soil is strongly influenced by the mode of measurement. The KCl extract is required to counteract the dilution effect, which gives a higher pH reading than expected. $K^+$ ions displace $H^+$ ions from cation exchange sites on clays into solution and give a more representative indication of the pH in the real soil solution (Rowell, 1998). Another source of error using water for measuring pH is the junction potential. This occurs when measuring the pH in colloidal solutions. If the solution contains no KCl, the potassium ions in the reference electrode are attracted to charged particles in suspension. The diffusion of $K^+$ and $Cl^-$ out of the electrode is unbalanced, creating a junction potential. If the particles are negatively charged, the apparent pH is lower than expected and the apparent pH is higher if the particles are positively charged (McBride, 1994). Three soils pH measurements were done in duplicate to verify the repeatability of the method. Results are given in Table A.17.

**Table A.16: Duplicate pH measurements**

| | | Repeat 1 | Repeat 2 | Difference | Average | Std dev | RSD (%) |
|---|---|---|---|---|---|---|---|
| KV-SS1b | pH | 8.22 | 8.20 | 0.02 | 8.21 | 0.01 | 0.17 |
| | pH ($H_2O$) | 8.79 | 8.81 | 0.02 | 8.80 | 0.01 | 0.16 |
| | pH (KCl) | 7.54 | 7.52 | 0.02 | 7.53 | 0.01 | 0.19 |
| RB-SS1 | pH | 8.96 | 8.99 | 0.03 | 8.98 | 0.02 | 0.24 |
| | pH ($H_2O$) | 9.66 | 9.79 | 0.13 | 9.73 | 0.09 | 0.95 |
| | pH (KCl) | 8.11 | 8.24 | 0.13 | 8.18 | 0.09 | 1.12 |
| YF-SS1b | pH | 7.39 | 7.39 | 0.00 | 7.39 | 0.00 | 0.00 |
| | pH ($H_2O$) | 7.87 | 7.88 | 0.01 | 7.88 | 0.01 | 0.09 |
| | pH (KCl) | 7.84 | 7.78 | 0.06 | 7.81 | 0.04 | 0.54 |

# B. XRD Scans

## B.1. BULK PAN SEDIMENT MINERALOGY

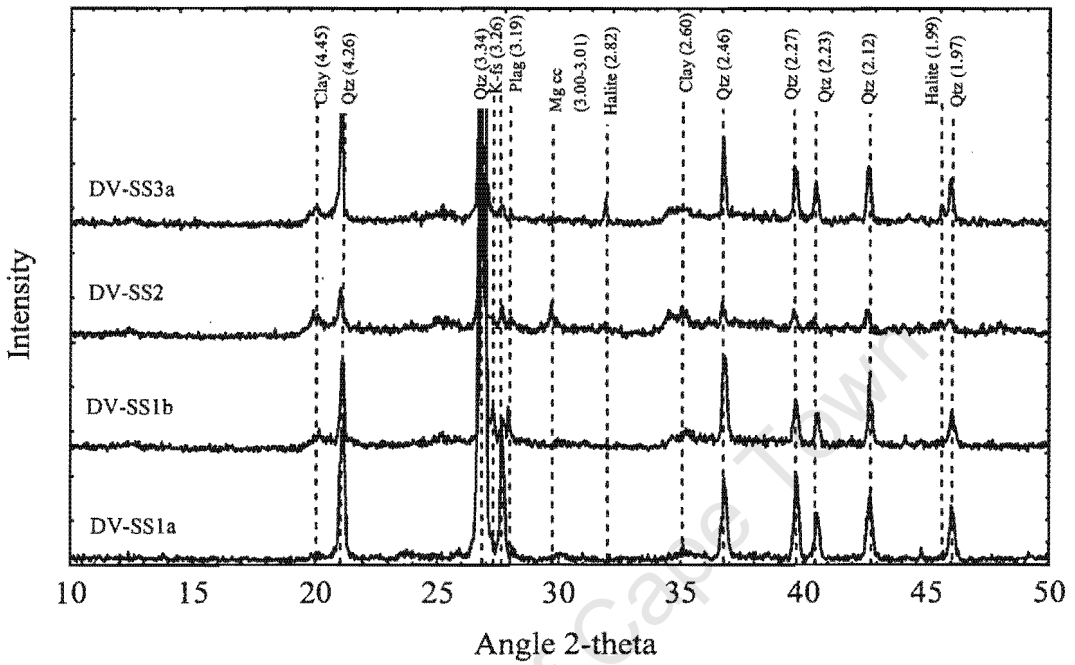


**Figure B.1: Bulk mineralogy XRD scan of samples from Droëvlei. (Qtz=quartz, K-fs = K-feldspar, Plag = plagioclase, Mg-cc = Mg calcite)**

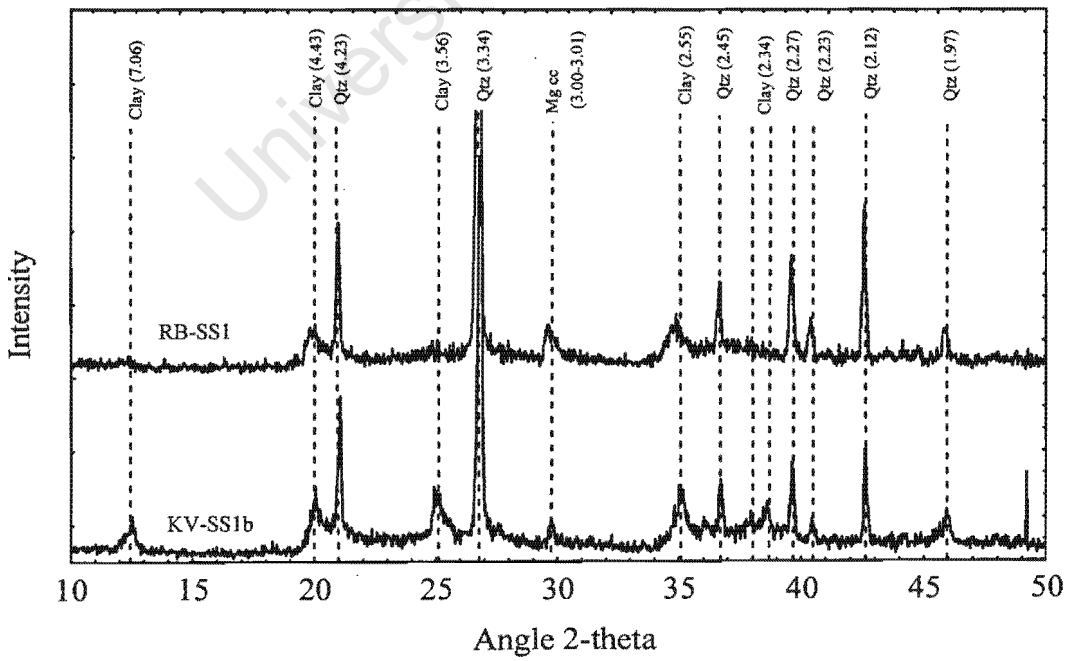


**Figure B.2: Bulk mineralogy XRD scan of samples from Rooipan north and Kiekoesvlei (Qtz = quartz, Mg-cc = Mg calcite)**

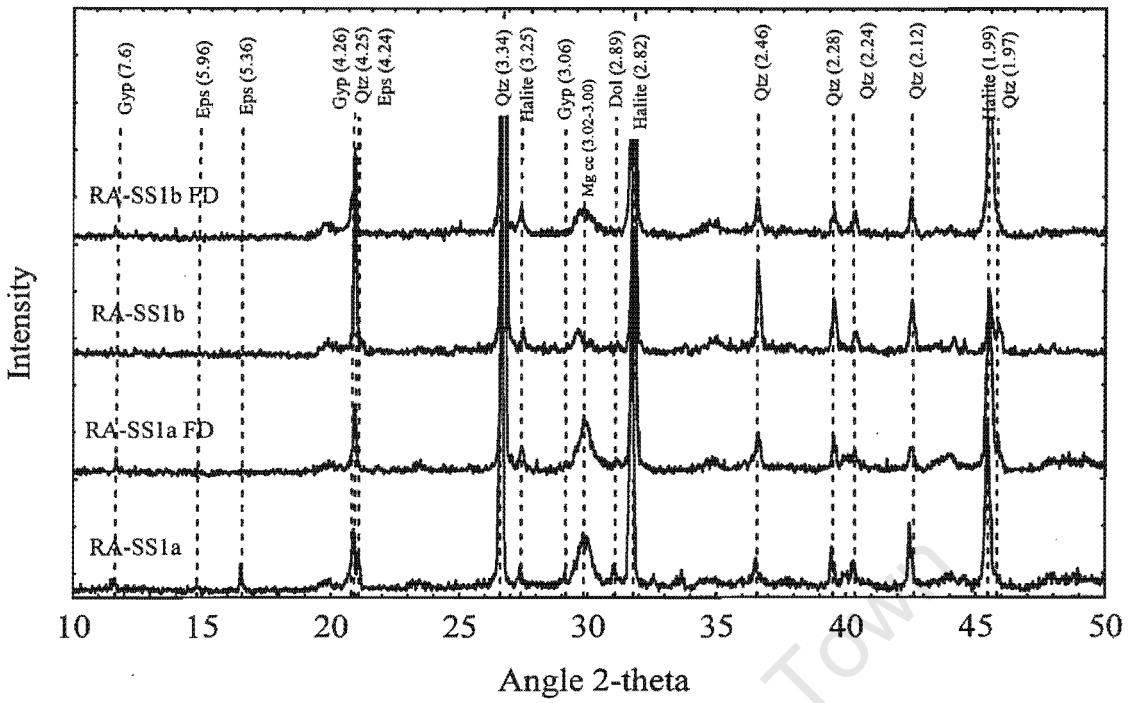


**Figure B.3: Bulk mineralogy XRD scans of pan floor samples from Rooipan south, air-dried and freeze-dried (FD = Freeze dried, Gyp = gypsum, Eps = epsomite, Qtz = quartz, Mg-cc = Mg calcite, Dol = dolomite)**

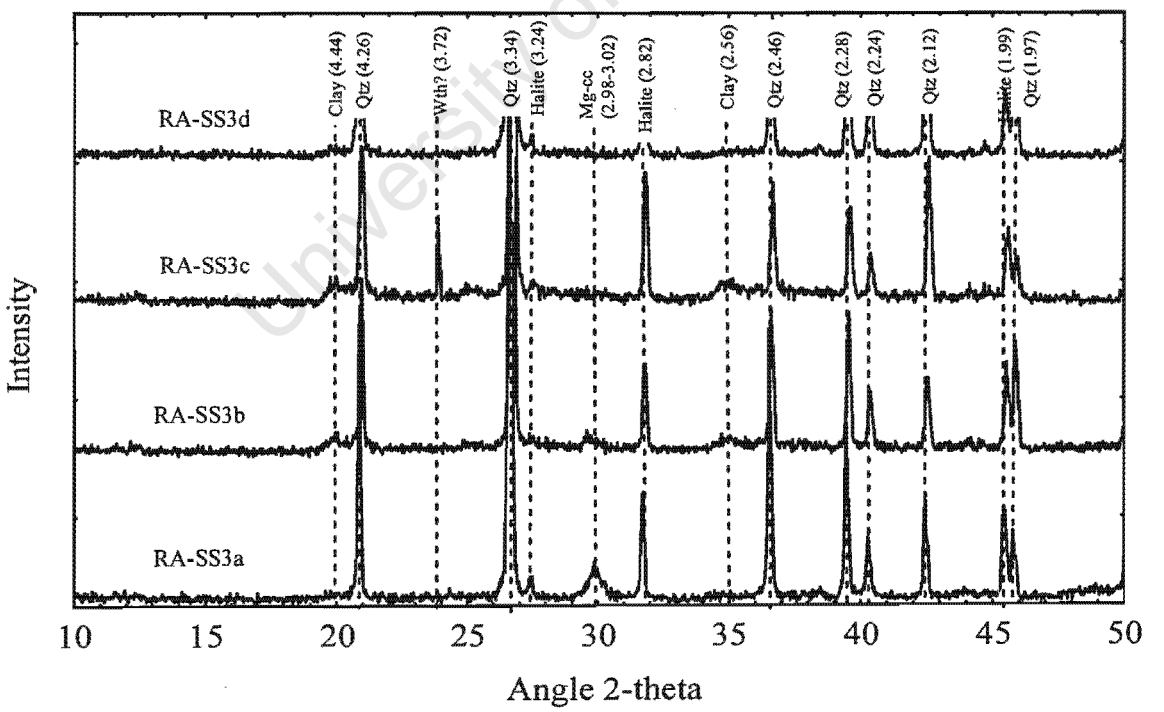


**Figure B.4: Bulk mineralogy XRD scans of samples from a pit dug adjacent to Rooipan south (Qtz = quartz, Wth = witherite, Mg-cc = Mg calcite)**

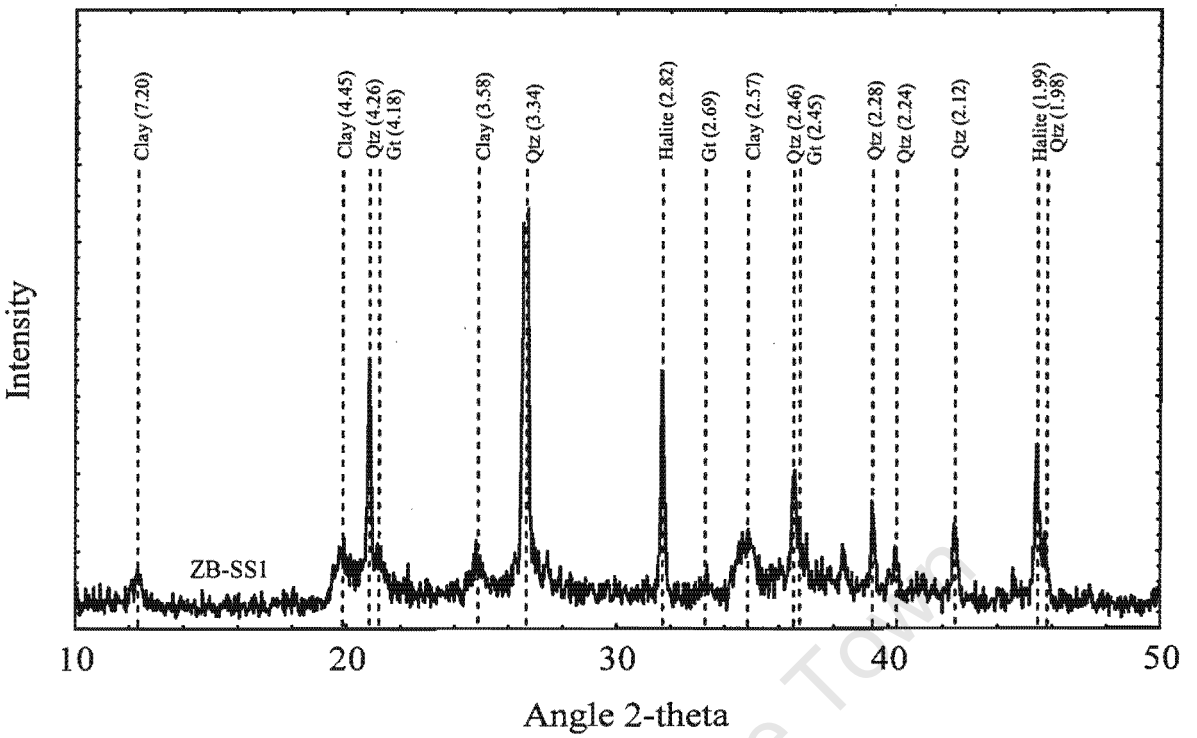


**Figure B.5: Bulk mineralogy of sample ZB-SS1 from adjacent to Zwartwater north (Qtz = quartz, Gt = goethite)**

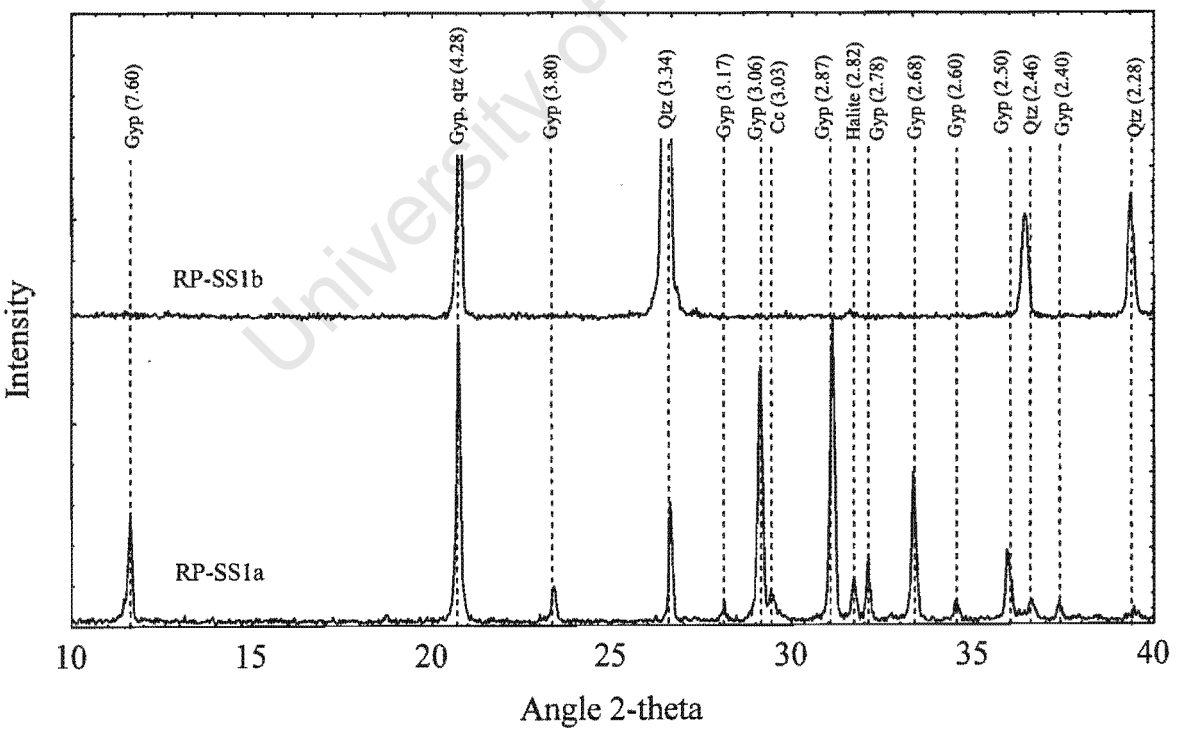


**Figure B.6: Bulk mineralogy of samples from coastal Rooipan (Gyp = gypsum, Qtz = quartz, Cc = calcite)**

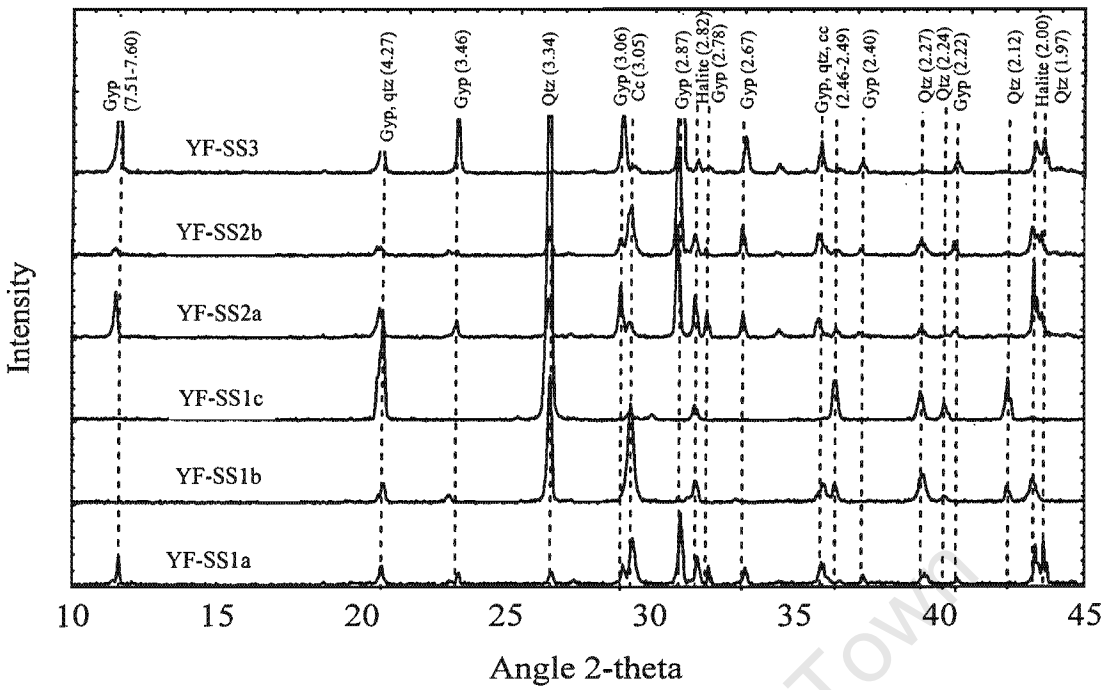


**Figure B.7: Bulk mineralogy XRD scan of samples from Ysterfontein pan (Gyp=gypsum, Qtz = quartz, Cc = calcite).**

## B.2. CLAY MINERALOGY

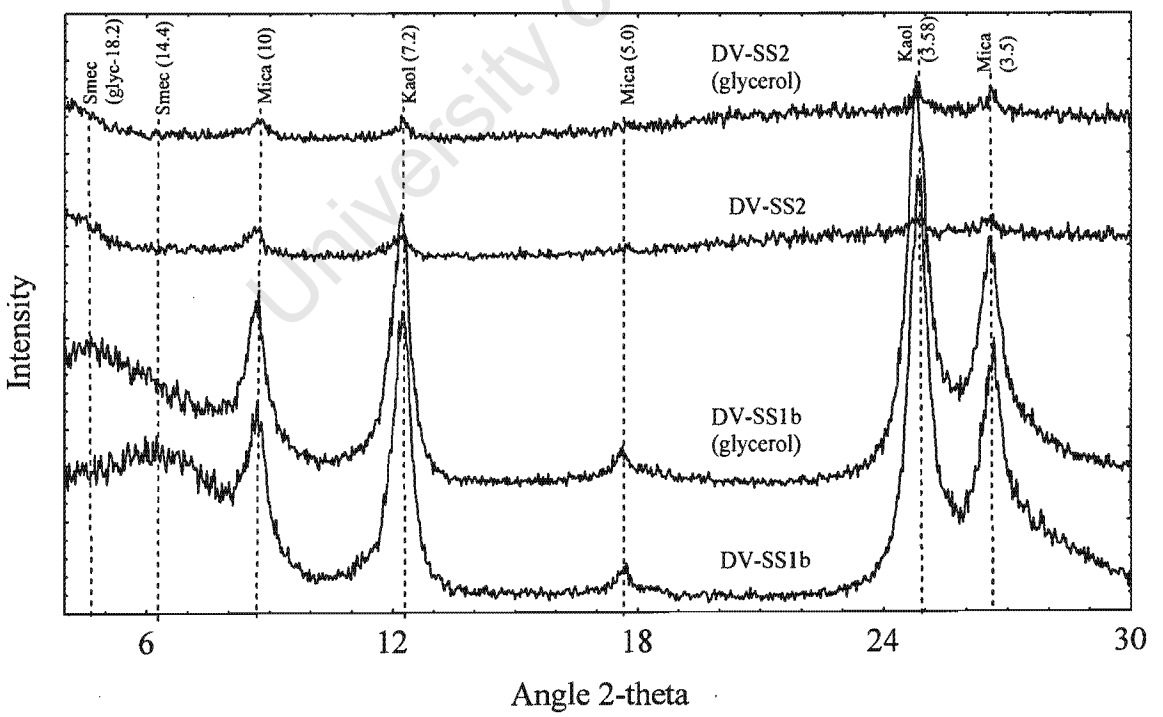


**Figure B.8: Clay XRD scan of samples from Droëvlei (Smec = smectite, glyc = glycerol, Kaol = kaolinite)**

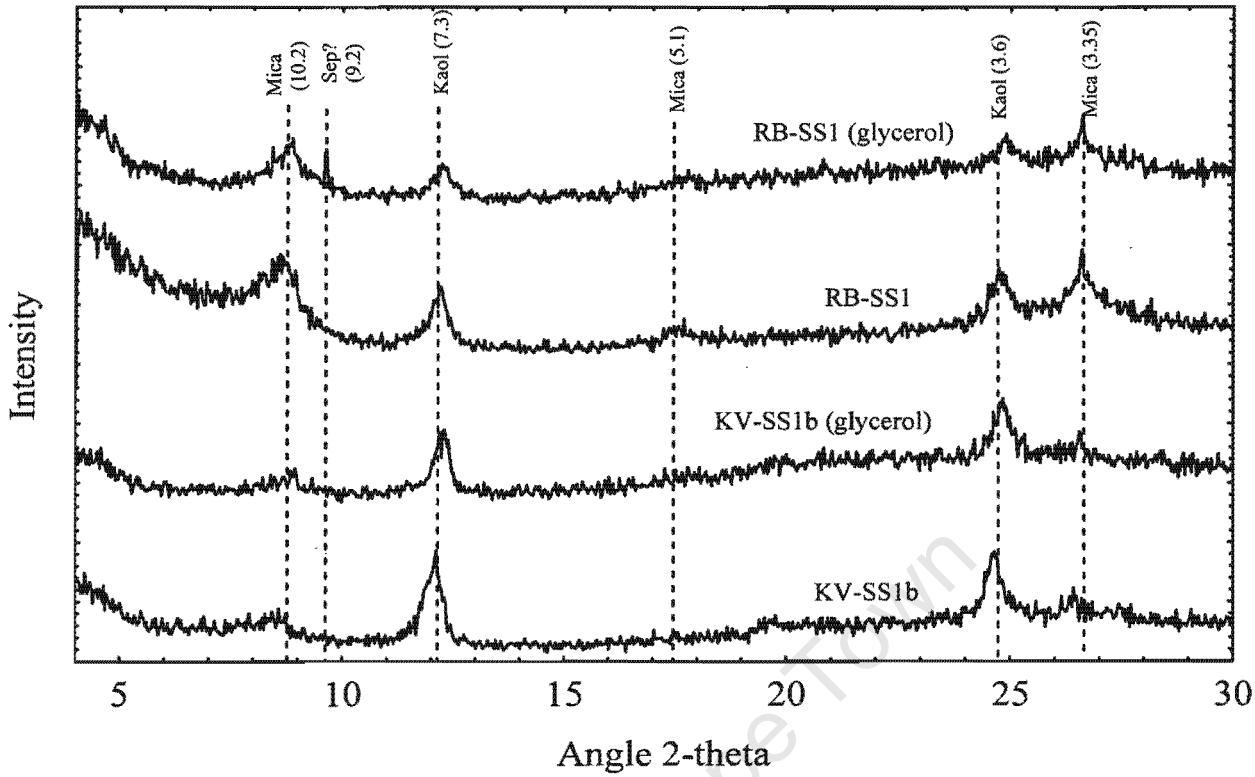


**Figure B.9: Clay XRD scan of samples from Rooipan north and Kiekoesvlei (Kaol = kaolinite; Sep = sepiolite)**

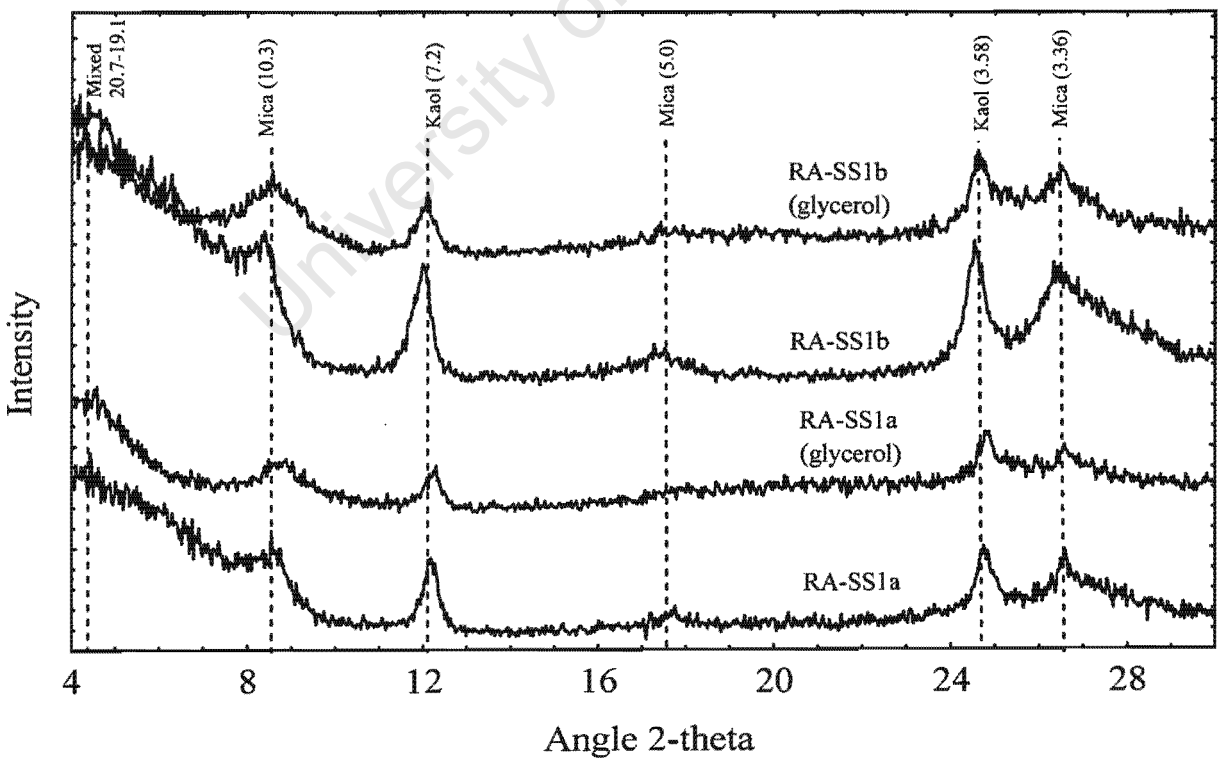


**Figure B.10: Clay XRD scans of subaqueous samples from Rooipan south (Mixed = randomly interstratified mica-smectite, Kaol = kaolinite)**

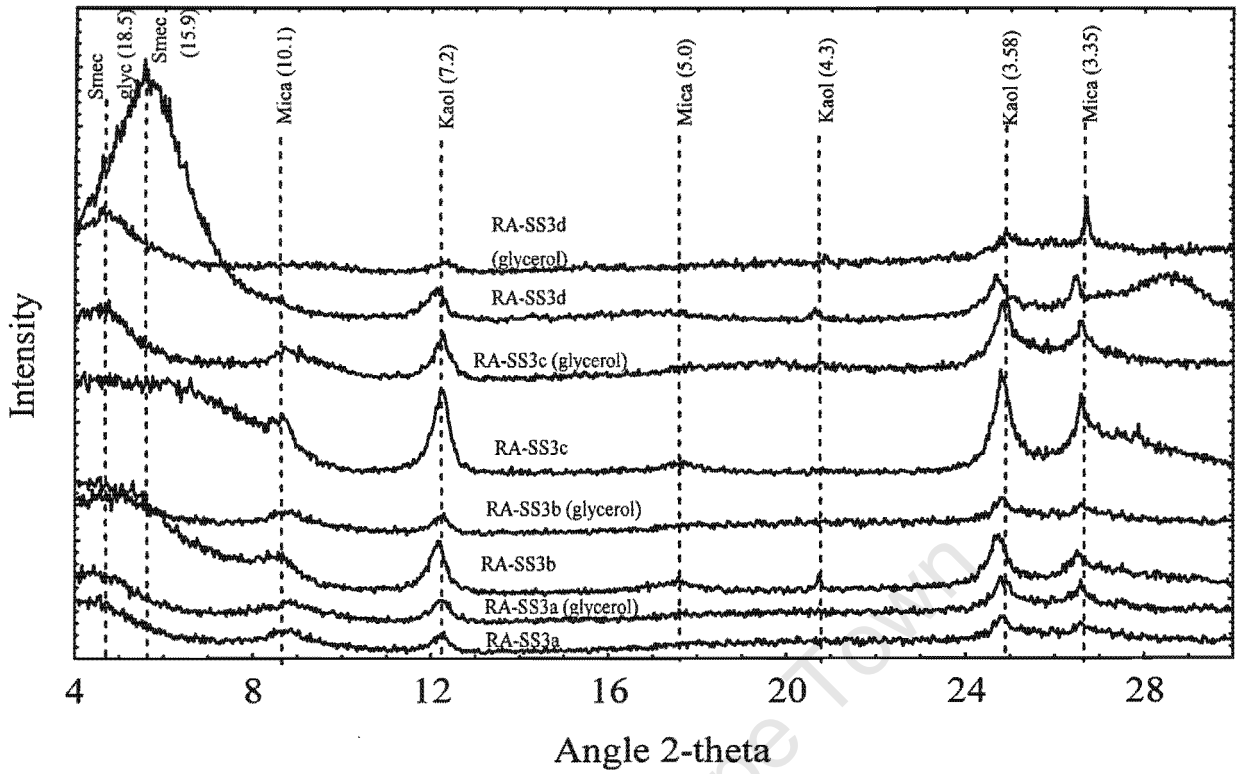


**Figure B.11: Clay XRD scans of samples from adjacent to Rooipan south (Smec = smectite, glyc = glycerol, Kaol = kaolinite)**

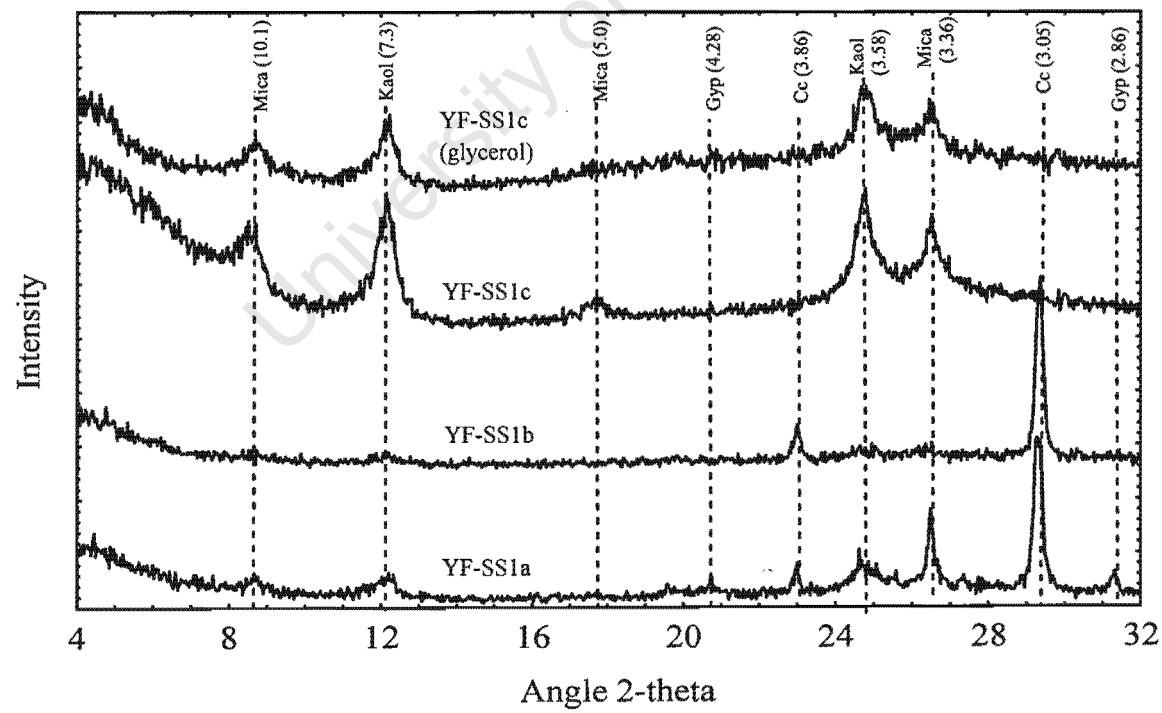


**Figure B.12: Clay XRD scan of samples from Ysterfontein pan (Kaol = kaolinite, Gyp = gypsum, Cc = calcite).**

## B.3. SECONDARY PRECIPITATE MINERALOGY

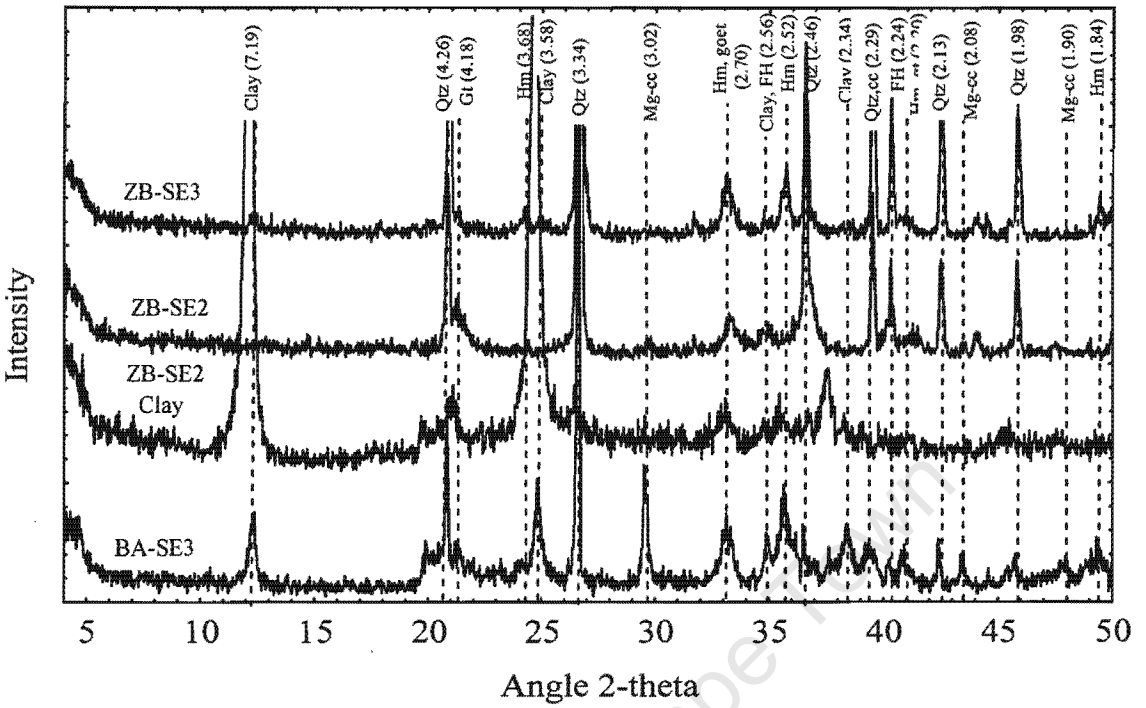


**Figure B.13: XRD scans of ferricrete samples (Qtz = quartz, Gt = goethite, Hm = haematite, Mg-cc = Mg calcite, FH = ferrihydrite).**

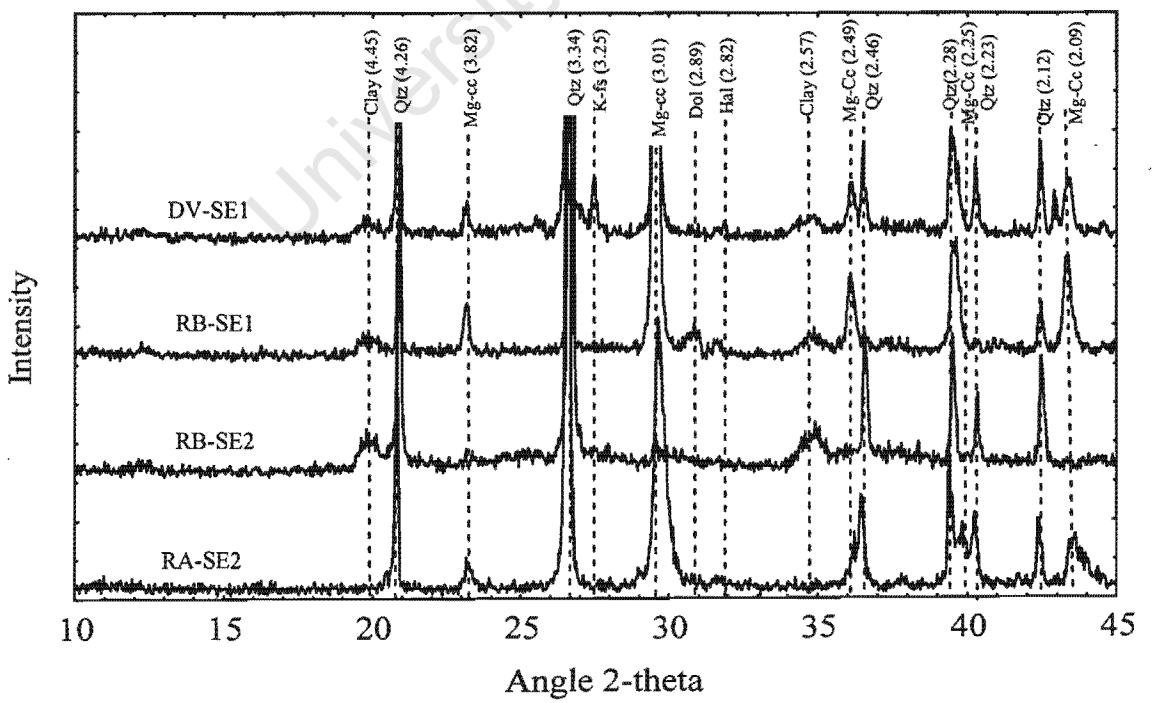


**Figure B.14: XRD scans of calcrete samples (Qtz = quartz, Mg-cc = high-Mg calcite, K-fs = K-feldspar, Dol = dolomite, Hal = halite).**

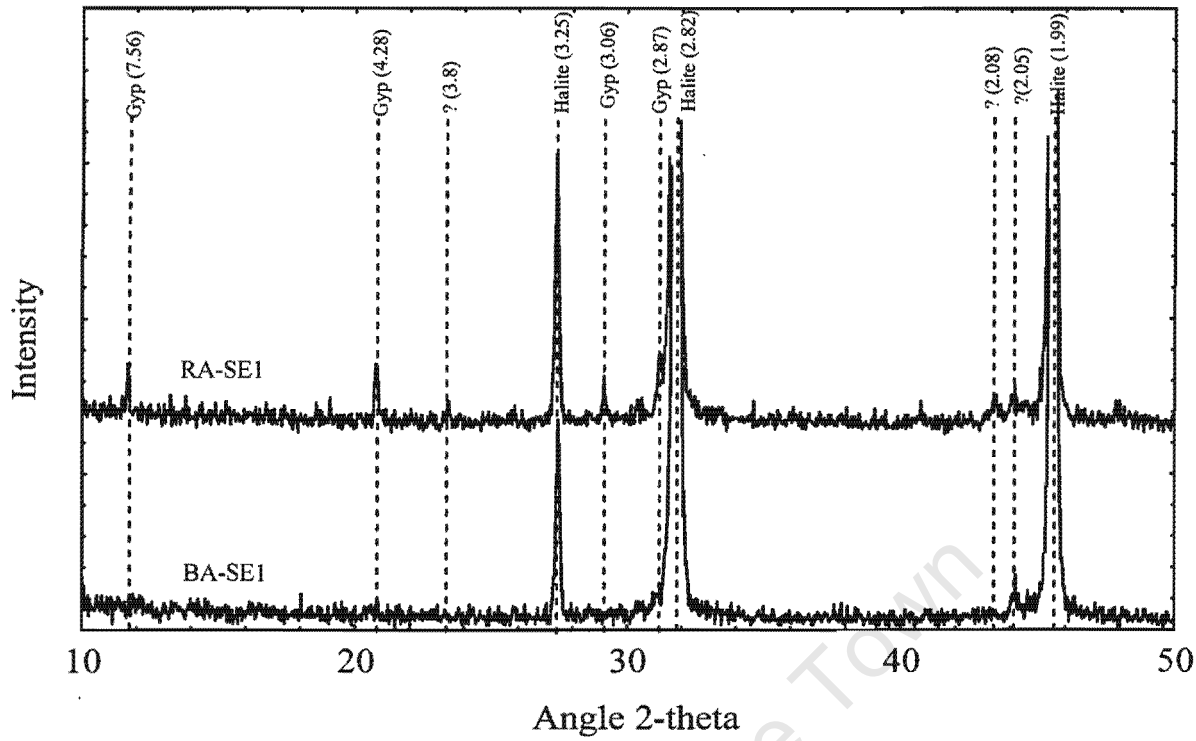


**Figure B.15: XRD scan of halite from two pans (Gyp = gypsum)**

## B.4. MINERALOGY OF SALTS FROM TDS

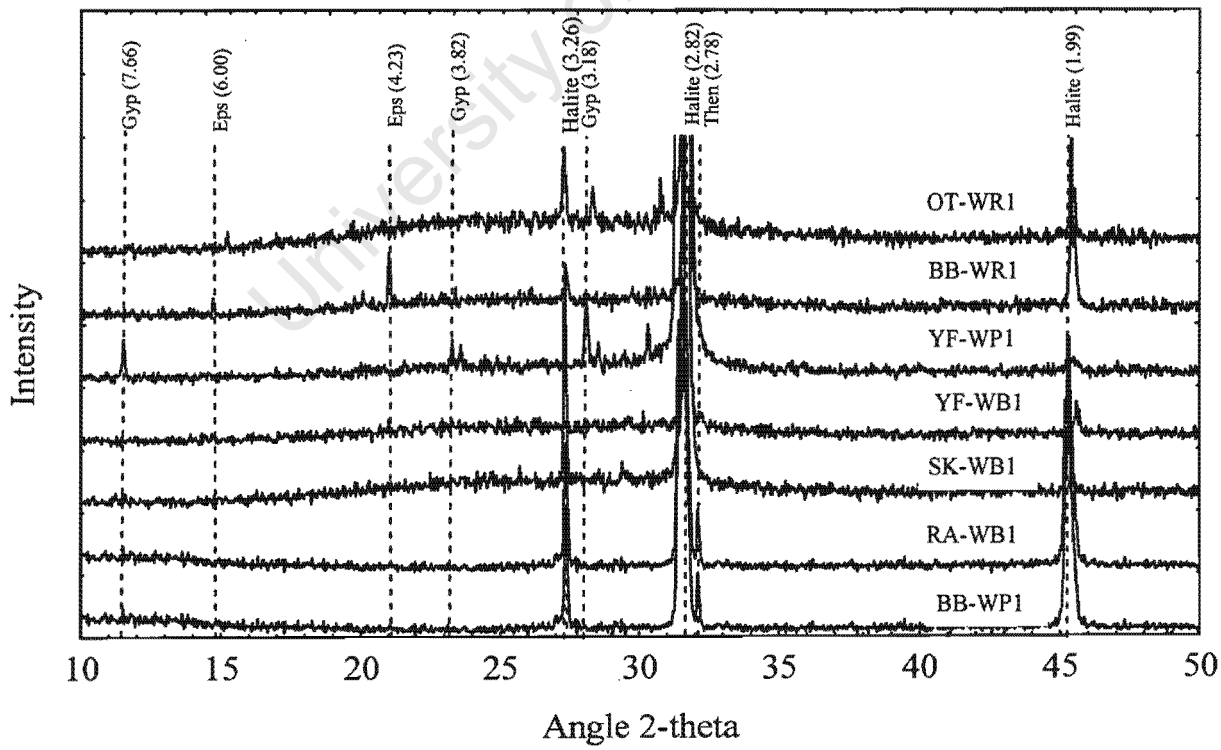


**Figure B.16: XRD scan of salts from drying water samples (Gyp = gypsum, Eps = epsomite, Then = thenardite)**

# C. Modelling

## C.1. OBTAINING PHRQPITZ

PHRQPITZ can be downloaded from the USGS website at the following URL:
http://water.usgs.gov/software/phrqpitz.html
Unfortunately the manual is not available for download, but part of the PHRQPITZ software is an application called PITZNPT.exe which allows easy creation of input files for PHRQPITZ. The following section explains the various options available for modelling.

## C.2. CREATING AN INPUT FILE IN PITZNPT

*Startup and options*
Run PITZNPT from Windows Explorer. The program offers a number of options for data input. It is best to read through the following questions and decide which options are appropriate before running the program, as there is no way to "undo" and the program has to be rerun from the beginning. Italics indicate text shown by the program.

*Name of PHRQNPT database file? Default: pitzinpt.dat*
Unless there is a reason to change the database file, hit return.
*Name of PHRQPITZ database file? Default: phrqpitz.dat*
Unless there is a reason to change the database file, hit return.
*Enter name of output file (input to PHRQPITZ). Default: pan.in*
This is the name of the file that PHRQNPT will generate and which can be used as an input file for PHRQPITZ. Sticking to the default will mean overwriting previous files.
*Input the title*
A name that will be displayed on the output.

The next section covers various options for modelling:

*Input IOPT(1)*
Options are:
0 – No print of thermodynamic data or coefficients of aqueous species
1 – Print the aqueous model data (which are stored on disk) once during the entire computer run.
*Input IOPT(2)*
Options are:
0 – Initial solutions are not to be charge balanced. Reaction solutions maintain the initial charge imbalance.
1 – pH is adjusted in initial solutions to obtain charge balance
2 – The total concentration of one of the elements (except H or O) is adjusted to obtain electrical balance. Neutral input is required.
*Input IOPT(3)*
Options are:
0 - No reactions modelled. Only the initial solutions are solved.

1 – Solution 1 is mixed (a hypothetical constant volume process) with solution 2 in specified reaction steps. **Steps** input and a value for *nsteps* are required. Minerals input may be included.
2 – Solution 1 is titrated with solution 2 in specific reaction steps. **Steps** input, a value for *nsteps* and a value for *V0* are required. Minerals input may be included.
3 – A stoichiometric reaction is added in specified reaction steps. **Reaction** input, **Steps** input, a value for *nsteps* and a value for *ncomps* are required. Minerals input may be included.
4 – A net stoichiometric reaction is added in *nsteps* equal increments. **Reaction** input, **Steps** input, a value for *nsteps* and a value for *ncomps* are required. Minerals input may be included. Only one value for the total reaction is read in **Steps.**

5 – Solution 1 is equilibrated with mineral phases only. No other reaction is performed. **Minerals** input is required.

6 – A reaction is added to solution 1 until equilibrium is attained with the first phase in mineral input (equilibrium with other minerals is maintained throughout the reaction). **Reaction** input, a value for *ncomps*, and **Minerals** input are required. No **Steps** input is required. Note: there should be a common element in the reaction and the first phase in **Minerals** input.

*Input IOPT(4)*

Options are:

0 – The temperature of the reaction solution is:

A: The same as the initial solution if adding a reaction.

B: Calculated linearly from the end members if mixing or titrating.

No **Temp** input is required.

1 – The temperature is constant during the reaction steps and differs from that of the initial solution(s). One value is read in **Temp** input.

2 – The temperature is varied from T(0) to T(F) in *nsteps* equal increments, during the reaction steps.

3 – The temperature of each reaction step is specified in **Temp** input, in order. *Nsteps* values are needed.

*Input IOPT(7)*

Options are:

0 – Do not save the aqueous phase composition at the end of a reaction for additional simulations.

1 – Save the final reaction solution in solution #1

2 – Save the final reaction solution in solution #2

*Input IOPT(8)*

Options are:

0 – The debugging print routine is not called

1 – A long printout is output at each iteration in each problem. This print is to be used only if there are convergence problems with the program (see subroutine Debug).

*Input IOPT(9)*

Options are:

0 – No printout of each array inverted.

1 – A long printout occurs of the entire array to be inverted at each iteration. This print is to be used only if there are convergence problems. (see subroutine SLNQ).

*Input IOPT(10)*

Options are:

0 – No convention for activity coefficient is used.

1 – MacInnes convention is used.

*Input nsteps*

Number of steps. A value is required if **IOPT(3)** =1, 2, 3 or 4 or if **IOPT(4)** =2 or 3

*Input V0*

Initial volume of solution #1 when modelling a titration. This unit of *V0* must be the same as that of *xstep* (see **Steps** input) if IOPT(3)=2. Otherwise *V0* is not required.

*Input ncomps*

The number of constituents in a net stoichiometric reaction. A constituent may be any element with an index number between 4 and 30 inclusive. No aqueous species with index numbers >30 may be included as reaction constituents except $H_2$ and $O_2$. Any constituent with index number greater than 30 is assumed to be either $H_2$ or $O_2$ and has the effect of raising or lowering the redox state of the solution depending on the assigned valence (*thmean*). A value for *ncomps* is required if **IOPT(3)** = 3, 4 or 6.

*Keyword data blocks*

There are 11 keywords which can be used to design the modelling input.

**ELEMENTS**

Defines a name and indices of all elements in the aqueous model database.

*Input tname*

Alphanumeric name of element. Type **LIST** to bring up a list of the elements currently in the database (Table C.1)

**Table C.1: Elements in the PHRQPITZ database**

| Elements | Index number | Gram formula weight | Input formula corresponding to GFW | Master species | OPV |
|---|---|---|---|---|---|
| ***** | 1 | 0 | ***** | ***** | +0.00 |
| ***** | 2 | 0 | ***** | ***** | +0.00 |
| ***** | 3 | 18.0152 | ***** | ***** | +0.00 |
| Ca | 4 | 40.0800 | $Ca^{2+}$ | $Ca^{2+}$ | +0.00 |
| Mg | 5 | 24.3050 | $Mg^{2+}$ | $Mg^{2+}$ | +0.00 |
| Na | 6 | 22.9898 | $Na^{+}$ | $Na^{+}$ | +0.00 |
| K | 7 | 39.0983 | $K^{+}$ | $K^{+}$ | +0.00 |
| Fe | 8 | 55.8470 | $Fe^{2+}$ | $Fe^{2+}$ | +2.00 |
| Mn | 9 | 54.9380 | $Mn^{2+}$ | $Mn^{2+}$ | +2.00 |
| Ba | 11 | 137.3300 | $Ba^{2+}$ | $Ba^{2+}$ | +0.00 |
| Sr | 12 | 87.6200 | $Sr^{2+}$ | $Sr^{2+}$ | +0.00 |
| Cl | 14 | 35.4530 | $Cl^{-}$ | $Cl^{-}$ | +0.00 |
| C | 15 | 44.0098 | $CO_2$ | $CO_3^{2-}$ | +4.00 |
| S | 16 | 96.0600 | $SO_4^{2-}$ | $SO_4^{2-}$ | +6.00 |
| B | 18 | 10.8100 | B | $B(OH)_3$ | +0.00 |
| Li | 21 | 6.9410 | $Li^{+}$ | $Li^{+}$ | +0.00 |
| Br | 22 | 79.9040 | $Br^{-}$ | $Br^{-}$ | +0.00 |

*Input NELT*

Index number assigned to element. Number must be between 4 and 30 inclusive.

*Input TGFW*

GFW of species used to report analytical data. If solution data is to include alkalinity, *TGFW* for element C must be the equivalent weight of the reported alkalinity species.

**SPECIES**

Defines names, index numbers and composition of all aqueous species in the aqueous model data base.

*Input I*

Index number assigned to aqueous species. Numbers 4 through 30 are reserved for master species. 250 is the maximum index number for an aqueous species.

*Input SNAME*

Alphanumeric species name

*Input NSP*

Total number of master species in the association reaction that forms this species. Do not count the species itself unless the species is a master species.

*Input KFLAG*

Options are:

0 – Van't Hoff expression is used to calculate temperature dependence of the association constant for this species.

1 – an analytical expression is used to calculate temperature dependence of the association constant.

*Input GFLAG*

Options are:

0 – The extended Debye-Huckel or Davis expression (according to **IOPT(6)**) is used to calculate the activity coefficient for this species.

1 – The Wateq-Debye-Huckel expression is used to calculate the activity coefficient for this species (regardless of the value of **IOPT(6)**).

*Input ZSP*

Charge on this aqueous species.

*Input DHA*

The extended Debye-Huckel A-0 term.

*Input ALKSP*

The alkalinity assigned to this aqueous species.

*Input LKTOSP*

Log K at 25°C where $\log K = A1 + A2(T) + A3/T + (A4 * \log(T)) + A5/T^2$

*Input DHSP*

Standard enthalpy of association reaction at 25°C (H(R), in kcal/mol).

**SOLUTION**

Used to define starting solution.

*Input solution number*

A number, either 1 or 2, indicating the solution number of the following data.

*Input solution heading*

Title or comments about the solution.

*Input NTOTS*

The number of total concentrations to be read from card input, for example, if the starting solution is $MgCl_2$-$NaHCO_3$ solution, *NTOTS*=4 (for Mg, Cl, Na and C).

*Input IALK*

Flag which indicates whether total C or total alkalinity is to be input.

0 – indicates total concentration of C (not alkalinity) is input in the units specified by *IUNITS.*

N – 4<N<30 where N is the index number for the element C (in our database, N =15), indicates total alkalinity is being entered. **Elements** input may be required. The units of alkalinity are specified by *IUNITS* and if units>0, the GFW of the element C is critically important. The FGW in the case of alkalinity must be the gram equivalent weight (g/equivalent) of the chemical species in which alkalinity is being reported. The following is a list of species commonly used for reporting alkalinity and their corresponding equivalent weight:

$CaCO_3$ = 50.0446 g/eq
$HCO_3^-$ = 61.0171 g/eq
$CO_3^{2-}$ = 30.0046 g/eq

In our database, 44.010 is the GFW of C which is suitable for entering C as total $CO_2$. This GFW must be changed via **Elements** input if alkalinity is to be entered as mg/l or ppm (*IUNITS* = 2 or 3). If *IUNITS*=0, alkalinity myst be input as eq/kg $H_2O$ and in this case the GFW need not be changed since no conversion is necessary.

*Input IUNITS*

Flag describing units of input concentrations. The program makes all of its calculations in terms of molality and any other allowed concentration units (mmol/l, mg/l, ppm or mmol/kg) must be converted to molality before calculation may begin. To make the conversions it is necessary to know the GFW in g/mole of the chemical formula in which elemental analyses are reported. The GFW is an input parameter under **Elements** input and must be in agreement with the analytical units for each solution dataset. (If the units are molality, no conversion is necessary and the GFW's are not used). Note: All elements must have the same units. It is not possible to enter mg/l of one element and molality of another.

0 – concentration of elements entered as molality of each element, or for alkalinity, equivalents/kg $H_2O$.

1 – concentration of elements entered as mmol/l of each element, or for alkalinity meq/l

2 – concentration of elements entered as mg/l of the species which has a GFW given in **Elements** input (**Elements** input may be required)

3 – concentration of elements entered as ppm of the species which has a GFW given in **Elements** input. (**Elements** input may be required).

4 – concentration of elements entered as mmol/kg solution.

*Input pH*

The pH of the solution (approximate if *IOPT(2)* =1)

*Input Temp*

Temperature of solution in °C.

*Input LT(NTOTS)*

LT = index number of element N

*Input DTOT(NTOTS)*

Total concentration of element in molality, mmols/kg, mg/l or ppm according to *Iunits*.

**MINERALS**

Defines phases which will be maintained at equilibrium with each of the reaction solutions.

*Preconstructed mineral data are available. Do you wish to have any of them?* (see Table C.2)

**Table C.2: Minerals in the PHRQPITZ database**

| | | | | |
|---|---|---|---|---|
| 1. Anhydrite | 2. Aragonite | 3. Arcanite | 4. Bischofite | 5. Bloedite |
| 6. Brucite | 7. Burkeite | 8. Calcite | 9. Carnallite | 10. Dolomite |
| 11. Epsomite | 12. Gaylussite | 13. Glaserite | 14. Glauberite | 15. Gypsum |
| 16. Halite | 17.Hexahydrite | 18. Kainite | 19. Kalcinite | 20. Kieserite |
| 21. Labile S | 22. Leonhardite | 23. Leonite | 24. Magnesite | 25. Mirabilite |
| 26. Misenite | 27. Nahcolite | 28. Natron | 29. Nesquehonite | 30. $P_{CO2}$ |
| 31. Pentahydrite | 32. Pirssonite | 33. Polyhalite | 34. Portlandite | 35. Schoenite |
| 36. Sylvite | 37. Syngenite | 38. Trona | 39. Borax | 40. B-Acid, S |
| 41. KB5O84W | 42. K2B4O74W | 43. NABO24W | 44. NAB5O85W | 45. Teepleite |

*More minerals to be typed in from the terminal?*
*Input MNAME*
Alphanumeric name of mineral
*Input NMINO*
Number of different species in the mineral dissociation reaction (including $H^+$, $e^-$, and $H_2O$). *NMINO* must be < 10.
*Input THMIN*
The sum of the valencies of the redox species in the mineral dissociation reaction.
*Input LKTOM*
Log of the equilibrium constant at 25°C for reaction
*Input DHMIN*
Delta H® (kcal/mol) for the Van't Hoff expression
*Input MFLAG*
0 – The Van't Hoff expression is used to calculate the temperature dependence of the equilibrium constant.
1 – The analytical expression is used to calculate the temperature dependence of the equilibrium constant.
*Input SIMIN*
Saturation index (log $IAP/K_{sp}$) desired in the final solution. *SIMIN* = 0.0 would produce equilibrium with the mineral while 1.0 would produce a solution 10x supersaturated. This variable is useful inspecifying the partial pressure of a gas. The Henry's Law constant for the gas would be entered using the Van't Hoff (*LKTOM*) or analytical expression (*AMIN*) and the log of the partial pressure would be entered for *SIMIN*.
*Input LMIN(NMINO)*
Index number of species (not necessarily master species) in the dissocation reaction for this mineral.
*Input CMIN(NMINO)*
Stoichiometric coefficient of species in dissociation reaction.

**LOOKMIN**
Provide information on the saturation state of aqueous phases with respect to desired minerals. Minerals in this block of input do not affect calculations of initial solution or any of the reaction solutions. Never mandatory.

*Do you want to delete all old minerals?*
Input variables as for **Minerals** keyword block.

**TEMP**
Varies temperature during reaction steps. It is not required when IOPT(4) = 0.
*Input XTEMP(NSTEP)*
Temperature in degrees C.

**STEPS**
Defines steps of reaction process. Not required when IOPT(3) = 0, 5 or 6.
*Input XSTEP(NSTEP)*
The value of XSTEP will vary depending on IOPT(3).
1 – The fraction of solution 1 to be mixed with solution2.

2 – Volume of solution 2 to be titrated into solution 1. Units must be the same as V0.
3 – The moles of reaction to be added to solution 1.
4 – Total number of moles of reaction to be added in *NSTEPS* steps. *NSTEPS* reaction solutions will be calculated. The Ith solution will have I x *XSTEP/NSTEP* moles of reaction added to solution 1.

**REACTION**
Describes the stoichiometry and valence of elements to be added as reaction.
*Input LREAC(1)*
Index number of element for the reaction. *LREAC* must be between 4 and 30 inclusive. If *LREAC*>30 the program considers this constituent to be $H_2$ or $O_2$ and only uses *CREAC* and *THMEAN* to change the oxidation state of the reaction solution.
*Input CREAC(1)*
Stoichiometric coefficient of element in reaction.

**NEUTRAL**
Input defines elements to be used to adjust the initial solutions to electrical neutrality (i.e. IOPT(2) =2).
*Input LPOS*
Index number of an element with a cation master species.
*Input LNEG*
Index number of an element with an anion master species.

**SUMS**
Sums the molalities of aqueous species which are then printed in the output of reaction. These sums do not affect the calculations in any way and are never mandatory.
*Do you want to delete all old sums?*
*Input SUNAME*
Alphanumeric name to be printed to identify reaction.
*Input NSUM*
The number of index numbers to be read (<50)
*Input LSUM(NSUM)*
Index numbers of species in sum.

**END**
Terminates input operations for single simulation. Any computer has at least one end card.
*More simulations?*
*Do you wish to define the previous output as your new reference?*
Enter reference file name? Etc.....

## C.3. EXAMPLE OF PHRQPITZ INPUT FILE

```
RA-WP1
0000020000 0 0      0.0
SOLUTION 1
RA-WP1
12  0 0  7.6      4.0     25.       1.0
  4 0.0102      5 0.141       6 4.642       7 0.0269      11 0.000000085
 12 0.0001872   14 4.767      15 0.00062    16 0.350      18 0.001082
 21 0.00002262  22 0.00119
LOOK MIN
Barite    2  0.      -9.97    6.35        0      2.       11 1.       16 1.
Celestit  2  0.      -6.63    -1.037      0      2.       12 1.       16 1.
Strontia  2  0.      -9.271   -0.4        0      2.       12 1.       15 1.
witherit  2  0.      -8.562   0.703       0      2.       11 1.       15 1.
END
```

Where: Line(1): Title
Line(2): Iopt(1);Iopt(2);Iopt(3);Iopt(4);0;2;Iopt(7);Iopt(8);Iopt(9);Iopt(10) Nsteps Ncomps V.O.
Line(3): Keyword "Solution" plus solution number

Line(4): Solution heading
Line(5): Ntots; Ialk; Iunits; pH; 4.0; Temp; Solution number
Line(6-8): Concentration input in format: Index number of element (from Table x); Total concentration of element in units according to Iunits
Line(9): Next keyword, LOOKMIN – used to add minerals to database to determine saturation.
Line(10-17): Mname;Nmino;Thmin;Lktom;Dhmin;Mflag;Simin;Lmin(1);Cmin(1); Lmin(2);Cmin(2)

## C.4. EXAMPLE OF PHRQPITZ OUTPUT FILE

SOLUTION NUMBER 1
RA-WP1

TOTAL MOLALITIES OF ELEMENTS

| ELEMENT | MOLALITY | LOG MOLALITY |
|---|---|---|
| CA | 1.020000D-02 | -1.9914 |
| MG | 1.410000D-01 | -0.8508 |
| NA | 4.642000D+00 | 0.6667 |
| K | 2.690000D-02 | -1.5702 |
| BA | 8.000000D-08 | -7.0969 |
| SR | 1.872000D-04 | -3.7277 |
| CL | 4.767000D+00 | 0.6782 |
| C | 6.200000D-04 | -3.2076 |
| S | 3.500000D-01 | -0.4559 |
| B | 1.082000D-03 | -2.9658 |
| LI | 2.262000D-05 | -4.6455 |
| BR | 1.190000D-03 | -2.9245 |

----DESCRIPTION OF SOLUTION----

PH = 7.6000
ACTIVITY H2O = 0.8107
OSMOTIC COEFFICIENT = 1.1719
IONIC STRENGTH = 5.7215
TEMPERATURE = 25.0000
PRESSURE = 1.0000 ATM
DENSITY OF H2O = 0.9971 G/CC
ELECTRICAL BALANCE = -4.9740D-01
TOTAL ALKALINITY = 9.0634D-04
ITERATIONS = 1

DISTRIBUTION OF SPECIES

| I | SPECIES | Z | UNSCALED MOLALITY | LOG MOLAL | UNSCALED ACTIVITY | LOG ACT | GAMMA | LOG GAM |
|---|---|---|---|---|---|---|---|---|
| 1 | H+ | 1.0 | 8.718E-09 | -8.060 | 2.512E-08 | -7.600 | 2.881E+00 | 0.460 |
| 3 | H2O | 0.0 | 8.107E-01 | -0.091 | 8.107E-01 | -0.091 | 1.000E+00 | 0.000 |
| 4 | CA+2 | 2.0 | 1.019E-02 | -1.992 | 6.639E-03 | -2.178 | 6.515E-01 | -0.186 |
| 5 | MG+2 | 2.0 | 1.409E-01 | -0.851 | 1.607E-01 | -0.794 | 1.141E+00 | 0.057 |
| 6 | NA+ | 1.0 | 4.642E+00 | 0.667 | 3.943E+00 | 0.596 | 8.493E-01 | -0.071 |
| 7 | K+ | 1.0 | 2.690E-02 | -1.570 | 1.296E-02 | -1.887 | 4.817E-01 | -0.317 |
| 11 | BA+2 | 2.0 | 8.000E-08 | -7.097 | 9.610E-09 | -8.017 | 1.201E-01 | -0.920 |
| 12 | SR+2 | 2.0 | 1.872E-04 | -3.728 | 6.606E-05 | -4.180 | 3.529E-01 | -0.452 |
| 14 | CL- | -1.0 | 4.767E+00 | 0.678 | 4.104E+00 | 0.613 | 8.610E-01 | -0.065 |
| 15 | CO3-2 | -2.0 | 1.939E-05 | -4.713 | 3.744E-07 | -6.427 | 1.932E-02 | -1.714 |
| 16 | SO4-2 | -2.0 | 3.500E-01 | -0.456 | 6.761E-03 | -2.170 | 1.932E-02 | -1.714 |
| 18 | B(OH)3 | 0.0 | 8.841E-04 | -3.053 | 9.265E-04 | -3.033 | 1.048E+00 | 0.020 |

| | | | | | | | |
|---|---|---|---|---|---|---|---|
| 21 LI+ | 1.0 | 2.262E-05 | -4.646 | 4.503E-05 | -4.347 | 1.991E+00 | 0.299 |
| 22 BR- | -1.0 | 1.190E-03 | -2.924 | 1.273E-03 | -2.895 | 1.070E+00 | 0.029 |
| 31 OH- | -1.0 | 7.108E-07 | -6.148 | 3.242E-07 | -6.489 | 4.562E-01 | -0.341 |
| 34 HCO3- | -1.0 | 5.410E-04 | -3.267 | 2.054E-04 | -3.687 | 3.797E-01 | -0.421 |
| 35 H2CO3 | 0.0 | 5.059E-06 | -5.296 | 1.384E-05 | -4.859 | 2.736E+00 | 0.437 |
| 40 HSO4- | -1.0 | 2.815E-08 | -7.551 | 1.618E-08 | -7.791 | 5.748E-01 | -0.240 |
| 41 B(OH)4- | -1.0 | 1.404E-04 | -3.853 | 1.725E-05 | -4.763 | 1.229E-01 | -0.911 |
| 42 B3O3()4- | -1.0 | 8.685E-09 | -8.061 | 1.428E-09 | -8.845 | 1.645E-01 | -0.784 |
| 43 B4O5()-- | -2.0 | 3.747E-11 | -10.426 | 1.610E-13 | -12.793 | 4.297E-03 | -2.367 |
| 44 CAB()4+ | 1.0 | 5.594E-06 | -5.252 | 5.115E-06 | -5.291 | 9.143E-01 | -0.039 |
| 45 MGB()4+ | 1.0 | 5.189E-05 | -4.285 | 6.947E-05 | -4.158 | 1.339E+00 | 0.127 |
| 76 CACO3 | 0.0 | 3.522E-06 | -5.453 | 3.522E-06 | -5.453 | 1.000E+00 | 0.000 |
| 85 MGOH+ | 1.0 | 1.891E-05 | -4.723 | 8.052E-06 | -5.094 | 4.258E-01 | -0.371 |
| 86 MGCO3 | 0.0 | 5.099E-05 | -4.292 | 5.099E-05 | -4.292 | 1.000E+00 | 0.000 |

| SPECIES | UNSCALED TOTAL MOL | UNSCALED ACTIVITY | TOTAL GAMMA |
|---|---|---|---|
| H+ | 3.6866D-08 | 2.5119D-08 | 6.8136D-01 |
| CA+2 | 1.0200D-02 | 6.6391D-03 | 6.5090D-01 |
| MG+2 | 1.4100D-01 | 1.6072D-01 | 1.1398D+00 |
| NA+ | 4.6420D+00 | 3.9426D+00 | 8.4932D-01 |
| K+ | 2.6900D-02 | 1.2959D-02 | 4.8175D-01 |
| BA+2 | 8.0000D-08 | 9.6095D-09 | 1.2012D-01 |
| SR+2 | 1.8720D-04 | 6.6058D-05 | 3.5288D-01 |
| CL- | 4.7670D+00 | 4.1043D+00 | 8.6098D-01 |
| CO3-2 | 7.3902D-05 | 3.7443D-07 | 5.0665D-03 |
| SO4-2 | 3.5000D-01 | 6.7614D-03 | 1.9318D-02 |
| B(OH)3 | 1.0820D-03 | 9.2651D-04 | 8.5629D-01 |
| LI+ | 2.2620D-05 | 4.5026D-05 | 1.9906D+00 |
| BR- | 1.1900D-03 | 1.2731D-03 | 1.0699D+00 |
| OH- | 2.1749D-04 | 3.2424D-07 | 1.4908D-03 |
| HCO3- | 5.4104D-04 | 2.0541D-04 | 3.7966D-01 |
| H2CO3 | 5.0586D-06 | 1.3843D-05 | 2.7365D+00 |

---- MEAN ACTIVITY COEFFICIENT ----

| FORMULA | MEAN GAMMA | | |
|---|---|---|---|
| CACL2 | 7.8433D-01 | CASO4 | 1.1213D-01 |
| CACO3 | 5.7426D-02 | CA(OH)2 | 1.1310D-02 |
| MGCL2 | 9.4539D-01 | MGSO4 | 1.4839D-01 |
| MGCO3 | 7.5994D-02 | MG(OH)2 | 1.3632D-02 |
| NACL | 8.5513D-01 | NA2SO4 | 2.4064D-01 |
| NAHCO3 | 5.6785D-01 | NA2CO3 | 1.5403D-01 |
| NAOH | 3.5583D-02 | KCL | 6.4403D-01 |
| K2SO4 | 1.6489D-01 | KHCO3 | 4.2767D-01 |
| K2CO3 | 1.0555D-01 | KOH | 2.6799D-02 |
| HCL | 7.6592D-01 | H2SO4 | 2.0777D-01 |
| HBR | 8.5379D-01 | | |

---- LOOK MIN IAP ----

| PHASE | LOG IAP | LOG KT | LOG IAP/KT | PHASE | LOG IAP | LOG KT | LOG IAP/KT |
|---|---|---|---|---|---|---|---|
| ANHYDRIT | -4.3479 | -4.3617 | 0.0138 | MISENITE | -75.8892 | -10.8060 | -65.0832 |
| ARAGONIT | -8.6045 | -8.2195 | -0.3851 | NAHCOLIT | -13.4309 | -10.7420 | -2.6889 |
| ARCANITE | -5.9448 | -1.7760 | -4.1688 | NATRON | -6.1465 | -0.8250 | -5.3215 |
| BISCHOFI | -0.1143 | 4.4551 | -4.5694 | NESQUEHO | -7.4940 | -5.1670 | -2.3270 |
| BLOEDITE | -4.3069 | -2.3470 | -1.9599 | PCO2 | -4.8588 | -1.4679 | -3.3908 |
| BRUCITE | -13.7722 | -10.8840 | -2.8882 | PENTAHYD | -3.4196 | -1.2850 | -2.1346 |

| | | | | | | | |
|---|---|---|---|---|---|---|---|
| BURKEITE | -7.1919 | -0.7720 | -6.4199 | PIRSSONI | -14.0219 | -9.2340 | -4.7879 |
| CALCITE | -8.6045 | -8.4062 | -0.1983 | POLYHALI | -17.7867 | -13.7440 | -4.0427 |
| CARNALLI | -1.3885 | 4.3300 | -5.7185 | PORTLAND | -15.1562 | -5.1900 | -9.9662 |
| DOLOMITE | -15.8251 | -17.0830 | 1.2579 | SCHOENIT | -9.4555 | -4.3280 | -5.1275 |
| EPSOMITE | -3.6019 | -1.8809 | -1.7210 | SYLVITE | -1.2742 | 0.8998 | -2.1740 |
| GAYLUSSI | -14.2953 | -9.4210 | -4.8743 | SYNGENIT | -10.3838 | -7.4480 | -2.9358 |
| GLASERIT | -9.4064 | -3.8030 | -5.6034 | TRONA | -18.8482 | -11.3840 | -7.4642 |
| GLAUBERI | -5.3263 | -5.2450 | -0.0813 | BORAX | 3.8033 | 12.4640 | -8.6607 |
| GYPSUM | -4.5301 | -4.5805 | 0.0504 | B-ACID,S | -3.0331 | -0.0300 | -3.0031 |
| HALITE | 1.2090 | 1.5700 | -0.3610 | KB5O84W | -9.1798 | 4.6710 | -13.8508 |
| HEXAHYDR | -3.5107 | -1.6346 | -1.8761 | K2B4074W | -0.6163 | 13.9060 | -14.5223 |
| KAINITE | -4.5115 | -0.1930 | -4.3185 | NABO24W | 4.8892 | 9.5680 | -4.6788 |
| KALICINI | -15.9141 | -10.0580 | -5.8561 | NAB5085W | -6.7877 | 5.8950 | -12.6827 |
| KIESERIT | -3.0550 | -0.1230 | -2.9320 | TEEPLEIT | 6.2805 | 10.8400 | -4.5595 |
| LABILE S | -6.4869 | -5.6720 | -0.8149 | Barite | -10.1873 | -9.9700 | -0.2173 |
| LEONHARD | -3.3284 | -0.8870 | -2.4414 | Celestit | -6.3500 | -6.6300 | 0.2800 |
| LEONITE | -9.2733 | -3.9790 | -5.2943 | Strontia | -10.6067 | -9.2710 | -1.3357 |
| MAGNESIT | -7.2206 | -7.8340 | 0.6134 | witherit | -14.4439 | -8.5620 | -5.8819 |
| MIRABIL | -1.8898 | -1.2135 | -0.6762 | | | | |

## C.5. EVAPORATION MODELLING IN PHREEQC

### C.5.1. EXAMPLE OF INPUT FILE

```
TITLE OT-WR1
Solution 1
        Units ppm
        temp 25.0
        pH 8.6
        C 83.41 as CO3-2
        Ca 223.65
        Mg 315.9
        Na 1896.675
        K 82.89
        S(6) 904.15 as SO4
        Cl 4147.65
        Br 4.714
        F 0.684
        Si 8.07
reaction
        H2O -1
        44.405 moles
save solution 2
end
use solution 2
mix
        2 20
save solution 3
end
use solution 3
equilibrium_phases 2
Gypsum 0.0 0.0
Calcite 0.0 0.0
halite 0.0 0.0
CO2(g) -3.5 1.0
fluorite 0.0 0.0
end
```